

**Characterisation of Cardiosphere Derived Cells:  
investigating hypoxic pre-conditioning on pro-  
angiogenic properties and tracking the cardiac  
fibroblast component**

**Thesis submitted for the degree of  
Doctor of Philosophy**



**Muhammad Mehdi Amirrasouli  
Institute of Genetic Medicine  
Faculty of Medical Sciences  
Newcastle University  
February 2014**

## **Abstract**

Coronary heart disease is still the leading cause of death in the UK, despite significant advances in clinical treatments. Stem cell transplantation has the potential to improve cardiac function and patient outcome, but optimal cell types, cell preparation methods and cell delivery routes are yet to be established.

The heart contains a small population of progenitor cells that, in culture, contribute to spontaneously formed spheroids known as cardiospheres (Csphs). Following further culture, Csphs give rise to cardiosphere derived cells (CDCs). Both Csphs and CDCs show paracrine benefit including neovascularisation in myocardial ischaemia, leading to improvement in heart function. The aims of this project were to use mouse models to (i) investigate the effect of hypoxic preconditioning on the pro-angiogenic potential of CDCs and (ii) characterise the contribution of cardiac fibroblasts (CFs) to CDCs.

I used *Colla2-CreERT;Rosa26-STOP-YFP* mice to track YFP-expressing CFs in myocardial tissue and in CDC culture. Co-staining experiments showed only partial overlap of YFP with other CF markers (vimentin and Fsp1) in heart tissue, which may be due to the heterogeneity of CFs and/or incomplete activation of YFP in CFs. I showed that CF-derived cells exist in all stages of CDC culture, and a small subset of these cells also expressed the stem cell markers Sca-1 or cKit, suggesting CF derived cells may contribute to the progenitor cell population.

My results showed that preconditioning CDCs with 3%O<sub>2</sub> enhances cell outgrowth from heart explants and promotes expression of stem cell and pro-angiogenic markers. I then assessed the pro-angiogenic potential of CDCs in vivo using a sub-dermal matrigel plug assay and showed that CDCs alone have limited pro-angiogenic potential. However, 3%O<sub>2</sub> preconditioning of CDCs significantly enhances this process.

Further research will increase our understanding of CDC-mediated angiogenesis and improve clinical therapies for MI patients.

## **Declaration**

The work presented in this thesis was undertaken in the laboratory of Prof Helen Arthur at the institute of Genetic Medicine (Newcastle University). The contents are original and are my own work and I have acknowledged the contributors where appropriate in the text. No material of this thesis has been submitted by me for any qualification and publications. The word limit of this thesis follows the guidelines presented by the Faculty of Medical Science.

Muhammad Mehdi Amirrasouli

February 2014

## **Acknowledgments**

Foremost I would like to express my sincere gratitude to my supervisor Prof Helen Arthur for continuous help and support of my research and passing her knowledge and guidance to me. Her guidance helped me in all time of research and writing every parts of this thesis. I would like to thank Prof Ioakim Spyridopoulos, my second supervisor for his valuable comments and suggestion to write my thesis.

I would also like to thank Dr Racheal Redgrave for teaching me CDC culture and for her valuable suggestion to improve this research and I wish her best of luck and success for the future. My special thanks also go to Dr Zhenhua Zhai for sharing his experience in cell and tissue staining and statistics, good luck mate. I would also like to thank to the rest of my research group both past and present. I would like to acknowledge Lisa Hodgson for her great help to set up confocal microscopy with my experiments.

My very special thanks go to Azadeh for loving me and always supporting me and building my confidence throughout my studies in the UK. Without her I could not have done this. Above all I would like to thank my lovely son Yousef and my little princess Sarah for letting me to write my thesis at home instead of watching Batman together, although they pour once a whole cup of tea on my laptop.

I would also like to thank my brothers Benyamin and Mousa for always making me laugh with their funny texts, jokes and pictures.

And finally I would like to thank my parents Dada & Ouza for their never ending love and unconditional support throughout my degree. I wish them health and happiness for the future.

## List of contents

<b>Chapter 1 Introduction</b>	<b>1</b>
<b>1.1 The heart</b>	<b>2</b>
1.1.1 Vascularity of the heart	2
1.1.2 Cellular composition of the heart	3
<b>1.2 Coronary heart disease and myocardial infarction</b>	<b>4</b>
<b>1.3 CF morphology and functions</b>	<b>6</b>
1.3.1 Origin and heterogeneity of CFs	7
1.3.2 CF markers	8
1.3.3 Origins of CFs in cardiopathy	8
1.3.3.1 Endothelial-mesenchymal transition (End-MT)	9
1.3.3.2 Bone-marrow-derived CFs	10
1.3.4 CFs and myocardial remodelling	11
<b>1.4 Vasculogenesis and angiogenesis</b>	<b>12</b>
<b>1.5 Angiogenesis and its role in cardiac remodelling</b>	<b>13</b>
1.5.1 Therapeutic angiogenic therapies in myocardial infarction	14
<b>1.6 Cardiac stem cells (CSCs)</b>	<b>15</b>
1.6.1 Stem cell antigen-1 (Sca-1)	16
1.6.2 cKit	17
1.6.3 Cardiac side population, Abcg2 <sup>+</sup> progenitors	18
1.6.4 Characterisation of EDCs, Csphs and CDCs	18
1.6.5 The origin of Csphs and CDCs	21
1.6.6 EDC and Csph culture from the MI model	22
1.6.7 The role of EDCs, Csphs and CDCs in neovascularisation	22
<b>1.7 Hypoxia and Hif proteins</b>	<b>24</b>
1.7.1 Hif proteins	25
1.7.2 Hypoxia signalling in adult stem cells	26
<b>1.8 Hypoxia and cardiac progenitor cells</b>	<b>27</b>
1.8.1 Hypoxia preconditioning of EDCs and CDCs	28
<b>1.9 Clinical trials using CDCs in MI patients</b>	<b>30</b>
<b>1.10 Aims of thesis</b>	<b>31</b>
<b>Chapter 2 Material and Methods</b>	<b>32</b>
<b>2.1 Suppliers</b>	<b>33</b>
<b>2.2 Mouse strains</b>	<b>33</b>
<b>2.3 Genotyping and DNA extraction from ear clips and tail tips</b>	<b>34</b>
2.3.1 Genotyping	34
2.3.1.1 Standard PCR	34
2.3.1.2 Agarose gel electrophoresis solutions and preparation:	35
<b>2.4 Cardiosphere-Derived Cells (CDCs) culture:</b>	<b>36</b>
2.4.1 Explant culture	36
2.4.2 Cardiosphere culture	37
2.4.3 Cardiosphere-derived cell culture	37

<b>2.5 Cell staining</b>	<b>38</b>
2.5.1 Immunofluorescent cell staining	38
<b>2.6 <i>In-vitro</i> cell proliferation and viability assay of CDCs</b>	<b>38</b>
<b>2.7 Clonogenicity assay with CDCs</b>	<b>38</b>
<b>2.8 Flow cytometry</b>	<b>39</b>
2.8.1 Immunophenotyping of murine CDCs	39
<b>2.9 ELISA (Enzyme-Linked Immunosorbent Assay)</b>	<b>39</b>
<b>2.10 Quantitative RT-PCR</b>	<b>40</b>
2.10.1 Primer design	40
2.10.2 RNA isolation	40
2.10.3 RNA isolation with Trizol	41
2.10.4 Complementary DNA (cDNA) preparation	41
2.10.5 qRT-PCR analysis of CDCs	42
<b>2.11 Histological staining procedures</b>	<b>43</b>
<b>Solutions:</b>	43
2.11.1 Interaperitoneal (IP) injection of tamoxifen	43
2.11.2 Tissue processing and preparation of frozen samples	43
2.11.3 Cryosectioning of frozen tissue.	43
2.11.4 Immunohistochemistry with Vectastain ABC system	44
2.11.5 H & E staining	44
2.11.6 Immunofluorescent staining of heart and matrigel plugs	45
2.11.7 Double Immunofluorescent Staining	45
<b>2.12 Mouse model of <i>in vivo</i> angiogenesis using sub-dermal matrigel plugs</b>	<b>47</b>
2.12.1 Matrigel preparation	47
2.12.2 Pre injection preparation	47
2.12.3 Induction of anaesthesia	47
2.12.4 Sub-dermal cell/matrigel injection with neonatal CDCs	47
2.12.5 Sub-dermal cell/matrigel injection with adult CDCs	48
2.12.6 <i>In-vivo</i> perfusion analysis of sub-dermal matrigel plugs with adult-derived CDCs	48
<b>2.13 Microscopy and imaging</b>	<b>49</b>
<b>2.14 Statistical analysis</b>	<b>49</b>
<b>Chapter 3 The effect of 3% O<sub>2</sub> culture on neonatal CDCs proangiogenic and stem cell potential</b>	<b>50</b>
<b>3.1 Introduction</b>	<b>51</b>
<b>3.2 Results</b>	<b>52</b>
3.2.1 Optimizing CDC culture with 3% O <sub>2</sub>	52
3.2.2 3% O <sub>2</sub> increases phase bright cell outgrowth but delays Csph maturation	53
3.2.3 3% O <sub>2</sub> stabilises Hif-1 $\alpha$ protein in CDCs	55
3.2.4 The effect of 3% O <sub>2</sub> on P2 neonatal CDC proliferation and viability	56
3.2.5 The effect of 3% O <sub>2</sub> on CDC clonogenicity	57
3.2.6 Selection of housekeeping genes for qRT-PCR experiments with CDCs cultured in normoxia and 3% O <sub>2</sub>	58
3.2.7 The effect of 3% O <sub>2</sub> on gene expression in neonatal CDCs	59
3.2.8 3% O <sub>2</sub> leads to variable protein expression of endothelial, mesenchymal and stem cell markers in neonatal CDCs.	63

<b>3.3 Discussion</b>	<b>66</b>
3.3.1 Validation of hypoxia	66
3.3.2 The effect of 3% O <sub>2</sub> on different stages of CDC culture	67
3.3.3 The effect of 3% O <sub>2</sub> on superficial markers of neonatal CDCs	69
3.3.3.1 Defining the proper combination of housekeeping genes for 3% O <sub>2</sub> studies with CDCs	69
3.3.3.2 The effect of 3% O <sub>2</sub> on CDC stem cell markers	70
3.3.3.3 The effect of 3% O <sub>2</sub> on mesenchymal markers of CDCs	71
3.3.3.4 The effect of 3% O <sub>2</sub> on endothelial markers of CDCs	71
<b>Chapter 4 The effect of 3% O<sub>2</sub> culture on adult CDCs proangiogenic and stem cell potential</b>	<b>74</b>
<b>4.1 Introduction</b>	<b>75</b>
<b>4.2 Results</b>	<b>76</b>
4.2.1 Optimisation of adult CDC culture	76
4.2.2 Preparing CDCs from atria and ventricles of the adult murine heart	76
4.2.3 Defining an effective 3% O <sub>2</sub> pre-treatment duration for adult P2 CDCs	78
4.2.4 Stabilisation of Hif-1 $\alpha$ protein in adult P2 CDCs following 48 hours of 3% O <sub>2</sub> culture	78
4.2.5 The effect of 3% O <sub>2</sub> on adult CDC clonogenicity	79
4.2.6 The effect of 3% O <sub>2</sub> on adult P2 CDC proliferation and viability	80
4.2.7 The effect of 3% O <sub>2</sub> on passage 2 adult CDC gene expression	82
4.2.8 3% O <sub>2</sub> increases Vegf protein in the supernatant of adult-derived P2 CDC	86
4.2.9 The effect of 3% O <sub>2</sub> on stem cell (Sca-1, cKit), Mesenchymal (CD90, Eng) and endothelial (CD31, CD34, Flk1) markers of adult P2 CDCs	87
4.2.10 Sca-1 <sup>+</sup> and cKit <sup>+</sup> CDCs are predominantly CD45 <sup>-</sup>	88
4.2.11 Sca-1 expression increases following extended passaging of adult CDCs	91
<b>4.3 Discussion</b>	<b>92</b>
4.3.1 The efficiency of adult murine CDC culture	92
4.3.2 Possible reasons for low efficiency of adult CDC culture in comparison with neonatal CDCs	92
4.3.3 Adult murine atria generate a higher yield of EDCs and Csphs than ventricles	93
4.3.4 Defining the optimal 3% O <sub>2</sub> culture duration for adult CDCs	94
4.3.5 The effect of 3% O <sub>2</sub> on adult CDC clonogenicity, viability and proliferation	94
4.3.6 Possible implications of 3% O <sub>2</sub> culture in phenotypic heterogeneity of adult murine CDCs	95
4.3.7 Sca-1 expression in expanded adult CDC culture	95
<b>Chapter 5 Lineage tracing of cardiac fibroblasts in murine hearts and CDC culture</b>	<b>97</b>
<b>5.1 Introduction</b>	<b>98</b>
<b>5.2 Results</b>	<b>100</b>
5.2.1 Transgenic <i>Col1a2-Cre(ER)<sup>T2</sup>; Rosa26-floxed-STOP-eYFP</i> mouse model	100
5.2.2 Activation of Cre-recombinase and eYFP reporter expression in CFs	101
5.2.3 Co expression of eYFP with FSP1 and vimentin in healthy murine myocardium	102
5.2.4 YFP and FSP1 co-expression in the infarct and border zone of <i>Col1a2 CreERT; Rosa26-STOP-eYFP</i> hearts following myocardial infarction	105
5.2.5 Elimination of the autofluorescent artefacts in the border zone (BZ) and the infarct region (IR) of hearts following MI of <i>Col1a2 CreERT; Rosa26-floxed STOP eYFP</i> and <i>Rosa26-STOP-eYFP</i> mice	106
5.2.6 The pattern of eYFP/FSP1 and eYFP/vimentin expression in the border zone and the infarct region	108

5.2.7 Quantification of CFs in healthy and MI hearts and assessing eYFP co-staining with FSP1 or vimentin _____	113
5.2.8 eYFP expression at different stages of CDC culture _____	114
5.2.9 eYFP <sup>+</sup> EDCs from atria are able to form Csphs _____	118
5.2.10 eYFP expression in passage 2 CDCs derived from <i>Coll1a2CreERT; Rosa26-floxed-STOP-eYFP</i> P mice _____	119
5.2.11 eYFP expression (derived from <i>Coll1a2 CreERT; Rosa26-floxed STOP eYFP</i> mice) increases by extending CDC passage number _____	122
<b>5.3 Discussion _____</b>	<b>124</b>
5.3.1 Myocardial infarction causes autofluorescence in the border zone and in the injured region _____	126
5.3.2 Co-localisation of FSP1 and vimentin with eYFP in the border zone and the infarct region _____	126
5.3.3 Possible implications of MI experimental design on eYFP expression in CFs _____	128
5.3.4 Cardiac fibroblasts are able to form Csphs _____	129
5.3.5 Evaluation of eYFP expression at different stages of CDC culture _____	129
<b>Chapter 6 Angiogenic potential of neonatal and adult CDCs in sub-dermal matrigel plugs _____</b>	<b>134</b>
<b>6.1 Introduction _____</b>	<b>135</b>
<b>6.2 Results _____</b>	<b>136</b>
6.2.1 Mouse model of angiogenesis using subcutaneous injection of CDCs _____	136
6.2.2 Investigating the role of neonatal CDCs on <i>in-vivo</i> angiogenesis in subcutaneous matrigel plugs _____	138
6.2.3 <i>In-vitro</i> expression analysis of GFP in P2 neonatal and adult-derived CDCs _____	139
6.2.4 Neonatal CDC transplantation with matrigel-increased microvessel density (MVD) in recipient C57BL/6 mice _____	139
6.2.5 Tracking eGFP <sup>+</sup> neonatal CDCs in the neovasculature of the matrigel _____	143
6.2.6 Investigating the effect of adult-derived CDCs <i>CAG-farnesyl-eGFP</i> preconditioned with normoxia and 3% O <sub>2</sub> on <i>in-vivo</i> angiogenesis using matrigel plug assay _____	144
6.2.7 Adult CDCs led to increased microvessel density (MVD) in subdermal matrigel plugs in recipient C57BL/6 mice and preconditioning CDCs with 3% O <sub>2</sub> enhanced this process _____	146
6.2.8 Tracking GFP positive adult CDCs two weeks following sub-dermal transplantation in matrigel plugs _____	151
6.2.9 CDC <sup>3%O<sub>2</sub></sup> matrigel implants showed more cytoplasmic protrusions than the other groups _____	155
6.2.10 Perfusion analysis of microvasculature formed by adult CDCs cultured in normoxia and 3% O <sub>2</sub> within subdermal matrigel plugs _____	159
<b>6.3 Discussion _____</b>	<b>161</b>
6.3.1 MVD analysis of P2 neonatal CDCs in the matrigel plug angiogenesis assay _____	161
6.3.2 <i>In-vivo</i> angiogenesis with adult CDCs _____	162
6.3.3 eGFP and CD31 co-expression in matrigel plugs implanted with adult CDCs. _____	164
6.3.4 Assessing eGFP and CD11b co-expression in matrigel plugs _____	165
6.3.5 CDCs pre-treated with 3% O <sub>2</sub> may enhance connection of new vessels within the matrigel plugs to the host vasculature _____	166
<b>Chapter 7 Final discussion and future directions _____</b>	<b>169</b>
<b>References _____</b>	<b>177</b>



## **List of figures**

Figure 1-1. The cellular composition of the heart and the coronary arteries. _____	3
Figure 1-2 Three different phases of infarct healing in a mouse cardiac reperfusion model. _____	6
Figure 1-3 Schematic representation of CF function. _____	7
Figure 1-4 A schematic illustration of End-MT process in tissue fibrosis. _____	9
Figure 1-5 Origin of CFs in physiological and pathological heart tissue. _____	11
Figure 1-6 Schematic representations of vasculogenesis and two types of angiogenesis.. _____	13
Figure 1-7 Schematic representation of three stages of CDC culture. _____	19
Figure 1-8 Electron microscopic analysis of human Csph _____	20
Figure 1-9 Oxygen quenching in a rat MI model,. _____	25
Figure 1-10 Hif-1 $\alpha$ regulation in Normoxia and Hypoxia. _____	26
Figure 3-1 Different stages of Csph and CDC culture. _____	52
Figure 3-2 The effect of 3% O <sub>2</sub> on different stages of CDC culture. _____	53
Figure 3-3 3% O <sub>2</sub> increases EDC outgrowth from neonatal cardiac explants _____	54
Figure 3-4 Hif-1 $\alpha$ protein stabilization in passage 2 neonatal CDCs _____	55
Figure 3-5 Evaluating the effect of 3% O <sub>2</sub> on total cell count and viability _____	56
Figure 3-6 The effect of 3% O <sub>2</sub> on the clonogenicity of passage 2 neonatal CDCs. _____	57
Figure 3-7 qRT-PCR experiments showing gene expression levels ( $\Delta$ Ct) in neonatal CDCs _____	61
Figure 3-8 Flow cytometric analysis of murine neonatal CDCs _____	64
Figure 4-1. Evaluating explant productivity and Csph yield. _____	77
Figure 4-2 Hif-1 $\alpha$ protein stabilization in adult passage 2 CDCs _____	79
Figure 4-3 The effect of 3% O <sub>2</sub> on Adult CDC clonogenicity. _____	80
Figure 4-4 Evaluating adult passage 2 CDC total cell viability and cell count _____	81
Figure 4-5 Gene expression changes in adult CDCs at passage 2 _____	84
Figure 4-6 The level of Vegf protein in supernatant of adult P2 CDCs _____	86
Figure 4-7 Sca-1 <sup>+</sup> and cKit <sup>+</sup> adult CDCs, at passage 2 _____	88
Figure 4-8 Flow cytometric analysis of murine adult CDCs at passage 2 _____	89
Figure 4-9 Flow cytometric analysis of P2 and P4 adult CDCs _____	91
Figure 5-1 Schematic representation of Cre-mediated recombination _____	100
Figure 5-2 Co-expression of eYFP and collagen 1 _____	102
Figure 5-3 Immunofluorescent staining of healthy hearts (n=6) with FSP1/eYFP, vimentin/eYFP ____	103
Figure 5-4 Immunofluorescent staining of healthy atria with FSP1 or vimentin _____	104
Figure 5-5 Immunofluorescent staining of remote myocardium _____	106
Figure 5-6 Auto fluorescent background elimination _____	107
Figure 5-7 Evaluation of the autofluorescence in the border zone _____	108
Figure 5-8 Co localisation of FSP1 or vimentin with eYFP _____	109
Figure 5-9 eYFP expression in EDCs and Csphs _____	116
Figure 5-10 eYFP expression in Csphs derived from _____	117
Figure 5-11 Evaluating the potential of eYFP <sup>+</sup> versus eYFP <sup>-</sup> EDCs. _____	119
Figure 5-12 eYFP <sup>+</sup> , eYFP <sup>+</sup> Sca-1 <sup>+</sup> and eYFP <sup>+</sup> cKit <sup>+</sup> cells in P2 CDCs _____	121
Figure 5-13 The proportion of Sca-1 <sup>+</sup> and cKit <sup>+</sup> CDCs which express eYFP _____	122
Figure 5-14 The effect of cell passage on eYFP expression in P2 and P4 CDCs. _____	123
Figure 6-1 Schematic depicting different stages of in-vivo angiogenesis _____	137

Figure 6-2 Assessing the viability of neonatal CDCs after passing through an insulin syringe _____	138
Figure 6-3 In-vitro expression of eGFP in passage 2 CDCs _____	139
Figure 6-4 Angiogenesis in subdermal matrigel plugs seeded with neonatal CDCs. _____	141
Figure 6-5 Fluorescent staining of GFP and CD31 in matrigel plugs _____	144
Figure 6-6 eGFP expression in matrigel plugs _____	145
Figure 6-7 The level of Vegf protein supernatant of adult P2 CDCs _____	147
Figure 6-8 Angiogenesis in matrigel plugs seeded with adult atrial CDCs, _____	149
Figure 6-9 Majority of eGFP positive adult CDCs do not express the vascular marker CD31. _____	152
Figure 6-10 GFP positive adult CDCs do not co-express $\alpha$ -SMA _____	153
Figure 6-11 eGFP and CD31 co-expression analysis. _____	154
Figure 6-12 Cytoplasmic protrusions _____	156
Figure 6-13 The assessment of immune response within the matrigel plugs. _____	157
Figure 6-14 Pre-treatment of adult CDCs with 3% O <sub>2</sub> has a limited effect on the in-vivo perfusion _____	160

## **List of tables**

Table 1-1 Frequently used terminology and the relative oxygen level. Table is adapted from [90].	25
Table 2-1 Primer details used for genotyping.	35
Table 2-2 PCR program steps for genotyping mouse lines.	36
Table 2-3 Antibodies used for immunofluorescent cell staining.	38
Table 2-4 The primary (Rat antibodies) and secondary antibodies used to immunophenotype CDCs.	40
Table 2-5 The list of primers used for qRT-PCR analysis	42
Table 2-6 Primary and secondary antibodies used to stain cryosections	46
Table 2-7 The combination of antibodies used in double immunofluorescent staining experiments.	46
Table 3-1 The summary of three independent clonogenicity assays.	58
Table 3-2 Summary of the Ct values from four candidate housekeeping genes	59
Table 3-3 The effect of 3% O <sub>2</sub> on the expression of Sca-1, cKit, Abcg2, Eng and Vegf	62
Table 3-4 Summary of 3 independent FACS analysis	65
Table 4-1 Summary of three independent clonogenicity experiments	80
Table 4-2 Summary of three independent analyses of proliferation and cell viability	82
Table 4-3 Time-course analysis of the effect of 3% O <sub>2</sub> on gene expression	85
Table 4-4 Summary of 3 independent FACS analyses	90
Table 4-5 A summary of three independent flow cytometric	91
Table 5-1 Quantification of eYFP, FSP1 and vimentin expressing cells	104
Table 5-2 (A) The mean proportion of FSP1 and eYFP expression	110
Table 5-3 (A) The mean proportion of vimentin and eYFP	111
Table 5-4 Evaluating the efficiency of Col1a2 CreERT; Rosa26-floxed STOP eYFP transgenic mice	113
Table 5-5 A summary of three independent FACS experiments for eYFP, Sca-1 and cKit	121
Table 6-1 Summary of MVD assessment	143
Table 6-2 Number and type of cells injected with matrigel plugs in adult CDC	146
Table 6-3 Summary of MVD assessment	151
Table 6-4 The summary of immune response assessment with CD11b expression	158

## **List of Abbreviations**

AML	Acute myeloid leukaemia
ADSCs	Adipose derived stem cells
Ang 1	Angiopoietin 1
Ang 2	Angiopoietin 2
ARNT	Aryl Hydrocarbon Nuclear Translocator
Abcg2	ATP-binding cassette sub-family G member 2
bFGF	Basic fibroblasts growth factor
$\alpha$ -SMA	$\alpha$ smooth muscle actin
BMC	Bone marrow cells
BSA	Bovine serum albumin
CFs	Cardiac fibroblasts
CSCs	Cardiac stem cells
CLK	Cardiosphere derived cells, Lin-/cKit+
CGM	Cardiosphere Growth Medium
Csphs	Cardiospheres
CDCs	Cardiosphere derived cells
CXCR4	Chemokine receptor 4
CD45	Cluster of differentiation 45
CEM	Complete Explant Medium
CHD	Coronary heart disease
CDKIs	Cyclin-dependent kinase inhibitors
DAB	3,3'-diaminobenzidine tetrahydrochloride
DH <sub>2</sub> O	Distilled water
DMEM	Dulbecco's modified Eagle's medium
DNA	Deoxyribonucleic acid
dNTPs	Deoxyribonucleotide triphosphate
DEPC	Diethylpyrocarbonate
DDR2	Discoidin domain receptor
ESCs	Embryonic stem cells
ECs	Endothelial cells
EGF	Epidermal growth factor
End-MT	Endothelial- mesenchymal transition
EPCs	Endothelial progenitor cells

ELISA	Enzyme Linked Immunosorbent Assay
EPDC	Epicardial derived cells
EMT	Epithelial-mesenchymal transition
Eng	Endoglin
EDTA	Ethylene-diamine-tetra-acetic acid
EDCs	Explant derived cells
ECM	Extracellular matrix
Erk	Extracellular signal-regulated kinases
FACS	Fluorescent activated cell sorting
FIH	Factor-inhibiting HIF-1 $\alpha$
Flk1	Fetal liver kinase-1
FGF-2	Fibroblast growth factor 2
FITC	Fluorescein isothiocyanate
FSP1	Fibroblast specific protein 1
FST	Fine Science Tools
FSS	Fluid shear stress
GLUT1	Glucose transporter 1
GCPs	Glycolytic cardiac progenitors
GFP	Green fluorescent protein
HSCs	Hematopoietic stem cells
HDAC2	Histone deacetylase 2
hCMPCs	Human cardiomyocyte progenitor cells
HMSCs	Human mesenchymal stem cells
Hif-1 $\alpha$	Hypoxia inducible factor- 1- $\alpha$
Hif-2 $\alpha$	Hypoxia inducible factor- 2- $\alpha$
Hif-3 $\alpha$	Hypoxia inducible factor- 3- $\alpha$
Hif-1 $\beta$	Hypoxia inducible factor- 1- $\beta$
HRE	Hypoxia-response-element
iPSCs	Induce pluripotent stem cells
iPDGF	Including platelet-derived growth factor
IDT	Integrated DNA Technologies
IL-1 $\beta$	Interleukin-1 $\beta$
IMG	Intussusceptive microvascular growth
LVEF	Left ventricular ejection fraction

MMP	Matrix metalloporinase
MAPK	Mitogen-activated protein kinase
MCP-1	Monocyte chemoattractant protein 1
MI	Myocardial infarction
MLECs	Mouse lung endothelial cells
mRNA	Messenger RNA
NSC	Neural stem cell
PBS	Phosphate buffered saline
PCR	Polymerase chain reaction
PECAM-1	Platelet and endothelial cell adhesion molecule-1
PFA	Para-formaldehyde
PHD	Prolyl hydroxylase domain
PKB	Protein kinase B
qRT-PCR	Quantitative reverse transcription polymerase chain reaction
RTK	Receptor tyrosine kinase
RNA	Ribonucleic acid
Sca-1	Stem cell antigen
SCID	Severe combined immunodeficiency
SD	Standard deviation
STR	Short tandem repeat
SP	Side populations
SDF-1	Somatic cell-derived factor-1
SSEA-1	Stage-specific embryonic antigen 1
SF	Stem cell factor
SCPIO	Stem Cell Infusion in Patients with Ischemic Cardiomyopathy
TAE	Tris-acetate EDTA
TIMP	Tissue inhibitor of metalloproteinase
TGF- $\beta$	Transforming growth factor - $\beta$
TNF- $\alpha$	Tumour necrosis factor- $\alpha$
VEGF	Vascular endothelial growth factor
VHL	Von Hippel–Lindau
YFP	Yellow fluorescent protein

# **Chapter 1 Introduction**

## **1.1 The heart**

The mammalian heart is composed of four chambers, two atria and two ventricles. The role of the right atrium is to collect blood from the body and pump it to the right ventricle then the right ventricle pumps the blood to the lungs. When the blood is oxygenated in the lungs it returns to the left atrium. From there the blood goes into the left ventricle, and is pumped through the aorta to all the body. In order to generate the proper blood flow within the heart, cardiac valves including tricuspid valve (between the right atrium and ventricle), mitral valve (between the left atrium and ventricle), pulmonary valve (between the right ventricle and the pulmonary artery) and finally the aortic valve are present[1].

The cardiac skeleton is a very dense connective tissue, mainly composed of collagen, and has three main roles: (i) to maintain the atrial and ventricular structure; (ii) to anchor the four valves of the heart and (iii); to electrically insulate the ventricles from the atria. Each heart beat is an electrical impulse which is generated from specialised myocardial cells located in the sinoatrial (SA) node located in the groove where the superior vena cava meets the right atrium. Cells in this region are smaller than ordinary cardiac muscle cells and have the ability to spontaneously depolarise and conduct the electric impulses through the other cardiac regions[1].

### **1.1.1 Vasculature of the heart**

Anatomically, human heart has two main coronary arteries, originating from the aorta. The left main coronary artery (LM) originates from the left coronary sinus of the aorta and forms the left anterior descending coronary artery (LAD) and left circumflex coronary artery (LCX). The right coronary artery (RCA) originates from the right coronary sinus of aorta and gives three branches; proximal, mid, and distal. The coronary venous system is variable, but generally in humans there are two cardiac veins; the great cardiac vein (GCV) and the middle cardiac (MCV) vein. The GCV runs in parallel with the LAD and then courses superiorly, crossing the LCX and posteriorly draining into the coronary sinus. This vascular system is responsible for circulating blood to the heart muscle [1]. Figure 1-1 depicts schematically the coronary arteries and their branches.



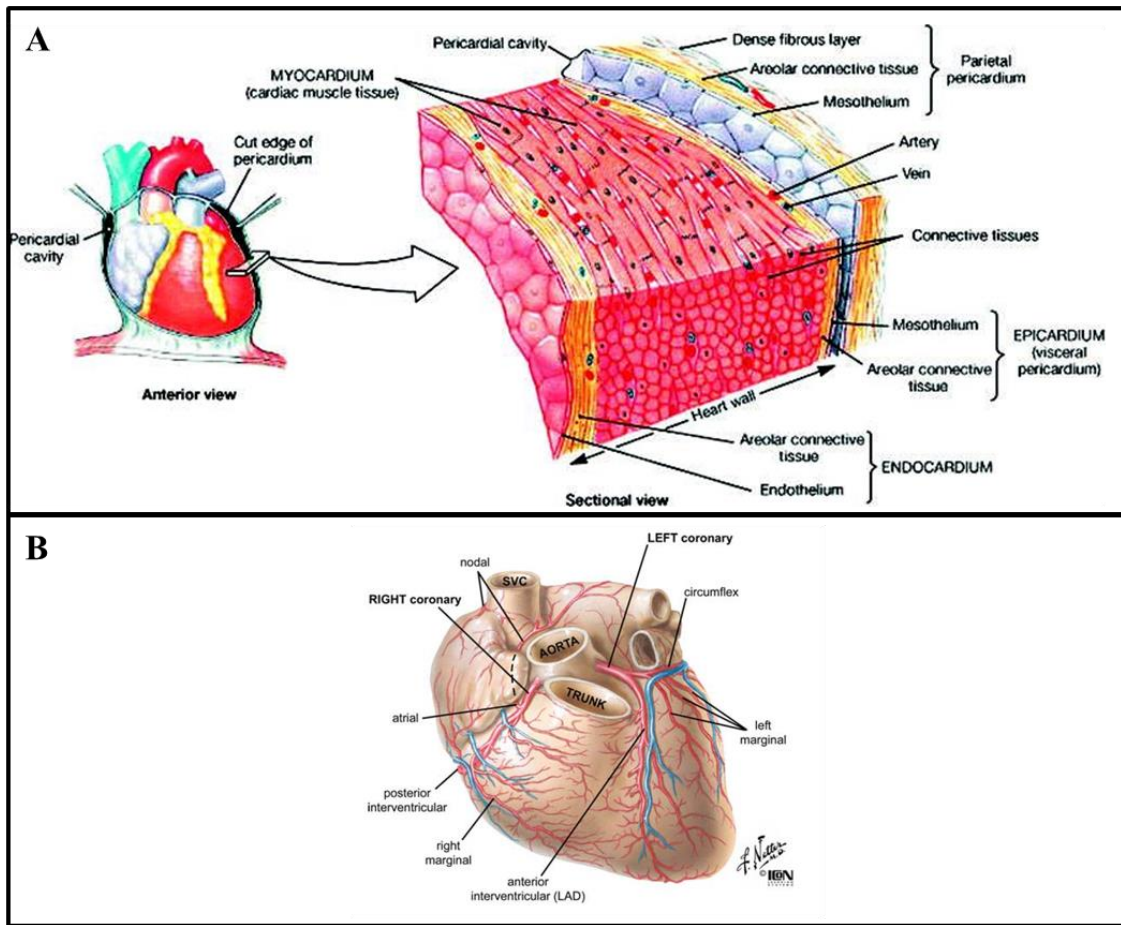


**Figure 1-1. The cellular composition of the heart and the coronary arteries.** A) shows a cross section through the myocardium. The heart contains three layers: (i) the epicardium, (ii) the myocardium composed of cardiomyocytes, connective tissue, blood vessels and non-cardiomyocyte cells; (iii) the inner endocardium. Note that non-cardiomyocyte cellular fraction of the heart contains: cardiac fibroblast, endothelial cells, vascular smooth muscle cells, immune cells and stem cells. The communication between all cell types within the heart is an important aspect in order to maintain cardiac homeostasis and its electrophysiological actions. B) shows the vascular supply to the heart with left and right coronary arteries and their branches. The image is adapted from [1].

### 1.1.2 Cellular composition of the heart

In a normal healthy heart, its cellular components interact in a fashion to respond to developmental, homeostatic, and pathological stimuli. The main cellular components that make up the heart include cardiomyocytes, cardiac fibroblasts (CFs), endothelial cells (ECs), and vascular smooth muscle cells (VSMCs), with the majority being CFs and cardiomyocytes. Transient cell populations of the heart include; lymphocytes, mast cells, and macrophages, which can interact with permanent cell types to affect cardiac

function. The adult heart also contains a limited number of cardiac stem cells which express stem cell markers such as; cKit and Sca-1 and are able to differentiate into different cell types. It has also been observed that there are significant differences in the makeup of the cardiac cell populations between the species, this could be important when examining myocardial remodelling. Current dogma claims that fibroblasts makes up the largest cell population of the heart; however, this appears to vary for different species, for example in mice and rats. However the cell composition of the heart maintains the electrical and biomechanical responsive reactions of the organ as well as the three-dimensional structure through autocrine, paracrine, and cell-cell interactions reviewed in [7]. Interruption of these interactions via cardiac remodelling can cause interference in this system leading to pathological conditions.

## **1.2 Coronary heart disease and myocardial infarction**

Acute myocardial infarction (MI) is a persistent public health issue and coronary heart disease (CHD) is the main cause of death in the UK (British Heart Foundation, 2012 statistics). MI is the most common and clinically significant form of acute cardiac injury, which results in significant cardiomyocyte death. The underlying cause of MI is coronary atherosclerosis, and MI frequently happens as a result of an acute rupture of an atherosclerotic plaque. Following infarction a complex cascade of myocardial responses happen which are reviewed by Frangogiannis [8] (2008), but will be briefly discussed here. Infarct healing consists of three phases: (i) inflammatory phase, (ii) proliferative phase and (iii) maturation phase (Figure 1-2). In the inflammatory phase, the injured tissue secretes chemokine and cytokine cascades that result in recruitment of neutrophils and macrophages to clear the necrotic debris. Activated macrophages release some cytokines and growth factors which then increase vascularization of the infarct region. Then at the proliferative stage the expression of pro-inflammatory mediators is reduced, and fibroblasts and endothelial cells (ECs) proliferate. Inflammatory leukocytes secrete a variety of cytokines which activate fibroblasts to form extracellular matrix (ECM). After myocardial infarction, the environment of the scar region draws further development of fibroblasts into myofibroblasts. For instance, Willems *et al.* (1994) showed that some interstitial cells within the human myocardial infarct regions express alpha-smooth muscle actin ( $\alpha$ SMA), and vimentin. The authors used electron microscopy and showed that these cells have features of myofibroblasts [9].

Desmoulière *et al.* (1993) showed that the subcutaneous administration of transforming growth factor-beta 1 (TGF- $\beta$ 1) to rats results in enhanced  $\alpha$ -SMA expression in the granulation tissue. Furthermore administration of TGF- $\beta$ 1 also increases  $\alpha$ -SMA expression at mRNA and protein level in the *in-vitro* fibroblast culture [10]. As the human heart has negligible cardiac regenerative potential, the fibrotic scar is permanent and significantly reduces the cardiac output. Therefore, to understand myocardial remodelling post-MI, it is valuable to address cardiac fibrosis and the cellular content of this event.

There is some evidence which show that following MI, different cytokines and growth factors are produced, which cause different structural and functional changes. For instance, interleukin-1 $\beta$  (IL-1 $\beta$ ) and tumour necrosis factor- $\alpha$  (TNF- $\alpha$ ) result in decreased expression of collagen and enhance matrix metalloproteinase (MMP) expression in the *in vitro* culture of rat-derived cardiac fibroblasts [11]. It has been shown TGF- $\beta$ /Smad3 signaling is activated in healing infarcts and induces fibrotic remodeling of the infarcted hearts. For instance Dobaczewski *et al.* (2010) showed that Smad3 Null murine infarcts had higher number of proliferating myofibroblast ( $\alpha$ -SMA<sup>+</sup> / Ki67<sup>+</sup>) than wild type infarcts after 72 hours of reperfusion[12]. Angiogenic factors such as vascular endothelial growth factor (Vegf) and basic fibroblast growth factor (bFGF) are enhanced significantly and initiate neo-vessel formation. In this respect, Fukuda *et al.* (2004) showed a marked increase in arteriolar density of the hearts of rat MI models (+ischemic preconditioning with 4 repetitive coronary artery banding) at 7, 14 and 21 days after MI when compared to the control groups; further investigations showed that the level of Vegf protein was significantly higher in MI + ischemic preconditioning models versus the control groups [13]. Hif-1 $\alpha$  overexpression in the murine heart resulted in attenuated infarct size and improved cardiac function 4 weeks post MI; furthermore, over expression of Hif-1 $\alpha$  increased Vegf expression and capillary density in peri-infarct and infarct regions in the hearts of constitutive Hif-1 $\alpha$  expressing animals versus control mice [14].

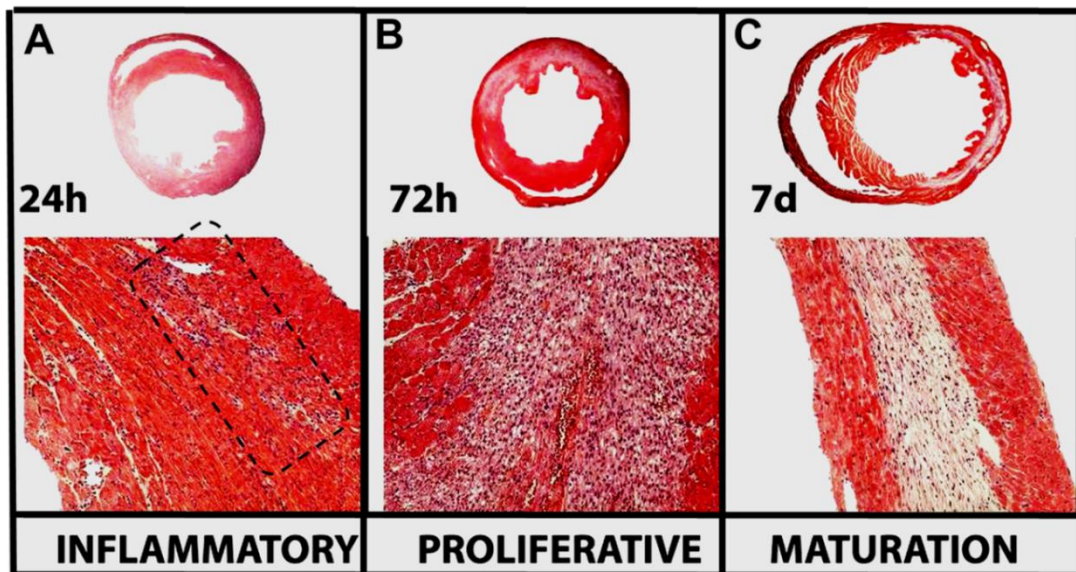


**Figure 1-2 Three different phases of infarct healing in a mouse cardiac reperfusion model.** Top panel is depicting fibrosis and ventricular atrophy of the infarct region during three phases of infarct healing. (A) During the inflammatory phase, chemokines and cytokines are induced in the infarct and marked leukocyte infiltration is noted (highlighted in the box). In this phase dead cells and matrix debris are cleared by neutrophils and macrophages. (B) Activated macrophages release angiogenic cytokines and growth factors and the number of fibroblasts, endothelial cells and extra cellular matrix (ECM) increases dramatically. (C) During the maturation phase macrophages and fibroblasts apoptose and the collagen scar stabilises. The image is adapted from [8].

### 1.3 CF morphology and functions

The characteristic of cardiac fibroblasts (CFs) is a challenging topic and several articles have reviewed CFs in detail [15-18]. Here some important facts about CFs are discussed. CFs are defined as mesenchymal derived cells which produce collagen I, III and VI and associate directly with ECM. Morphologically, they all lack a basement membrane with spindle-shaped and multiple cytoplasmic processes emanating from the main cell with a speckled nucleus that typically has 1 or 2 nucleoli, reviewed in [15,16]. In general, fibroblasts are believed to be phenotypically heterogeneous based on morphology, collagen production, glycogen reservoirs and expressing fibroblast markers. For instance, gene array analysis has shown extreme diversity in the pattern of gene expression in 50 fibroblast cell cultures [19].

Resident CFs are quiescent, and become active and proliferative by signalling molecules that are produced due to a cardiac injury. CFs are involved in different cardiac functions such as the production of cytokines and growth factors, cell proliferation, apoptosis, cardiomyocyte hypertrophy, ECM homeostasis, cell-to-cell

junctions with cardiomyocytes, conduction of electrical features of heart, cardiac remodelling, and angiogenesis reviewed in [18]. Figure 1-3 shows the different functions in which CFs are involved.

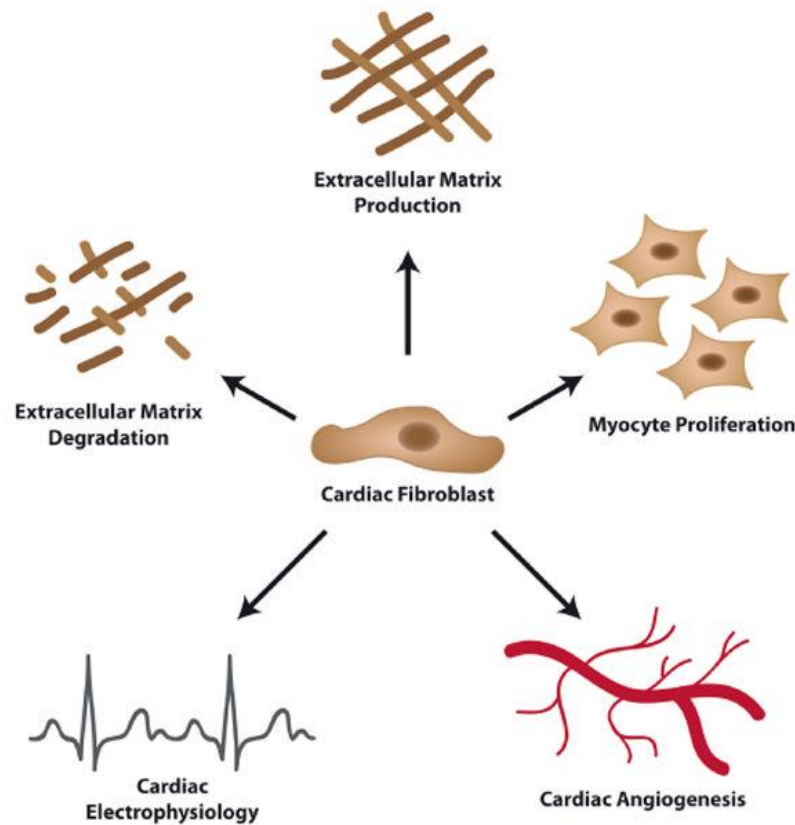


**Figure 1-3 Schematic representation of CF function.** CFs produce different growth factors and cytokines in order to produce or degrade ECM components such as collagen I and III, and fibronectin. They may also promote cardiomyocyte proliferation, angiogenesis and cardiac electrophysiology. The image is adapted from [17].

### 1.3.1 Origin and heterogeneity of CFs

During embryonic life, interstitial CFs are derived from different origins. For instance, fibroblasts within the cardiac interstitium and the annulus are derived from mesenchymal cells of the embryonic pro-epicardium [20], which migrate over the embryonic heart and make the epicardium. Epicardial cells under the influence of growth factors, including platelet-derived growth factor (PDGF), FGF and TGF- $\beta$ , undergo epithelial-mesenchymal transition (EMT) to form epicardium-derived cells (EPDC). These cells then further differentiate into fibroblasts and other cardiac cell types [21]. In addition to interstitial CFs, valvular fibroblasts are derived from the

cardiac endocardium during embryonic life, through a process called endothelial-mesenchymal transition (End-MT) [22].

### **1.3.2 CF markers**

The limitation and the specificity of different fibroblast markers have been extensively discussed in the following reviews [15,23,24]. For instance, the discoidin domain receptor (DDR2), which is expressed in the majority of CFs, is a collagen receptor and mediates a wide range of cellular functions, such as migration, growth and differentiation. In fact, 26% of the cellular content of murine hearts are DDR2-expressing cells [25]. Fibroblast specific protein 1 (FSP1), also known as S100A4, is also proposed to be a discriminative marker for fibroblasts. However, the validity of this marker has been questioned as FSP1 expression has been reported in a variety of other cell types such as leukocytes and cancer cells. In addition, not all CFs express FSP1. Vimentin also has been used widely to detect CFs but this marker is also expressed in endothelial cells and mesenchymal cells. Other markers such as periostin, fibronectin and connexin 40 (expressed in fibroblast-to-fibroblast boundaries) or connexin 45 (expressed in fibroblast-to-myocyte boundaries) have also been shown to be CF markers, and are reviewed in [15,23,24]. Therefore, it seems that the identification of CFs may be more accurate by using a combination of several fibroblast markers in the context of their location and the physiological or pathological stages of the heart. Further identification of definitive fibroblast-specific markers will be necessary to better understand this heterogeneous cell type of the heart.

### **1.3.3 Origins of CFs in cardiopathy**

As mentioned above the lack of a robust CF specific marker makes CF studies difficult and, due to the variability among lineage-tracking tools, it is believed that there are multiple sources of CF. Specially, following cardiac injury several mechanisms and origins have been shown to be involved in CF composition in the heart.

### 1.3.3.1 Endothelial-mesenchymal transition (End-MT)

As discussed above End-MT happens during cardiac development, however Zeisberg *et al.* (2007) used an aortic banding model to determine the role of End-MT in cardiac fibrosis [26]. The authors performed aortic banding in *Tie1Cre;R26R-stop-lacZ* adult mice and showed the expression of *LacZ* positive staining throughout the fibrotic region, whereas in the normal hearts *LacZ* expression was detected in blood vessels associated with endothelial cells [26]. Transition of endothelial cells into fibroblasts happens when endothelial cells are targeted by specific stimuli such as TGF- $\beta$  ligands. TGF- $\beta$  ligands mediate End-MT through the activation of the Snail family of transcription repressors which depends on Smad, MEK, PI3K and p38 MAPK activation, reviewed in [27]. Widyantoro *et al.* (2010), showed that diabetes mellitus–induced cardiac fibrosis is associated with the emergence of fibroblasts from EC due to End-MT process, triggered by endothelin-1 (ET-1) [28]. These data suggest the distinct origins of CFs in physiological and pathological conditions. Figure 1-4 represents the schematic process of End-MT in tissue fibrosis.

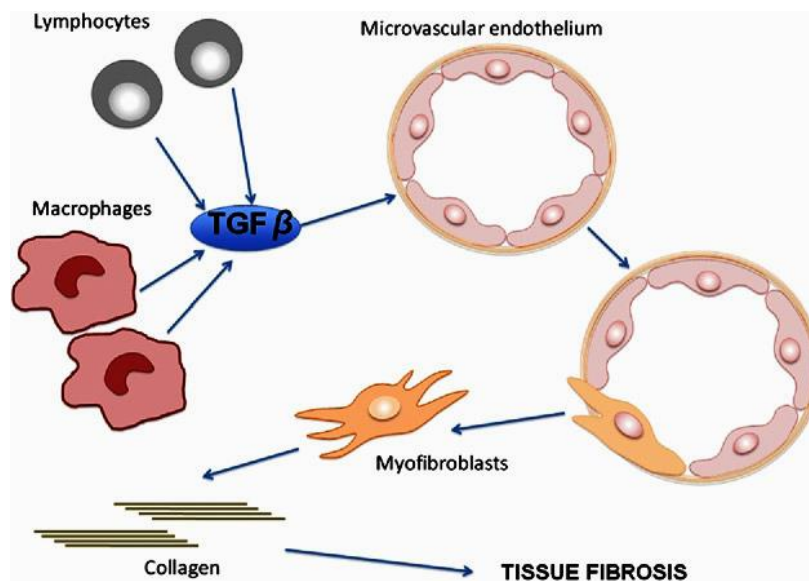


**Figure 1-4** A schematic illustration of End-MT process in tissue fibrosis. TGF- $\beta$  secretion by tissue-infiltrating inflammatory cells, such as lymphocytes and macrophages, triggers the transition of endothelial cells into myofibroblasts and then leads to the accumulation of myofibroblasts within the fibrotic tissue. The image is adapted from [29].

### 1.3.3.2 Bone-marrow-derived CFs

Van Amerongen *et al.* (2008) studied the quantitative and functional aspects of bone marrow-derived (BMD) myofibroblasts in myocardial scar formation and showed that following the transplantation of GFP-labelled or mismatched bone marrow (BM) cells, significant numbers of donor BM cells were observed in the fibrotic scar of the recipient hearts post-MI [30]. An interesting study compared the autopsy samples from male patients who had received a female donor heart with samples from such patients who developed MI after transplantation. They showed that in the fibrotic areas of MI about  $24.1 \pm 6.5\%$  of cells carried the Y chromosome, compared to  $5.3 \pm 1.1\%$  of transplanted control patients without infarction [31]. When female mice were transplanted with male donor mice BM, the Y chromosome was detected in 13% of FSP1 and 21% of  $\alpha$ -SMA fibroblasts in aortic-banded heart models, indicating that these CFs are derived from BM [26]. Van Amerongen *et al.* (2008) showed in the recipient mice which had undergone GFP<sup>+</sup> BM transplantation, after myocardial injury, that GFP<sup>+</sup> cells were observed in the fibrotic cardiac region and on average 21% of BMD cells were myofibroblasts which was 15% of the myofibroblast population in the infarct area [30]. However, there is a lot of controversy concerning the role of bone-marrow-derived (BMD) cells in the fibrotic reaction following cardiac injury, whether they are really fibroblasts or really inflammatory cells that are expressing fibroblast markers. In one study of mouse models of fibrotic ischemia/reperfusion cardiomyopathy a population of fibroblasts were identified that were highly proliferative and expressed collagen I and  $\alpha$ SMA, CD34, and CD45 (a hematopoietic marker). These cells represented 3% of all non-myocyte cells [32]. More importantly, van Amerongen *et al.* (2007) used a murine cryo-injury model to induce left ventricular damage and showed that following infiltrating macrophage depletion, the CF population diminished in the infarct region and impaired the wound-healing process and subsequently reduce the heart failure rate [33], which suggest a key role of monocytes in fibrosis following MI. In general, these findings support the idea that hematopoietic stem cells and epicardium-derived cells are important sources of CF turnover in different regions of the adult heart and CFs are likely to have distinct sources in physiological and pathological states of the heart.



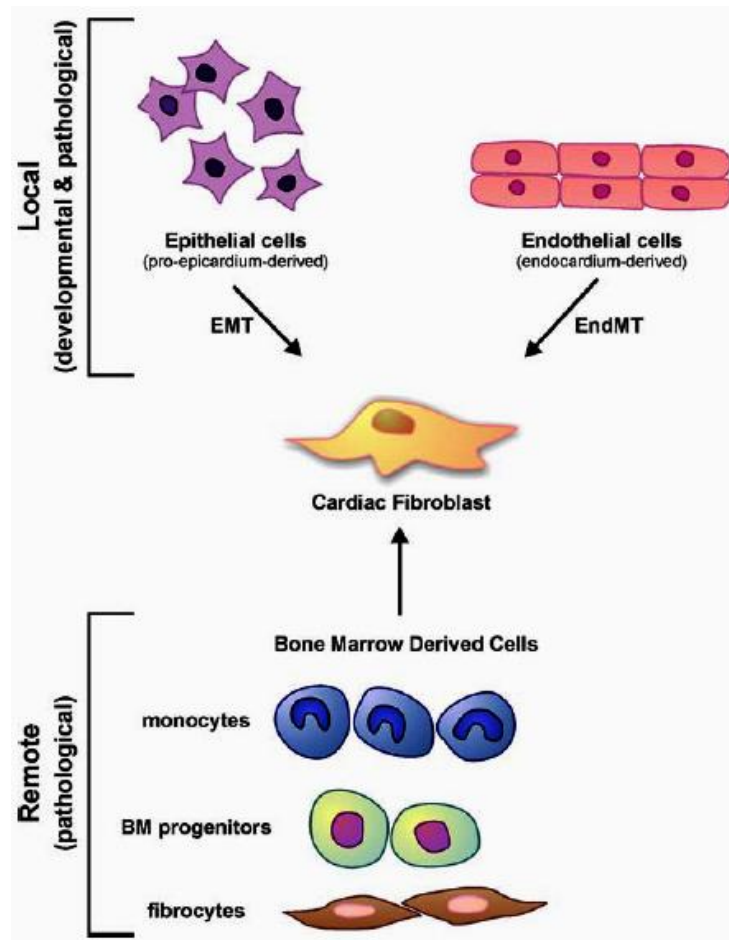


**Figure 1-5 Origin of CFs in physiological and pathological heart tissue.** EMT and End-MT are believed to be the two main sources of CFs during embryonic development. Proepicardial cells form interstitial fibroblasts through EMT, and End-MT is responsible for valvular fibroblast differentiation from endothelial cells. However, following cardiac injury CF recruitment occurs due to cell plasticity and pro-fibroblasts are mainly derived from endothelial or epithelial cells through EMT and End-MT. Other cell types such as monocytes, circulating-BM progenitors, pericytes and fibrocytes are also proposed to be a source of CFs. Image is adapted from [18].

### 1.3.4 CFs and myocardial remodelling

One of the most significant responses of the injured heart after MI is enhanced angiogenesis of the peri-infarct zone which happens in response to the release of cytokines and growth factors from the infarcted heart. In order to understand the role of angiogenesis in myocardial remodelling, a brief review of vasculogenesis and angiogenesis will be helpful.

## 1.4 Vasculogenesis and angiogenesis

In vertebrates, blood vessel formation is through two distinct processes: 1) vasculogenesis and 2) angiogenesis. In embryonic development the heart and primitive vascular plexus formation is through vasculogenesis which is defined as *de novo* differentiation of mesoderm-derived precursor cells (angioblasts) to endothelial cells. However, vasculogenesis can also happen in adult life when circulating BMD or endothelial progenitor cells (EPCs) contribute to new vessels following injury, reviewed in [34]. Angiogenesis occurs in both development and in adult life. In the embryo, it is the process that remodels a pre-existing primary plexus formed by vasculogenesis into a complex vessel network that supports growth and development of the vertebrate organism reviewed in [34]. Angiogenesis refers to two processes (i) endothelial sprouting and (ii) intussusceptive microvascular growth (IMG) (figure 1-6). The sprouting process involves the degradation of the basement membrane, endothelial cell migration, proliferation and tube formation, in response to a growth factor stimulus such as Vegf. IMG refers to the splitting and growing of vessels by folding of the interstitial tissue pillars into the lumen of the vessel. New vessel formation is supported by pericytes, vascular smooth muscle cells and the extra-cellular matrix. Neighbouring mesenchymal cells migrate towards the neo-vessel in response to cytokines such as PDGF and then differentiate into vascular SMCs (vSMCs) in response to TGF- $\beta$  signalling, reviewed in [35]. These supporting mechanisms provide a stable environment for new vessels to develop.

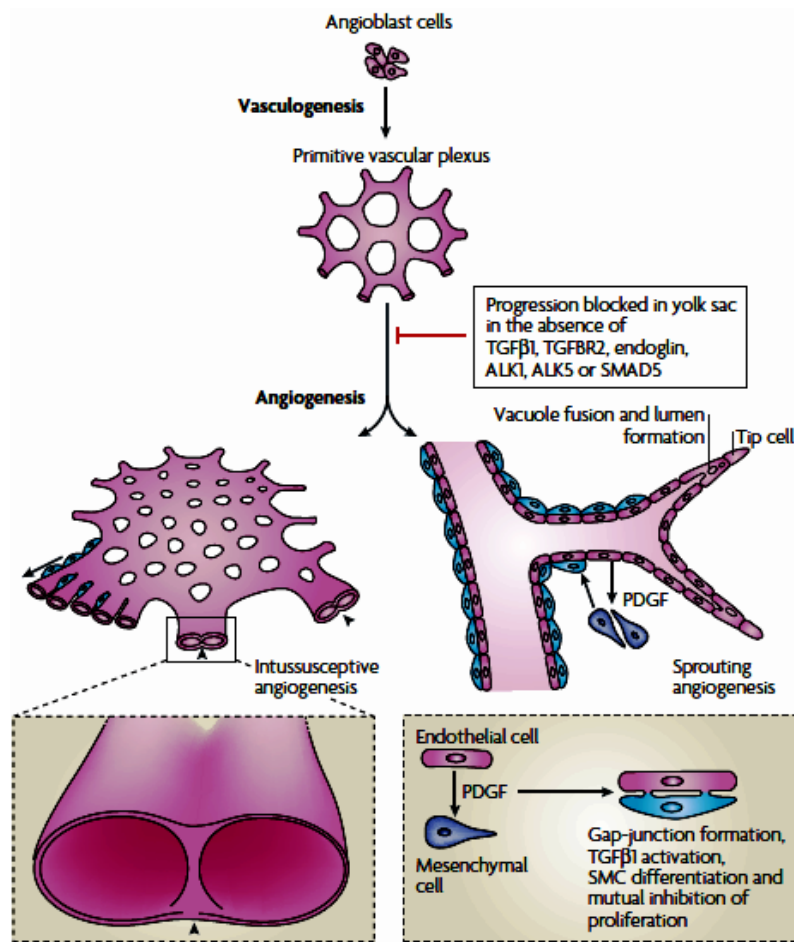


**Figure 1-6 Schematic representations of vasculogenesis and two types of angiogenesis.** Vasculogenesis starts with the differentiation of angioblasts to form a primary capillary plexus, which then expands by angiogenesis. In sprouting angiogenesis, ECs proliferate behind the tip cells and form a lumen. Intussusceptive angiogenesis involves the folding of vascular interstitial tissue into the lumen of the vessel. In both mechanisms smooth muscles are required for stabilisation of the nascent vessels: resident mesenchymal cells migrate towards the new vessel in response to platelet-derived growth factor (PDGF) and then differentiate into vascular smooth muscle cells following intimate associations with endothelial cells and the activation of TGF- $\beta$ . The image is modified from [35].

### 1.5 Angiogenesis and its role in cardiac remodelling

During adulthood the majority of blood vessels remain quiescent and angiogenesis is limited to the female reproductive cycle in the placenta during pregnancy. However, ECs retain their angiogenic response to different stimuli, reviewed in [34]. For instance, angiogenesis is reactivated during wound-healing in order to repair tissue damage. But in some disorders angiogenesis changes from a balanced to either an insufficient or an enhanced state. Tumours and related malignancies are examples when angiogenesis has been enhanced. In this respect, new vessels feed the tumours and allow tumour cells to metastasise. On the other hand, insufficient angiogenesis happens when

the level of angiogenesis cannot respond sufficiently well to meet the metabolic demands of the tissue [34].

Arteriogenesis, the process of enlargement and muscularisation of small arterioles, can happen following stenosis or occlusion of a major artery, and leads to enhanced reperfusion capacity of the injured tissue by acting as an alternative blood perfusion route. Scholz *et al.* (2000) investigated the structural and molecular histology of growing collateral arteries that develop after femoral artery occlusion in rabbits between 2 hours to 240 days. They showed that arteriogenesis starts with arteriolar thinning, followed by the proliferation of ECs and smooth muscle cells (SMCs). Interestingly, these cellular modifications happen quickly as EC and SMC division start 24 hours after artery occlusion. Expression of the adhesion molecules such as intercellular adhesion molecule-1 (ICAM-1) and vascular cell adhesion molecule-1 (VCAM-1) is enhanced after 12 hours [36]. Physical stimuli such as increasing blood pressure or fluid shear stress (FSS) have been shown to be a possible stimulator for arteriogenesis through the activation of ECs. In this respect, Scholz *et al.* (2000) showed the effect of *in vitro* FSS in cultured ECs which increased the expression of ICAM-1 and VCAM-1 between 2 h and 6 h after shear onset [36]. However, the healing processes with consequent angiogenic and arteriogenic responses are frequently insufficient to protect the myocardium from ischemic disease, which results in cardiomyocyte apoptosis and tissue necrosis. Hence therapeutic angiogenic strategies have the potential to improve myocardial function following MI.

### **1.5.1 Therapeutic angiogenic therapies in myocardial infarction**

The urgent treatment for the infarcted myocardium is to restore the blood flow via angioplasty combined with medical treatment to stabilise the patient. This method is able to overcome the cause of the infarction which is coronary artery occlusion and has led to a major improvement in patient survival. However angioplasty can lead to ischemia/reperfusion injury that is associated with EC apoptosis and loss of the local microcirculation. Therefore, much research has focussed on promoting angiogenesis in order to improve current treatments and decrease the level of cardiac injury in MI patients. Three main therapeutic routes, namely gene, protein and cell therapies, have been introduced. However, pro-angiogenic strategies with genes and proteins such as

Vegf and FGF resulted in limited and unstable success, probably due to their short half-lives. Using angiogenic cytokines, although they activated rapid neo-vessel formation in MI models, the newly formed vessels were fragile and failed to anastomose with the coronary circulation properly [37]. Therefore, therapeutic angiogenesis with cells such as relevant progenitor cells could potentially provide a prolonged effect, because progenitor cells have been shown to be able to differentiate into vascular and cardiomyocytes. Furthermore, the transplanted cells are able to secrete growth factors which could activate paracrine mechanisms and help to stimulate host angiogenic cells to form new vessels. Several stem/progenitor cells have been used in order to assess their pro-angiogenic potential following cell transfer. BMDs, embryonic stem cells (ESCs), induced pluripotent stem cells (iPSCs), skeletal cells and adipose-derived stem cells (ADSCs) have been used in myocardial infarct models; although some improvements have been reported, the optimal cell therapy is remains uncertain. BMD cells are the most widely used cells in clinical trials for myocardial repair. They are autologous, so no need for immunosuppression. However, in a clinical trial study with 200 patients which received BM cells after acute MI, the results showed very limited improvement of the left ventricular ejection fraction (LVEF) and did not have any obvious long term benefit [38]. It has been shown that the efficiency of BMC transplantation in old patients, diabetics and advanced cardiovascular disease is considerably reduced [39,40].

## **1.6 Cardiac stem cells (CSCs)**

Recent studies have shown that the mammalian adult heart has regeneration potential [41-44] so the heart is in principle capable of regeneration. CSCs have been isolated from adult human and different animals and are classified based on expression of stem cell markers such as Sca-1<sup>+</sup> (stem cell antigen), cKit<sup>+</sup> (CD117, the receptor of stem cell factor) Abcg2<sup>+</sup> or a side population (a population of progenitors which are able to efflux Hoechst dye) and Isl1<sup>+</sup> (an embryonic cardiac progenitor). Bearzi *et al.* (2007) isolated cKit<sup>+</sup> hCSCs from samples of human myocardium and showed that these cells have the ability to form functionally competent human myocardium after delivery to the infarcted heart of immunocompromised mice and rats. These stem cells were self-renewing, clonogenic, and multipotent. They also were able to differentiate into cardiomyocytes and occasionally into SMCs and ECs [45]. However, it has been shown

that the number of CSCs in the myocardium is relatively low which could explain that why the heart is unable to repair itself sufficiently following ischemic disease. The quantitative data have shown that on average there is 1 CSC per 18,000 myocytes in dog hearts [46]. Urbanek *et al.* (2005) studied the hearts from patients who died due to infarction, and hearts from patients who underwent cardiac transplantation after MI. The quantification of CSC showed that there were 40,000 CSCs per cm<sup>3</sup> of tissue in the border zone region and less than 20,000 per cm<sup>3</sup> in the remote region [47]. The true origin of CSCs is an interesting topic. For instance, it is possible that cKit<sup>+</sup> expressing CSCs might have originated from extra cardiac tissue, as HSCs including cKit<sup>+</sup> cells are shown to leave BM to the other extra myeloid organs [48]. Lineage tracing of cardiomyocytes from heart transplant patients showed that endothelial and cardiomyocytes derived from the recipient have been reported within the donor heart which suggests the possibility of the recipient cells' synchronisation with the donor heart [49].

As discussed above, CSCs are classified based on their superficial stem cell markers. In this thesis I used Sca-1 and cKit to characterise cardiosphere derived cells (CDCs), so it is useful to consider Sca-1, cKit and Abcg<sub>2</sub> in more detail.

### **1.6.1 Stem cell antigen-1 (Sca-1)**

Sca-1 is a common marker for murine hematopoietic stem cells (HSCs), and is used to isolate pure populations of HSCs. Sca-1 is a member of Ly-6 gene superfamily with diverse functions. Its expression in HSCs seems to be a subject to strain bias. For example, all HSCs in *Ly6.2* strains such as C57BL/6 are Sca-1 positive [50], whereas 25% of HSCs in *Ly6.1* strains such as BALB/c express Sca-1 [51]. Sca-1 positive cells have been shown to be involved in the derivation of stem/progenitor cells from different tissues such as the heart, liver, mammary gland, dermis and skeletal muscle. However it is not yet clear if tissue Sca-1 progenitors are truly tissue specific or are derived from BM. Sca-1 is involved in different pathways such as lymphocyte maturation, stem cell maintenance, cell adhesion, haematopoiesis and tumorigenesis, reviewed in [52]. Batts *et al.* (2011) showed that silencing Sca-1 expression in mammary cell lines decreases cell migration and the silenced Sca-1 cells showed higher adhesion to ECM molecules.

The results from this study suggested that the delayed migration exhibited by Sca-1-silenced cells could be due to increased cell-matrix interaction[53].

In the heart, majority of adult-side population cells are Sca-1<sup>+</sup>, CD45<sup>-</sup>, CD34<sup>-</sup> and expressing telomerase activity similar to the neonatal myocardium [54]. One hypothesis is that the Sca-1 population of CSCs may have a regenerative function after MI, as the number of Sca-1<sup>+</sup> and CD31<sup>-</sup> cells increase after 7 days post-MI as did the expression of the Sca-1 protein [55]. Transplantation of Sca-1 cells into the border zone of murine MI model, which attenuated post-MI ventricular remodelling, increased LVEF and angiogenesis [55]. It is already shown that Sca-1<sup>+</sup>/CD45<sup>-</sup> CSCs are clonogenic (5.6%) and are able to reduce infarct scar size, and promote angio/cardiogenesis post-transplantation into the MI heart [56].

### **1.6.2 cKit**

cKit, also known as CD117, is a type III receptor tyrosine kinase (RTK) and another cardiac stem cell marker. It plays important roles in the amplification and tissue recruitment of mesenchymal stem cells. The gene encodes a ligand that maps to the steel locus and was hence named steel factor or stem cell factor (SF), and is reviewed in [57]. In the heart, cKit-expressing cells were the first cardiac stem cell population isolated. Although these cells are originally mesenchymal stem cells, they are negative for some blood lineage markers such as CD34 and CD45. cKit cells have been isolated successfully from human atrial biopsies and almost 1% of the cells derived from tissue samples were cKit<sup>+</sup> [58]. Furthermore, cKit<sup>+</sup>-expressing cells have been shown to be clonogenic, self-renewing and multipotent, and have been shown to differentiate into smooth muscle, endothelial and cardiomyocyte cell types. Transplantation of human cKit<sup>+</sup> cells into nude rat MI models significantly increased LVEF 3 weeks after cell delivery (LVEF  $\approx$  48% treated vs. LVEF  $\approx$  36% untreated) and enhanced angiogenesis in rat MI models [45].

### **1.6.3 Cardiac side population, Abcg2<sup>+</sup> progenitors**

The adult heart contains a group of progenitor cells termed cardiac side populations (SPs), which are able to efflux metabolic markers such as Hoechst dye which represented 1% of total cardiac cells of adult heart[59]. These cells express a type of membrane pump encoded by a group of multidrug resistance genes. Martin *et al.* (2004) first attributed cardiac SP cells to ATP binding cassette transporter gene (*Abcg2*) and showed that the adult mouse heart has SP cells. Further characterisation of murine SP cells showed that 42.3% of SPs express Sca-1 and 2.1% cKit [60]. Interestingly, SPs were predominantly distinguished from myeloid lineages by the low expression of CD45 (1.5%). In another study, Pfister *et al.* (2010) showed that 84% of murine SPs are Sca-1<sup>+</sup> and 75% are CD31<sup>+</sup>, although the cardiogenic potential of the Sca-1<sup>+</sup>/CD31<sup>-</sup> fraction of SPs is shown to be the highest, and this fraction corresponds only to 10% of SP cells [61]. In another study, Oyama *et al.* (2007) showed that after the intravenous injection of cardiac GFP-SP cells into adult cardiac cryo-injured models, GFP-SP cells migrated towards to site of injury (12 fold more than normal controls) and formed cardiomyocytes, endothelial cells, smooth muscle cells and fibroblasts [62]. Human endothelial cells also express *Abcg2* [63], suggesting the possible endothelial fate of these cells.

### **1.6.4 Characterisation of EDCs, Csphs and CDCs**

In 2004, a group in Italy first showed that *ex vivo* culturing of human cardiac biopsies (explant) could yield cardiospheres (Csphs). Messina *et al.* (2004) showed that explant-derived cells (EDCs) were able to form Csphs spontaneously and that Csphs expressed cardiac stem cell markers such as cKit and Sca-1 [42]. Although spheroid formation of progenitor cells is a controversial characteristic, Khaitan *et al.* (2006) showed that glucose consumption of spheroids from human Glioma cells is 2-3 times more than the monolayer cell culture [64]. This could be due to the hypoxic environment of the core of the spheroids and the expression of Hif-1 $\alpha$  which activates glycolysis pathways to generate energy and decreased mitochondrial activity [64]. These findings suggest that spheroids are likely to provide a more beneficial niche for stem cells within the Csph 3D structure as hypoxic conditions cause less oxidative damage.



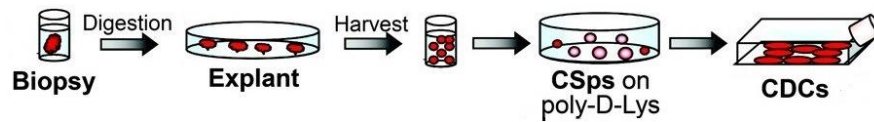


**Figure 1-7 Schematic representation of three stages of CDC culture.** Heart biopsies from humans or whole hearts from mice cultured as cardiac explant after a brief enzymatic digestion. After several days when the explant-derived cells are confluent, they are then transferred into a high growth factor medium and cultured till the Csphs are fully formed. Finally, at the CDC stage Csphs are passaged twice and used for experiments. Figure is adapted from [65].

Using electron microscopy Barile *et al.* (2013) showed that Csphs have a unique microenvironment which contains secretory granules and intercellular contacts (figure 1-8) [66]. Li *et al.* (2010) studied the effect of the 3D structure of Csphs on the stem cell niche and showed that the internal cells of the spheroids express cKit, shielded by Endoglin (Eng) and collagen IV expressing cells. Interestingly the authors showed that the proportion of cKit expression was significantly higher in Csphs in comparison with monolayers (16.9% vs. 9.1%) [67]. This finding marries with those of Smith *et al.* (2007), who proposed that mesenchymal cells could provide physical and secretory benefit to cKit-expressing cells [68]. In addition, Li *et al.* (2010) showed that Csphs show increased gene expression of: (i) some genes involved in ECM (such as MMPs), and collagen IV); (ii) stem cell markers such as Sox2, Nanog; and (iii) stem cell growth-related factors such as HDAC2, Tert and IGF-1 in comparison to the monolayer culture [67]. Although this study indicated the importance of the Csph culture stage and its benefits for the subsequent derivative cells; there are some reports that even some terminally differentiated cells such as fibroblasts can make spheroids when cultured in the Csph culture medium [69]. Another point about Csph culture is that it needs expensive growth factors and it is time consuming. Therefore, Davis *et al.* (2010) characterised EDCs from rat atrial and ventricular samples. The authors repeatedly harvested rat cardiac explants and analysed the expression of cKit and its co-expression with two other stem cell markers: either Abcg2 or SSEA-1. Although the expression of cKit reached its peak at harvest 3, Abcg2 expression increased following extended culture. And SSEA-1 had negligible expression even at the highest peak in harvest 1 (approximately 1%). However, this study was also important in showing the ability of rat-derived EDCs and CDCs to form tubes in a 2D matrigel assay and both cell groups were able to form cellular grafts following cell transplantation leading to improved cardiac contractility and angiogenesis mainly through paracrine activities [70].

Smith *et al.* (2007) modified the Csph culturing method and added a monolayer cell expansion post-cardiosphere stage to acquire cardiosphere-derived cells. This modification could be used to increase the yield of therapeutic cells for further investigations or clinical uses [68]. Davis *et al.* (2009) showed that CDCs had clonogenic properties (9 out of 65 single cells generated colonies) [71] and Messina *et al.* (2004) reported that the clonogenicity efficiency of GFP<sup>+</sup> cardiosphere cells were 1%-10% [42]. Following CDC expansion and characterisations, the heterogeneous expression of range markers was observed by Smith *et al.* (2007). Their CDCs at passage 2 express markers including gap junction protein (connexin 43), cKit (20%), CD90 (40%), Eng (>90%), CD34 (5%), CD31 (10%). The majority of CDCs at passage 2 were negative for CD45 and lineage markers [68], indicating that the majority of CDCs are distinct from BMD haematopoietic progenitor cells.

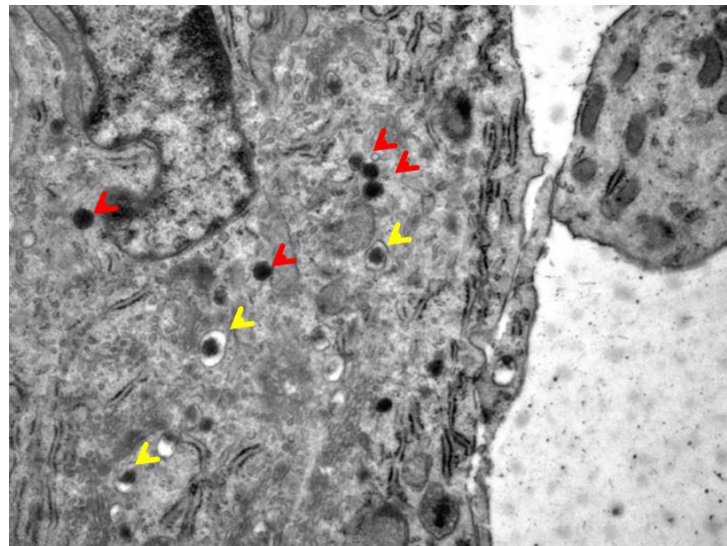


**Figure 1-8 Electron microscopic analysis of human Csph showing secretory granules (red arrows) and primary lysosomes (yellow arrows). Image is modified from [66].**

Validation of Csphs and CDCs to culture cardiac progenitor cells have been reported in several species including the Rhesus monkey [44], pig [43], mouse [42,72,73], rat [70,74], dog [75,76] and humans [77]. However, not all scientists consider that Csph culture is an accepted method of propagating cardiac stem cells. For instance, Andersen *et al.* (2009) claimed that Csphs are not clonogenic and they do not represent CSC populations, but rather they express CD45 or Collagen 1 which suggests they are BMD cells or fibroblasts [78]. Subsequently Davis *et al.* (2009) confirmed that EDCs, Csphs and CDCs contain cKit-expressing cells and do not express haematopoietic

lineage markers. Finally, they concluded that Andersen's group's findings could be due to technical differences in the Csph-culturing method that could significantly change their yield and phenotype [71]. However, CDCs share some immunophenotypic characteristics with fibroblasts such as CD90 expression. Although Mishra *et al.* (2011) showed by immunofluorescent staining that human CDCs are negative for Collagen 1 expression [79], Carr *et al.* (2011) showed that 10% of rat-derived CDCs express DDR2 (collagen receptor) [80], indicating the contribution of CFs in the CDC population.

### 1.6.5 The origin of Csphs and CDCs

Massberg *et al.* (2007) showed that cKit<sup>+</sup> cells occasionally leave the BM in order to provide local immune response in peripheral tissues such as the heart in response to pathogen invasions [48]. In human heart transplants, recipient cardiomyocyte and ECs have been observed in the donor hearts, suggesting that circulating stem cells could come into the donor heart and differentiate into different cell lineages [49]. Furthermore, it has been shown that almost 5% of cardiomyocytes of allogeneic BM-recipient patients are chimeric [81], suggesting that the possible recruitment of cardiogenic progenitors from the circulating system could reach the heart. However, another study showed only 18.4±4.5% of cells in murine Csphs were derived from BM. Csphs were cultured from hearts at 2 weeks post-MI and from no surgery controls in chimeric mice (transplanted BM cells from GFP transgenic mice into the lethally irradiated C57BL/6 mice,) and cells that co-expressed GFP and CD45 were used to indicate their BM origin. However, in this study, all Sca-1<sup>+</sup> CD45<sup>-</sup> cells (a proportion of cardiac progenitors in CDC culture) were GFP negative, suggesting their distinct origin from BM [56]. White *et al.* (2011) studied heart transplant patients and showed that CDCs have an intrinsic origin using molecular methods such as qRT-PCR, short tandem repeat (STR) analysis and fluorescence *in situ* hybridisation [82]. However, there are two points which need to be considered in this work. First is the sample size which is very small and is not significant for statistical analysis (n=2) and the other issue is that all of the cases were in a physiological state, even though they were transplanted, thus it is possible that pathological stimuli such as MI might generate different results [83]. Finally, Barile *et al.* (2007) transplanted BM donor cells in which GFP was under the control of the cKit promoter into irradiated mice, and after experimental MI, the majority of the Csphs made from the recipient mice showed GFP expression; this study

suggested that in pathological conditions, BM cells can repopulate the CSC pool and contribute into the Csph culture [84]. Therefore, these studies suggested that the purity of Csphs and CDCs in terms of cardiac origin is likely to depend on the physiological or pathological state of the heart. However, it is still not clear what the true origin of the resident cardiac stem cells is, and further lineage tracing by using different transgenic animal models would increase our knowledge regarding this matter.

### **1.6.6 EDC and Csph culture from the MI model**

Ye *et al.* (2012) showed that EDCs derived from 1, 2 & 4 weeks post-MI, took less time to form a confluent monolayer of cells in comparison to no surgery controls ( $14\pm 1$ ,  $13\pm 1$  and  $18\pm 2$  days from 1, 2 and 4-week post-MI hearts, respectively), versus to explants derived from sham-operated and non-operated hearts ( $21\pm 1$  and  $32\pm 2$  days, respectively). However, no significant difference was observed between the groups at 4 weeks post-MI. This study also showed that the number of Csphs formed was significantly greater at 1-week ( $5.12\times 10^5\pm 0.45\times 10^5/\text{heart}$ ) and 2-week ( $3.75\times 10^5\pm 0.52\times 10^5/\text{heart}$ ) post-MI versus sham-operated ( $2.20\times 10^5\pm 0.70\times 10^5/\text{heart}$ ) and non-operated hearts ( $1.67\times 10^5\pm 0.26\times 10^5$  cells/heart) ( $p<0.045$ ). Ye *et al.* (2012) also showed that Csphs derived from MI mice engrafted in the ischemic myocardium and differentiated into smooth muscle and endothelial cells. MI-derived Csphs were also able to promote angiogenesis and reduce the infarct size after transplantation in the MI models, suggesting that MI has improved the efficacy of Csphs *in vitro* and *in vivo* [56].

### **1.6.7 The role of EDCs, Csphs and CDCs in neovascularisation**

Several studies have shown the pro-angiogenic potential of EDCs [70,73], Csphs [42,67,85] and CDCs [65,68,74,79,80,86] *in vitro* or *in vivo* or both. There is evidence of successful cell engraftments in recipient heart tissues and promotion of a significant increase in the capillary density of the ischemic myocardium. EDCs, Csphs and CDCs have all been shown to express endothelium-related cell markers such as CD31, CD34, Vegf, Flk1 and Eng *in vitro*, to improve myocardial function and increase capillary density in the peri-infarct region through paracrine mechanisms in comparison with no-

cell recipient or sham-operated control groups. EDCs, Csphs and CDC also have a limited autocrine capacity to differentiate towards endothelial, smooth muscle cells and cardiomyocytes post-transplantation in MI models although the autocrine pathway seems to be not very efficient [68,70,83]. Some studies have compared the efficacy of Csphs with CDCs: for instance, Li *et al.* (2010) showed that transplantation of human Csphs into the mouse model of MI enhances cardiac function significantly better than CDCs [67]. In another study using a pig model of anteroseptal myocardial infarction, injection of CDCs or Csphs enhanced the cardiac function and attenuated myocardial remodelling in comparison with the placebo group; however, the authors concluded that Csphs were superior in improving hemodynamics, regional function, and in attenuating ventricular remodelling [43]. As discussed above, the benefit of CDC culture is due to its faster proliferation and higher therapeutic cellular yield than Csphs (3 folds vs. 1.2 fold increase in CDC vs. Csph growth rate after 7 days of culture) [67]. On the other hand, Csphs produce more growth factors *in vitro*, such as Vegf, compared with CDCs that could improve neo-vessel formation. However, Csphs have a large size (50-200  $\mu\text{m}$  in diameter) which limits their application due to the risk of embolism following intra-coronary delivery [43]. Even CDCs which are considered to be relatively large cells (20.6 $\pm$ 3.9  $\mu\text{m}$  diameter), could potentially cause microvessel blockage, as some microvessels are 7-10  $\mu\text{m}$  in diameter [86]. Furthermore, the addition of 100U/ml of heparin into the cell suspension solution, prior to cell transplantation is important to reduce cell-related thrombus formation [86]. Tang *et al.* (2009) showed that 4 weeks after transplantation of cardiosphere-derived Lin<sup>-</sup>/cKit<sup>+</sup> progenitor cells in a mouse model of MI, the capillary density of the peri-infarct region increased in comparison with mice which received only the culture medium [73]. In another study the authors showed that CD31 expression was enhanced by 44% in the peri-infarct region of CDC-transplanted rat models after 16 weeks of MI in comparison to controls [80].

However, the main barrier in the field of cardiac cell transplantation therapy is low cell survival after cell transplantation, this is irrespective of the applied cell type. It has been reported that cell retention in many studies is low. Variable cell retention could be due to a number of factors: (i) technical differences of cell culture protocols; (ii) animal models of MI; (iii) cell delivery route; and (iv) the harsh anoxic conditions of the host tissue (ischemic myocardium) [87]. Moreover, the constant activity of the heart and consequent mechanical forces and venous drainage could also decrease the cell retention efficacy [88]. Thus low cell survival could be detrimental for both autocrine

and paracrine routes of neo-vessel formation by CDCs. To this end some strategies have been applied in order to adapt cells prior to transplantation. In relation to CDCs, hypoxia pre-treatment could potentially increase their tolerance following cell transplantation into the harsh ischemic region. In 1994, Rumsey *et al.* used oxygen-sensitive phosphorus to measure the oxygenation of the healthy and infarcted rat heart in real time and showed that after cardiac infarction the heart is divided into three regions based on oxygen pressure: (i) Remote region, with almost physiological level of O<sub>2</sub>, equivalent to 5%; (ii) peri infarct zone, which extends only several millimetres and has the range of 3% O<sub>2</sub>; and (iii) the core of the infarct which has nearly 0-0.2% oxygen [89] (Figure 1-9).

### **1.7 Hypoxia and Hif proteins**

The range of normoxia is very narrow in mammalian cells as the risk of oxidative damage due to hyperoxia and metabolic deterioration due to insufficient O<sub>2</sub> (hypoxia) are extremely detrimental. In general, hypoxia means a reduction in the oxygen level in the cellular microenvironment and may result from vascular dysfunction or malignancy. Hypoxia activates a number of genes which are important to adapt cells to survival in low levels of O<sub>2</sub>. Mammalian cells have a system to respond to hypoxic conditions very quickly and efficiently which is initiated by Hif proteins, reviewed in [90]. Hifs are sequence-specific DNA-binding proteins that can promote or repress the expression of downstream genes which are involved in O<sub>2</sub> homeostasis. Genes that are under the control of hypoxia have been implicated in functions such as cell survival, cell proliferation, apoptosis, glucose metabolism and angiogenesis [91]. Overall, Hifs trigger a cascade of gene activation which helps cells to adapt to low concentrations of O<sub>2</sub>. This adaptation is useful to mammalian cells in the context of embryonic development, angiogenesis and ischemic disorders, or it may be detrimental in the context of tumorigenesis or apoptosis. Table 1-1 summarises the common terminology and the relative oxygen level.

Condition	pO <sub>2</sub> (mmHg)	% O <sub>2</sub>
Normoxia (ambient)	159	21%
Mild hypoxia	8-38	1-5%
Hypoxia	<8	<1%
Anoxia	<0.08	<0.1%

**Table 1-1** Frequently used terminology and the relative oxygen level. Table is adapted from [90].

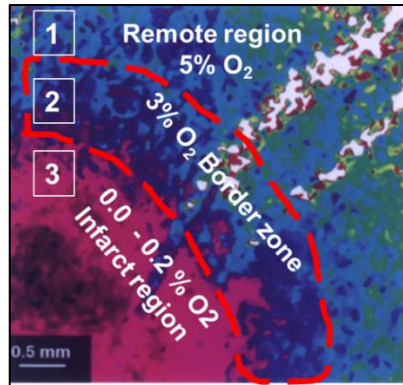


**Figure 1-9** Oxygen quenching in a rat MI model, showing that the heart is divided into three regions: 1) remote region with physiological oxygen levels (5% O<sub>2</sub>); 2) the peri-infarct/border zone containing 3% O<sub>2</sub>; and finally, the injured region with 0-0.2% O<sub>2</sub>. The image is modified from [89].

### 1.7.1 Hif proteins

Three isoforms of Hif- $\alpha$  have been identified in mammals: Hif-1 $\alpha$ ; Hif-2 $\alpha$ ; and Hif-3 $\alpha$ . Hif protein expression is regulated at transcriptional, translational and post-translational stages. Hif-1 $\alpha$  is highly sensitive to protein degradation in normal oxygen concentrations, reviewed in [90]. Figure 1-10 shows the inactivation of Hif- $\alpha$  in normoxic conditions. In hypoxia, Hif- $\alpha$  is stabilised mainly due to the inactivation of Hif- $\alpha$  hydroxylation enzymes (PHD and FIH) and enters into the nucleus where it binds to Hif-1 $\beta$  (ARNT) to produce a stable complex which is now able to activate the target genes [92]. The specific promoter sequence that Hif- $\alpha$  protein recognises is called an hypoxia-response-element (HRE) and contains 5'-RCGTG-3', in which R refers to A or G [93]. Erythropoietin and Vegf are some typical examples of Hif- $\alpha$  target genes which activate erythropoiesis and angiogenesis, respectively [90].

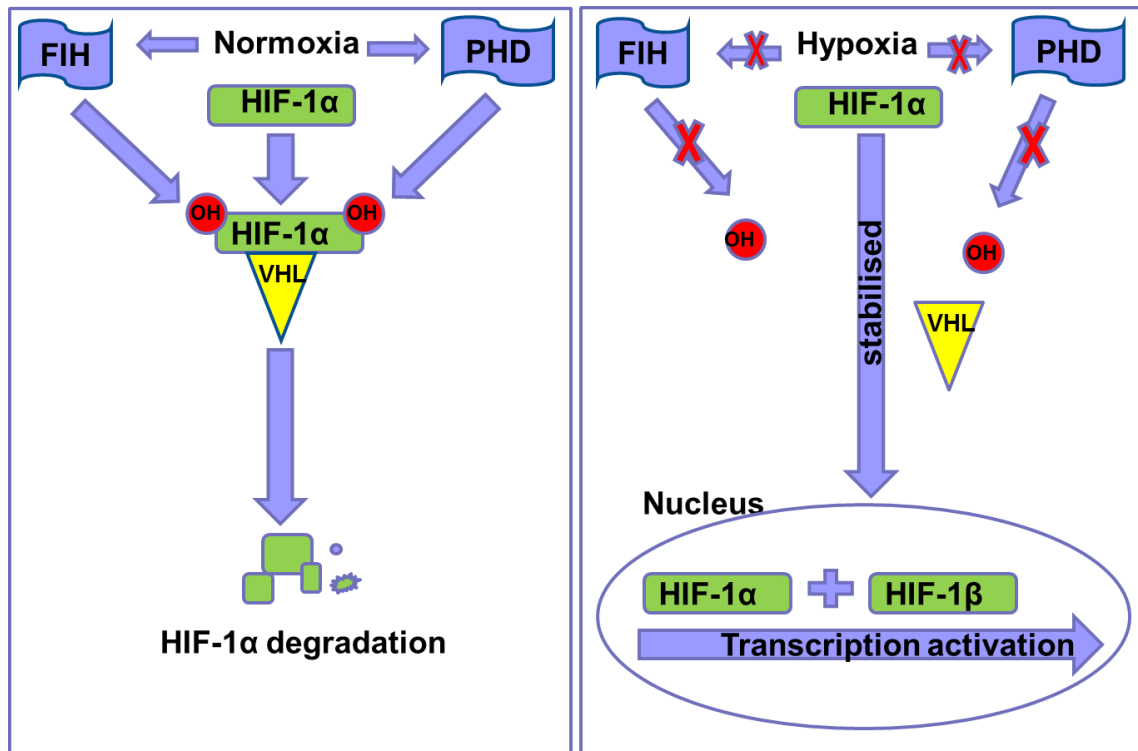


**Figure 1-10 Hif-1 $\alpha$  regulation in Normoxia and Hypoxia.** While O<sub>2</sub> is available in the cellular niche hydroxylation of proline residues by PHD 1-3 enzymes occurs and modifies the structure of Hif-1 $\alpha$ , which is then introduced to the VHL tumour suppressor gene and ubiquitin-mediated proteosomal degradation (Left). In contrast Hif-1 $\alpha$  is stable if O<sub>2</sub> availability is decreased. Hypoxia inhibits proline and asparagine hydroxylation, which allows Hif-1 $\alpha$  to accumulate and dimerise with Hif-1 $\beta$  in the nucleus and eventually activate the transcription of target genes involved in the adaptation of cells to hypoxic conditions.

### 1.7.2 Hypoxia signalling in adult stem cells

HSCs in BM are the classic example of adult stem cells which are capable of replenishing all types of myeloid blood cells. One of the important hallmarks of the BM microenvironment is hypoxia. It has been shown that the hypoxic niche of BM is essential for its resident stem cell maintenance and improves clonogenicity, reviewed in [94]. In addition to HSCs, the hypoxic niche also plays important roles in other adult stem cell populations such as the sub-ventricular zone of the hippocampus, which contain neural stem cells (NSCs). Moreover, Hif proteins are up-regulated in several cancer stem cells and this affects their proliferation, metastasis, vasculogenesis, survival and differentiation, reviewed in [95]. In addition, inhibition of Hif-1 $\alpha$  eradicates lymphoma and acute myeloid leukaemia (AML) by eliminating cancer stem cells [96]. Therefore, hypoxia and Hif proteins appear to be important regulators of stem cell maintenance and proliferation. In fact, hypoxia has variable effects on stem cell



proliferation. For instance, Grayson *et al.* (2007) showed that culturing human mesenchymal stem cells (hMSCs) in low oxygen (5%) resulted in a nine fold increase in cell expansion compared to normoxia [97]. However, in another study Holzwarth *et al.* (2010) showed that MSC cultured in 1% O<sub>2</sub> did not proliferate as fast as MSC cultured in atmospheric oxygen (21% O<sub>2</sub>) [98]. On the other hand, some studies have shown the benefit of hypoxic culture on the maintenance of stem cell pluripotency and the expression of embryonic stem cell markers such as Oct4. It has been shown that culturing human embryonic stem cells in 2% O<sub>2</sub> maintained their pluripotency for up to 18 months [99]. Taking all this together, it seems that the effect of hypoxia on the stem cell phenotype is cell type and cell culture dependent. Therefore, to elucidate better the effect of hypoxia on stem cells, it is specifically recommended to examine different O<sub>2</sub> levels on different characteristics of the candidate stem cell directly.

### **1.8 Hypoxia and cardiac progenitor cells**

Recently, a physiological cardiac hypoxic niche was identified in the epicardium and subepicardium, as these regions have the smallest capillary density. It was shown that 50% and 10% of epicardial and sub epicardial cells, respectively, express Hif-1 $\alpha$  in uninjured murine hearts. These cells also have clonogenic and multilineage differentiation capacity to form endothelial, cardiomyocyte and smooth muscle cells *in vitro* [100]. Another item of evidence to support the hypoxic niche in the epicardium and subepicardium regions is that cells of these regions mostly rely on cytoplasmic glycolysis rather than mitochondrial oxidative phosphorylation to generate energy, so they have been named as glycolytic cardiac progenitors (GCPs) [100]. Hif-1 $\alpha$  knock-down in these cells significantly reduced their proliferation and spontaneous differentiation potential. These findings suggest the similarity of the epicardium and subepicardium niche to the BM hypoxic niche. Hif proteins are likely to be the key regulators of self-renewing stem/progenitor cells within the hypoxic niche of the epicardium and sub epicardial regions [100]. But it is not yet clear whether GCPs could contribute to cardiac remodelling and myocardial repair after infarction. However, there is a possibility that hypoxia could activate migration of any types of cardiac progenitors towards the injured myocardium. For instance, it has been shown that cardiac progenitors, Sca-1<sup>+</sup> cells, migrate towards the injured myocardium after myocardial infarction and differentiate into cardiomyocytes and endothelial cells [56]. *In vitro*

studies have shown that the cardiac stem cell responds to hypoxic stimuli based on the duration of the culture. For instance Van Oorschot *et al.* (2011) showed that short- and long-term hypoxic culture have different effects on human cardiomyocyte progenitor cells (hCMPCs). In their study, short-term hypoxia increased the migratory and invasiveness of hCMPCs. Although long-term culture did not initiate differentiation of hCMPCs into endothelial or mature cardiomyocytes, it significantly increased their proliferation and growth factor secretion (such as Vegf) [101].

### **1.8.1 Hypoxia preconditioning of EDCs and CDCs**

SDF-1 is a transcriptional target of the Hif-1 $\alpha$  protein. Following the stabilisation of Hif-1 $\alpha$ , the migration and homing of circulating CXCR4 expressing progenitor cells to ischemic tissue was enhanced. Furthermore, the inhibition of SDF-1/CXCR4 signalling pathway decreased progenitor cell recruitment to the site of injury [102]. Tang *et al.* (2009) showed that preconditioning of the cardiosphere-derived cell Lin<sup>-</sup> cKit<sup>+</sup> progenitors (CLK) by severe hypoxia (0.1%) induces their recruitment (2.5 fold) to ischemic myocardium through the SDF-1/CXCR4 pathway. Tang *et al.* (2009) showed that it takes only 4 hours of hypoxic culture for CLK to show an increased expression of CXCR4. They also showed that the migratory activity of CLK towards the injured region was increased under the control of Hif-1 $\alpha$  and CXCR4 activation. In this study, CLK pre-treated with severe hypoxia (0.1% O<sub>2</sub>) produced more chemokines (TCA-3, SDF-1, 6Ckine), vascular growth factors (Vegf, osteopontin, bFGF, erythropoietin, stem-cell factor) and cardiac differentiation growth factors (Activin A, TGF- $\beta$ , and Dickkopf homolog-1) more efficiently than CLK treated with normoxia. Interestingly, intravenous injection of preconditioned CLK improved the LVEF and left ventricular fractional shortening in CLK pre-treated with hypoxia [73]. In a similar study, Yan *et al.* (2012) showed that after pre-treatment of adult murine CPCs (purified cKit<sup>+</sup> EDCs) with severe hypoxia for 6 hours, cell survival was increased in a serum-depleted condition and the expression of Bcl2 (an anti-apoptotic gene) increased three fold in comparison to normoxia-treated CPCs [72]. After the transplantation of hypoxia pre-treated CPCs into the ischemic myocardium, cell retention and survival were improved and the infarct size was reduced. The authors also showed that hypoxia increased the pro-angiogenic potential of CPCs by inducing an elevated release of Vegf and SDF-1 into the cell culture medium [72]. The benefits of physiological O<sub>2</sub> on human EDCs and

CDCs have also been shown. Li *et al.* (2011) showed that EDC proliferation was doubled following the culture of EDCs in 5% O<sub>2</sub> in comparison with normoxic counterparts. They also showed that *ex-vivo* expansion of human CDCs in 5% O<sub>2</sub> decreased the incidence of chromosomal abnormalities (1/16 versus 6/16 of CDC samples, p=0.02). Although no difference was observed for *in-vitro* angiogenesis (tube formation) between the groups, CDCs grown in 5% O<sub>2</sub> showed better engraftment and improved myocardial function in the recipient SCID mice [103]. However, Bonios *et al.* (2011) showed that the constitutive expression of Hif-1 $\alpha$  blunts the functional benefits of CDCs after myocardial transplantation. *In vitro* angiogenesis and proliferation were not changed in CDC with constitutive Hif-1 $\alpha$  expression versus the control CDCs. However, the expression of some growth factors such as Vegf and Endothelin-1 were enhanced in the CDC-Hif-1 $\alpha$  group [104].

In one study CDCs were harvested in a hypoxic environment mimicking the environment of the ischemic myocardium accompanied by the oxygen-releasing hydrogel system (containing hydrogen peroxide releasing microspheres which could release oxygen sustainably at least for 2 weeks). In this method CDCs were co-cultured with oxygen-releasing hydrogel for different time periods and the results showed augmented cell survival and an enhanced differentiation capacity of CDCs towards cardiac phenotypes [105]. However, there are some data showing that hypoxia has a negative effect on stem cell tissue recruitment. For instance, Eliasson *et al.* (2010) showed that hypoxia (0.1%) decreases HSC proliferation, as cells cultured in hypoxia showed reduced Ki-67 expressing cells (21%) compared to normoxia (29%), indicating that hypoxic exposure leads to the accumulation of HSCs in G<sub>0</sub>. The authors also compared the proliferation rate of LSK (Lin<sup>-</sup>, Sca-1<sup>+</sup> and cKit<sup>+</sup>) cells in hypoxic and normoxic conditions and showed that cells cultured in hypoxia had almost a 28 fold increase while cells in normoxia had a 168 fold increase in their proliferation rate. They also showed that the expression of some cyclin-dependent inhibitors (CDKIs) such as p21, p27 and p57 were up-regulated in hypoxic conditions after 24 hours of Hif-1 $\alpha$  activation [106].

Taking this together, moderate hypoxia has been shown to be a beneficial treatment for CDCs and increase their proliferation, cell survival and retention following transplantation into the MI model.

## 1.9 Clinical trials using CDCs in MI patients

Recently, the final results of a clinical trial with CDCs from Marban's group has been published as CADUCEUS; Cardiosphere-Derived Autologous Stem Cell to Reverse Ventricular dysfunction. In this trial, 17 male subjects with a recent MI (10 weeks) and with LVEF ranging between 25-45% received  $12.5-25 \times 10^6$  autologous CDCs through the intracoronary route and eight patients received conventional treatments. Results at 1 year showed no significant change in LVEF between CDC recipients and the control group; however, CDC recipients showed some significant improvements, such as the reduction of the infarct size ( $p < 0.001$ ). Moreover, both scar mass ( $-12 \pm 6.8$  g) and viable mass ( $+22.6 \pm 9.4$ g) significantly improved in CDC-treated patients over the reporting period of one year. Conversely, in the control group, there were no significant changes in scar mass or viable myocardial mass. An important finding in this trial is that CDCs could be safely transplanted into the patients with an ischemic myocardium. The authors concluded that these results provide important evidence of the potential of CDCs to enhance regional improvement in MI patients; however, further studies needed to be done in order to validate these preliminary findings and improve CDC functional efficiencies [77,107].

In another clinical trial of heart-derived stem cells, Stem Cell Infusion in Patients with Ischemic Cardiomyopathy (SCIPIO), 16 patients received autologous cKit<sup>+</sup> cells ( $0.5-1 \times 10^6$ ) derived from atrial biopsies four months after cell harvesting through the intracoronary route and seven patients were assigned to the control group. The strategy of cell delivery in this study was to deliver cKit<sup>+</sup> cells when the patients are in a critical condition due to ischemic myocardial disease in order to treat heart failure [108]. Using MRI and echocardiography the results showed that the cardiac function of the patient treated with cells improved significantly. In eight patients LVEF improved significantly in comparison to the control group (42.5% vs. 30%) [108]. The main limitations of these studies ((i) no placebo control group and (ii) the small sample size) make interpretation of the results difficult.

To summarise, three different stages of CDC culture: EDCs; Csphs; and CDCs are able to improve cardiac function in different clinically relevant animal models. Sub-populations of EDCs, Csphs and CDCs have limited autocrine pro-angiogenic and cardiogenic potential. It is believed that CDCs use paracrine mechanisms to activate angiogenesis and cardiogenesis, but do not show significant cell retention.

Preconditioning of human and murine CDCs with hypoxia has been shown to improve their engraftment and increase their angio/cardio-genic potential after injection into the MI models, although there are some reports which question the efficacy of these preclinical models. And finally, the clinical trials with CDCs showed that CDCs are safe to be used in MI patients leading to some important improvements such as an increase in viable myocardial mass and a decrease in scar size.

### **1.10 Aims of thesis**

Different groups have shown that CDCs offer a potential cell source for cellular transplantation and neovascularisation therapy. CDCs contain populations of progenitor cells that express some key markers of mesenchymal stem cells (cKit, Sca-1) that may be critical for this function. In my thesis I have investigated whether preconditioning CDCs with 3% O<sub>2</sub> (a mild hypoxia approximately equivalent to the level of oxygen in the infarct border zone) could enhance their stem cell component. In addition, in light of the recent debate regarding the extent to which Csphs and CDCs are cardiac progenitors or cardiac fibroblasts, I used lineage tracing to characterise the CF component of EDCs, Csphs and CDCs. In the final results chapter, I investigated the effect of mild hypoxia on the pro-angiogenic potential of CDCs by using an established *in-vivo* angiogenesis model.

Therefore the aims addressed in this thesis are:

1. To determine whether pre-treatment with 3% O<sub>2</sub> affects the stem cell phenotype of neonatal and adult murine CDCs;
2. To use lineage tracing to investigate the contribution of cardiac fibroblasts (CFs) to EDCs, Csphs and CDCs in culture;
3. To use lineage tracing to investigate the contribution of cardiac fibroblasts to the scar forming tissue in vivo;
4. To determine whether pre-treatment of CDCs with 3% O<sub>2</sub> can promote their pro-angiogenesis potential using a sub-dermal matrigel plug assay *in vivo*.

## **Chapter 2 Material and Methods**

## 2.1 Suppliers

All chemicals and reagents were purchased from the following companies:

eBioscience; BD Bioscience; Amsbio; Vector Laboratories; Sigma Aldrich; Fisher scientific; VMR International; GE Healthcare; Polyscience Inc. Qiagen; Invitrogen; Roche; Fisher Scientific; and Santa Cruz.

All cell and tissue culture flasks, plates, plastic apparatus and general laboratory use were purchased from BioRad Laboratories, Grenier, Iwaki and RA Lamb.

Medium and cell culture supplements were purchased from Gibco Invitrogen, Peprotech and Promocell. Oligonucleotides were purchased from Integrated DNA Technologies (IDT) and surgical instruments were purchased from Fine Science Tools (FST).

## 2.2 Mouse strains

All animal experiments were performed under UK Home Office Licence and according to the national guidelines for laboratory animal care.

All mice were maintained in a ventilated germ free facility in a 12 hour light/dark cycle and fed with standard diet and water.

*Rosa26-floxed stop eYFP*. [109] This line was originally generated by Srinivas *et al.* (2001). This line contains a stop sequence flanked by LoxP sites up stream to the *eYFP* gene. The expression of *eYFP* is driven by the ubiquitous *Rosa26* promoter and depends on the removal of the stop codon by Cre-recombinase activation.

*Collagen1- $\alpha$ 2-CreERT*. line was generated by Zheng *et al.* (2002) [110] and was obtained from Prof. David Abraham's Laboratory, UCL. This line expresses tamoxifen-inducible Cre recombinase (*CreERT*) and contains 6 kb of the upstream 5' flanking region of the *Coll1a2* promoter fused to a sequence encoding Cre-ER(T2)-IRES-hpAP.

*CAG-farnesylated-eGFP* (*CAG-farnesyl-eGFP*). This line was obtained from Prof. A. Medvinski (Edinburgh University). In this line eGFP expression is under the control of the *CAG* promoter and farnesyl maintains eGFP protein at the cell membrane. These

mice were used for the CDC culture in order to track eGFP-expressing CDCs in the subdermal matrigel angiogenesis assay.

### **2.3 Genotyping and DNA extraction from ear clips and tail tips**

#### Buffer 1 (25mM NaOH and 0.2 mM EDTA)

2.5ml of 0.5M NaOH + 0.02ml of 0.5M EDTA in 50ml of mill Q H<sub>2</sub>O and pH was adjusted to 12 with NaOH

#### Buffer 2 (40 mM Tris-HCl)

4ml of 0.5 M Tris-HCl in 50ml milli-Q H<sub>2</sub>O, adjust to pH 5 with HCl.

For genotyping ear clips were taken from adult mice and tail tips were taken from neonates. Tissue samples were incubated for 45 minutes in 100µl buffer 1 in a thermomixer at 95°C and 350-400 rpm to lyse the tissue. Then 100µl of buffer 2 was added to neutralize the pH. After vortexing the tubes were centrifuged at 13,000 rpm for 5 minutes to pellet the debris. Finally the extracted DNA (supernatant) was either stored at -20 °C or used immediately for genotyping.

#### **2.3.1 Genotyping**

Polymerase chain reaction (PCR) was used for all genotyping experiments.

##### **2.3.1.1 Standard PCR**

25µl reaction was used in all PCR reactions in 200µl PCR tubes. Each reaction consisted of: 2.5µl reaction buffer (10x), 2.5µl MgCl<sub>2</sub> (25mM), 0.2µl hot *Taq* DNA polymerase (AB gene) 0.25µl of forward and reverse primers (20µM), 0.5µl 10mM dNTPs and, finally, 2µl of DNA sample with autoclaved dH<sub>2</sub>O used to make up to the final volume of 25µl. All PCR reactions included negative and positive controls and were performed according to the cycle schedule in Table 2-2.



### 2.3.1.2 Agarose gel electrophoresis solutions and preparation:

Solutions:

1x TAE buffer: 40mM Tris base-acetate 1mM EDTA


DNA loading Dye: 0.25% xylene cyanol FF, 0.25% bromophenol blue with 40% sucrose in dH<sub>2</sub>O.

2% agarose gel was used for all PCR product electrophoresis. The gels were made by dissolving 2 grams of agarose powder in 100 ml of 1x TAE buffer and boiled in microwave till the agarose dissolved completely. Then the gel was partially cooled under tap water and poured into the gel tray with well-forming combs in place. After 30-45 minutes when the gel was solidified, the combs were removed and the gel placed in the electrophoresis tank which was filled with 1x TAE buffer. Loading samples were made by mixing PCR product with loading dye (according to the concentration of the dye), and pipetted into the wells. 1kb DNA ladder (Invitrogen) was used to assess the size of PCR products. The gels were run at 80-85 volts for 50-60 minutes and DNA bands were visualised first by immersing the gels in Ethidium Bromide solution (1µg/ml in dH<sub>2</sub>O) for 30 minutes and then exposing to UV light using the GeneGnome System. To capture the images GeneSnap Software (Syngene Bio Imaging) was used.

Line	Primer name	Primer sequence	Expected product size (bps)
<i>Col-Cre</i>	Cre F	GATCGCTGCCAGGATATACG	574
	Cre R	AATCGCCATCTTCCAGCAG	
<i>CAG-GFP</i>	eGFP F	TCGTCCTTGAAGAAGATGGTG	244
	eGFP R	ACGTAAACGGCCACAAGTTC	
<i>Rosa26R</i>	WT-R26	GCGAAGAGTTTGTCCCTCAACC	600 <sup>WT allele</sup>
	R26	GGAGCGGGAGAAATGGATATG	310 <sup>R26 allele</sup>
	R26GTRgeo	AAAGTCGCTCTGAGTTGTTAT	

**Table 2-1** Primer details used for genotyping.

Reaction steps	Step temperature	Step duration
1	95°	1 minute
2	95°	15 seconds
3	58°	30 seconds
4	74°	1 minute
5	74°	7 minutes
6	4°	-



**Table 2-2 PCR program steps for genotyping mouse lines.**

## **2.4 Cardiosphere-Derived Cells (CDCs) culture:**

All cell culture procedures were carried out in sterile conditions in a cell culture hood

### Media and solutions:

Complete Explant Medium (CEM). IMDM supplemented with 20% foetal calf or bovine serum (heat inactivated), 1% L-Glutamine, 0.1mM 2-mercaptoethanol, 1-unit/ml penicillin and 100µg/ml streptomycin.

Cardiosphere Growth Medium (CGM). DMEM F12 and CEM (35%/65%), supplemented with 2% B27, 80ng/ml bFGF, 20 ng/ml EGF, 40nmol/L Cardiotropin -1, 40nmol/L thrombin and 0.1 mmol/L 2-mercaptoethanol

### **2.4.1 Explant culture**

Mouse neonates (3-6 days old) or adult mice (6-8 weeks old) were culled via cervical dislocation and whole hearts were dissected with sterile instruments. The hearts were stored in ice cold PBS until cultured as explants. Under the cell culture hood the hearts were washed three times with ice cold PBS and then digested with 1 ml of 0.05% trypsin for 3-5 minutes (neonatal hearts) or 10 minutes (adult hearts). Trypsinisation proceeded at the same time as the heart tissue was cut into small pieces using fine scissors. Trypsin activity was inhibited by adding the equal volume of CEM and then 25-30 cardiac explants were put on each fibronectin (1 mg/ml BD) pre-coated 35 mm plate and cultured in 2 ml of CEM. Every third day 0.5 ml CEM was added to each plate. The explant culture stage was continued till the plates were confluent with an

outgrowth of phase bright cells. This time period was 12-14 days for neonatal heart explants and 25-30 days for adult mice. To proceed to the cardiosphere culture stage, explants were washed with PBS once and then incubated for 2 minutes with Versene (Invitrogen) followed by 3-5 minutes of digestion with trypsin for neonates and Accutase cell detachment reagent (eBioscience) for adults at 37°C. Then all of the contents of the plates were transferred into a 50 ml falcon tube and allowed to settle at room temperature for 1 minute in order to obtain tissue fragment free explant-derived cells.

#### **2.4.2 Cardiosphere culture**

EDCs were seeded at a density of  $10^5$  cells per well of a 24 well plate pre-coated with polyD lysine (BD Bioscience) using 2.4 µg/ml for neonatal EDCs and 1.2 µg/ml for adult EDCs, and 400 µl of CGM was added per well. Every 4<sup>th</sup> day 200µl of CGM was added to each well. At day 6-7 of culture (neonate) and day 12-14 (adult), loosely adherent cardiospheres were gently collected in 50 ml falcon tubes. To obtain a purer population, cardiospheres were allowed to settle at the bottom of the tube and the single cells remaining in the supernatant were discarded. Then 10 ml PBS was added and the sedimentation process was repeated 2 times. Finally, the cardiospheres were spun down at 1000rpm for 8 minutes and followed by 2-3 minutes trituration with 1ml pipette in order to promote dissociation of cardiospheres.

#### **2.4.3 Cardiosphere-derived cell culture**

Dissociated cardiosphere cells from one 24-well plate were transferred to one fibronectin pre-coated T75 flask. Cells were passaged twice when reaching 80-90% confluence. To do this, cells were treated with accutase for 10 minutes at 37°C and collected after knocking the flasks harshly to remove adherent cells. In addition, cell scrapers were used to remove any remaining cells. Finally, the cells were centrifuged at 1000 rpm for 8 minutes and seeded on fibronectin pre-coated T75 flasks in 1:2 dilution.

All EDCs, Cardiospheres and CDCs were cultured at 37°C in humidified air with 5% CO<sub>2</sub> and atmospheric O<sub>2</sub> (for normoxic culture) and 3% O<sub>2</sub> (for hypoxic culture).

## 2.5 Cell staining

### 2.5.1 Immunofluorescent cell staining

$2 \times 10^4$  CDCs were seeded onto 4 chamber glass slides (Lab-Tek, Nunc) and allowed to settle for 24 hours. CDCs were then cultured at normoxia or 3% O<sub>2</sub>. Cells were washed with 1x PBS and fixed with acetone for 15 minutes on ice. Then the acetone was removed and the chambers were washed three times with ice cold PBS. Cells were blocked with blocking solution (5% goat serum, 1% BSA and 0.5% tween 20) for 30 minutes at room temperature inside a humidity chamber. Then the blocking solution was removed and the appropriate primary antibody (diluted in blocking solution) was added to the chambers and incubated at 4°C overnight. The slides were washed with ice cold PBS three times and the secondary antibody (1/200 dilution in blocking solution) was applied for 1 hour at room temperature. Cells were then washed three times in PBS and mounted with hard set mountant (vector laboratories) containing DAPI under a coverslip. Finally, the slides were kept at 4°C overnight to allow to the mountant to set and fluorescent microscopy was performed the following day.

Primary Antibody	Stock Concentration	Working concentration	Source Cat. No
Anti-Hif-1 $\alpha$ (Rabbit)	200 $\mu$ g/ml	1/50	Santa Cruz (sc-10790)
Anti-GFP-alexa 488	2mg/ml	1/50	Invitrogen (A21311)
Secondary Antibody	Stock concentration	Working concentration	Source Cat. No
Goat anti-Rabbit IgG alexa 594	2mg/ml	1/200	Invitrogen (A11012)

**Table 2-3 Antibodies used for immunofluorescent cell staining.**

### 2.6 *In-vitro* cell proliferation and viability assay of CDCs

CDCs were seeded at  $2 \times 10^4$  cell density per well in a 24-well plate. After resting the cells for 24 hours to let them adhere, cells were transferred into normoxia or 3% O<sub>2</sub> incubators. Cell density and viability were measured at different time points: 0; 24; 48; and 72 hours with Vi cell XR (Coulter) automated cell viability and total cell counter.

### 2.7 Clonogenicity assay with CDCs

CDCs in T75 flasks, at passage 1 were cultured in 3% O<sub>2</sub> or normoxia. Then the cells were treated with accutase for 10 minutes at 37°C. Cell suspensions were collected in

50 ml falcon tubes and centrifuged at 1000 rpm for 8 minutes. The cell pellet was re-suspended in 1ml PBS and viable cells were quantified with an automated cell counter (Vi cell). Using 96-well plates, the FACS aria cell sorter automatically put 1cell/well. After 1 hour, wells which have received a single cell were labelled and all plates were transferred to a normoxic incubator (overnight) to let the cells settle. Then the clonogenicity of CDCs was assessed for 42 days. In each experiment three 96-well plates were used for each condition.

## **2.8 Flow cytometry**

### **2.8.1 Immunophenotyping of murine CDCs**

CDCs at passage 2 were incubated with accutase for 10 minutes at 37°C. The cell suspension was collected in a 50 ml falcon tube and cell pellets were collected after centrifuging at 1000 rpm for 8 minutes. The resultant cell pellet was quantified with the Vi-cell automated cell counter.  $1 \times 10^5$  cells in 100 $\mu$ l volume were added to one round bottom glass FACS tube. Then the appropriate primary antibody was added to each tube (Table 2-4). Separate tubes were allocated for the appropriate IgG isotype and negative controls. All tubes were incubated on ice for 20 minutes and protected from light. Then all samples were washed three times with BD Bioscience wash assist. In case of unconjugated antibodies, cells were stained with the appropriate secondary antibody and incubated again on ice for 20 minutes, protected from light. Finally, the cells were washed three times and DAPI (1 $\mu$ g/ml) was added. FACS analysis was performed with LSRII or FACS Canto (BD Bioscience). FITC was detected using 488/520 channels, Alexa 647 was detected with 638/660 channel, Dapi, PE-Cy5.5 and PE were detected using 407/450, 488/710 and 488/585 settings.

Each analysis was performed with  $3 \times 10^4$  events and all viable cells were included in the final data analysis. All FACS data were displayed as dot plots or histograms and the gates were allocated based on negative and isotope controls. In all FACS experiments each marker was tested with three technical replicates.

## **2.9 ELISA (Enzyme-Linked Immunosorbent Assay)**

$5 \times 10^4$  CDCs at passage 2 were seeded per well of a six-well plate and 3ml of CGM was added into each well. Cells were incubated in normoxia or 3% O<sub>2</sub> for 48 hours. Three

technical replicate wells were used for each condition. At 80-90% cell confluency, the cell culture medium was removed and centrifuged at 1000 rpm for 8 minutes to remove cell debris. Vegf levels in the cell supernatant were measured after a 2-step dilution with Vegf ELISA kit, following the manufacturer's instructions (RD system) and the optical density was measured with MultiScan Ascent, Thermo LabSystems at 560 nm. Finally, the results were normalised against the standard controls provided with the kit and the results presented as pg/ml of the supernatant.

Primary Antibody	Stock concentration	Working concentration	Source & Cat. No
Sca-1	0.2mg/ml	1µl in 100µl	eBioscience (558162)
cKit	0.2mg/ml	1µl in 100µl	eBioscience (14-1172-82)
CD90	0.5mg/ml	1µl in 100µl	BD Pharmingen (553006)
CD31	0.5mg/ml	1µl in 100µl	BD Pharmingen (550274)
CD34	0.5mg/ml	1µl in 100µl	BD Pharmingen (560230)
Flk1	0.5mg/ml	1µl in 100µl	BD Pharmingen (561252)
Eng	0.5mg/ml	1µl in 100µl	eBioscience (14-1051-85)
CD45	0.5mg/ml	1µl in 100µl	eBioscience (11-0451-81)
Secondary Antibody	Stock concentration	Working concentration	Source
Goat anti-Rat Alexa-647	2mg/ml	1µl in 100µl	Invitrogen (A-21247)

**Table 2-4 The primary (Rat antibodies) and secondary antibodies used to immunophenotype CDCs.**

## 2.10 Quantitative RT-PCR

### 2.10.1 Primer design

Primer sequences used in this study were obtained from the primer Bank website. Further assessment of each primer pair in terms of cDNA sequence of the gene of the interest was obtained from the NCBI genome browser and BLAST search in order to confirm their specificity and coverage of exon boundary regions. This step was important to eliminate products that derived from possible genomic contaminations.

### 2.10.2 RNA isolation

Two methods were used for RNA isolation (Trizol and Qiagen RNA isolation kit) from approximately 10<sup>6</sup> neonatal or adult derived CDCs at passage 2.

Trizol is a hazardous chemical therefore all steps with Trizol were carried out in a designated hood. Due to the vulnerable nature of RNA, all tips were filter protected and

UV light was used for at least 20 minutes followed by cleaning the working area with RNase Zap wipes (Invitrogen) prior to RNA and qRT-PCR procedures in order to eliminate any possible RNase contamination.

### **2.10.3 RNA isolation with Trizol**

CDCs at passage 2 were incubated with accutase for 10 minutes at 37°C. For each 3% O<sub>2</sub> on normoxia conditions, cell suspension from 1 T75 flask at 80-90% confluency was transferred into 50 ml falcon tubes and centrifuged at 1000 rpm for 8 minutes. Then 1 ml trizol was added to the cell pellet and incubated for 5 minutes. After transferring the suspension into an Eppendorf tube, 200µl chloroform was added and shaken vigorously for 15 seconds. Following 2-3 minutes' incubation at room temperature and centrifugation at 12,000 G for 15 minutes, the upper layer was transferred into a new tube and 500µl isopropanol was added; after a vigorous mixing for 30 seconds the samples were incubated for 10 minutes on ice. Following another centrifugation (12,000 G for 15 minutes, 4°C) and removing the supernatant, 500 µl of 75% ethanol (diluted with RNA-free Diethylpyrocarbonate (DEPC) treated dH<sub>2</sub>O) was added. After vortexing for 20 seconds and spinning down at 7,500 G for 5 minutes 4°C, the ethanol was removed and the RNA pellet was air dried for 5 minutes. Before drying completely, RNase-free water was added to the pellets. After measuring the amount of RNA in each sample, all RNA samples were treated with DNase turbo (Life Technologies) to minimize genomic DNA contamination. 7.5µg of RNA was mixed with 5µl of DNase I Reaction Buffer. Then 1 unit of DNase enzyme was added and the mixture and total volume were made up to 50 µl. After 30 minutes' incubation at 37°C, 5µl of inactivation buffer was added. The solution was centrifuged at 7,500G at 4°C then the supernatant removed and the concentration of RNA in each sample was measured with nanodrop (ND-1000 Thermo spectrophotometer) at 260 nm absorbance. The purity of the RNA was assessed based on the ratios displayed. If A<sub>260</sub>/A<sub>280</sub> was above 2.0 and A<sub>260</sub>/A<sub>230</sub> was between 1.8-2.2, the samples were considered as pure RNA and were used directly for cDNA preparation.

### **2.10.4 Complementary DNA (cDNA) preparation**

cDNA preparation was performed using the high capacity cDNA reverse transcription kit (Applied Bioscience). The procedure started with 1µg RNA in 10µl DEPC-dH<sub>2</sub>O,

then 2µl of 10X reverse transcription buffer, 2µl 10X random primers, 0.8µl of dNTP, 2µl of reverse transcriptase enzyme were added and the final volume made up to 20µl with DEPC treated dH<sub>2</sub>O. Using BioRad C1000 thermal cycler the mixture was incubated for 10 minutes at 25°C and followed by 120 minutes at 37°C and 85°C for 5 minutes. Finally, the samples were cooled down to 4°C and stored at -20°C till required.

### 2.10.5 qRT-PCR analysis of CDCs

All experiments were carried out in 10µl reaction in a 384-well plate containing 5µl SYBR Green Master Mix (Sigma), and 10 µM (1µl) of forward and reverse primers (listed in table 2-5). The final volume was made up to 10µl by adding 3µl of DEPC-treated dH<sub>2</sub>O. The thermal profile for all SYBR Green qRT-PCR reactions was 95°C for 10 min, followed by 40 cycles of 95°C for 10s and 60°C for 30s using an ABI Fast Real Time PCR System (7900 HT). All samples were analysed in triplicate with three housekeeping genes used as reference controls (*Gapdh*, *B-actin* and *Rps19*).

Gene	Sequence 5'-3'	Expected size bps	Tm °C	Efficiency
<i>Gapdh</i>	F: AACTTTGGCATTGTGGAAGG	132	60	95%
	R: AGAACATCATCCCTGCATCC			
<i>B-Actin</i>	F: GGCTGTATCCCCCTCCATCG	154	60	98%
	R: ACATGGCATTGTTACCAACTGG			
<i>Rps19</i>	F: GCTTGCCTCTAGTGTCC	75	60	97%
	R: TGAGACCAATGAAATCGCCAA			
<i>Hprt</i>	F: TCAGTCAACGGGGGACATAAA	124	60	93%
	R: CTGGTTAAGCAGTACAGCCCC			
<i>Sca-1</i>	F: TCAGGAGGCAGCAGTTATTGTG	160	60	95%
	R: CGTGAAGACTTCCTGTTGCCA			
<i>cKit</i>	F: CTCCCCAACAGTGTATTAC	90	60	95%
	R: TAGCCCGAAATCGAAATCTT			
<i>Abcg2</i>	F: GATGAACTCCAGAGCCGTTAGGAC	169	60	94%
	R: AACCTGGCCTTAATGCTATTCTG			
<i>Eng</i>	F: CTGCCAATGCTGTGCGTGAA	191	60	95%
	R: ACTTGGCCTACGACTCCAGCC			
<i>Vegf</i>	F: CTTGTTTCAGAGCGGAGAAAGC	125	60	97%
	R: AACGAACGTA CTTGCAGAGTG			

**Table 2-5 The list of primers used for qRT-PCR analysis of CDCs.** All primers are from pga.mgh.harvard.edu. Primer efficiency was measured automatically with applied bio systems real-time PCR software using 5 dilutions of DNA sample from neonatal and adult CDCs (100ng, 10ng, 1000pg-100pg and 10pg).



## **2.11 Histological staining procedures**

### **Solutions:**

10x Phosphate Buffered Saline (PBS). KCl (2g), NaCl (80g), Na<sub>2</sub>HPO<sub>4</sub> (14.4g) and KH<sub>2</sub>PO<sub>4</sub> dissolved in 800ml of ddH<sub>2</sub>O and the pH adjusted to 7.4 with HCl and the final volume made up to 1 litre with milli-Q H<sub>2</sub>O.

0.2% Para Formaldehyde (PFA)/PBS. 0.2g of para-formaldehyde powder was added to 100ml of 1x PBS and dissolved at 60°C.

Scott's tap water. 30.0g of MgSO<sub>4</sub> and 2.0g Sodium bicarbonate, dissolved in 3 litres of Tap water

### **2.11.1 Interaperitoneal (IP) injection of tamoxifen**

In order to activate *Cre-ERT*, 5 interaperitoneal injections of 2 mg (10mg/ml) Tamoxifen, diluted in peanut oil (Sigma) over 5 consecutive days were administered in adult mice (6-8 weeks). At 48 hours following the last injection the mice were euthanized and the hearts were processed for tissue staining.

### **2.11.2 Tissue processing and preparation of frozen samples**

Sub-dermal matrigel plugs and heart tissues were dissected from adult mice (age 6-8 weeks) after cervical dislocation. The tissue was washed in ice cold PBS twice and fixed with 0.2% PFA/PBS at 4°C overnight. The next day the tissue was incubated in 30% sucrose/PBS with gentle agitation at 4°C. Finally the tissue was frozen down with OCT freezing medium on dry ice and transferred to a -80°C freezer until sectioning.

### **2.11.3 Cryosectioning of frozen tissue.**

All frozen tissue blocks were sectioned using a Microm HM 560 Cryostat (Thermo Scientific). Frozen tissue blocks were kept at -20°C for 30 minutes prior to sectioning. 8-12µm-thick serial sections were prepared for heart tissue and 10-25µm-thick serial sections were prepared for matrigel plugs. Sections were mounted on polylysine glass

slides (VWR International). Then the slides were left to dry for 30-45 minutes at room temperature before storing in slide mailers in a -80°C freezer.

#### **2.11.4 Immunohistochemistry with Vectastain ABC system**

Matrigel plug cryo-sections were removed from the -80°C freezer and allowed to reach room temperature for 30 minutes inside the slide mailers in order to minimise condensation. Then the slides were air-dried outside of the slide mailers (RT) for 30-45 minutes. When the slides dried completely they were washed with 1x PBS and circled with a hydrophobic barrier pen. The sections were blocked with a blocking solution (5% Rabbit serum diluted in 1x PBS). To block unspecific biotin binding sites the sections were blocked with Avidin/Biotin buffers (Vector Laboratories). The sections were incubated with Avidin block for 15 minutes and washed with PBS. Then the sections were treated with Biotin block for 15 minutes and washed again. All sections were then incubated with primary anti-CD31 antibody (BD Pharmingen, diluted to 1/50 with blocking solution) overnight at 4°C. The next day, the slides were washed for three times with 1x PBS (each 5 minutes) and then incubated with secondary rabbit anti rat antibody (Vector Laboratories 1/200 diluted in blocking solution) for 30 minutes at room temperature. All sections were washed again for 3x5 minutes in 1x PBS and incubated with ABC reagent for 30 minutes. After 3 x 5 minutes washes with 1x PBS, all sections were incubated for 1 minute at room temperature with the liquid DAB kit (BioGenex). Then the slides were quickly rinsed under tap water and then stained with Mayer's haematoxylin counterstain (RA Lamb) for 3 minutes and rinsed under running tap water. Then the sections were dehydrated with 50%, 70% and 100% ethanol respectively (5 minutes each), and finally, the slides were incubated in histoclear for 10 minutes and mounted with histomount (National Diagnostics) and allowed to dry in the fume hood.

#### **2.11.5 H & E staining**

Cryosections from matrigel plugs and murine hearts were stained in Mayer's Haematoxylin for 2-3 minutes and then rinsed in tap water for 2 minutes. Then the slides were treated with Scott's tap water for 10-15 seconds to allow the sections to turn

into a blue colour. After one more wash with tap water the slides were then stained with Eosin for 45 seconds. Then the slides were washed once in tap water and dehydrated through the series of ethanol steps (50%, 70% and 100% ethanol for 5 minutes each). Finally, the slides were treated with histoclear for 10 minutes and mounted with histomount and the slides left to dry in the fume hood.

### **2.11.6 Immunofluorescent staining of heart and matrigel plugs**

Matrigel plug cryo-sections and heart sections were removed from the -80°C freezer and allowed to reach room temperature for 30 minutes inside the slide mailers in order to minimise condensation. When the sections dried completely outside the slide mailers in room temperature, they were washed with 1x PBS and circled with a hydrophobic barrier pen. The sections were blocked with blocking solution (5% Goat serum + 1% BSA and 0.5% Tween 20 diluted in 1x PBS). The sections were then incubated with the appropriate primary antibody (table 2-6) at 4°C overnight. After 3x5 minute washes in PBS, the sections were incubated with the appropriate secondary antibody for 1 hour at room temperature. After the final 3x5 minute washes with PBS, the sections were mounted with DAPI prolong gold mountant (vector laboratories) and allowed to dry overnight at 4°C before analysis.

### **2.11.7 Double Immunofluorescent Staining**

Directly conjugated antibodies including (SMA-Cy3 or anti GFP-alexa 488) were added to sections and after 1 hour's incubation at room-temperature, the unconjugated antibodies including CD31, CD11b, FSP1, vimentin and Coll $\alpha$  were used and the co-localisation was assessed. Negative or no primary control sections were prepared for all primaries above to assess the specificity of the staining. Please see tables 2-6 and 2-7 for more details.

Primary antibody Cat. No.	Working concentration	Incubation	Secondary Antibody Cat. No.
CD31(550274) BD Pharmingen	1/50	Overnight @4°C	Anti-Rat alexa-594 (Invitrogen A11007)
SMA-Cy3.3 Sigma(C6198)	1/200	30 minutes room Temperature	n/a
CD11bBD Pharmingen (553308)	1/100	30 minutes room Temperature	Anti-Rat alexa-594 (Invitrogen A11007)
GFP-alexa 488 Invitrogen (A21311)	1/25	30 minutes room Temperature	n/a
GFP (Ab13970) Abcam	1/100	Overnight @4°C	Anti-chicken alexa-488 (Life technologies A11039)
GFP (TP401) Amsbio	1/100	Overnight @4°C	Anti-rabbit alexa-594 (Invitrogen A11012)
FSP1(07-2274) Milipore	1/200	Overnight @4°C	Anti-rabbit alexa-594 (Invitrogen A11012)
vimentin (Ab24525) Abcam	1/200	Overnight @4°C	Anti-chicken alexa-488 (Life technologies A11039)
Col1 $\alpha$ 2 Abcam	1/100	Overnight @4°C	Anti-Rabbit alexa-594 (Invitrogen A11012)

**Table 2-6 Primary and secondary antibodies used to stain cryosections of heart and sub-dermal matrigel plugs.** All secondary antibodies were diluted in 1/200 ratio in the blocking solution using serum of the species in which the secondary antibody had been raised.

Experiment	Antibody set one( primary Ab + secondary Ab)	Antibody set two (YFP or GFP)	Tissue type
Vimentin+eYFP	Vimentin (24525) + Anti- chicken alexa-488 (A11039)	GFP (TP401) + Anti-rabbit alexa- 594 (A11012)	Adult murine heart
FSP1+eYFP	FSP1(07-2274) + Anti-rabbit alexa-594 (A11012)	GFP (Ab13970) + Anti-chicken alexa-488 (A11039)	Adult murine heart
CD31+eGFP	CD31(550274) + Anti-Rat alexa-594 (A11007)	GFP-alexa 488 (A21311)	Matrigel plug
$\alpha$ SMA+eGFP	SMA-Cy3.3 (C6198)	GFP-alexa 488 (A21311)	Matrigel plug
CD11b+eGFP	CD11b (553308) + Anti-Rat alexa-594 (A11007)	GFP-alexa 488 (A21311)	Matrigel plug

**Table 2-7 The combination of antibodies used in double immunofluorescent staining experiments.**

## **2.12 Mouse model of in vivo angiogenesis using sub-dermal matrigel plugs**

### **2.12.1 Matrigel preparation**

Growth factor reduced Matrigel (BD Bioscience) was thawed at 4°C and kept on ice to maintain its liquidity. Other equipment including all pipettes, tips and syringes were kept at 4°C in order to prevent matrigel solidification during preparation, cell inoculation and subdermal injection.

### **2.12.2 Pre injection preparation**

Prior to sub-dermal injection the small animal heat pad (Harvard apparatus) was cleaned with 70% ethanol and the ventilator was checked for functionality. A detailed record of the mice was taken including the genotype, sex and age.

### **2.12.3 Induction of anaesthesia**

The mice were placed one by one into the anaesthesia induction chamber (97% O<sub>2</sub>/3% isoflurane, flow rate: 3 litres per minute) for 2 minutes. Then the mice were transferred to an anaesthetic nose cone on the thermal pad to maintain body temperature at 37°C. Isoflurane was reduced to 2.5% at a rate of 2 litres per minute. The flanks were shaved and cleaned with a cotton bud soaked in 70% ethanol.

### **2.12.4 Sub-dermal cell/matrigel injection with neonatal CDCs**

Neonatal CDCs at passage 2 derived from *CAG-farnesylated-eGFP* mice were washed and prepared as a single cell suspension in growth factor reduced matrigel diluted with PBS (200µl matrigel+100µl PBS).  $2 \times 10^6$  cells were suspended in 300µl ice cold Matrigel and were kept for up to 20 minutes on ice prior to sub-dermal injection into C57BL/6 mice, 6 weeks old. At 14 days following matrigel injection the animals were humanely killed and matrigel plugs were dissected and washed twice in ice cold PBS before being frozen in the OCT freezing medium on dry ice. Samples were kept in the -80°C freezer until required.

For vessel quantification with neonatal derived CDCs, the matrigel plugs were serially sectioned (3-6 sections per slide) and every fifth slide was chosen for CD31 staining. One representative section from each slide was imaged and vessel density was measured by manual counting. The total numbers of vessels were normalised against the surface area of the matrigel used.

#### **2.12.5 Sub-dermal cell/matrigel injection with adult CDCs**

CDCs at P2 derived from *CAG-farnesylated-eGFP* adults (6-8 weeks old) were cultured in normoxia or 3% O<sub>2</sub> for 48 hours. CDCs were then washed and prepared as a single cell suspension in undiluted growth factor reduced matrigel. 2 x10<sup>6</sup> cells were suspended in 300µl Matrigel and stored in ice for up to 20 minutes prior to sub-dermal injection. After 14 days the animals were humanely killed and matrigel plugs were dissected. Plugs were washed twice in ice cold PBS, fixed with 0.2% PFA overnight at 4° and then treated with 30% sucrose/PBS overnight at 4°. Finally the plugs were frozen by OCT freezing medium on dry ice and kept in a -80°C freezer until required.

For vessel quantification with adult-derived CDCs, the matrigel plugs were serially sectioned with approximately (3-6 sections per slide) and every fifth slide was chosen for CD31 staining. One representative section from each slide was imaged and vessel density was measured using image J software. The results were normalised against the whole surface area of the matrigel used. Whole surface areas of the matrigel were measured using the Axio vision software (version 4.8) and Carl Zeiss stemi microscope.

#### **2.12.6 *In-vivo* perfusion analysis of sub-dermal matrigel plugs with adult-derived CDCs**

In a separate experiment 2x10<sup>6</sup> adult-derived CDCs from *CAG-farnesylated-GFP* mice were cultured in normoxia or 3% O<sub>2</sub> and suspended in 300µl growth factor reduced matrigel sub-dermally into adult mice recipients (6 weeks old, C57BL/6). After 14 days of the implant injection, 100µl of 50µg of fluorescein-labelled esculentum (tomato) isolectin (Vector Laboratories) was injected through the tail vein. 15 minutes later, the animals were killed humanely, and the plugs were removed and fixed as mentioned above. One ear from each mouse was removed and washed in PBS and imaged directly to assess the perfusion; isolectin expression with the vessels of the ear was used to

confirm the functionality of the perfusion test, prior to examining the perfusion of the matrigel plugs. The matrigel plugs were processed in the same way as sub-dermal matrigel plugs with adult CDCs (please see section 2.12.5) and kept in the -80 freezer (in light-protected boxes) until required.

### **2.13 Microscopy and imaging**

Light microscopy was used to assess cell morphology and clonogenicity using a Zeiss Axiovert 200 inverted microscope. Histochemical stained sections were imaged using Zeiss Axioplan and Zeiss Stemi microscopes. For fluorescent-stained sections a Zeiss Axio Imager II with apotome was used. A Nikon confocal A1-R microscope was used for live cell fluorescent imaging and for spectral analysis of some fluorescent-stained sections. All of the images were taken by digital camera and analysed by ZEN 2013 software for the images taken with Zeiss microscopes, NIS element software was used for the images taken by Nikon microscopes. Image J was used for quantification and for measuring the staining intensity.

### **2.14 Statistical analysis**

To analyse the data SPSS software (version 19, SPSS Inc) was used. To test for normal distribution of data the Shapiro-Wilki normality test was used and if the data were not normally distributed, the data were transformed by taking the log of the data before statistical analysis. The transformed data then were assessed by the Shapiro-Wilki test again to assess their normality and, finally, the subsequent statistical tests were performed. For multiple group data analysis (groups >2) one-way ANOVA was used and subsequent Post-Hoc (Tukey test) was used to compare two independent groups. In all experiments paired t-test and *p* value of <0.05 was defined as being statistically significant.

**Chapter 3 The effect of 3% O<sub>2</sub> culture on neonatal CDCs proangiogenic and stem cell potential**



### 3.1 Introduction

As outlined in the main introduction to the thesis (see sections 1.5.4-7) CDCs have been shown to promote heart repair following myocardial infarction (MI). However, the low survival of transplanted cells into recipient hearts poses a major limitation. This may partly be due to the harsh ischemic condition of the infarcted heart tissue. Strategies designed to overcome this problem such as pre-treating CDCs with physiological O<sub>2</sub> levels [103] or severe hypoxic conditions [73] have been investigated. Tang *et al.* (2009) showed that severe hypoxia (0.1%) can increase murine CLK's ability to survive, though up-regulation of CXCR4/SDF1 and CLKs showed augmented cell migration (*in vitro*). CLKs which have been treated with 0.1% O<sub>2</sub> showed more efficient recruitment into the ischemic myocardium and the infarct size, vascular density and myocardial function were significantly better than in mice treated with cell culture under normoxic conditions[73]. Furthermore, physiological oxygen (5% O<sub>2</sub>) treatment improved EDC production from human cardiac explants and diminished chromosomal aneuploidies. The authors also showed that human-derived CDC cultured in 5% O<sub>2</sub> for 3 days decreased reactive O<sub>2</sub> levels and reduced cell senescence. *In vivo* studies showed that human CDC cultured in 5% O<sub>2</sub> (whole CDC culture duration) showed better cell engraftment and better recovery in comparison to CDC cultured in normoxia [103]. However, the effect of 3% O<sub>2</sub> on CDC characteristics and pro-angiogenic potential is not known. As discussed in section 1.6 this is important to address because the infarct border zone which contains 3% O<sub>2</sub> and is the region of interest for myocardial cell delivery in preclinical and clinical studies. Culturing CDCs in 3% O<sub>2</sub> could be beneficial in three ways: (i) it is very close to the O<sub>2</sub> level of the infarct border zone, which may help to adapt CDCs prior to transplantation; (ii) activation of Hif-1 $\alpha$  in CDCs cultured in 3% O<sub>2</sub> may improve CDC survival and facilitate their pro angiogenic potential; (iii) as 3% O<sub>2</sub> is a mild hypoxia condition, extended CDC culture is possible to achieve more efficient cardiosphere and CDC yields. This chapter aims to address the role of 3% O<sub>2</sub> culture in CDCs, by testing its effect on CDC culture and the possible modifications of the expression of stem cell (Sca-1, cKit, Abcg2) mesenchymal (Eng, CD90) and endothelial (CD31, CD34, Flk1) cell markers.

## 3.2 Results

CDCs were obtained from neonatal hearts (3-6 days old) and cultured in normoxia or 3% O<sub>2</sub>. Figure 3-1 schematically represents different stages of CDC culture in neonatal and adult CDCs.

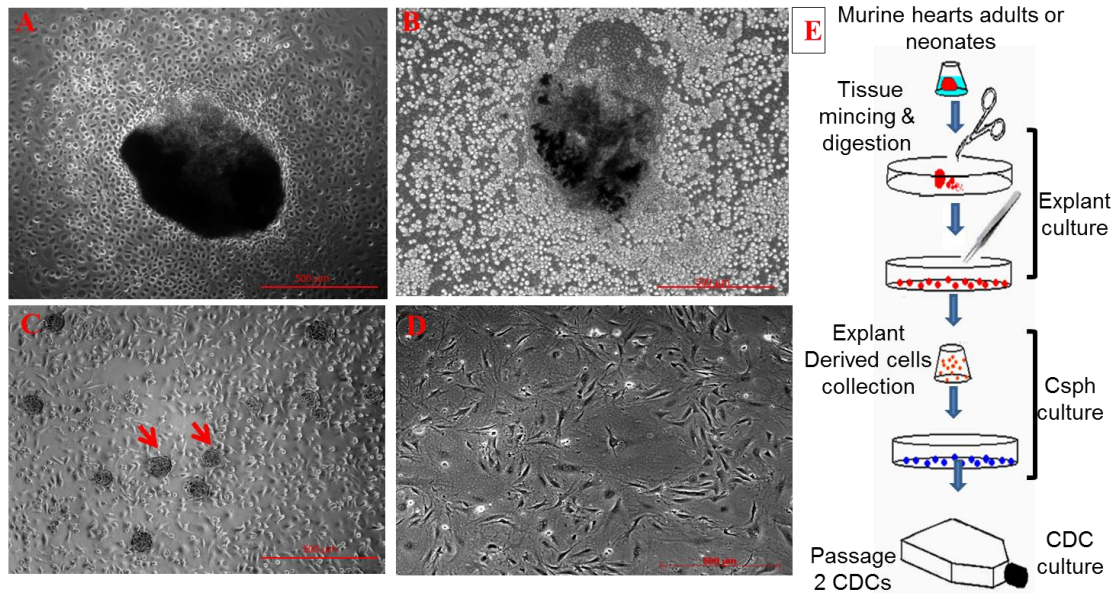


**Figure 3-1 Different stages of Csph and CDC culture.** (A) A small heart explant at day 6, with stromal cells migrating out of the dense explant; (B) the same explant at day 14 with surrounding phase bright cells, myocardial tissue gradually disappears in parallel with increasing explant-derived cell (EDC) density; (C) fully formed Csphs at day 6 (arrows) and, finally, (D) a monolayer cell culture of CDCs – this image is of CDCs at passage 2 (P2), the Scale bar is 500μm. (E) Schematic representation of CDC culture.

### 3.2.1 Optimizing CDC culture with 3% O<sub>2</sub>

CDCs were prepared as described in chapter 2 (Sections 2.4.1-3) and the culture details are summarised in Figure 3-1. I first investigated whether 3% O<sub>2</sub> could improve EDC and Csph yield. In this experiment, explants were cultured in 3% O<sub>2</sub> or normoxia from the date of tissue harvest and the readouts were: (i) extent of phase bright cell outgrowth from cardiac explants; and (ii) number of Csphs generated in normoxia and 3% O<sub>2</sub>. Explant culture was 14 days in normoxia and 3% O<sub>2</sub> groups. The average number of explants analysed per experiment was 111±21 in normoxia and 96±22 in 3% O<sub>2</sub> culture. Csph quantification was from 12 wells of 24-well plates.

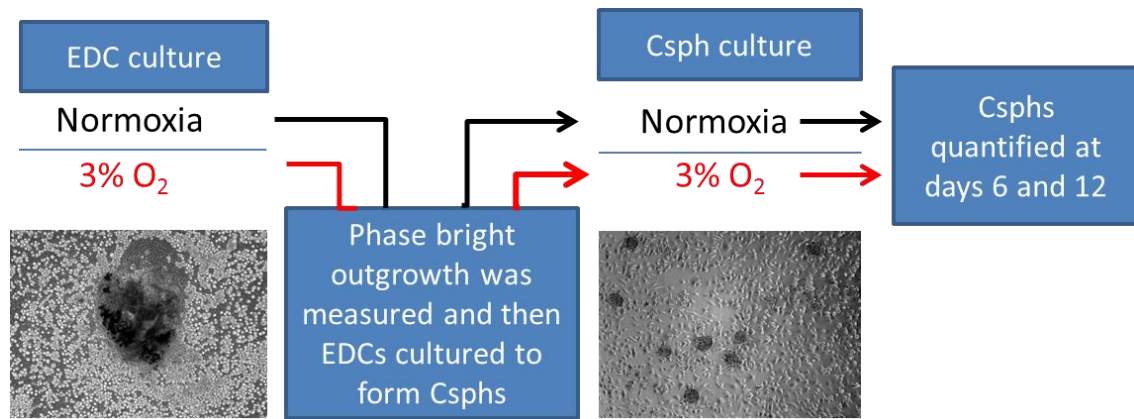


**Figure 3-2 The effect of 3% O<sub>2</sub> on different stages of CDC culture.** CDC culture consists of three stages including: 1) explant culture; 2) cardiosphere; and 3) CDC culture. As shown in the figure each stage was cultured in hypoxia and then the cardiosphere yield were quantified in subsequent stages. This experiment was repeated three times.

### 3.2.2 3% O<sub>2</sub> increases phase bright cell outgrowth but delays Csph maturation

Cardiac explants from 3-6 day-old neonates (strain C57BL/6) were cultured in 3% O<sub>2</sub> and normoxia for 2 weeks. The length of EDC outgrowth was measured at 4 points from the heart explant tissue and presented as the mean outgrowth distance (in micrometres). Despite the positive effect of 3% O<sub>2</sub> on increasing EDC outgrowth (1097±226 μm in normoxia vs. 1502±250 μm in 3% O<sub>2</sub>, p<0.05), further culture in 3% O<sub>2</sub> decreased Csph number and delayed Csph formation time from 6±1 days in normoxia to 10±2 days in 3% O<sub>2</sub> (281±44 Csphs in normoxia vs 201±32 in 3% O<sub>2</sub> p<0.05). Figure 3-3 shows the effect of 3% O<sub>2</sub> treatment on EDC and Csph culture. My findings are in agreement with Li *et al.* (2011)[103], who showed that physiological O<sub>2</sub> (5%) increased EDC outgrowth from human cardiac explants. These results also showed that culturing Csphs in 3% O<sub>2</sub> is not as efficient as normoxia in terms of Csph yield. It is also likely that removing plates from hypoxic incubator in order to change or add fresh media would have introduced oxygenation of cell supernatant, as a result, the level of Hif-1α stabilisation and downstream gene expression and cytokine production involved in Csph formation may have been changed. However, as a result of the detrimental effect of prolonged 3% O<sub>2</sub> culture on Csph maturation, I chose not to continue experiments using EDC culture in 3% O<sub>2</sub>.

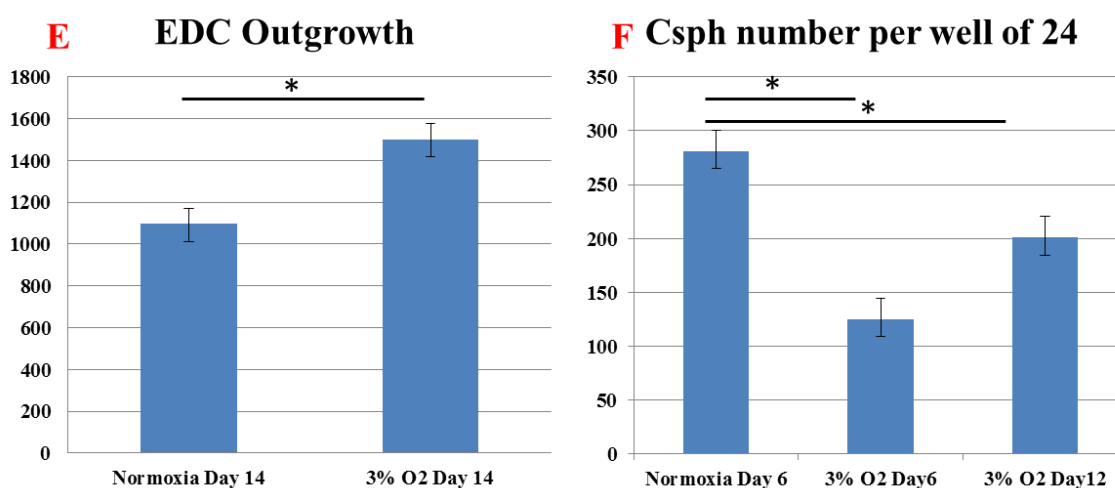
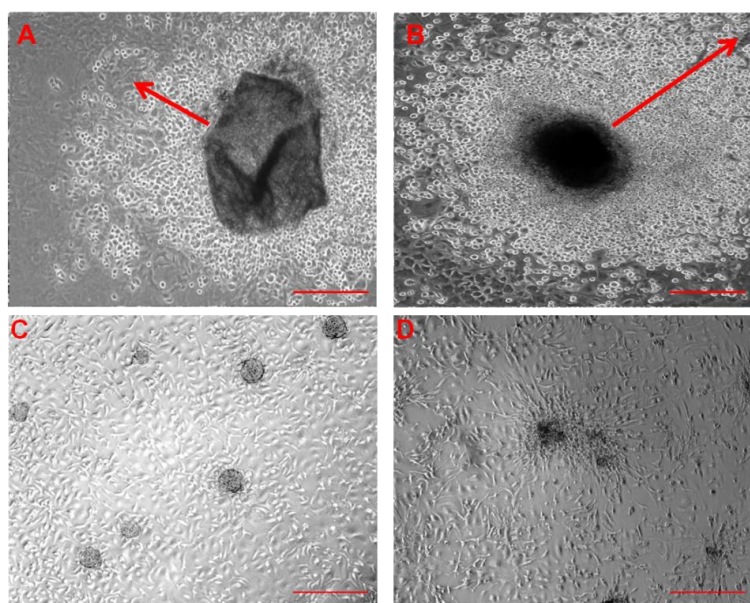


**Figure 3-3 3% O<sub>2</sub> increases EDC outgrowth from neonatal cardiac explants but delays Csph formation.** Cardiac explants cultured in normoxia and 3% O<sub>2</sub> for two weeks and the length of EDC outgrowth were measured for each explant at 4 different points and presented as the mean outgrowth in micrometres. 3% O<sub>2</sub> slightly increased EDC outgrowth in comparison to normoxia. (A) Explant outgrowth in normoxia and (B) in 3% O<sub>2</sub>. To evaluate Csph formation, 10<sup>5</sup> EDCs which had been cultured in normoxia or 3% O<sub>2</sub>, were plated in each well of 24-well plates and cultured in normoxia or 3% O<sub>2</sub> for approximately 2 weeks. While Csphs were fully formed at day 6 in normoxia (C) and were ready for CDC culture, Csphs cultured in 3% O<sub>2</sub> were not mature (D) and remained attached to the plates. E and F show the summary of three independent experiments. (F) The summary of three independent quantifications of Csphs cultured in normoxia (at day 6) and 3% O<sub>2</sub> (at day 6 and 12). (\* p value <0.05)

### 3.2.3 3% O<sub>2</sub> stabilises Hif-1 $\alpha$ protein in CDCs

It is already known that Hif-1 $\alpha$  protein is stabilized in mammalian cells cultured in hypoxic environments. Therefore, any evidence of Hif-1 $\alpha$  protein stabilization would validate the effects of a hypoxic environment. Hif-1 $\alpha$  stabilization in CDCs was evaluated by immunocytochemistry using a specific Hif-1 $\alpha$  antibody in three independent experiments. Passage 2 neonatal CDCs cultured in normoxia or 3% O<sub>2</sub> for 72 hours were analysed and quantified based on the stabilization of Hif-1 $\alpha$  protein and the results are summarised in Figure 3-4.C. The numbers of cells expressing Hif-1 $\alpha$  was quantified in 20 microscopic fields of view (x60) and normalised against the total cell number and presented as the mean percentage  $\pm$  SEM. Results showed that 69.8 $\pm$ 1.8% of CDCs express Hif-1 $\alpha$  following 72 hours of culture in 3% O<sub>2</sub> vs 6.7 $\pm$ 4.3% in normoxia,  $p < 0.05$ .

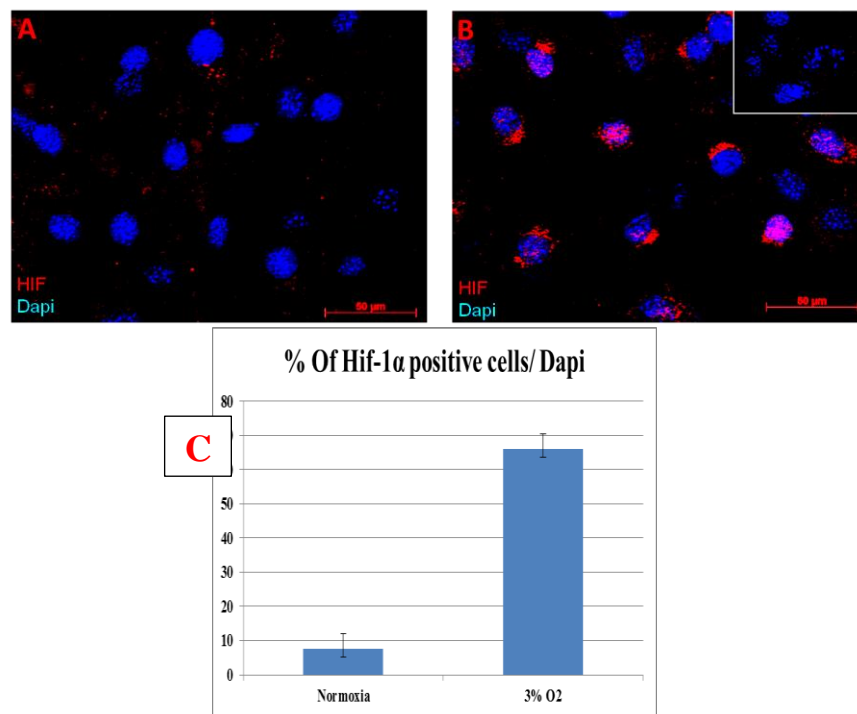


**Figure 3-4 Hif-1 $\alpha$  protein stabilization in passage 2 neonatal CDCs cultured in 3% O<sub>2</sub>.** CDCs stained with anti-Hif-1 $\alpha$  specific antibody and detected with an anti-rabbit secondary antibody conjugated with alexa 594 (red). CDCs were cultured in (A) normoxia or (B) 3% O<sub>2</sub> for 72 hours and Dapi (blue) was used to stain nuclei. (C) A summary of three independent quantification of Hif-1 $\alpha$  positive cells in 20 different microscopic fields from each experiment. It appears that Hif-1 $\alpha$  is stabilized in the majority of P2 murine CDCs after 72 hours of 3% O<sub>2</sub> culture. Inset image B is the no primary control. Scale bar = 50  $\mu$ m.

### 3.2.4 The effect of 3% O<sub>2</sub> on P2 neonatal CDC proliferation and viability

Hif-1 $\alpha$  is shown to activate hypoxia-mediated apoptosis and reduces proliferation in embryonic stem cells [111]. However, it seems that the effect of hypoxia on cell proliferation is cell- and context-dependent. Therefore, I performed proliferation and viability assays to assess the effect of 3% O<sub>2</sub> on CDC proliferation and viability. Passage 2 neonatal CDCs cultured in normoxia or 3% O<sub>2</sub> for 24, 48 and 72 hours were enzymatically detached and assessed for viability and proliferation using automated cell counter Vi-Cell XR 2.03 (Beckman/Coulter). Results showed no difference in viability or cell proliferation in normoxia and 3% O<sub>2</sub> (Figure 3-5). The total cell count revealed that CDCs grow at a similar rate in normoxia and 3% O<sub>2</sub> culture. This experiment was done three times independently, which suggested that 3% O<sub>2</sub> treatment of CDCs did not increase cell death in comparison to normoxic culture and would be suitable for pre-conditioning of CDCs prior to injection into the infarct border zone in heart repair therapy.

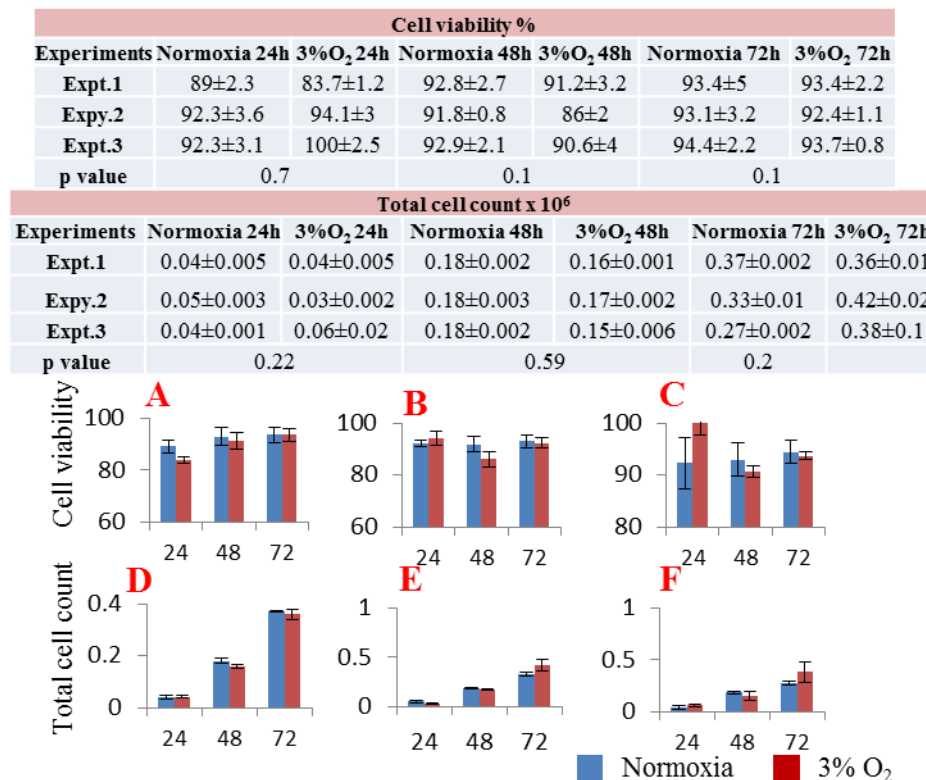


**Figure 3-5. Evaluating the effect of 3% O<sub>2</sub> on total cell count and viability of neonatal CDCs.** Viability and total cell count were analysed with the automated cell counter (Coulter) after single cell suspension in PBS. (A-C) Three independent experiments evaluating viability of neonatal CDCs cultured in normoxia and 3% O<sub>2</sub>. The results revealed that 3% O<sub>2</sub> has no significant effect on the viability of CDCs. (D-F) Three independent experiments evaluating total cell count of CDCs cultured in normoxia and 3% O<sub>2</sub>, shows that 3% O<sub>2</sub> had no significant effect on the total cell count. The bar graphs show the mean (and standard error) of three technical replicates in each case.

### 3.2.5 The effect of 3% O<sub>2</sub> on CDC clonogenicity

Physiological (5 % O<sub>2</sub>) and severe hypoxia (0.1% O<sub>2</sub>) have been shown to improve cardiac stem cell production and potency for myocardial repair [73,103]. However, application of severe hypoxia (0.1%) used in one of these publications led to a high mortality of CDCs (Gangjian Qin, personal communication) so I investigated if 3% O<sub>2</sub> as a mild hypoxic cell culture environment could increase CDC clonogenicity. To analyse clonogenicity, neonatal CDCs at passage 1 were cultured for 72 hours in normoxia or 3% O<sub>2</sub>. 100µl of cell suspension (diluted to 1 cell/100µl of media) were added to each well of 96-well plates. All wells which received one cell were identified under the microscope and clonogenicity was monitored over the following 6 weeks in normoxia. At day 42 the number of colonies were quantified and normalized against the total number of wells with one cell and results presented as clonogenicity percentage ± SEM. This experiment was performed independently three times and results showed that 3% O<sub>2</sub> did not significantly change CDC clonogenicity. Figure 3-6 shows a representative single cell (3-6.A), the colony formed after 14 days from the same cell (3-6.B) and (3-6.C) is the summary of clonogenicity percentage derived from three independent studies. Table 3-1 summarises the results of three independent clonogenicity experiments.

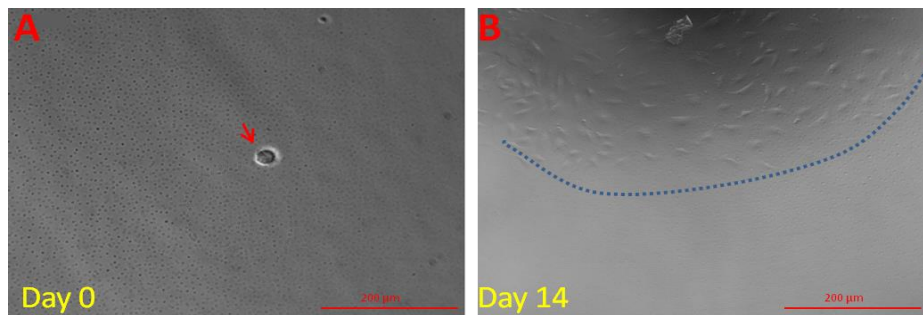


**Figure 3-6 The effect of 3% O<sub>2</sub> on the clonogenicity of passage 2 neonatal CDCs.** Single cell suspensions of CDCs were prepared and 100µl of cell suspension (diluted to 1cell/100µl of media) was manually placed in each well of a 96-well plate. (A) A single CDC at day 0. (B) The colony formed from the same cell after 14 days: the edge of the colony is highlighted with a blue line. Scale bar =200 µm. (C) The graph summarise three independent clonogenicity experiments with neonatal CDCs cultured in normoxia and 3% O<sub>2</sub>.

Experiments	Normoxia	3% O <sub>2</sub>
Expt.1	8.48±1.4%	6.8±1.4
Expt.2	7.07±4.4	7.4±1.9
Expt.3	5±2	5.9±2.7
P value	0.9	

**Table 3-1 The summary of three independent clonogenicity assays performed with neonatal mouse CDCs at passage 2 cultured in 3% O<sub>2</sub> or normoxia.** CDCs cultured in 3% O<sub>2</sub> or normoxia for 72 hours at passage 1, then single cells were manually placed in each well of a 96-well plate and clonogenicity assessed after 6 weeks. Data presented as mean percentage ± SEM, derived from 3 technical replicates. Paired t-test showed that there is no significant difference between normoxia and 3% O<sub>2</sub>.

As this study is aiming to assess the effect of 3% O<sub>2</sub> on progenitor and endothelial sub-populations of CDCs, I next assessed expression of stem cell and endothelial markers at mRNA and protein levels. qRT-PCR is an efficient method for assessing the level of gene expression in *in-vitro* and *in-vivo* studies; however, choosing suitable housekeeping genes is crucial in gene expression analysis.

### 3.2.6 Selection of housekeeping genes for qRT-PCR experiments with CDCs cultured in normoxia and 3% O<sub>2</sub>

Due to the mixed population of CDCs, validating housekeeping genes with a relatively constant level of expression in normoxia and 3% O<sub>2</sub> is very important as it directly influences the interpretation of qRT-PCR. During the gene expression analysis of stem cell markers (*Sca-1*, *cKit*, *Abcg2*) and endothelial genes (*Vegf* & *Eng*), in CDCs treated with normoxia and 3% O<sub>2</sub>, I noticed that the *Hprt* housekeeping gene had the least stable Ct values at different time points of the 3% O<sub>2</sub> culture, which was consistent in three independent experiments. Simultaneously, a group at Oxford University reported that *Hprt* is not a suitable housekeeping gene for studies with CDCs [112]. Therefore, in subsequent qRT-PCR studies the *Hprt* gene was excluded from the list of housekeeping genes used for data normalisation. However in general I noticed that the Ct value of all genes increased at 72 hours in comparison to the other time points, (either in normoxia or 3% O<sub>2</sub> culture). This could be due to some technical issues such as cell pellet preparation and RNA isolation at 72 hours. It is also possible that the increased Ct levels at this time point is due to the effect of high cell density on gene expression. In



this respect Pallen and Tong (1991) showed that high cell density in fibroblast culture increased cell density-dependent growth-arrest [113] and in another study high cell confluency increased DNA methylation (~50%) of the MGMT CpG island in fibroblast cells and modified significantly gene expression levels [114]. Table 3-2 summarises the Ct values from three independent qRT-PCR analyses with neonatal CDCs treated with normoxia and 3% O<sub>2</sub> for different time points.

Exp.	Time points	<i>Gapdh</i>		<i>B-actin</i>		<i>Rps19</i>		<i>Hprt</i>	
		3% O <sub>2</sub>	Normoxia	3% O <sub>2</sub>	Normoxia	3% O <sub>2</sub>	Normoxia	3% O <sub>2</sub>	Normoxia
Exp.1	3 hours	16.9±0.3	16.5±0.2	14.4±0.56	14.3±0.3	-	-	19.3±0.2	18.1±0.3
	6 hours	16.4±0.26	16.2±0.12	14.1±0.32	14.7±0.5	-	-	19.7±0.11	19.4±0.43
	24 hours	16.2±0.45	16.3±0.3	14.7±0.14	13.4±0.4	-	-	21.5±0.24	19.5±0.2
	48 hours	15.8±0.25	16±0.4	14.4±0.2	14.5±0.4	-	-	20.4±0.21	19.4±0.3
	72 hours	19±0.41	18.40±0.5	18.2±0.38	17.7±0.2	-	-	22.6±0.23	22.5±0.4
Exp.2	3 hours	18.6±0.27	18.2±0.21	15.4±0.31	14.9±0.3	17.7±0.21	17.6±0.2	22.3±0.41	20.6±0.4
	6 hours	18.3±0.25	18.6±0.3	14.9±0.48	15.2±0.4	17.4±0.52	17.3±0.2	21.9±0.21	20±0.3
	24 hours	18.7±0.17	18.2±0.18	15.9±0.24	15.3±0.3	17.4±0.37	17.9±0.4	23.4±0.34	21.1±0.4
	48 hours	18.7±0.24	18.4±0.4	15.3±0.31	15.2±0.14	17.3±0.3	16.9±0.4	24.3±0.41	21.7±0.3
	72 hours	19.9±0.48	20.2±0.4	17±0.22	16.8±0.34	18.4±0.41	18.2±0.3	23.9±0.46	24.1±0.5
Exp.3	3 hours	18.1±0.51	17.9±0.3	14.5±0.28	14.2±0.4	18.4±0.46	18.7±0.1	21.7±0.15	21.3±0.4
	6 hours	18±0.23	18±0.3	14.4±0.24	14.2±0.34	17.3±0.21	18.1±0.3	22.4±0.32	21.6±0.43
	24 hours	17.4±0.31	18.1±0.32	14.1±0.44	13.8±0.52	17.5±0.28	17.8±0.4	23.1±0.24	20.4±0.6
	48 hours	17.5±0.36	17.3±0.38	13.9±0.32	1.5±0.28	17.4±0.1	17.1±0.3	22.6±0.17	21.8±0.43
	72 hours	18.2±0.34	18.5±0.48	14.8±0.41	15.1±0.3	18.5±0.2	18.2±0.4	24.4±0.1	24.4±0.5

**Table 3-2 Summary of the Ct values from four candidate housekeeping genes: *Gapdh*, *B-Actin*, *Rps19* and *Hprt*, in qRT-PCR experiments performed with RNA isolated from neonatal CDCs cultured in normoxia or 3% O<sub>2</sub> for 3, 6, 24, 48 and 72 hours. As shown in the table, Ct values from the *Hprt* housekeeping gene was the least stable of the housekeeping genes; therefore, the *Hprt* gene was excluded from the list of housekeeping genes.**

### 3.2.7 The effect of 3% O<sub>2</sub> on gene expression in neonatal CDCs

Using qRT-PCR I analysed neonatal CDCs at passage 2 cultured in 3% O<sub>2</sub> or normoxia for 3, 6, 24, 48 and 72 hours. I compared the gene expression profile of 3 stem cell markers *Sca-1*, *cKit*, *Abcg2*, and the mesenchymal/endothelial marker *Eng* as well as the pro-angiogenic factor, *Vegf*. This experiment was independently preformed three times and data was normalised against *Gapdh*, *B-actin* and *Rps19* at each time point. Figure 3-7 and table 3-3 summarises the results of all three experiments. Among stem cell

markers, *Sca-1* showed the highest expression at 48 hours in experiment 1 and at 24 hours in experiment 2 but in experiment 3 the highest expression of *Sca-1* was observed after 6 hours of 3% O<sub>2</sub> culture. Although variability was observed in all experiments, paired t-test analysis showed that culturing neonatal CDCs in 3% O<sub>2</sub> for 3-6 hours increased *Sca-1* expression and culture for 6 hours in 3% O<sub>2</sub> increased *cKit* expression significantly. Also the levels of *Vegf* and *Eng* increased significantly in comparison to the normoxia counterparts at 24 and 48 hours, respectively. In general, the expression of the majority of the genes decreased after 72 hours of culture in 3% O<sub>2</sub> and normoxia which could be due to the fact that the cells reached confluency at 72 hours and cell-cell contact inhibits cell proliferation and induces quiescence. Also, as discussed above this may impact on gene expression in general and the 72hour time point data may be less robust than the earlier time points.

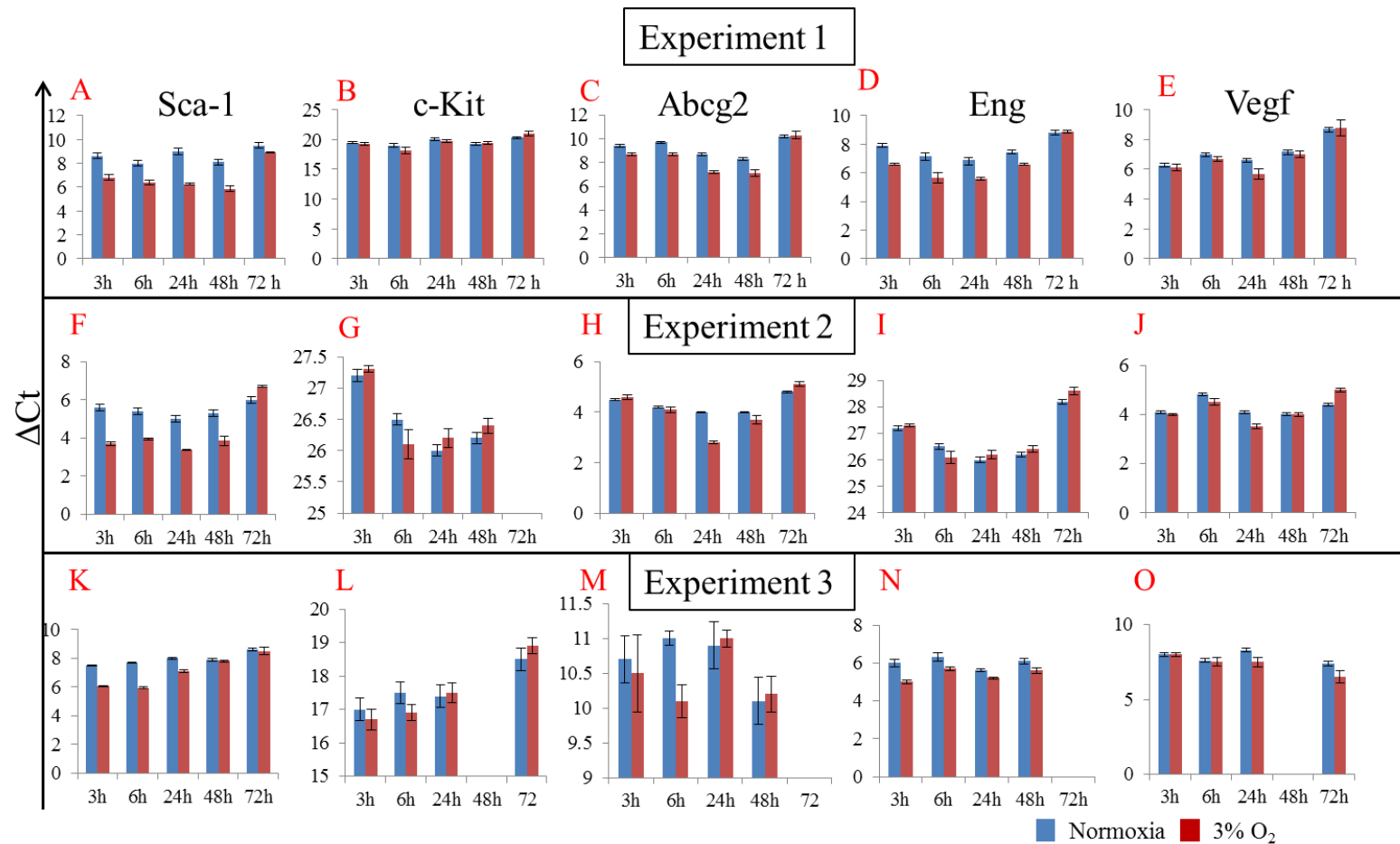


**Figure 3-7 qRT-PCR experiments showing gene expression levels ( $\Delta$ Ct) in neonatal CDCs at passage 2 cultured in 3% O<sub>2</sub> versus normoxia for 3, 6, 24, 48 and 72 hours. *Sca-1*, *cKit*, *Abcg2*, *Eng* and *Vegf* expression was analysed using qRT-PCR at 5 different time points. Ct values were normalised against *Gapdh*, *B-actin* and *Rps19* at all-time points and then 3% O<sub>2</sub> values were compared to the counterpart control cells cultured in normoxia. Results are presented as the mean  $\Delta$ Ct of each gene calculated from three technical replicates per experiment.**

Sca-1										
	Normoxia	3% O <sub>2</sub>	Normoxia	3% O <sub>2</sub>	Normoxia	3% O <sub>2</sub>	Normoxia	3% O <sub>2</sub>	Normoxia	3% O <sub>2</sub>
Experiments	3 hours		6 hours		24 hours		48 hours		72 hours	
Expt.1	8.6	6.8	8	6.4	9	6.25	8.1	5.85	9.5	8.9
Expt.2	5.6	3.7	5.4	3.95	5	3.37	5.3	3.85	6	6.7
Expt.3	7.5	6.04	7.7	5.95	8	7.1	7.9	7.8	8.6	8.5
p value	0.005		0.002		0.08		0.1		1	
cKit										
	Normoxia	3% O <sub>2</sub>	Normoxia	3% O <sub>2</sub>	Normoxia	3% O <sub>2</sub>	Normoxia	3% O <sub>2</sub>	Normoxia	3% O <sub>2</sub>
Experiments	3 hours		6 hours		24 hours		48 hours		72 hours	
Expt.1	19.5	19.3	19	18.1	9	6.25	19.3	19.4	20.3	21
Expt.2	27.2	27.3	26.5	26.1	5	3.37	26.2	26.4	-	-
Expt.3	17	16.7	17.5	16.9	8	7.1	-	-	18.5	18.9
p value	0.38		0.04		0.08					
Abcg2										
	Normoxia	3% O <sub>2</sub>	Normoxia	3% O <sub>2</sub>	Normoxia	3% O <sub>2</sub>	Normoxia	3% O <sub>2</sub>	Normoxia	3% O <sub>2</sub>
Experiments	3 hours		6 hours		24 hours		48 hours		72 hours	
Expt.1	9.4	8.7	9.7	8.7	8.7	7.17	8.3	7.1	10.2	10.3
Expt.2	4.5	4.6	4.2	4.1	4	2.8	4	3.7	4.8	5.1
Expt.3	10.7	10.5	11	10.1	10.9	11	10.1	10.2	-	-
p value	0.3		0.1		0.2		0.34			
Eng										
	Normoxia	3% O <sub>2</sub>	Normoxia	3% O <sub>2</sub>	Normoxia	3% O <sub>2</sub>	Normoxia	3% O <sub>2</sub>	Normoxia	3% O <sub>2</sub>
Experiments	3 hours		6 hours		24 hours		48 hours		72 hours	
Expt.1	7.9	6.6	7.1	5.66	6.9	5.6	7.4	6.6	8.8	8.9
Expt.2	3	2.7	3.8	3.7	3.6	2.5	3	2	3	2.56
Expt.3	6	5	6.3	5.7	5.6	5.2	6.1	5.6	-	-
p value	0.09		0.2		0.07		0.03			
Vegf										
	Normoxia	3% O <sub>2</sub>	Normoxia	3% O <sub>2</sub>	Normoxia	3% O <sub>2</sub>	Normoxia	3% O <sub>2</sub>	Normoxia	3% O <sub>2</sub>
Experiments	3 hours		6 hours		24 hours		48 hours		72 hours	
Expt.1	6.2	6.1	7	6.7	6.6	5.7	7.2	7	8.7	8.78
Expt.2	4.1	4	4.8	4.5	4.1	3.5	4	4	4.4	5
Expt.3	8	8	7.6	7.5	8.3	7.5	7.4	6.5	-	-
p value	0.18		0.07		0.01		0.3			

**Table 3-3** The effect of 3% O<sub>2</sub> on the expression of *Sca-1*, *cKit*, *Abcg2*, *Eng* and *Vegf* in passage 2 neonatal CDCs using qRT-PCR. The table shows the relative expression of *Sca-1*, *ckit*, *Abcg2*, *Eng* and *Vegf* genes cultured in 3% O<sub>2</sub> in comparison to normoxia from 3 hours up to 72 hours. Each value in the table is the mean of three technical replicates and there are a total of three biological replicate experiments (data summarised in Figure 3-7). Data were normalised against three housekeeping genes: *Gapdh*; *B-actin*; and *Rps19* and analysed using the  $\Delta$ Ct of each gene in 3% O<sub>2</sub> versus the normoxia control group. Therefore, the lower the value, the higher the expression. Paired t tests were used to assess significant differences in  $\Delta$ Ct values. The significant differences ( $p < 0.05$ ) are highlighted in red.

### **3.2.8 3% O<sub>2</sub> leads to variable protein expression of endothelial, mesenchymal and stem cell markers in neonatal CDCs.**

To evaluate further the increase seen in *Sca-1* gene expression at the RNA level in P2 CDCs following treatment with 3% O<sub>2</sub>, I used flow cytometry to determine whether there was a similar increase in Sca-1 expression at the protein level. To place this in context I also used a panel of endothelial (Flk1, CD34, CD31), mesenchymal (*Eng*, CD90), haematopoietic (CD45) and stem cell (*cKit*) markers. Figure 3-8 shows representative FACS plots and summarises the results of all three independent experiments as a percentage of positive events for all cell populations analysed. Although CDCs cultured in 3% O<sub>2</sub> showed a trend towards higher levels of Sca-1 and Flk1 compared with normoxia, these differences did not reach statistical significance, likely due to the variability between replicate experiments (Table 3-4). Also the protein levels of *cKit*, CD90, CD45, CD31 and CD34 showed little change between normoxia and 3% O<sub>2</sub>. *cKit* mRNA showed a slight increase at 6 hours of culturing in 3% O<sub>2</sub> ( $p=0.04$ ) but, its protein expression remained unchanged between normoxia and hypoxia. However, there is a noticeable discrepancy between *Eng* and *cKit* mRNA and protein levels. *Eng* appeared to be up-regulated at the mRNA level following treatment with 3% O<sub>2</sub> (48 hours,  $p=0.03$ ), but there was no change in the number of *Eng* positive CDCs in the FACS assay. This difference could be due to protein degradation or a delayed translation rate in *Eng* or *cKit* expressing sub-population of CDCs. It is possible that culturing neonatal CDCs in 3% O<sub>2</sub> for 72 hours was not sufficient enough in order to increase *cKit* and *Eng* protein, although this time point was initially chosen based on qRT-PCR experiments in order to allow enough time for protein translation of the elevated genes. As shown in table 3-4 there is a noticeable degree of variation of protein expression between CDC preparations. For example, Sca-1 expression in normoxia ranged from 9.8% to 28.5%. The highest variability was observed in the CD90 and Sca-1 expression patterns and the lowest variability was seen in the *cKit* and CD45 expressing cells. CD31 and CD34 expression remained below 10% in both 3% O<sub>2</sub> and normoxia groups except experiment 1, where CD31 expression was 16-18%. CD45, the common leukocyte antigen, remained unchanged and at low levels in normoxia and 3% O<sub>2</sub>. CD45 expression analysis showed that the majority of CDCs are not derived from haematological contamination and they are likely to have originated from the heart tissue.

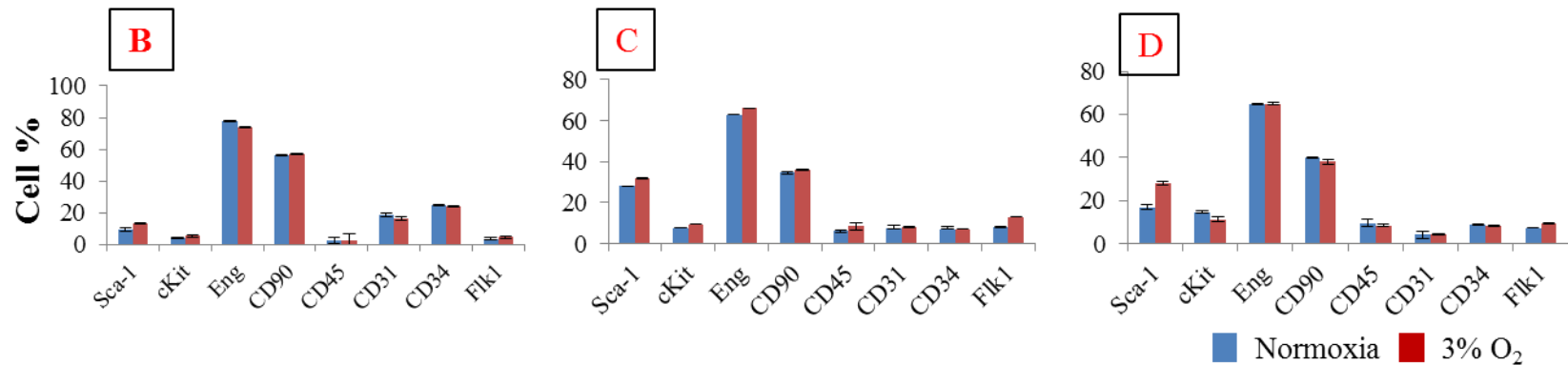
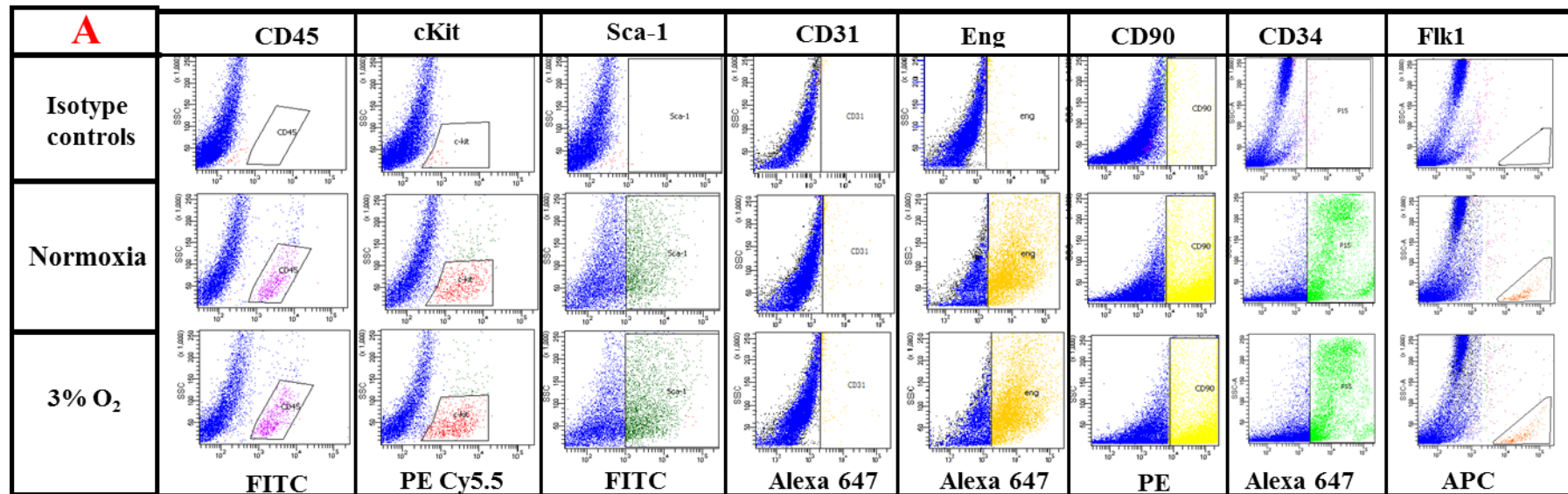


**Figure 3-8** Flow cytometric analysis of murine neonatal CDCs at passage 2 harvested for 72 hours in normoxia and 3% O<sub>2</sub>. CDCs were analysed for the expression of Sca-1, cKit, Eng, CD90, CD45, CD31, CD34 and Flk1. A) Dot plots are showing populations of CDCs at passage 2 expressing the representative markers in normoxia and 3% O<sub>2</sub>. CD45 the pan-leukocyte marker was expressed only in a small fraction of P2 CDCs. B,C and D are the summary of three independent FACS experiments showing the proportion of the cells expressing each marker.

Experiments	Sca-1		cKit		Eng		CD90		CD45		CD31		CD34		Flk1	
	Normoxia	3% O <sub>2</sub>	Normoxia	3% O <sub>2</sub>	Normoxia	3% O <sub>2</sub>	Normoxia	3% O <sub>2</sub>	Normoxia	3% O <sub>2</sub>	Normoxia	3% O <sub>2</sub>	Normoxia	3% O <sub>2</sub>	Normoxia	3% O <sub>2</sub>
Expt.1	9.8 ±0.3	13.1±0.4	4.4 ±0.15	5.3±0.1	78.1±1.8	74.73±3.3	56.6±0.2	57.5±0.5	2.7±0.2	2.5 ±0.1	18.6 ±0.2	16.6	25.5 ±0.2	24. ±0.05	3.7±0.2	4.6±0.2
Expt.2	28.5 ±2.4	32.2 ±1	7.5±1	9.4±1	65.5±3.6	63.5±7.5	35.9±1.9	36.9±1.8	6.5±0.8	8.4±0.4	7.5±0.4	8.0±0.2	7.0±0.8	6.9±0.8	8±1.3	13±1.3
Expt.3	17.4±1.5	28.2±1.7	14.7±0.9	11.3±1.9	65.6±2.9	66.2±1	40.6±3	38.5±0.6	9.6±0.6	8.4±0.9	4.1±0.7	4.4±1.2	8.8±0.5	8.3±0.9	7.3±0.2	9.3±0.4
p value	0.1		0.9		0.3		0.9		0.8		0.6		0.2		0.1	

**Table 3-4 Summary of 3 independent FACS analysis performed with neonatal murine CDCs at passage 2 cultured in normoxia and 3% O<sub>2</sub>.** Culturing CDCs in 3% O<sub>2</sub> has changed the expression of some genes such as Sca-1, cKit, Flk1 and CD45 slightly, but not significantly. As shown in the table Sca-1 and Flk1 showed slight increase in 3% O<sub>2</sub> compared to normoxia but these differences did not reach to significant level due to the variability among the groups. Data presented as mean percentage ± SEM, derived from 3 separate replicates. Paired t-test was performed using the technical means from each experiment and no significant difference observed between the groups.

### 3.3 Discussion

In this chapter I investigated the effect of 3% O<sub>2</sub> on neonatal CDCs and analysed its influence on different stages of CDC culture, gene expression and immunophenotyping. However, my studies of gene expression analysis at mRNA and protein levels showed inter-culture variation in stem cell (Sca-1, cKit, Abcg2), mesenchymal (Eng, CD90) and endothelial (CD31, CD34, Flk1) markers of neonatal CDCs, cultured in normoxia and 3% O<sub>2</sub>. Although I tried to reduce inter-culture variability by following the same cell culture protocol, the following reasons could explain the inter-culture variability: (i) the sex of pups, although Drowley *et al.* (2009) showed that the sex of muscle stem cell donors has no effect on the regenerative capacity of recipients [115], but Crisostomo *et al.* (2007) discovered that female MSC-treated rat hearts had a greater recovery [116]. Due to the high yield of CDCs which I needed for my experiments, I never focused on a specific sex of pups which could have generated variability in CDC culture. (ii) Age of the pups: it has been shown that BM stem cells from young donors have better cellular engraftments after transplantation into rats after MI [117]. In this chapter I used pups aged 3-6 days which could be another reason for variable results with CDCs. For future experiments it would be useful to use pups of the same sex and age (same day) for all CDC experiments.

#### 3.3.1 Validation of hypoxia

As many cellular responses to hypoxia are mediated by Hif-1 $\alpha$ , I validated the stabilisation of this protein in CDCs treated with 3% O<sub>2</sub> for 72 hours and observed that the majority of CDCs (69.8%) show stabilisation of Hif-1 $\alpha$  protein (figure 3-4). It would be more informative to assess Hif-1 $\alpha$  at different time points, in this respect Tang *et al.* (2009) showed that Hif-1 $\alpha$  has the highest stabilisation in CDCs at 10-12 hours in severe hypoxic conditions (0.1%). However, the gold standard of assessing Hif-1 $\alpha$  is western blot experiments – unfortunately, my experiments with Hif-1 $\alpha$  western blotting and its stabilisation timing analysis was not successful, possibly due to its very short half-life (5-8 minutes)[73]. Vegf is a well-known direct target gene of the Hif-1 $\alpha$  pathway, reviewed in [90]. Following the transfer of CDCs to 3% O<sub>2</sub>, I found that *Vegf* mRNA reached a peak of expression after 24 hours compared with the normoxia-treated cells. However, Steinbrech *et al.* (2000) showed that Vegf expression in osteoblasts in



culture increased in 35-40 mmHg (hypoxia), beginning from 6 hours after exposure and peaking (3 folds) at 24 hours [118]. I only observed a modest 1.5 to 1.9 increase in *Vegf* mRNA levels in CDCs cultured in 3% O<sub>2</sub> for 24-48 hours, pre-treating CDCs with severe hypoxic conditions such as (0.1-1% O<sub>2</sub>) could increase *Vegf* more significantly.

### **3.3.2 The effect of 3% O<sub>2</sub> on different stages of CDC culture**

To evaluate the effect of 3% O<sub>2</sub> on different stages of CDC culture, I observed that culturing neonatal explants in 3% O<sub>2</sub> increased EDC outgrowth significantly compared to normoxia (figure 3-3), this result is consistent with Li *et al.* (2011), which showed that EDCs grow faster in physiological O<sub>2</sub> (5%) than in normoxia [103]. As hypoxia is shown to stimulate cell migration via the *perk/atf4/lamp3*-arm pathway [119], it is possible that 3% O<sub>2</sub> may increase cell migration out of the explant. However, careful analysis of the cytokines involved in paracrine activities of EDCs in normoxia and 3% O<sub>2</sub> could explain this finding. My results showed that culturing Csphs in 3% O<sub>2</sub>, delayed their maturation significantly. I observed that culturing cells in 3% O<sub>2</sub> generally increases the acidity of the supernatant (based on the yellow colour of the supernatant of the cells cultured in 3% O<sub>2</sub>, data not shown), and it is already known that cellular acidity enhances apoptosis [120]. As discussed above, hypoxia increases cell migration, and this could possibly explain how Csph-forming cells in hypoxia favour cell spreading and invasion rather than cell accumulation. In this matter Koh *et al.* (2011) showed that overexpressing hypoxia associated factor (HAF) cells grow slowly and had diffused colonies in comparison to the controls. This was due to the effect of HAF on switching from the Hif-1 $\alpha$  to Hif-2 $\alpha$  pathway [121]. Hif-2 $\alpha$  is shown to affect cellular migration and invasion and is shown to be activated in prolonged hypoxia culture, reviewed in [90]. As Csph-forming cells had been in 3% O<sub>2</sub> since the explant culture, thus the Hif-2 $\alpha$  pathway may have been activated and had caused cell migration rather than accumulation. Furthermore, it is possible that the acidity of the media cultured in 3% O<sub>2</sub> reduced the Csph maturation efficiency. According to the CDC culture protocol, every 4 days 200  $\mu$ l of Csph media are added to the plates. To prevent acidification of the media, adding more media with shorter intervals could be useful.

Analysing the effect of 3% O<sub>2</sub> on P2 CDC showed that culturing P2 CDCs in 3% O<sub>2</sub> for 72 hours did not show any significant difference in CDC proliferation and clonogenicity, this finding is consistent with Li *et al.* (2011) and Van Oorschot *et al.*

(2011) [101,103]. Li *et al.* (2011) concluded that proliferation of CDCs at early passages (P1-P3) in physiological O<sub>2</sub> did not change CDC proliferation, although proliferation was higher in later passages (P4-P5) [103]. Van Oorschot *et al.* (2011) also showed that short-term hypoxia culture (1% O<sub>2</sub>/5 days) did not change cardiac progenitor proliferation; however, prolonged hypoxic culture (<6 days) increased cell growth and migration [101]. To increase CDC yields, culturing CDCs at a later passage could generate better yields; however, careful immunophenotyping of CDCs at a later passage seems to be necessary as it is likely that passaging and prolonged cell culture change their stem cell phenotype.

However, there are some other issues that needed to be addressed about the nature of Hif proteins and possible implications for CDC culture variability: (i) stability of Hif-1 $\alpha$  protein. Hif-1 $\alpha$  is shown to have the shortest half-life of approximately 5-8 minutes among all the other proteins [122]. I always changed the medium in a laminar flow hood under room air, which took approximately 3-4 minutes. The hypoxic incubator required almost 5 minutes to re-equilibrate with 3% O<sub>2</sub>. Therefore, the fluctuation in O<sub>2</sub> during the medium change and O<sub>2</sub> recalibration may affect the quality of the expression of the markers at protein and mRNA level; also changing cell culture medium could introduce oxygenation of cell supernatant which could affect the expression of Hif-1 $\alpha$  downstream genes in CDCs. Further experiments with stricter controls of the O<sub>2</sub> level could be useful to decrease the level of variability in CDC surface marker expression. (ii) Hif-2 $\alpha$  which is shown to be another isoform of Hif-1 $\alpha$  has some antagonist effect on Hif-1 $\alpha$ , reviewed in [90]. For instance, while Hif-1 $\alpha$  stabilization produces cell cycle arrest by inhibiting the MYC activation and decreasing cell proliferation [123], activation of Hif-2 $\alpha$  exclusively exhibits enhanced MYC activity and cell proliferation [124]. Further experiments will be necessary to elucidate which isoform of the Hif protein is dominantly active in CDCs following 3% O<sub>2</sub> culture. (iii) It has been shown that Hif expression can be selectively regulated by post-translation activities and epigenetic modifications, reviewed in [125], which could influence Hif-1 $\alpha$  expression and subsequently downstream genes. Due to the heterogeneity of CDCs it is possible that Hif-1 $\alpha$  is selectively regulated in different sub-types of CDCs which leads to the variable expression of surface markers. As I also noticed, not all CDCs cultured for 72 hours in 3% O<sub>2</sub> had their Hif-1 $\alpha$  stabilised (figure 3-4).

### 3.3.3 The effect of 3% O<sub>2</sub> on superficial markers of neonatal CDCs

In order to assess the effect of 3% O<sub>2</sub> on the phenotype of different sub-populations of P2 CDCs, I investigated if 3% O<sub>2</sub> could increase the expression of stem cell (Sca-1, cKit, *Abcg2*), mesenchymal (Eng, CD90) and endothelial (CD31, CD34, Flk1) markers. To do this I used a quantitative RT-PCR approach which depends on data normalisation using housekeeping genes.

#### 3.3.3.1 Defining the proper combination of housekeeping genes for 3% O<sub>2</sub> studies with CDCs

The effect of hypoxia on the expression of housekeeping genes in neonatal and adult CDCs has been studied [112]. Housekeeping genes are considered to have a constitutive level of expression regardless of the age and culture condition, genes such as *Gapdh*, *β-actin*, *Hprt*, and ribosomal proteins are some examples of housekeeping genes which have been used extensively in gene expression analysis such as qRT-PCR. In one study the authors evaluated the most reliable housekeeping genes in CDCs cultured under normoxia, hypoxia or with prolyl-4-hydroxylase inhibitors (PHDIs) derived from both neonatal and adult rats. The aim of study was to determine the effects of ageing and different culture conditions on the stability of the housekeeping gene for CDCs. The results revealed that *Gapdh* was the most constant housekeeping gene for normoxia studies, whereas *β-actin* was the most stable housekeeping gene under hypoxia. The authors also showed that three housekeeping genes *β2M*, *Hprt-1* and *Rplp-1* stability was age-dependent. However they concluded that it is better to combine values from 2 housekeeping genes *Gapdh* and *β-actin* for hypoxia studies with CDCs[112].

During the analysis of qRT-PCR results I noticed that the *Hprt* housekeeping gene did not produce stable Ct values at the different time points of the 3% O<sub>2</sub> culture. However, Yao *et al.* (2012) showed that *Hprt* has no fluctuations of Ct values among other housekeeping genes in neural progenitor cells cultured in normoxia or hypoxia [126]. Yao *et al.* (2012) used neural stem cells from rats which could represent different transcriptome to CDCs, besides they have compared different time points of hypoxic preconditioning with a single normoxic control group. Maybe comparing each specific time point with the same normoxic counterpart could give a better idea of the effect of hypoxia on different housekeeping genes.

### 3.3.3.2 The effect of 3% O<sub>2</sub> on CDC stem cell markers

It has been shown that a considerable population of CDCs express cardiac stem cell markers such as cKit and Sca-1 [63,110]. The benefit of hypoxia preconditioning in CDCs has been shown in humans [97] and mice [65]. qRT-PCR analysis of Sca-1 showed that 3 to 6 hours of 3% O<sub>2</sub> treatment, significantly increased Sca-1 transcript expression in P2 CDCs, (p=0.005 and 0.002 respectively). However the protein level of Sca-1 expressing CDCs cultured in 3% O<sub>2</sub> did not change. Although in all experiments there was a noticeable trend towards an increase in Sca-1 expression following culture in 3% O<sub>2</sub>, this did not reach significance, likely due to variability of the data. It is possible that more FACS experiments with CDCs cultured in 3% O<sub>2</sub> and normoxia could provide more significant results. It has been shown that hypoxia increased Sca-1-expressing mesenchymal stem cells and enhanced their adipogenic potential [128]. Activation of downstream genes of Hif-1 $\alpha$  depends on the hypoxia response element of the target gene, which contains the core sequence (5'-ACGTCG-3') and in some genes such as erythropoietin, HRE contains 50 base pairs, reviewed in [129]; therefore, I investigated the promoter region of the Sca-1 gene in ensembl genome browser and I could not find a potential HRE in the promoter region, but I observed three potential HREs in intron 2, 3 and exon 3, which may be involved in Hif-1 $\alpha$  dependent regulation of Sca-1 and could possibly explain why 3% O<sub>2</sub> increased Sca-1 expression. Functional HRE have previously been found in intronic regions; for instance, Tazuke *et al.* (1998) reported the existence of functional HRE in intron 1 of the insulin-like growth factor binding protein 1 (IGFBP-1) gene [130]. In another study, lactate dehydrogenase-B gene (LDH-B) of fundulus was shown to contain an HRE in intron 2 [131]. However, the significance of my findings requires more investigations, including a more detailed study of the direct and indirect effect of Hif-1 $\alpha$  on the expression of Sca-1.

I also observed that culturing P2 CDC in 3% O<sub>2</sub> changed *cKit* mRNA expression slightly at 6 hours (p=0.03) at mRNA but not at protein level. These results are consistent with Jögi *et al.* (2002) who showed that hypoxia increased cKit expression in neuroblastoma cells [132]. However, it is in contrast with Li *et al.* (2011), who did not see any significant change in cKit expression of human CDCs cultured in 5% O<sub>2</sub> [103]. It would be interesting to assess the effect of severe hypoxic conditioning could be tested on CDCs to analyse cKit expression, but the cell survival and viability of cKit-expressing cells should be investigated simultaneously as cKit-expressing cells among

CDCs are not abundant. qRT-PCR analysis showed that *Abcg2* mRNA expression did not change after culturing P2 CDCs in 3% O<sub>2</sub> for 3-72 hours. This is in contrast to previous findings showing that hypoxia increases bone marrow side populations, *Abcg2* expressing cells, 24 fold in comparison to normoxia [133]. Therefore it would be interesting to assess the *Abcg2* expression and side population content of CDCs in normoxia and 3% O<sub>2</sub> by Hoechst dye staining, which could be done by FACS on CDCs treated with 3% O<sub>2</sub> and normoxia.

### **3.3.3.3 The effect of 3% O<sub>2</sub> on mesenchymal markers of CDCs**

Exposure to 3% O<sub>2</sub> had no effect on the expression on CD90 in neonatal CDCs, which is in agreement with Valorani *et al.* (2012) who did not observe a significant difference in mesenchymal markers such as CD90 and CD73 in adipose tissue progenitors cultured in normoxia and hypoxia (2% O<sub>2</sub> for 7 days) [134]. But my findings are in contrast with Adesida *et al.* (2012), who showed that culturing BM stromal cells in 3% O<sub>2</sub> for 14 days depleted CD90 expression in comparison to normoxia [135], but this was a much longer time course. Although *Eng* mRNA expression was variable in three independent experiments, 3% O<sub>2</sub> treatment significantly increased *Eng* mRNA expression at 48 hours following the transfer to 3% O<sub>2</sub> (p=0.03), but endoglin protein expression was not increased. This could be due to three reasons: (i) the expression of *Eng* in a hypoxic environment is up-regulated due to co-operation between the TGF- $\beta$  signalling and hypoxia pathway [136]. Therefore *Eng* might need TGF- $\beta$  signalling ligands in order to be up-regulated more significantly in CDCs cultured in 3% O<sub>2</sub>. (ii) It is possible that to activate *Eng* a more hypoxic environment is necessary; to answer this it would be useful to test if culturing CDCs in severe hypoxia could increase *Eng* mRNA and protein. As *Eng* is shown to have an important role in angiogenesis, enhancing cell viability and inhibiting apoptosis, reviewed in [137], more expression of *Eng* could possibly help to obtain more therapeutic quantities of CDCs in a shorter time in clinical studies.

### **3.3.3.4 The effect of 3% O<sub>2</sub> on endothelial markers of CDCs**

I observed that 3% O<sub>2</sub> had variable effects on the expression of endothelial markers (CD31, CD34 and Flk1) in CDCs. However, in three independent qPCR experiments, *Vegf* and *Eng* showed a significant increase in passage 2 neonatal CDCs pre-treated with 3% O<sub>2</sub>. This is consistent with data from Hu *et al.* (2008), who showed that

hypoxia preconditioning (0.5%, 24 hours) improves mesenchymal stem cell engraftment into MI models and increases Flk1 expression [138]. My investigations with FACS analysis of CD31 expression in P2 CDCs cultured in normoxia and 3% O<sub>2</sub> showed no significant difference between the two groups. Hu *et al.* (2008) showed that the preconditioning of mesenchymal stem cells with hypoxia increased the proportion of CD31/Hoechst positive cells. Han *et al.* (2010) also showed that hypoxia preconditioning increased the number of CD31-expressing embryonic stem cells [139]. The differences between my experiment and these two studies are mainly the type of cells and the severity of hypoxia. For instance, in Hu *et al.*'s work, bone-marrow-derived mesenchymal cells were cultured in a 0.5% O<sub>2</sub> environment. It is possible that the hypoxic effect on the endothelial proportion of BM MSCs more is easily detectable than CDCs, because BM MSCs contain a significant number of endothelial progenitor and CD31-expressing cells while CDCs contain low numbers of CD31-expressing cells (table 3.4) and any change in CD31-expressing cells might not have been detected. As mentioned above, Han *et al.* (2010) used embryonic stem cells which are at the pluripotent stage with a different epigenetic structure, which could possibly make them capable of differentiating into different cell types such as endothelial progenitor cells. I observed that CD34, an endothelial cell marker, remained unchanged in normoxia and 3% O<sub>2</sub> in P2 neonatal CDCs. My finding is in agreement with Valorani *et al.* (2012), who showed that culturing adipose tissue mesenchymal stem cells in 2% O<sub>2</sub> did not change the CD34-expression potential [134]. However, to validate my data, more characterisation of CDCs with 3% O<sub>2</sub> and normoxia seems to be necessary; for instance, using multicolour FACS would provide more information regarding CDC-immunophenotyping analysis.

It would also be very interesting if we could analyse the co-expression of Hif-1 $\alpha$  or Hif-2 $\alpha$  with other stem cell (Sca-1, cKit, Abcg2) and endothelial (CD31, CD34 and Flk1) markers. This could possibly tell us more about the paracrine and autocrine pathways that contribute to expression of stem cell and endothelial markers in CDCs. Hif-1 $\alpha$  and Hif-2 $\alpha$  activate different genes on some occasions, reviewed in [90], which would inform future experimental designs with CDCs and hypoxia preconditioning. This will be helpful in terms of investigating which hypoxia pathway is more involved in CDC biology when cultured in 3% O<sub>2</sub>. It would also be useful to do FACS and qRT-PCR analyses at different time points. Possibly CDCs at earlier time points and earlier

passages (for example, P1 CDCs treated for 24 or 48 hours in 3% O<sub>2</sub>) may show increased expression of angiogenic and progenitor markers.

Culturing P2 CDCs in 3% O<sub>2</sub> increased EDC outgrowth from neonatal cardiac explants and increased the stem cell marker gene expression of *Sca-1* and *cKit*. 3% O<sub>2</sub> also increased endothelial marker gene expression (*Vegf* and *Eng*). Although 3% O<sub>2</sub> had a modest influence on endothelial markers, this may be very important in pro-angiogenic heart repair in clinical treatments. However, due to the clinical relevance of the pro-angiogenic potential of adult CDCs, I investigated the effect of 3% O<sub>2</sub> on adult-derived CDCs, which is discussed in chapter 4.

## **Chapter 4 The effect of 3% O<sub>2</sub> culture on adult CDCs proangiogenic and stem cell potential**



## 4.1 Introduction

So far my studies showed that the pre-treating of neonatal CDCs with 3% O<sub>2</sub> for up to 48 hours increased their pro-angiogenic and stem cell sub-populations *in vitro* by enhancing Sca-1, cKit, Eng, Vegf gene expression at mRNA level, although changes at protein level were less clear. However, neonatal CDCs are not used in patients. As the final goal of CDC studies is to provide a safe method of producing an autologous cell source for MI patients, I studied whether 3% O<sub>2</sub> has the same effect on adult CDCs as findings from adult cells will have more clinical relevance. The work described in this chapter therefore includes the establishment of adult CDC culture from C57BL/6 mice in normoxia and 3% O<sub>2</sub>, together with the re-validation of all of my findings with neonatal CDCs in chapter 3 and doing complementary immunophenotyping of adult-derived CDCs with FACS. The aim of this chapter is to assess whether culturing adult-derived CDCs in 3% O<sub>2</sub> benefits their pro-angiogenic and stem cell characteristics *in vitro*.

## **4.2 Results**

### **4.2.1 Optimisation of adult CDC culture**

Adult CDCs were derived using the protocol used for neonatal CDC culture with some modifications. Briefly, I used adult mouse hearts (6-8 weeks old) digested with trypsin, minced and cardiac explants plated on fibronectin-coated dishes. After several days, stromal cells grow from the explant, over which round phase bright cells migrate. Once confluent, all EDCs (stromal and phase bright cells) were removed after enzymatic digestion and plated on to Csph culture media with several growth factors. Following two weeks of Csph culture, loosely adherent Csphs were removed by gentle trituration. Csphs were then plated on fibronectin pre-coated flasks and passaged twice in media containing 20% foetal calf serum. In general, I observed that CDC culture from adult mouse hearts (C57BL/6 strain) is not as efficient as neonatal CDC culture and it is not always successful, especially at the Csph stage. Therefore, I made some modifications to the adult CDC culture protocol in order to obtain an optimal Csph and CDC yield. For instance, I observed that mincing adult cardiac tissue for 10 minutes instead of 3-5 minutes and harvesting smaller cardiac explants improve the phase bright cell production in explant derived cells. Likewise, the addition of 1 ml medium at three-day intervals during the explant culture was advantageous for phase bright cell outgrowth. While counting EDCs prior to the Csph stage, I noticed that there was a lot of debris and dead cells left from the adult explant tissue culture; therefore, careful cell counting and viability assessment were carried out by automated cell counter to gain accurate EDC counts. Using the optimised protocol I noticed that adult explants needed more time (25-30 days) to become confluent in comparison to neonates (12-14 days). EDCs were seeded in polylysine-D-coated wells at a seeding density of  $10^5$  EDCs per well of 24-well-plate to form cardiospheres. By day 12-14, Csphs formed completely and were then expanded as CDCs for 2 passages.

### **4.2.2 Preparing CDCs from atria and ventricles of the adult murine heart**

It has been reported that human atria from patients with chronic ischaemic heart disease generate more efficient EDCs compared to the ventricles [140] and Mishra *et al.* (2010) showed that, overall, human atria contain more cKit<sup>+</sup> cells than ventricles (right atrium: 5.2%, left atrium: 0.3%, right ventricle: 1.4% and left ventricle 1.4%) [79]. It is believed

that the minimised stress in the atrial wall favours cardiac progenitors and is permissive for their increased proliferation, reviewed in [141]. Therefore, to optimise adult CDC culture to obtain a better yield of CDCs, I compared the different stages of CDC culture between the atria and ventricles from C57BL/6 young adults (6-8 weeks old). The aim of this study was: (i) to define the productive explant capacity; and (ii) to measure the number of fully formed Csphs from the atria and ventricles. Both atrial and ventricular explants and Csphs were cultured for the same time (explants 25-30 days and Csphs 12-14 days). Eight plates with an average of 20 adhered explants in each plate were randomly selected for each experiment from atrial and ventricular culture. In total, 510 explants ( $170\pm 23$ ) from atrial explant cultures versus 492 explants ( $164\pm 34$ ) ventricular explants were analysed from three separate experiments and the number of productive explants (those which showed stromal and phase bright cell outgrowth) were normalized against the total number of adhered explants. Fully formed Csphs were quantified from eight wells for each experiment at the end of cardiosphere culture.

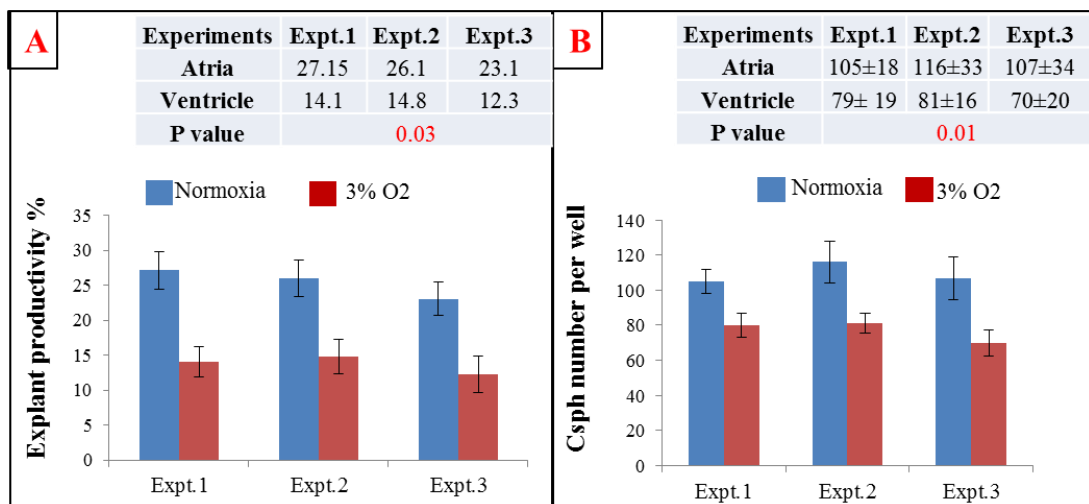


**Figure 4-1. Evaluating explant productivity (A) and Csph yield (B) from atrial and ventricular tissues.** (A) A summary of three independent experiments showing the mean percentage  $\pm$ SEM of productive explants, from atrial explant cultures versus ventricular explants. The mean number of explants per experiment was  $170\pm 23$  atrial explants and  $164\pm 34$  ventricular explants. Explant productivity was normalised to the total attached explant number and expressed as the productive percentage of explants for each experiment. The proportion of productive explants generated from atrial tissue was significantly higher than from the ventricles. (B) A summary of three independent experiments showing the mean number of fully formed Csphs at day 14 from atrial and ventricular explant-derived cells plated at  $10^5$  cells/well of 24-well plate. To assess the significance difference between the groups paired t-test was used and data showed that atrial EDCs produce significantly more Csphs in comparison to ventricular EDCs. In each experiment, at least 3 atria or ventricles were used from 6-8 week old mice.

Figure 4-1 shows that in all three experiments a significant difference was observed between atria and ventricles in explant productivity and Csph production. Combining the explant productivity from atria and ventricles (23-27% vs. 12-14%) gave a total explant productivity of 19.6% in young adult mice, aged 6-8 weeks from C57BL/6 line which is consistent with Davis *et al.* (2009) who showed ~ 20% explant culture productivity with C57BL/6 mice [71]. Due to the higher yield of EDCs and Csph from the atrial culture, I decided to use atria only in the subsequent CDC culture from adult hearts.

#### **4.2.3 Defining an effective 3% O<sub>2</sub> pre-treatment duration for adult P2 CDCs**

In chapter 3, I observed that passage 2 neonatal CDCs show elevated levels of Sca-1, Eng, Vegf mRNA at different time points following their transfer to culture in 3% O<sub>2</sub>. qRT-PCR analysis of stem cell (*Sca-1*), mesenchymal (*Eng*) and endothelial (*Vegf*) markers of neonatal CDC preconditioned in 3% O<sub>2</sub> showed that the expression of these genes increased at different time points between 3 and 48 hours. As neonatal CDCs were confluent after 72 hours of 3% O<sub>2</sub> culture and all genes of interest had either returned to baseline or below, in the subsequent adult CDC culture described in this chapter, 3% O<sub>2</sub> treatment was only continued for a maximum of 48 hours.

In order to investigate the effect of 3% O<sub>2</sub> culture on adult CDCs, three factors were evaluated: (i) the effect of 3% O<sub>2</sub> on clonogenicity, viability and proliferation; (ii) the effect of 3% O<sub>2</sub> on the expression of stem cell, mesenchymal and endothelial markers; and (iii) the level of Vegf in supernatant of P2 CDCs cultured in 3% O<sub>2</sub> for 6, 24, and 48 hours.

#### **4.2.4 Stabilisation of Hif-1 $\alpha$ protein in adult P2 CDCs following 48 hours of 3% O<sub>2</sub> culture**

As discussed in section 1.6, Hif-1 $\alpha$  protein is stabilised in mammalian cells cultured in hypoxic environments. Therefore, any evidence of Hif-1 protein stabilisation in all experiments associated with hypoxia is fundamental for the validation of the hypoxic environment. To assess hypoxia-associated protein in CDCs, Hif-1 $\alpha$  stabilisation was evaluated by immunocytochemistry by using the specific Hif-1 $\alpha$  antibody in adult-

derived P2 CDCs cultured for 48 hours in normoxia and 3% O<sub>2</sub>. Figure 4-2 shows the stabilisation of Hif-1 $\alpha$  in adult CDCs at P2 cultured in 3% O<sub>2</sub> for 48 hours.

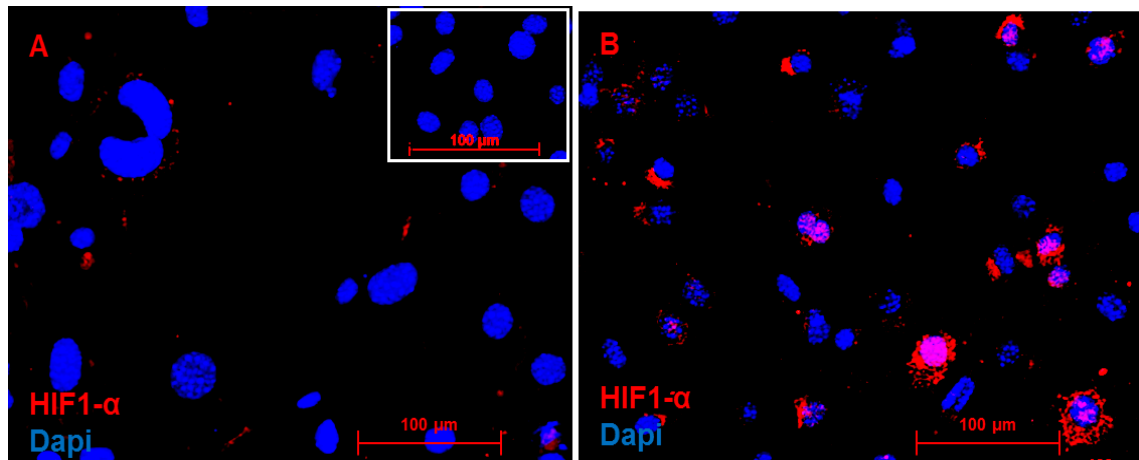


**Figure 4-2 Hif-1 $\alpha$  protein stabilization in adult passage 2 CDCs cultured in normoxia and 3% O<sub>2</sub> for 48 hours.** CDCs stained with anti-Hif-1 $\alpha$  specific antibody and detected with an anti-rabbit secondary antibody conjugated with alexa594 (red). Cells were cultured in (A) normoxia and (B) 3% O<sub>2</sub> for 48 hours. Hif-1 $\alpha$  protein appears to be stabilised in cytoplasm and nuclei of CDCs in 3% O<sub>2</sub>; however, cells appear to have a variable response, as some CDCs do express Hif-1 $\alpha$  neither in the nucleus nor in cytoplasm. And some cells in normoxia expressed detectable levels of Hif-1 $\alpha$ . Nuclei were stained with Dapi (blue). Inset image A is the no primary control with same scale bar = 100 $\mu$ m.

#### 4.2.5 The effect of 3% O<sub>2</sub> on adult CDC clonogenicity

My findings showed that neonatal CDCs are clonogenic and the rate of clonogenicity in normoxia and 3% O<sub>2</sub> were 5-8.5% and 5.9-7.4% respectively. I also investigated if 3% O<sub>2</sub> as a mild hypoxic cell culture environment that could modify adult CDC clonogenicity. To test this, adult CDCs at passage 1 were preconditioned with 3% O<sub>2</sub> for 48 hours, and then were sorted using an automatic cell sorter (FACS Aria) and one single cell placed automatically in each well of a 96-well plate. For extra assurance all wells were observed with light microscopy straight after cell sorting and all the clonogenicity sample cultures were continued in normoxia. Clonogenicity was monitored for 6 weeks and at day 42 the number of colonies was quantified and the clonogenicity percentage calculated. This experiment was performed independently three times and results showed that preconditioning of CDCs at passage 1 with 3% O<sub>2</sub> for 48 hours did not significantly change their clonogenicity as the rates were comparable. Figure 4-3 shows a representative single cell in the well of a 96-well plate (Fig 4.3.A) and a colony that formed after 14 days from the same cell (Fig 4.3.B). Table 4-1 summarises the results of three independent clonogenicity experiments with adult

CDCs, which have been cultured in normoxia and 3% O<sub>2</sub> for 48 hours while they were at the P1 stage.

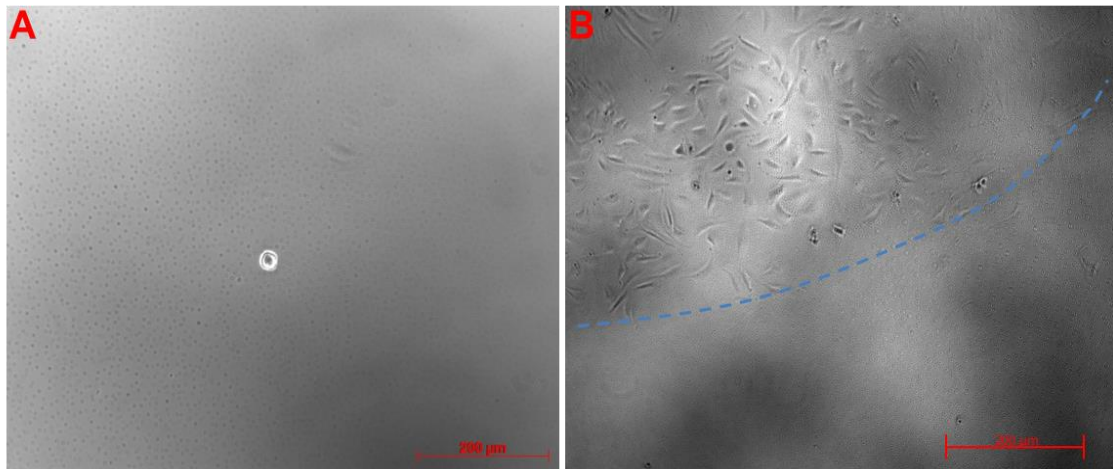


**Figure 4-3 The effect of 3% O<sub>2</sub> on Adult CDC clonogenicity.** Single cells from P1 CDCs exposed to either normoxia or 3% O<sub>2</sub> were sorted automatically using a FACS Aria sorter and placed in each well of 96-well plates. Clonogenicity was assessed weekly by light microscopy for 6 weeks. (A) A single adult CDC at day 0; (B) A colony from the same cell after 14 days; the edge of the colony is highlighted with a blue line. Scale bar =200 μm.

Experiments	Normoxia	3% O <sub>2</sub>
Expt.1	11±2.1	13.5±5.8
Expt.2	7.2±2	15.6±5.4
Expt.3	8.3±4.7	12.1±5.1
P value	0.1	

**Table 4-1 Summary of three independent clonogenicity experiments performed with adult murine CDCs preconditioned for 48 hours in normoxia and 3% O<sub>2</sub>.** CDCs at Passage 1 were cultured in normoxia and 3% O<sub>2</sub> for 48 hours. Then, using the cell sorter; one single cell was placed in each well of 96-well plates and clonogenicity measured after 6 weeks of culture. Data are presented as mean percentage of clonogenicity ± SEM from three technical replicates for each run. Paired t-test was used to assess the significant difference between biological replicates.

#### 4.2.6 The effect of 3% O<sub>2</sub> on adult P2 CDC proliferation and viability

In the literature there are different opinions about the effect of hypoxia on cell proliferation and viability. My experiments from neonatal CDCs cultured in 3% O<sub>2</sub> for 24, 48 and 72 hours showed no significant difference in terms of viability and cell proliferation in comparison to normoxia counterparts. To test the effect of 3% O<sub>2</sub> on the viability and proliferation of adult CDCs, I performed a proliferation and viability assay

using the automated cell counter Vi-Cell XR 2.03 (Beckman/Coulter). Passage 2 adult CDCs (seeded at the same cell density of  $2 \times 10^5$ /per well) were cultured in normoxia and 3% O<sub>2</sub> for 48 hours. CDCs were enzymatically detached at 24 and 48 hours of culture and assessed for viability and proliferation. This experiment was performed independently three times and Table 4-2 and Figure 4-4 summarise the results of these experiments. The data suggested that 3% O<sub>2</sub> treatment of CDCs leads to increased CDC proliferation rate after 24 hours ( $p=0.02$ ) but did not change the cell proliferation at 48 hours. Adult CDC viability remains stable for 48 hours without any significant change between normoxia and 3% O<sub>2</sub> groups.

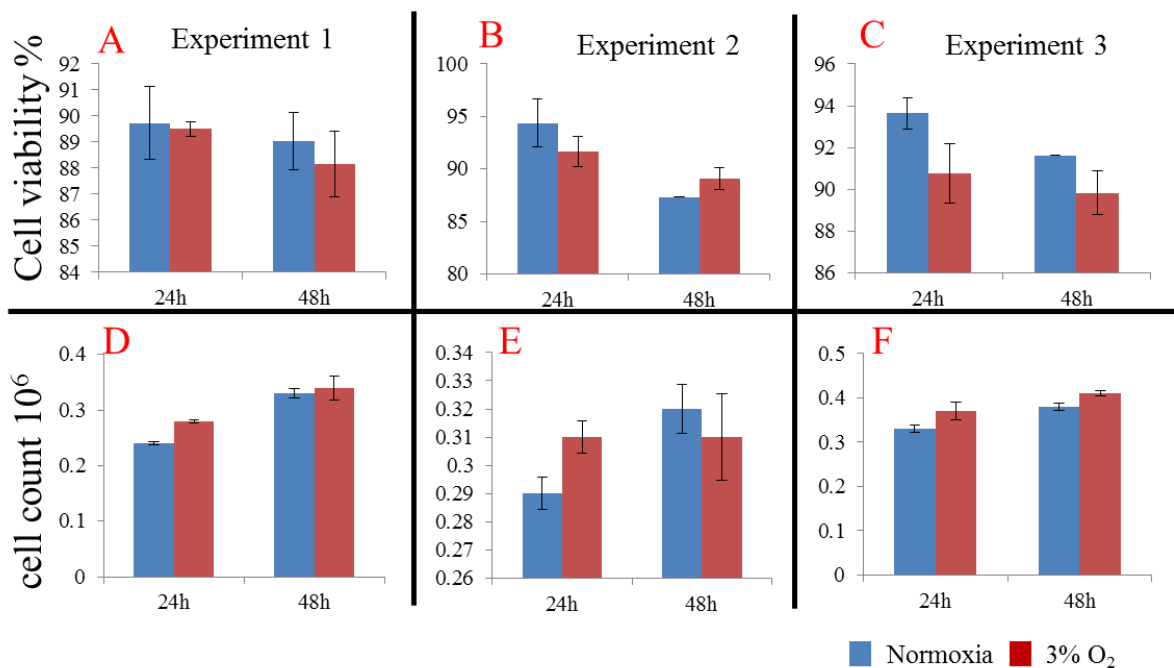


**Figure 4-4 Evaluating adult passage 2 CDC total cell viability and cell count in normoxia and 3% O<sub>2</sub> for 24 and 48 hours in three independent experiments.** Viability and total cell count were analysed with automated cell counter (Coulter) after single cell suspension in PBS. Bar graphs show mean +/-SEM from 3 technical replicates.

<b>A</b> Total cell count x 10 <sup>6</sup>				
Experiments	Normoxia 24h	3%O <sub>2</sub> 24h	Normoxia 48h	3%O <sub>2</sub> 48h
Expt.1	0.24±0.02	0.28±0.04	0.33±0.02	0.34±0.01
Expt.2	0.29±0.03	0.31±0.03	0.32±0.1	0.31±0.003
Expt.3	0.33±0.02	0.37±0.03	0.38±0.07	0.41±0.03
<i>p</i> value	0.02		0.59	

<b>B</b> cell viability %				
Experiments	Normoxia 24h	3% O <sub>2</sub> 24h	Normoxia 48h	3% O <sub>2</sub> 48h
Expt.1	89.7±2.4	89.5±0.5	89±2	88±2.1
Expt.2	94±4	91.6±3.5	87.3±2	89.1±1.6
Expt.3	92±1.2	90.7±2.4	91.6±1.3	89.8±1.7
<i>p</i> value	0.1		0.8	

**Table 4-2 Summary of three independent analyses of proliferation (A) and cell viability (B) performed with P2 adult murine CDCs (aged 6-8 weeks) cultured in 3% O<sub>2</sub> and normoxia.** CDCs at P2 were cultured in 3% O<sub>2</sub> and normoxia with the same cell seeding density. (A). Adult P2 CDC total cell count assessed at 2 different time points (24 and 48 hours). Data are presented as the mean total cell viability or total cell count ±SEM. Paired t test showed that total cell count increased significantly in 24 hours cell culture only. (B) Adult CDC cell viability was assessed at two different time points including 24 and 48 hours. Data presented as mean viability percentage ±SEM. It appears that viability remained un-changed. The full dataset for this experiment is depicted in figure 4-4.

#### 4.2.7 The effect of 3% O<sub>2</sub> on passage 2 adult CDC gene expression

Using qRT-PCR, I analysed adult CDCs at passage 2 treated with 3% O<sub>2</sub> and normoxia for 3, 6, 24 and 48 hours and compared the gene expression profile of *Sca-1*, *cKit*, *Abcg2*, *Eng* and *Vegf*. This experiment was independently performed three times and although results were variable, there was a significant up-regulation in expression of *Sca-1* (6 hours, p=0.04), *Abcg2* (3 hours, p=0.03), *Vegf* (6 hours, p=0.03 and 24 hours, p= 0.02) and *Eng* (24 hours, p=0.03), but generally a notable reduction of gene expression observed at 48 hours of culture. The significant increase in *Sca-1* mRNA expression was observed at 6 hours in all experiments, although in all time points the  $\Delta$ Ct value of *Sca-1* in CDCs cultured in 3% O<sub>2</sub> was lower than the normoxia counterparts. *cKit* mRNA level did not appear to change following 3% O<sub>2</sub> treatment ( $\Delta$ ct values were almost same as the normoxia control groups in the 3 experiments), however the amount of *cKit* mRNA was not detectable in experiment 2 (48 hours) and 3(24 hours), therefore not enough data were available for paired t-test in these two time points. *Abcg2* mRNA which was not changed in neonatal CDCs following exposure to 3% O<sub>2</sub>



increased significantly at 3 hours of 3% O<sub>2</sub> culture in adult-derived P2 CDC. *Eng* expression was also moderately elevated at 24 hours following 3% O<sub>2</sub> treatment in comparison with the normoxia group. *Vegf* also had a variable response to 3% O<sub>2</sub> culture, yet in all three experiments there was an up-regulation in the level of *Vegf* of at 6 to 24 hours of cell culture. Figure 4-5 and Table 4-3 depict qRT-PCR results from neonatal CDCs cultured in 3% O<sub>2</sub> in comparison with its normoxia counterpart.

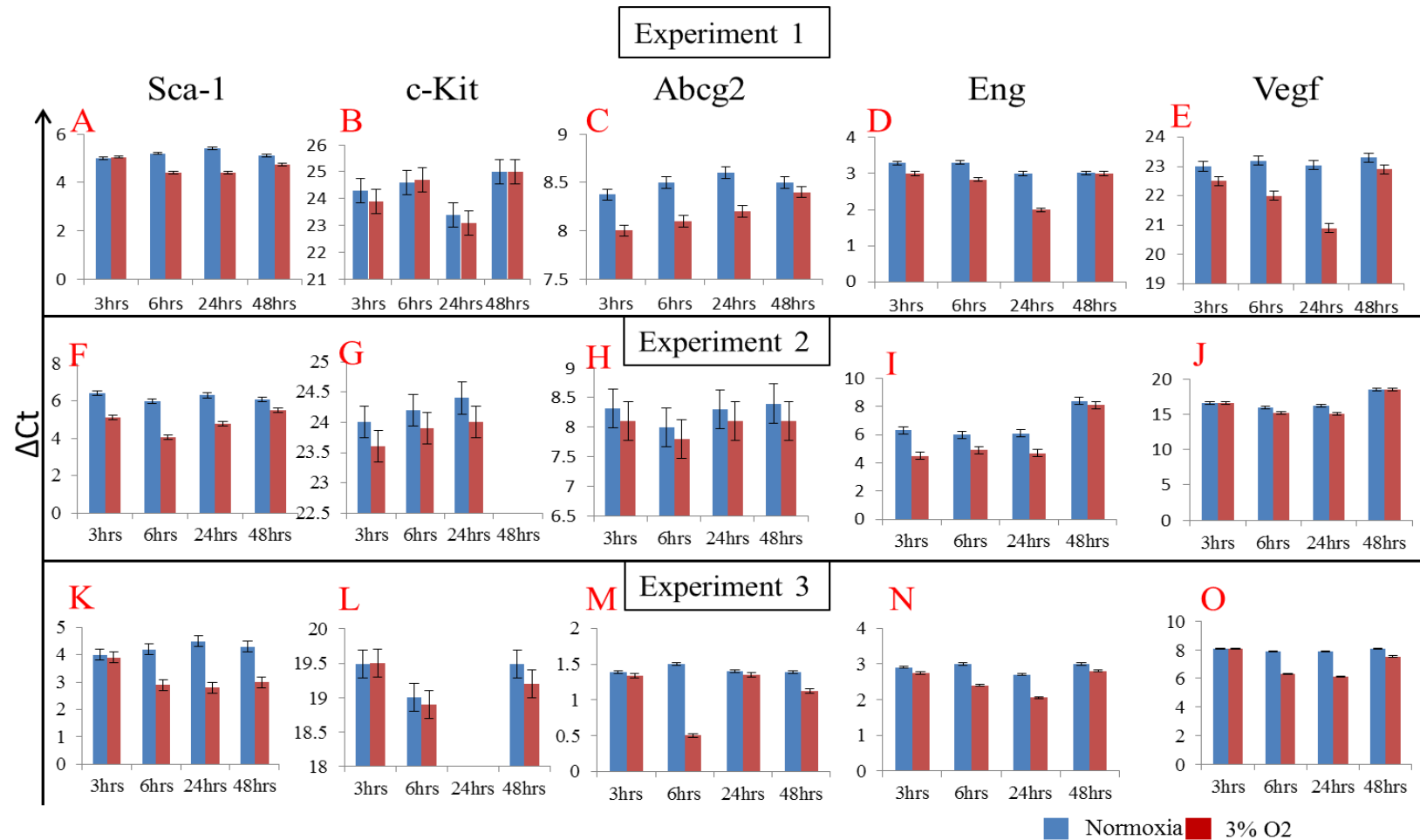


**Figure 4-5 Gene expression changes in adult CDCs at passage 2 cultured in normoxia and 3% O<sub>2</sub> for 3 to 48 hours.** *Sca-1*, *cKit*, *Abcg2*, *Eng* and *Vegf* expression was analysed using qRT-PCR at 4 different time points in three independent experiments. The  $\Delta$ Ct values of target genes are summarised in the graphs, blue bars (normoxia), red bars (3% O<sub>2</sub>) showing mean  $\pm$ SEM of 3 technical replicates and data were analysed as summarised in Table 4-3.

Sca-1								
	3 hours		6 hours		24 hours		48 hours	
Experiments	Normoxia	3% O <sub>2</sub>	Normoxia	3% O <sub>2</sub>	Normoxia	3% O <sub>2</sub>	Normoxia	3% O <sub>2</sub>
Expt.1	5	5	5.2	4.4	5.4	4.4	5.1	4.7
Expt.2	6.4	5.1	6	4	6.3	4.8	6.1	5.5
Expt.3	4	3.9	4.2	2.9	4.5	2.8	4.5	3
P value	0.3		0.04		0.96		0.1	
cKit								
	3 hours		6 hours		24 hours		48 hours	
Experiments	Normoxia	3% O <sub>2</sub>	Normoxia	3% O <sub>2</sub>	Normoxia	3% O <sub>2</sub>	Normoxia	3% O <sub>2</sub>
Expt.1	24.3	23.9	24.6	24.7	23.4	23.1	25	25
Expt.2	24	23.6	24.2	23.9	24.4	24		
Expt.3	19.5	19.5	19	18.9	-	-	19.4	19.2
P value	0.7		0.7					
Abcg2								
	3 hours		6 hours		24 hours		48 hours	
Experiments	Normoxia	3% O <sub>2</sub>	Normoxia	3% O <sub>2</sub>	Normoxia	3% O <sub>2</sub>	Normoxia	3% O <sub>2</sub>
Expt.1	8.3	8	8.5	8.1	8.6	8.2	8.5	8.4
Expt.2	8.3	8.1	8	7.8	8.3	8.1	8.4	8.1
Expt.3	1.39	1.34	1.5	0.5	1.4	1.35	1.39	1.1
P value	0.03		0.1		0.1		0.4	
Vegf								
	3 hours		6 hours		24 hours		48 hours	
Experiments	Normoxia	3% O <sub>2</sub>	Normoxia	3% O <sub>2</sub>	Normoxia	3% O <sub>2</sub>	Normoxia	3% O <sub>2</sub>
Expt.1	23	22.5	23.2	22	23	21	23.2	23
Expt.2	16.6	16.6	16	15.1	16.2	15.1	18.5	18.5
Expt.3	8.1	7.9	7.9	6.3	7.9	6.1	8.1	7.5
P value	0.3		0.03		0.02		0.2	
Eng								
	3 hours		6 hours		24 hours		48 hours	
Experiments	Normoxia	3% O <sub>2</sub>	Normoxia	3% O <sub>2</sub>	Normoxia	3% O <sub>2</sub>	Normoxia	3% O <sub>2</sub>
Expt.1	3.3	3	3.3	2.8	3	2	3	3
Expt.2	6.3	4.5	6	4.9	6.1	4.7	8.4	8.1
Expt.3	3	2.7	3	2.4	2.7	2	3	2.8
P value	0.2		0.05		0.03		0.5	

**Table 4-3** Time-course analysis of the effect of 3% O<sub>2</sub> on the expression of *Sca-1*, *cKit*, *Abcg2*, *Eng* and *Vegf* in passage 2 adult CDCs. Analysis of gene expression using qRT-PCR with  $\Delta$ Ct values (shown in table) generated following normalisation against the average Ct from three housekeeping genes: *Gapdh*; *B-actin*; and *RPL-19*. The table shows the relative expression of *Sca-1*, *cKit*, *Abcg2*, *Eng* and *Vegf* in CDCs cultured in 3% O<sub>2</sub> from 3 to 48 hours. Each  $\Delta$ Ct value shown is the mean of three technical replicates. Paired t test was performed using the mean value for each biological replicate and the significant differences, ( $p < 0.05$ ) are highlighted in red.

#### 4.2.8 3% O<sub>2</sub> increases Vegf protein in the supernatant of adult-derived P2 CDC

CDCs are shown to contain some pro-angiogenic potential [65,68,74,79,80,86], and show increased Vegf mRNA expression following exposure to 3% O<sub>2</sub>. Therefore, to validate the hypoxic environment in CDC culture and test the secreted levels of Vegf, I analysed the level of Vegf protein in CDC-conditioned media. Using Elisa, the level of Vegf was measured in adult P2 CDCs cultured in normoxia and 3% O<sub>2</sub> at 6, 24 and 48 hours. The same cell density of P2 CDCs was seeded in each well (5 x 10<sup>4</sup> cells/well of 6-well plates) and the same volume of media was added (3 ml/well). 250 µl of media were collected at 6, 24 and 48 hours from CDCs cultured in normoxia and 3% O<sub>2</sub>. Results showed that 3% O<sub>2</sub> culture of P2 CDCs significantly increased Vegf protein in the media in comparison with normoxia. As shown in figure 4-6 the level of Vegf protein in supernatants increased in normoxia from 172±14 pg/ml to 267±15.6 and 388±7 pg/ml at 6 and 24 hours respectively, but the highest level of Vegf was observed at 48 hours of 3% O<sub>2</sub> culture, 422.7±13 pg/ml. Figure 4-6 shows the level of Vegf at three different time points in comparison with the control group (48 hours normoxic culture).

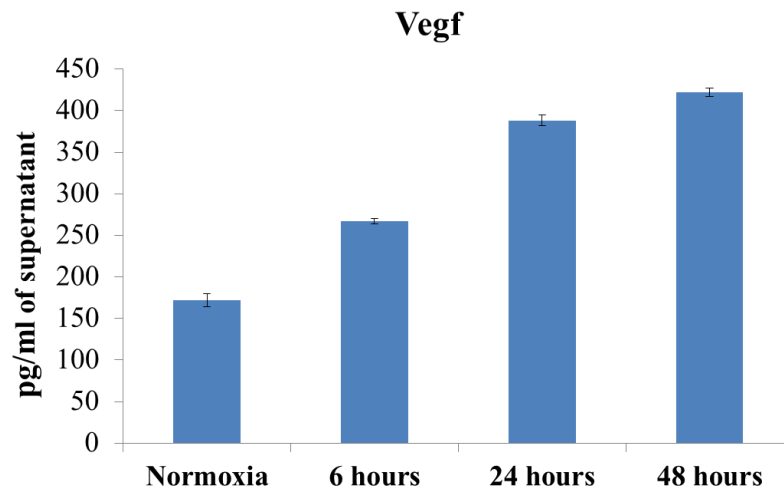


**Figure 4-6** The level of Vegf protein in supernatant of adult P2 CDCs cultured in normoxia( 48 hours) and 3% O<sub>2</sub>. Adult P2 CDCs cultured in normoxia and 3% O<sub>2</sub> with same cell density and same total volume of cell media. At each time point an aliquot of the media was used to measure Vegf level by Elisa. The graph clearly shows that the Vegf expression level from P2 CDCs cultured in 3% O<sub>2</sub> has an appreciably higher level of Vegf protein in comparison to normoxia group (\*p<0.05).

#### **4.2.9 The effect of 3% O<sub>2</sub> on stem cell (Sca-1, cKit), Mesenchymal (CD90, Eng) and endothelial (CD31, CD34, Flk1) markers of adult P2 CDCs**

FACS data showed that, Sca-1 expression was up regulated in all three experiments in 3% O<sub>2</sub> compared to normoxia which validates the data from neonatal derived CDCs. cKit expression remained stable in both groups in all three experiments which confirms the data from qRT-PCR analysis of cKit gene expression. Eng and CD90 also showed stable expression in normoxia and 3% O<sub>2</sub>. However, *Eng* mRNA expression has previously been shown to be up-regulated in a hypoxic environment (1% O<sub>2</sub>, 4-6 hours, 3.5 and 1.5 folds respectively) in trophoblast-derived cell lines [142]. CD31 expression was relatively low in three experiments and no significant change observed between 3% O<sub>2</sub> and normoxia. Unfortunately, in experiment 2, due to technical errors CD34 was not detectable, but 3% O<sub>2</sub> appeared to increase CD34 in experiments 1 and 3. However, this difference was not significant in experiment 1, only in the third experiment. Therefore, further investigations with CDCs cultured in 3% O<sub>2</sub> and normoxia is necessary to elucidate the effects on CD34 expression levels. Flk1, although expressed at low levels, showed a significant increase in CDCs cultured in 3% O<sub>2</sub> compared to normoxia (table 4-4). In this respect it has previously been shown that hypoxia (0.5% O<sub>2</sub> for 24 hours) increases Flk1 expression in murine MSN [143]. Overall, my findings from the immunophenotyping of CDCs share similarities with neonatal CDCs (chapter 3) and those published in the literature [83,144]. Figure 4-8 shows representative FACS plots and table 4-4 summarises the results of all three independent experiments as a percentage of positive events for all the cell populations analysed.

#### 4.2.10 Sca-1<sup>+</sup> and cKit<sup>+</sup> CDCs are predominantly CD45<sup>-</sup>

Flow cytometry demonstrated that passage 2 adult Sca-1<sup>+</sup> and cKit<sup>+</sup> CDCs were predominantly negative for the haematopoietic marker CD45 (1.8±0.2 and 0.6±0.12 respectively – figure 4-7). This result demonstrates that Sca-1 and cKit-expressing CDCs are predominantly distinct from cells of haematological origin.

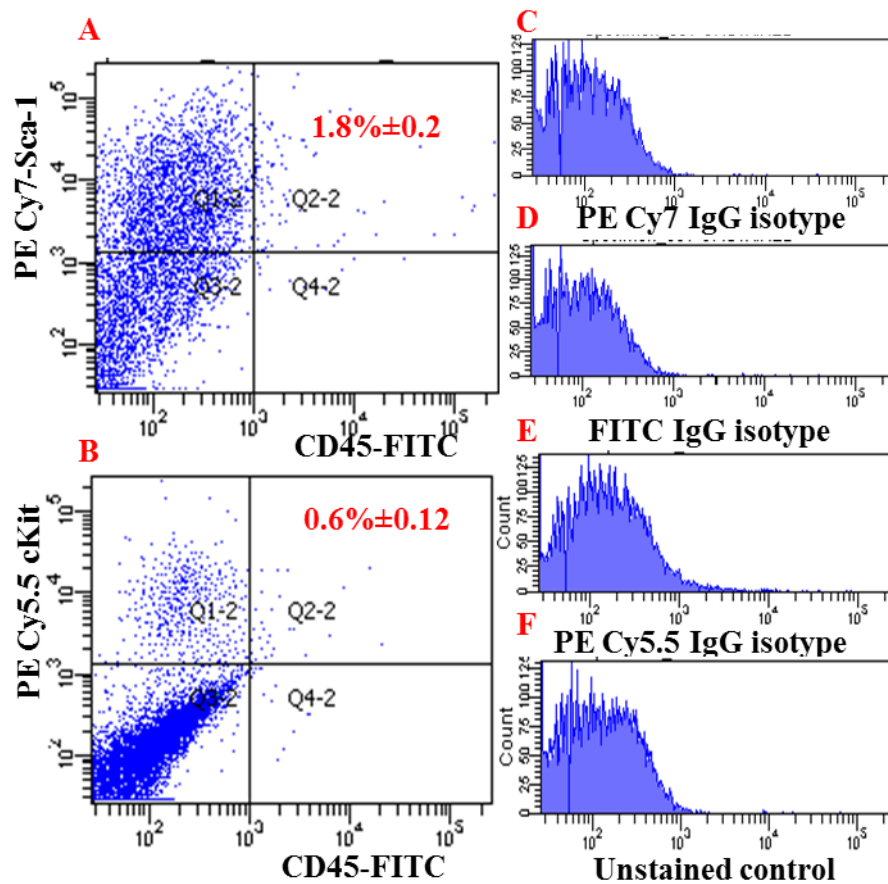


**Figure 4-7 Sca-1<sup>+</sup> and cKit<sup>+</sup> adult CDCs, at passage 2 are predominantly negative for CD45.** Flow cytometry analysis reveals that a very low population of adult CDCs at passage 2 expresses the pan-leukocyte marker CD45. Dot plots (A) & (B) showing 1.8% and 0.6% of adult CDCs at passage 2 co-express Sca-1 and cKit with CD45 respectively. (C), (D), (E) and (F) are isotype controls for PE Cy7, FITC, PE Cy 5.5 and unstained control respectively. Data are presented as mean percentage ± SEM.

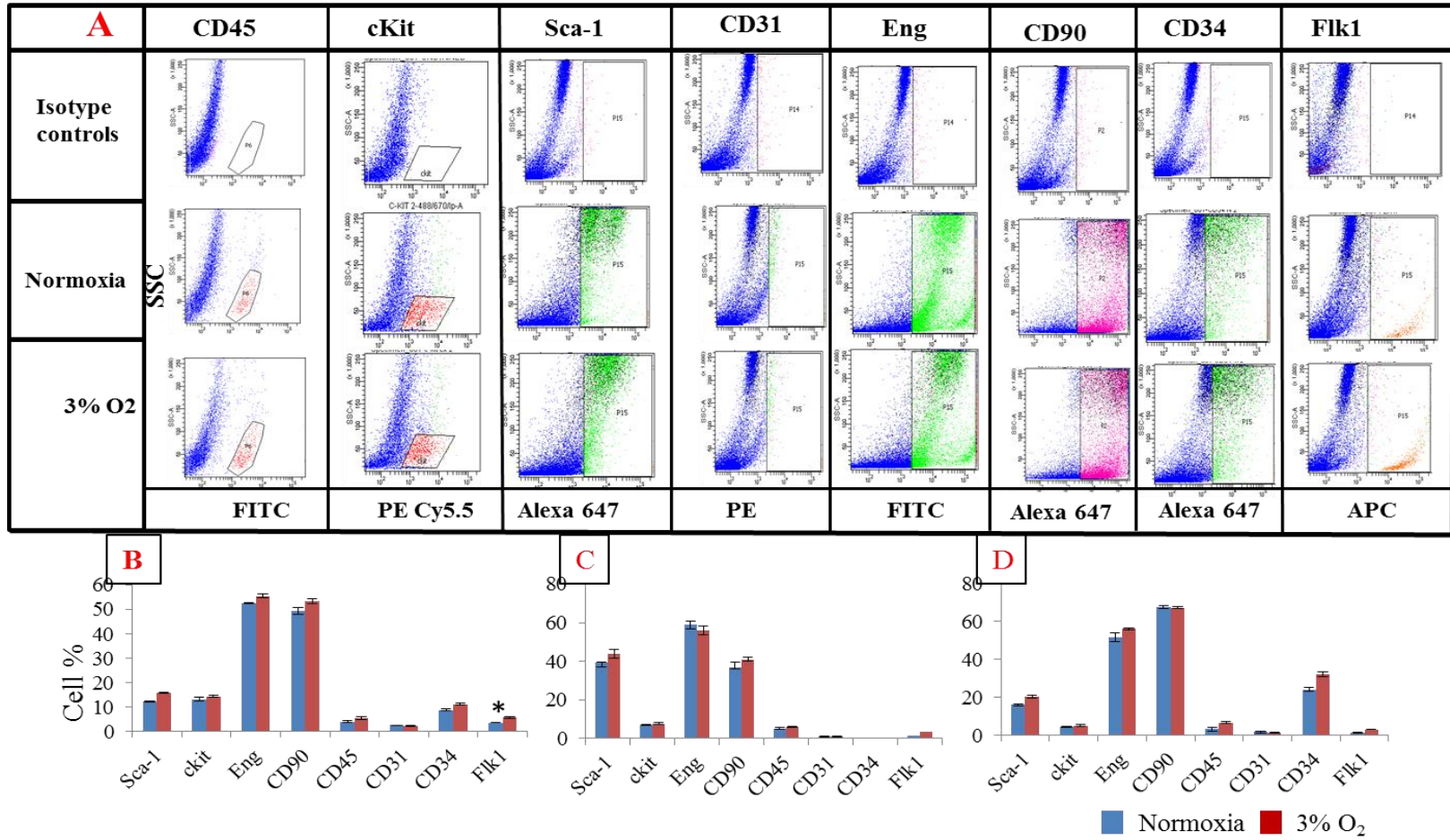


**Figure 4-8** Flow cytometric analysis of murine adult CDCs at passage 2 harvested for 48 hours in normoxia and 3% O<sub>2</sub>. A) CDCs were analysed for the expression of Sca-1, cKit, Eng, CD90, CD45, CD31, CD34 and Flk1. B,C and D are the summary of three independent FACS experiments showing the proportion of cells expressing each marker. Data was summarised and analysed as shown in Table 4-4.

Experiments	Sca-1		c-kit		Eng		CD90		CD45	
	Normoxia	3% O <sub>2</sub>	Normoxia	3% O <sub>2</sub>	Normoxia	3% O <sub>2</sub>	Normoxia	3% O <sub>2</sub>	Normoxia	3% O <sub>2</sub>
<b>Expt.1</b>	12.36±0.5	15.8±0.5	13.23±1.1	14.3±0.7	52.4±0.7	55.4±1.5	49.4±2.3	53.1±1.8	3.9±0.6	5.3±1.0
<b>Expt.2</b>	39.3±0.7	43.8±4	7±0.5	7.7±0.8	59.2±3.6	56±3	37.6±4	41.8±1	4.96±0.8	6.1±0.5
<b>Expt.3</b>	15.9±0.6	20.4±1.4	4.3±0.8	4.9±0.9	51.6±4	56.1±1.3	67.6±1	67.3±1	3.2±1.9	5.6±1
<b>P value</b>	0.006		0.05		0.5		0.5		0.1	

CD31		CD34		Flk1		Sca-1/cKit		Sca-1/Eng		cKit/Eng	
Normoxia	3% O <sub>2</sub>	Normoxia	3% O <sub>2</sub>	Normoxia	3% O <sub>2</sub>	Normoxia	3% O <sub>2</sub>	Normoxia	3% O <sub>2</sub>	Normoxia	3% O <sub>2</sub>
2.5±0.1	2.4±0.3	8.8±0.6	11.2±0.8	3.6±0.15	5.7±0.6	2.3±0.3	1.4±0.2	33.1±0.6	43.1±1.4	3.8±0.4	2.4±0.2
1.1±0.5	1.1±0.3	-	-	1.5±0.37	3.7±0.6	0.2±0.1	0.6±0.3	18.3±0.4	23±0.1	5.4±1.02	3.3±1.1
1.6±0.6	1.4±0.5	24.5±2	32.2±2.3	1.4±0.2	2.9±0.15	-	-	-	-	-	-
0.1		-		0.01		-		-		-	

**Table 4-4 Summary of 3 independent FACS analyses performed with adult murine CDCs at passage 2 cultured in normoxia and 3% O<sub>2</sub>.** Data represents the number of immuno-positive cells as a percentage of viable cells. Sca-1 and Flk1 are increased significantly after 48 hours of 3% O<sub>2</sub> treatment, but culturing CDCs in low oxygen had no significant effect on the expression of the other markers. All FACS experiments are summarised in Figure 4-8. Data presented as mean percentage ± SEM, derived from 3 separate replicates per experiment. Paired t-test was performed to compare biological replicates. Significant values are highlighted in red.



#### 4.2.11 Sca-1 expression increases following extended passaging of adult CDCs

As qRT-PCR and FACS analysis of CDC treated with 3% O<sub>2</sub> showed a significant increase in Sca-1 expressing a sub-population of CDCs, I next assessed whether prolonged CDC culture influences Sca-1 expression.

To test this hypothesis Sca-1 expression in adult CDCs was assessed with flow cytometric-based immunophenotyping at passages 2 and 4. Interestingly, FACS data showed a dynamic increase in the numbers of Sca-1 expressing cells following the extension of the *in-vitro* passaging of adult CDCs to P4. This experiment was independently performed three times. In all the experiments there was a significant increase in the number of Sca-1 expressing cells in P4 in comparison with P2. Figure 4-9 shows the summary of three independent FACS results depicting this change, while table 4-5 summarises the results of all three experiments.

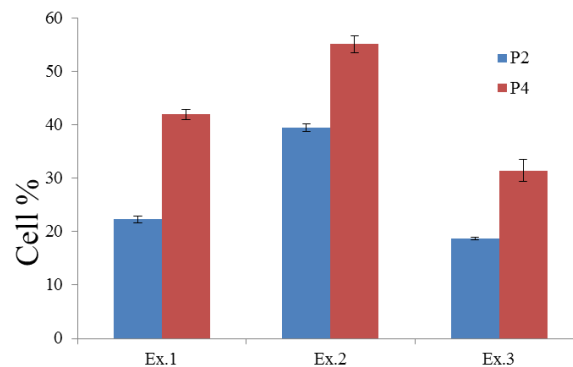


**Figure 4-9 Flow cytometric analysis of P2 and P4 adult CDCs showing up regulation of Sca-1 following extended passaging.** CDCs were expanded until passage 2 and 4 then, cells were sampled and analysed for the expression of Sca-1. The images clearly show that Sca-1 expression is appreciably increased from passage 2 to passage 4. Data are derived from three independent experiments and data are presented as mean percentage (from three technical replicates) ± SEM. Summary and analysis of data are shown in Table 4-5.

Experiments	P2	P4
expt.1	22.3±± 1.1	42± 1.7
expt.2	38.2± 1.1	57.2± 2.7
expt.3	18.9± 0.4	33.2± 3.4
p value	0.01	

**Table 4-5 A summary of three independent flow cytometric analyses of Sca-1 expression from adult murine CDCs at P2 and P4 stages.** Results showed that Sca-1 expression is significantly increased following prolonged CDC culture. Data are derived from three independent experiments and presented as mean percentage ± SEM. Paired t-test was used to analyse changes between biological replicates.

## **4.3 Discussion**

### **4.3.1 The efficiency of adult murine CDC culture**

Davis *et al.* (2010) showed that CDC culture is an efficient method to obtain cardiac progenitor cells, but they reported a variable success rate between different mouse strains such as C57BL/6, MerCreMer-Z/EG [71]. The authors reported that only 20% of cardiac explants derived from adult C57BL/6 mice were able to form phase bright outgrowth. This is consistent with my findings with the adult C57BL/6 cardiac explant culture, where I found that 19.6% of explants generated phase bright cells. Davis *et al.* did not report any difficulties with Csph stage culture using EDCs from adult C57BL/6 mice [71]. However, it is reported that Csphs grow slowly when EDCs are seeded at a low density and at least 40,000 EDCs are required for a successful Csph culture [140]. Using the established CDC protocol based on neonatal CDC culture, I seeded  $10^5$  adult EDCs per well of 24-well plate to culture Csphs, but fewer Csphs were generated at two weeks in comparison to neonatal Csphs. After EDC quantification with the haemocytometer I noticed that, along with EDCs, there are lots of cellular fragments and cardiac tissue remnants, which may have led to an overestimation of cell seeding density, so I added the automated cell quantification step and correlated the seeding density with the number of viable cells, which influenced positively the Csph yield.

### **4.3.2 Possible reasons for low efficiency of adult CDC culture in comparison with neonatal CDCs**

There are a number of possible explanations for the low yield of CDCs from adult hearts compared with neonatal hearts. Although Chan *et al.* (2012) [140] reported that there is no effect of age on EDC and CDC growth from human cardiac samples, they compared only adults over a limited age range ( $65 > \text{age} > 65$ ). Possibly culturing CDCs from different animal models, with different age ranges, could answer this question. It is possible that adult EDCs and Csphs proliferate more slowly than neonatal cells. It is reported that resident human CPCs are most abundant in the neonatal stage ( $< 30$  days) compared with children (age 2 to 13 years) and rapidly decrease over time; and also CPCs from younger children express more Ki67 (a marker for proliferating cells) than older CPCs [79]. In this respect, measuring the doubling time of phase bright cells and Csph-forming cells of adult and neonates could help to address this point. There may

also be technical issues affecting the CDC yield. It is already reported that EDC culture from C57BL/6 is difficult and technical variation in culture conditions such as initial explant enzymatic digestion, or the seeding density alters the efficiency of the CDC culture [71]. In our lab the established CDC culture protocol is based on neonatal CDCs in which all EDCs including stromal and phase bright cells are dissociated with enzymatic digestion using trypsin. I observed a considerable number of floating cells at the Csph culture stage following trypsin digestion. Therefore, I replaced trypsin with a milder cell disassociation enzyme: accutase, which decreased the numbers of dead floating cells at the Csph stage.

#### **4.3.3 Adult murine atria generate a higher yield of EDCs and Csphs than ventricles**

My findings from comparing EDCs and Csph formation from atria and ventricles showed that atria generate higher yields of EDC and Csphs in comparison to ventricles. This is in agreement with Chan et al. (2012) [140], who showed that EDCs could be expanded from all atrial biopsies, but sufficient cells were obtained from only 8/22 ventricular biopsies. This could be due to the less contractile activity of the atria in comparison to the ventricles as Leri *et al.* (2005) noted that CSC distribution within the heart appears to be related to the minimised levels of wall stress regions such as the atria and apex. The difference between the cellular components of the atria and ventricles could also affect EDC outgrowth from explants. In this respect, Burstein *et al.* (2008) compared secretory, morphological and proliferative indexes of canine atrial versus ventricular fibroblasts and showed that atrial fibroblasts express greater  $\alpha$ SMA and proliferate faster than ventricular fibroblasts. Therefore, it is possible the abundance of atrial fibroblasts facilitates phase bright cell migration by paracrine mechanisms [145]. It would be interesting to measure the level of growth factors and cytokines expressed in the supernatant of atrial versus ventricular explant culture and investigate the possible correlation between the EDC outgrowth rate and released paracrine pathways. Several pathways have been shown to be involved in cell migration such as CXCR4/SDF1 [146] and TGF- $\beta$  [147].

#### **4.3.4 Defining the optimal 3% O<sub>2</sub> culture duration for adult CDCs**

It has already been shown that hypoxia increases stem cell proliferation and clonogenicity and due to the relevance of the application of adult CDCs in ischemic heart regeneration, in this chapter I investigated whether the preconditioning of adult CDCs with 3% O<sub>2</sub> favours CDCs in terms of the proliferation, and expression of stem cell, mesenchymal and endothelial cell markers. My observations of neonatal CDCs (described in the previous chapter) showed that 3% O<sub>2</sub> increases EDC proliferation and up-regulates Sca-1, Abcg2, Vegf and Flk1 expression. This indicates that 3% O<sub>2</sub> improves the *in-vitro* stem cell and pro-angiogenic potential of neonatal CDCs. Therefore, in the first step I decided to find the best possible 3% O<sub>2</sub> culture duration for adult CDCs.

#### **4.3.5 The effect of 3% O<sub>2</sub> on adult CDC clonogenicity, viability and proliferation**

Culturing adult CDCs for 48 hours in 3% O<sub>2</sub> did not change their clonogenicity but increased their proliferation rate slightly after 24 hours of cell culture. Interestingly their viability remained same between normoxia and 3% O<sub>2</sub> which suggest that the hypoxic environment has no significant impact on cell viability in 24 or 48 hours of culture. However, it is known that the effect of hypoxia on cell proliferation is cell specific; for instance, 1% O<sub>2</sub> increases the proliferation and clonogenicity of neural stem cells [148] but decreases the proliferation and clonogenicity of mesenchymal stem cells [98]. As discussed in chapter 3, it is also possible that 3% O<sub>2</sub> is not sufficient to increase the clonogenicity and viability in adult CDCs. Therefore, it would be interesting to assess the effect of combining severe hypoxia cultures followed by 3% O<sub>2</sub> on CDC proliferation and clonogenicity. As it has been shown that Hif-1 $\alpha$  is more efficiently active below 2% O<sub>2</sub> and Hif-2 $\alpha$  has more activity above 2% O<sub>2</sub>, this could potentially stabilise both Hif-1 $\alpha$  and Hif-2 $\alpha$  which could activate the downstream activities of both genes and possibly the CDCs could get the benefit of the activation of both downstream pathways. Probably in future experiments, selecting specific sub-populations of CDCs (e.g. cKit<sup>+</sup> or Sca-1<sup>+</sup>) would provide a better understanding of the effect of 3% O<sub>2</sub> on their proliferation and clonogenicity.

#### **4.3.6 Possible implications of 3% O<sub>2</sub> culture in phenotypic heterogeneity of adult murine CDCs**

qRT-PCR and FACS analysis of stem cell (Sca-1, cKit, Abcg2), mesenchymal (Eng, CD90) and endothelial (CD31, CD34, Flk1) markers revealed inter-culture variation between CDCs at passage 2 as well as temporal variation in response to 3% O<sub>2</sub>. This finding is very similar to my results from studies on the neonatal CDCs and was discussed in the previous chapter. Sca-1 was the only marker which was expressed at higher levels in adult CDCs in comparison with neonatal CDC (p<0.05). CD31, Flk1 and Eng were all expressed at lower levels in adult CDCs compared with neonatal CDCs (p<0.05 for all three markers), suggesting that adult murine CDCs have a smaller angiogenic sub-population in comparison with neonatal CDCs.

#### **4.3.7 Sca-1 expression in expanded adult CDC culture**

Interestingly, FACS data showed that with prolonged CDC culture, Sca-1 expression increased progressively (table 4-5). My findings are in agreement with Zuba-Surma *et al.*, who showed that Sca-1<sup>-</sup> skeletal muscle progenitors become Sca-1<sup>+</sup> following expansion in the culture and reaches 98% of the total cells following 3 passages [149]. The elevation of Sca-1 expression following increasing CDC passage could be due to the fact that Sca-1 expressing CDCs proliferate faster than other CDC sub-populations following prolonged culture as Zuba-Surma *et al.* (2006) showed that Sca-1<sup>+</sup> cells proliferated faster than Sca-1<sup>-</sup> cells [149]. It would be interesting to analyse the proliferation rate and doubling time of sorted Sca-1<sup>+</sup> versus Sca-1<sup>-</sup> CDCs to test this possibility. It is also possible that adult murine atria contain more Sca-1<sup>+</sup> cells than neonatal hearts so consequent CDC cultures reflect levels of Sca-1 expressing cells in the cardiac tissue. In this respect Hidestrand *et al.* (2008) showed that Sca-1-expressing cells are more abundant in regenerating the aged (24 months old mice) than young adult (4 months old) tibialis anterior muscle [150]. According to Janson *et al.* (2013) serial passaging can be used as a model of *in-vitro* cell ageing studies [151]; therefore, it is possible that prolonged CDC culture has the same effect on Sca-1 expression by an *in-vitro* ageing mechanism. My experiments showed that culturing CDCs in 3% O<sub>2</sub> also led to an increase in Sca-1 expression. However, there could be a possible difference between Sca-1<sup>+</sup> cells induced by 3% O<sub>2</sub> and serial passaging. Sca-1 is expressed in mixed stem cells, progenitor and differentiated cells [127]. It would be interesting to

investigate the possible difference between Sca-1-expressing CDCs induced by 3% O<sub>2</sub> and serial passaging. Functional experiments such as clonogenicity and differentiation capacity to other lineages such as endothelial and cardiomyocytes could help to characterise Sca-1<sup>+</sup> CDCs. In this respect I further assessed Sca-1 expressing CDCs with other markers by flow cytometric analysis and noticed that the proportion of Sca-1<sup>+</sup>/Eng<sup>+</sup> CDCs cultured in 3% O<sub>2</sub> increased from 33.1±0.6% in normoxia to 43.1±1.4% in 3% O<sub>2</sub> (p <0.05). Furthermore, Sca-1-expressing cells were predominantly distinct from myeloid cells as they were mostly CD45<sup>-</sup>. However, to validate these findings, Sca-1 cells from aged mice and higher passages could also be assessed for co-expression of other angiogenic and stem cell markers.

My studies of adult CDCs and their response to 3% O<sub>2</sub>, showed that 3% O<sub>2</sub> favours murine adult CDCs in terms of the stem cell phenotype (by increasing sub-populations of Sca-1 and Abcg2) and pro-angiogenic potential (by increasing the expression of Eng, Vegf and Flk1). The results from this chapter suggested a potential treatment for cardiac stem cell pre-treatment in order to increase the pro-angiogenic sub-populations of CDCs and their application in clinical studies. However, the mice models used in this study were healthy and, therefore, in order to have a more clinically relevant scenario, it would be better to culture CDCs from diseased models such as the MI model and further characterise them in 3% O<sub>2</sub> and normoxia.

Fibroblasts in atria are shown to proliferate faster than ventricles [145] and there is evidence in the literature which suggests Csphs resemble fibroblasts and have little cardiogenic potential [78] and, finally, Zakharova *et al.* (2010) used immunocytochemical analysis of dissociated Csphs and showed that 17% of the cells expressed αSMA and 6% expressed vimentin [85]. As I am using atria to culture CDCs, there is a likelihood of culturing fibroblasts with CDCs. As the final aim of CDC culture is to provide a safe autologous cell source for MI patients, it is important to investigate the fibroblast content at different stages of CDC culture. This can be done by using transgenic mice in which cardiac fibroblasts are labelled with specific genetic tags and is described in the next chapter.

# **Chapter 5 Lineage tracing of cardiac fibroblasts in murine hearts and CDC culture**

## 5.1 Introduction

As discussed in section 1.5.7, EDCs, Csphs and CDCs have been shown to be pro-angiogenic, cardiogenic, clonogenic and capable of multilineage differentiation. However, the validity of the Csph culture method has been questioned and different laboratories have shown different outcomes. Csphs derived from neonatal WK rats were reported to contain a significant population of hematopoietic progenitor cells (CD45<sup>+</sup>); moreover, non-haematological Csph cells (CD45<sup>-</sup>) in this published study, expressed collagen Ia2 and may therefore be fibroblasts [78]. However, enhanced variable level of Collagen 1 expressing cells in explants and the Csph stage may be due to technical differences between different laboratories during the preparation of Csph cells. The Marban group proposed that the inclusion of non-standard steps such as filtering the EDC in order to omit tissue fragments, and using harsh enzymatic digestion to remove all EDCs (instead of light digestion to remove phase bright cells only) and using a different cell culture medium all had a detrimental effect on the CDC preparations [83]. My studies using murine neonatal and adult CDCs, used a standard preparation method and validated that CDCs are clonogenic (tables 3-1 and 4-1) and express stem cell, endothelial and angiogenic markers (tables 3-4 and 4-4), have shared some similarities with work from the Marban laboratory [68,70,71,83] and the work of Chen *et al.*, and Carr *et al.* [80,140]. However, my CDCs as well as those from other laboratories share some characteristics with mesenchymal cells and cardiac fibroblasts such as the expression of markers of mesenchymal cells (CD90). As myofibroblasts have been shown to form spheres [152] further investigations are required to characterise the fibroblast content of Csphs and CDCs.

Carr *et al.* (2011) showed that 10±2% of rat CDCs express DDR2 (a fibroblast marker) [80] and it is also shown that murine hearts contain 27% of DDR2-expressing cells [25]. CFs from atria are shown to have more proliferative and secretory activities in comparison with CFs derived from ventricles [145]. As the source of adult CDC culture in this study is atria, therefore assessing CF derived cells within CDC culture seems to be necessary. However, studying CF is complicated as fibroblasts and CFs lack specific markers, therefore to study fibroblasts it is useful to study them with a combination of markers reviewed in [15]. In the literature, there is contrasting evidence for the fibroblast content of Csphs and CDCs. For instance, it has been shown that Csphs overwhelmingly express Collagen 1 [78] but, in other work, researchers showed that CDCs at passage 2 derived from human congenital heart patients are Collagen 1



negative [79]. To address the question of the fibroblast content of Csphs and CDCs, I used a mouse model that permitted lineage tracing of fibroblasts (figure 5-1). This type of approach leads to the activation of a reporter gene (such as GFP or eYFP) in a specific cell population that can be used to track this cell population and its progeny over time. One commonly used lineage tracing system is the Cre-recombinase/loxP system. This complex consists of a Cre-recombinase enzyme driven by a specific promoter (allowing tissue or cell-type specific expression) and a reporter gene containing a floxed stop cassette (a region that prevents expression of the reporter gene which is flanked by 2 LoxP sites). A LoxP site consists of a 34-base-pair sequence and acts as a recognition site for Cre-recombinase. Binding of Cre-recombinase to 2 LoxP sites leads to the inversion or excision of the floxed DNA sequence depending on LoxP site orientation. In this way, Cre-recombinase can excise a specific genomic region which is flanked between 2 LoxP sites and this step can be used to activate the expression of a reporter gene (figure 5-1). Temporal activation of Cre-recombinase is achievable through the fusing of a mutated hormone binding site of an oestrogen receptor with Cre-recombinase. For instance, CreERT is obtained by fusing of Cre-recombinase with a mutated oestrogen receptor domain that leads to CreERT activation in the presence of Tamoxifen [153]. Cre activity is monitored using a genetic marker such as eYFP that can be used to identify activated cells and all daughter cells (figure 5-1).

Collagen I is produced by fibroblasts and is one of the main components of ECM, reviewed in [15]. In this chapter I have used a tamoxifen inducible *Colla2-CreERT*; *Rosa26-floxed STOP eYFP* transgenic mouse model (Figure 5-1) to trace and quantify CFs in cardiac tissue and at different stages of CDC culture.

## 5.2 Results

### 5.2.1 Transgenic *Col1a2-CreERT*; *Rosa26-floxed STOP eYFP* mouse model

The *Col1a2-CreERT* mouse was first reported by Zheng *et al.* (2002) [110] and was obtained from Prof. David Abraham's Laboratory (UCL). The *Col1a2-CreERT* transgene contains 6 kb of the upstream 5' flanking region of the *Col1a2* promoter fused to a sequence encoding Cre-ERT-IRES-hpAP. Zheng *et al.* (2002) showed by histological examination of *Col1a2-CreERT*; *Rosa26-floxed STOP eYFP* transgenic mice, that the *LacZ* reporter gene was essentially restricted to fibroblast cells in different tissues such as the skin, lung, kidney, skull, liver, and epicardium and intestine [110]. Using *LacZ* staining, Zheng *et al.* (2002) showed the expression of Collagen 1 expressing cells within the pericardium, suggesting the *in-vivo* activation of Cre recombinase in the heart. I therefore tested whether the *Col1a2-CreERT* line could be used to mark CFs. I did this by using a different reporter gene that expressed eYFP (Figure 5-1). *Col1a2-CreERT* mice were crossed with *Rosa26-floxed STOP-eYFP* reporter mice [109] in which eYFP has been introduced into the ubiquitously expressed *Rosa26* locus. In the presence of functional Cre-recombinase the STOP cassette upstream to the eYFP coding sequence is excised and the eYFP gene is expressed. Figure 5-1 depicts schematically the steps of Cre-recombinase activation and eYFP expression in CFs following administration of Tamoxifen.

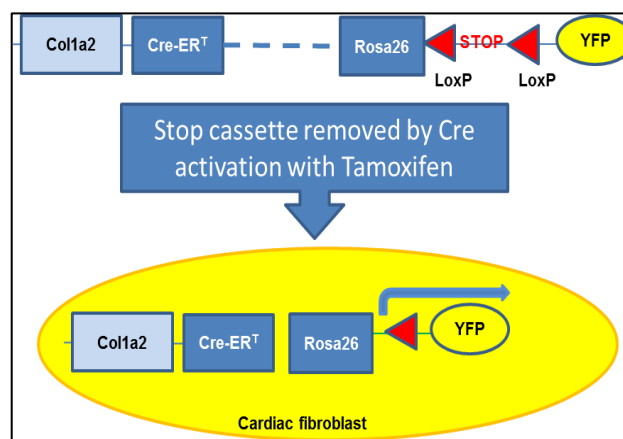


**Figure 5-1 Schematic representation of Cre-mediated recombination of the *Rosa26* floxed *STOP-eYFP* allele in *Col1a2-Cre-ERT* mice.** *Col1a2-Cre-ERT* mice were crossed with *Rosa26-floxed STOP eYFP* reporter mice to generate *Col1a2-Cre-ERT*; *Rosa26-floxed STOP eYFP* mice. The expression of eYFP is driven by the ubiquitously expressed *Rosa26* promoter and is conditional on the removal of the upstream LoxP flanked 'STOP' region. IP injection of 2 mg tamoxifen/day for 5 consecutive days activates Cre-recombinase to remove the floxed STOP region. As a result, all cells expressing *Col1a2* and their progenies will express eYFP, and this is anticipated to localise to CFs and their descendent cells.

### 5.2.2 Activation of Cre-recombinase and eYFP reporter expression in CFs

Studying CFs is complicated because evidence is emerging that CFs are a highly heterogeneous cell population. In this study I investigated co-localisation of two fibroblast markers: vimentin and FSP1 with endogenous eYFP expression in *Colla2-CreERT; Rosa26-floxed STOP eYFP* mice, using both healthy and MI models (please see section 2.11). To validate the eYFP expression in collagen 1 expressing cells, heart sections from tamoxifen treated *Colla2-CreERT; Rosa26-floxed STOP eYFP* mice were stained with an anti-collagen 1 antibody. Anti-GFP was used to stain cells expressing eYFP and the co-localisation of these two markers was quantified in three *Colla2-CreERT; Rosa26-floxed STOP eYFP* male mice (6-8 weeks old) 48 hours after the last tamoxifen injection (please see section 2.11). The results showed that eYFP is expressed in collagen 1 expressing cells in the heart. However, not all collagen 1 expressing cells were positive for the eYFP marker. Detailed quantifications showed that  $37.3 \pm 2.1\%$  of collagen 1 expressing cells express eYFP and  $59.2 \pm 1.8\%$  of eYFP expressing cells also co-expressed collagen 1. Figure 5.2 depicts the degree of co-expression of eYFP and collagen 1.

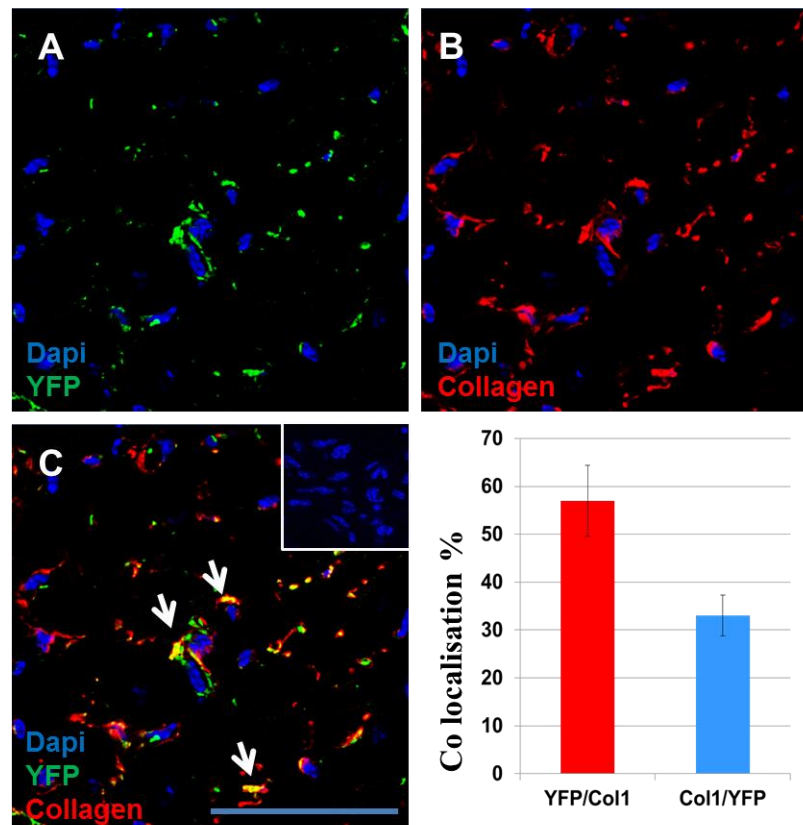


**Figure 5-2 Co-expression of eYFP and collagen 1 in tamoxifen-treated *Colla2-CreERT*; *Rosa26-floxed STOP eYFP* heart sections.** To assess the specificity of eYFP expression in collagen 1 expressing cells, heart sections from *Colla2-CreERT*; *Rosa26-floxed STOP eYFP* mice were stained with primary anti-collagen 1  $\alpha$  and anti-GFP antibodies and then the secondary antibodies conjugated with Alexa 594 and Alexa 488 respectively. (A) Dapi/eYFP, (B) Dapi/Collagen, (C) merged, the white arrow depicts the co-localisation of both YFP and Collagen 1, (D) shows the summary analysis of Collagen 1 and YFP co-expressing cells from three *Colla2-CreERT*; *Rosa26-floxed STOP eYFP* mice. As shown in the figure, endogenous eYFP expression in CFs was not detected in all Collagen 1 expressing cells. The inset in image C is a no primary control. The scale bar = 50  $\mu$ m.

### 5.2.3 Co expression of eYFP with FSP1 and vimentin in healthy murine myocardium

To analyse further whether eYFP is activated in the other sub-populations of CFs and represents a suitable genetic marker for CF lineage tracing studies, heart sections from tamoxifen-treated *Colla2-CreERT*; *Rosa26-floxed STOP eYFP* mice were stained with anti-FSP1 and anti-vimentin in combination with anti-GFP (please see chapter 2, sections 2.5.1 & 2.11.7). Quantitative analysis of FSP1, vimentin and eYFP expression on cardiac sections from *Colla2-CreERT*; *Rosa26-floxed STOP eYFP* transgenic mice, showed that  $37.5 \pm 9\%$ ,  $40.3 \pm 5.5\%$  of FSP1 and  $38.6 \pm 3.4\%$ ,  $46 \pm 6.6\%$  of vimentin expressing cells co-localised with YFP expression in the atria and ventricles,

respectively. Figure 5-3 depicts representative images showing the co-expression of FSP1/eYFP, and vimentin/eYFP in *Coll1a2-CreERT; Rosa26-floxed STOP eYFP* hearts compared with the hearts from *Rosa26-floxed STOP eYFP* mice, which served as the biological negative control (Figure 5-4).

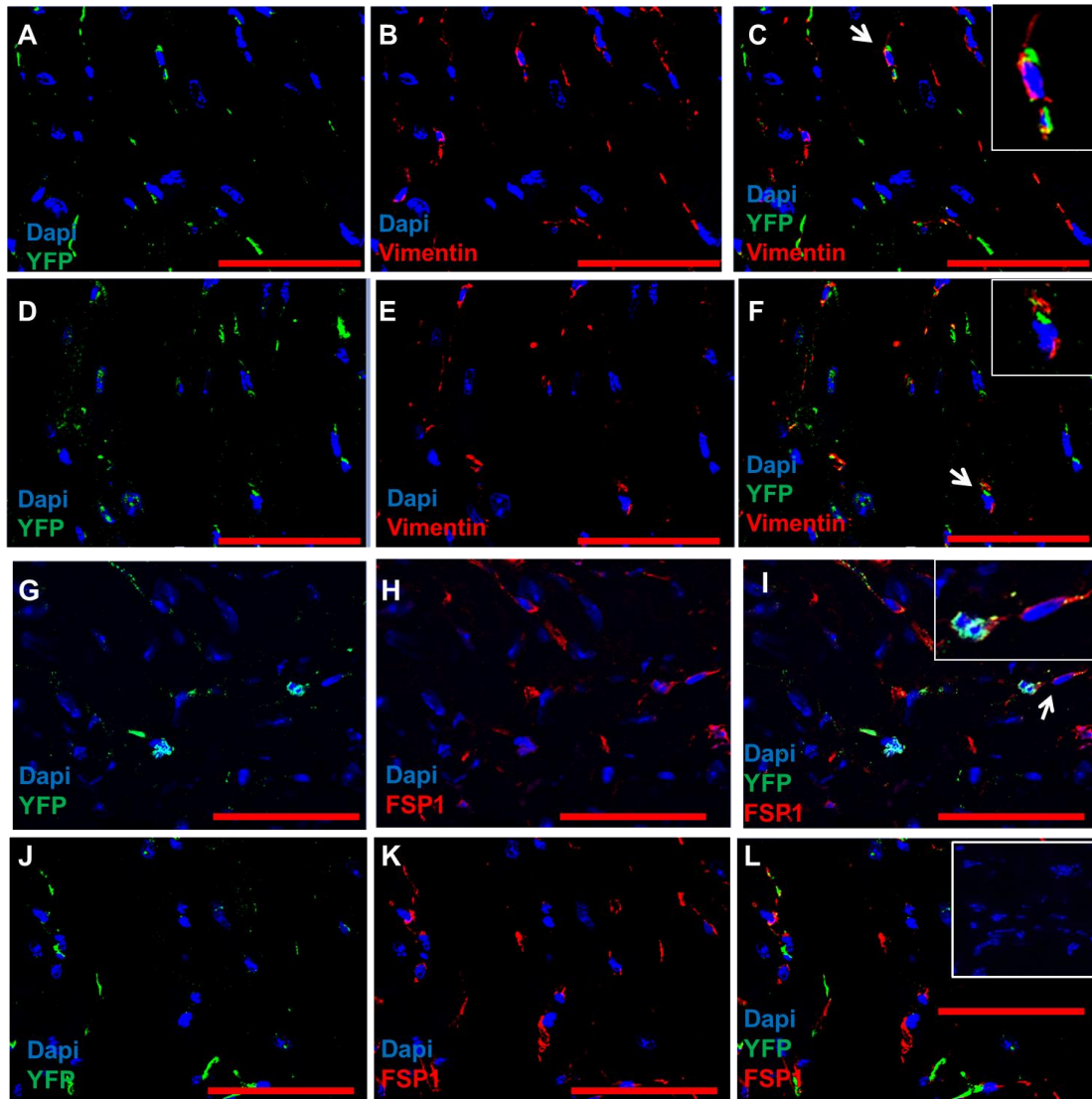


**Figure 5-3 Immunofluorescent staining of healthy hearts (n=6) with FSP1/eYFP, vimentin/eYFP in tamoxifen-treated *Coll1a2-CreERT; Rosa26-floxed STOP eYFP* mice.** Representative vimentin/eYFP co-expression in ventricles (A-C) and atria (D-F), tissue stained with anti-GFP (green), anti-vimentin (red) and nuclei stained with DAPI. Representative FSP1/eYFP co-expression in Ventricles (G-I) and atria (J-L) were stained with anti-GFP (green) and anti-FSP1 antibody (red), nuclei stained with Dapi. The inset image in L shows a no primary control. Cells highlighted by white arrow (digital zooms) in C,F and I, are examples of the cells which are considered positive for both markers. All cryosections were prepared as described in section 2.11.7. All mice were injected with Tamoxifen as described in 2.11.1 The scale bar = 50  $\mu$ m.

Table 5-1 summarises six independent quantification experiments to analyse the number of FSP1/eYFP and vimentin/eYFP co-expressing CFs in healthy hearts from tamoxifen-treated *Colla2-CreERT; Rosa26-floxed STOP eYFP* mice.

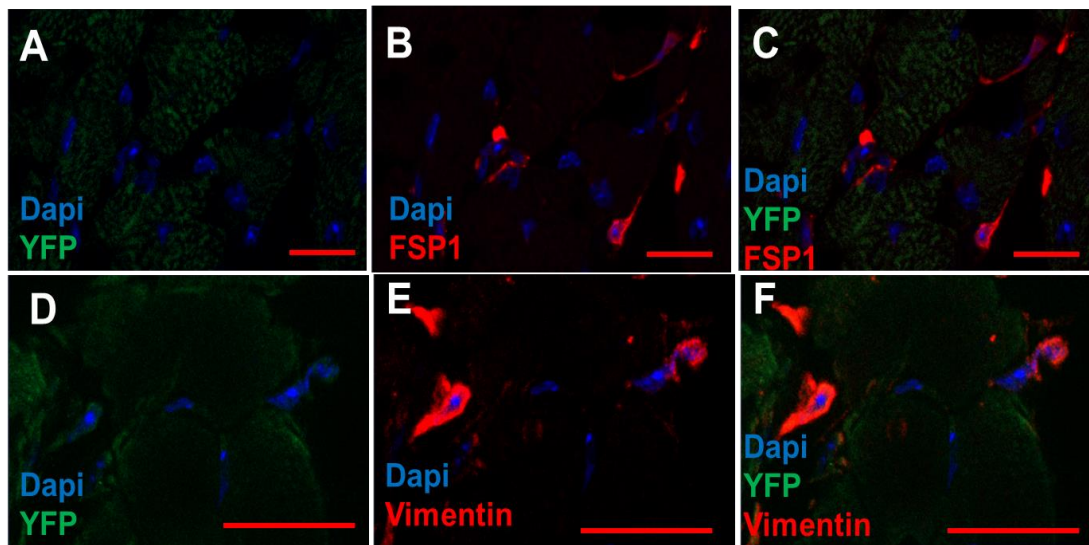


**Figure 5-4 Immunofluorescent staining of healthy atria with FSP1 or vimentin with eYFP in tamoxifen-treated *Rosa26-floxed STOP eYFP* control mice.** A-C: representative image of atrial tissue stained with anti-FSP1 antibody (red), anti-GFP (green) and nuclei stained with Dapi. Images (D-F) are representative images showing vimentin expression in adult mouse atria stained with anti-GFP (green), anti-vimentin (red), all mice and hearts were treated as before. This experiment with *Rosa26-floxed STOP eYFP* mice showed that there was no eYFP staining in the absence of *Colla2-CreERT* which confirms the efficiency of the STOP cassette. The pale green seen in these images is due to tissue autofluorescence from myocardium. The scale bar = 20  $\mu$ m.

<b>A</b>	CF Marker	% Atria	% Ventricle	<b>B</b>	CF Marker	% Atria	% Ventricle
	% YFP (Dapi cells)	15.2 $\pm$ 5.2	15.2 $\pm$ 3.03		%YFP (Dapi cells)	20 $\pm$ 3.4	22 $\pm$ 3.4
	%FSP1	28.9 $\pm$ 5.5	28.3 $\pm$ 4.4		%Vimentin	30 $\pm$ 5	33 $\pm$ 5.7
	% FSP1/YFP co expressing cells	8.2 $\pm$ 2.3	8.7 $\pm$ 1.8		% Vimentin /YFP co expressing cells	12.3 $\pm$ 3.8	13 $\pm$ 3.6
	% Total fibroblasts (YFP+FSP1)	36.3 $\pm$ 4.6	34.2 $\pm$ 4.7		Total fibroblast(Vimentin +%YFP)	34 $\pm$ 3.7	36 $\pm$ 7.6

**Table 5-1 Quantification of eYFP, FSP1 and vimentin expressing cells in atria and ventricle cryosections from *Colla2-CreERT; Rosa26-floxed STOP eYFP* healthy mice.** Detailed analysis of eYFP, FSP1 and vimentin expressing cells in the atria and ventricle showed that these three markers are expressed at the same levels in both regions. There is a considerable difference between eYFP expression between (A) and (B) which is probably due to the use of two different anti-eYFP antibodies that were required to be compatible with the antibodies used to detect FSP1 and vimentin. It is likely that the specificity of the YFP primary antibody used in co-staining with FSP1 (A) is higher than the one used in co-staining with vimentin (B).

#### **5.2.4 YFP and FSP1 co-expression in the infarct and border zone of *Col1a2 CreERT; Rosa26-floxed STOP eYFP* hearts following myocardial infarction**

To investigate the pattern of CF marker expression and assess their contribution to the injured heart tissue following MI, I followed the expression of FSP1 and vimentin and assessed their co-expression with endogenous YFP in the hearts of *Col1a2 CreERT; Rosa26-floxed-STOP-eYFP* and control *Rosa26-floxed-STOP-eYFP* mice following (i) Tamoxifen-activation of Cre (please see section 2.11.1) and (ii) subsequent myocardial infarction. A surgical myocardial infarct was introduced by ligation of the left anterior descending coronary artery by Dr. Rachael Redgrave. After 7 days from the last tamoxifen injection, 7 mice from the *Col1a2 CreERT; Rosa26-floxed STOP eYFP* line received a surgical myocardial infarct. At either 1 or 2 weeks post-surgery the mice were euthanized by cervical dislocation and the hearts were dissected, fixed and processed for cryosections (please see section 2.11). Immunohistochemical analysis of the healthy region (remote myocardium of the MI hearts showed that there was no significant difference in the pattern of eYFP, FSP1 and vimentin between the non-infarct controls, remote regions and the MI atria (Figure 5-5). However, in order to analyse the pattern of eYFP/FSP1 and eYFP/vimentin expression in the border zone and the infarct region, I had to overcome the autofluorescence problem that was associated with these areas.

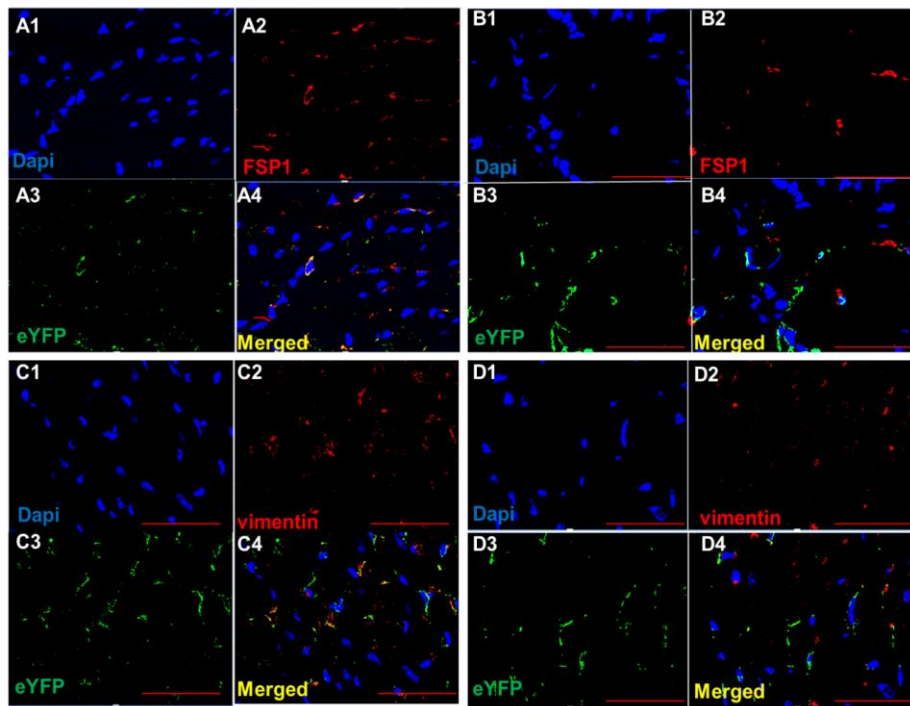


**Figure 5-5 Immunofluorescent staining of remote myocardium in an infarcted heart (n=7) with FSP1/eYFP, vimentin/eYFP in tamoxifen-treated *Colla2 CreERT; Rosa26-floxed STOP eYFP* mice.** The remote ventricular region (A1-A4) and atria (B1-B4) were stained with anti-FSP1 antibody (red), anti-GFP (green) and nuclei were stained with Dapi. Representative ventricle remote region (C1-C4) and atria (D1-D4) tissue were stained with anti-vimentin (red) and anti-GFP (green), nuclei stained with Dapi. All cryosections were prepared as described in section 2.11 and were injected with Tamoxifen as described in 2.11.1. Scale bar = 50 $\mu$ m.

### 5.2.5 Elimination of the autofluorescent artefacts in the border zone (BZ) and the infarct region (IR) of hearts following MI of *Colla2 CreERT; Rosa26-floxed STOP eYFP* and *Rosa26-floxed-STOP-eYFP* mice

Autofluorescence has emerged as a confounding factor in studies using endogenous fluorescent protein expression in muscular organs such as the heart and skeletal muscle cells. For instance, Jackson *et al.* (2004) showed significant levels of autofluorescence in skeletal muscles which could be mistaken for enhanced GFP expression [154]. Furthermore, Nussbaum *et al.* (2007) showed the level of autofluorescence in rat MI models and concluded the need for caution and appropriate negative controls when using immunofluorescence for cell lineage studies in injured hearts [155]. Therefore, to resolve autofluorescent issue, confocal microscopy with spectral unmixing was used to eliminate autofluorescence from all channels. To do this, the entire emission spectrum was scanned by the microscope and the spectral histogram was analysed in the unstained infarcted and healthy tissue samples and autofluorescent spectra were identified. Then this process was repeated for Dapi, Alexa 488 and Alexa 594 stained



sections. Then, the desired spectra which covered the majority of the autofluorescence ranges were chosen, and the autofluorescence was removed. Finally the remaining spectra matching the real emission from each fluorochrome was used to detect the real expression. Figure 5-6 shows the removal of autofluorescence from the infarct region of *Rosa26-floxed-STOP-eYFP* mice. As expected these mice did not express YFP after tamoxifen injection in the infarct region which again validates the efficiency of the *STOP* cassette. Figure 5-7 shows the removal of autofluorescence from the border zone of *Coll1a2 CreERT; Rosa26-floxed STOP eYFP* mice.

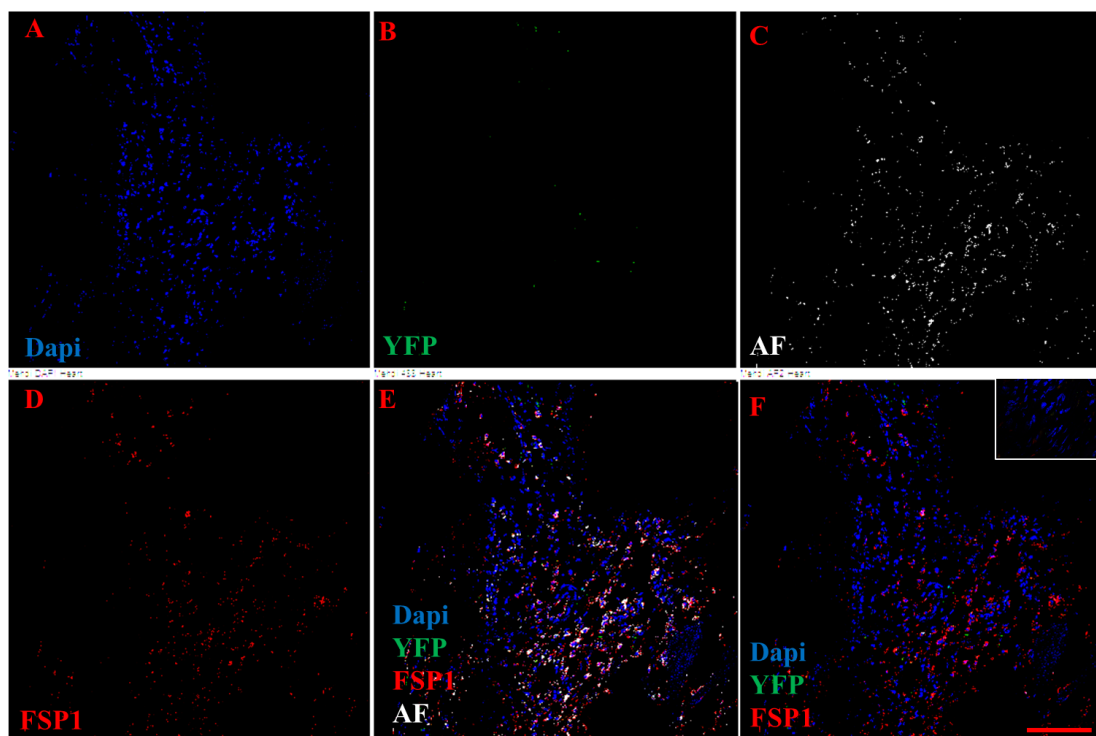


**Figure 5-6 Auto fluorescent background elimination in the infarct region of *Rosa26-floxed-STOP-eYFP* mice.** Cryopreserved sections of infarct regions from two *Rosa26-floxed-STOP-eYFP* mice were analysed with confocal microscopy and the fluorescent spectra from these sections were used to analyses fluorescent staining in the border zone and the infarct regions of *Coll1a2CreERT; Rosa26-floxed-STOP-eYFP*. A) Dapi, B) YFP, C) autofluorescent, D) FSP1,E) merged image with auto fluorescent and F) merged image after removing autofluorescent. Scale bar=100 $\mu$ m.

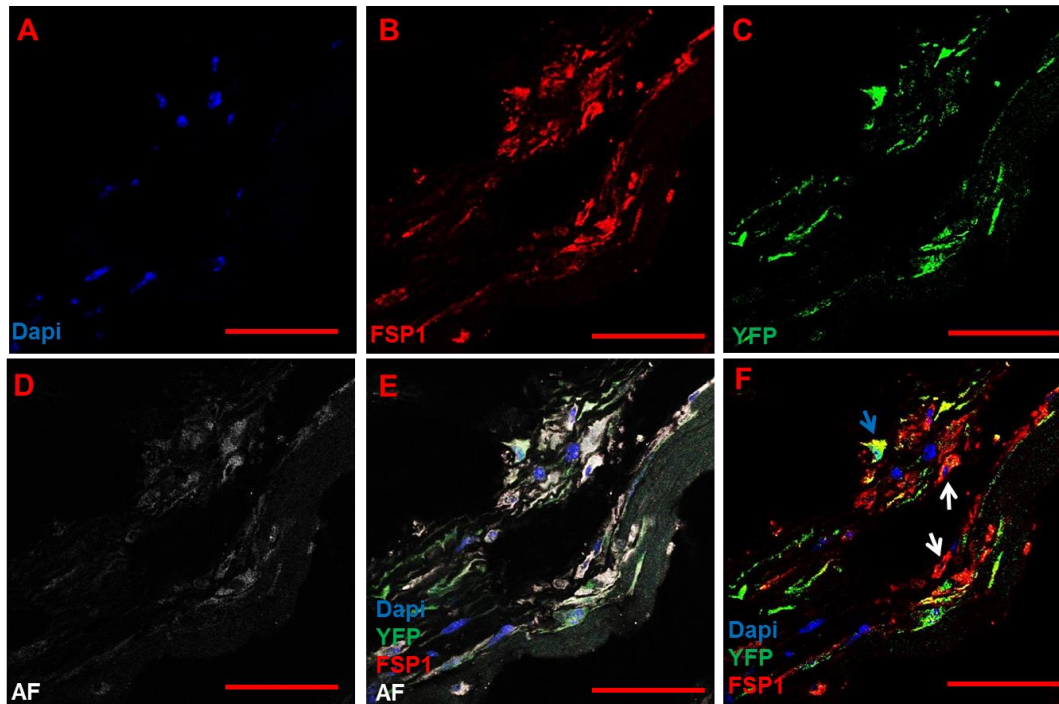


**Figure 5-7 Evaluation of the autofluorescence in the border zone of *Col1a2 CreERT*; *Rosa26-floxed STOP eYFP* mice, two weeks after MI.** 8-week old *CreERT*; *Rosa26-floxed-STOP-eYFP* mice received 5 intraperitoneal injections of tamoxifen (2 mg/ml) and two weeks after LAD ligation, the hearts were dissected and stained with anti-GFP and FSP1 conjugated with Alexa 594. To eliminate the autofluorescence from the tissue, I used confocal microscopy and analysed the spectral emissions from Dapi, Alexa 594 and Alexa 488 stainings. (A) Dapi, (B) FSP1, (C) eYFP, (D) autofluorescence, (E) Dapi, FSP1 and eYFP merged with autofluorescence and (F) merged without fluorescence. As shown in E and F, the spectral analysis has appreciably reduced the autofluorescent background. Co-localization analysis of eYFP and FSP1 showed that in the cells of the border zone, there is limited overlapping expression of FSP1 and eYFP. (F) Some cells express only FSP1 (highlighted by white arrows) and some co-express FSP1 and eYFP (highlighted by the blue arrows).

### 5.2.6 The pattern of eYFP/FSP1 and eYFP/vimentin expression in the border zone and the infarct region

After removing the autofluorescence from the samples, I observed that majority of FSP1, vimentin and eYFP, do not co-localise in the same cells in the infarct region. However, there was a significant increase in the numbers of cells that (individually) expressed these markers. These results are in agreement with Schneider *et al.* (2007), who showed that in normal rat and human hearts, FSP1 primarily co-localizes with markers of fibroblasts such as vimentin[156]. However, in hypertrophy induced by aortic banding, or stenosis or MI, FSP1 expression increased and macrophages and leucocytes within the infarct region stained strongly for FSP1[156]. Figure 5-8 illustrates the low level of eYFP/FSP1 or

eYFP/vimentin co-expression in the infarct regions of *Colla2 CreERT; Rosa26-floxed STOP eYFP* mice.

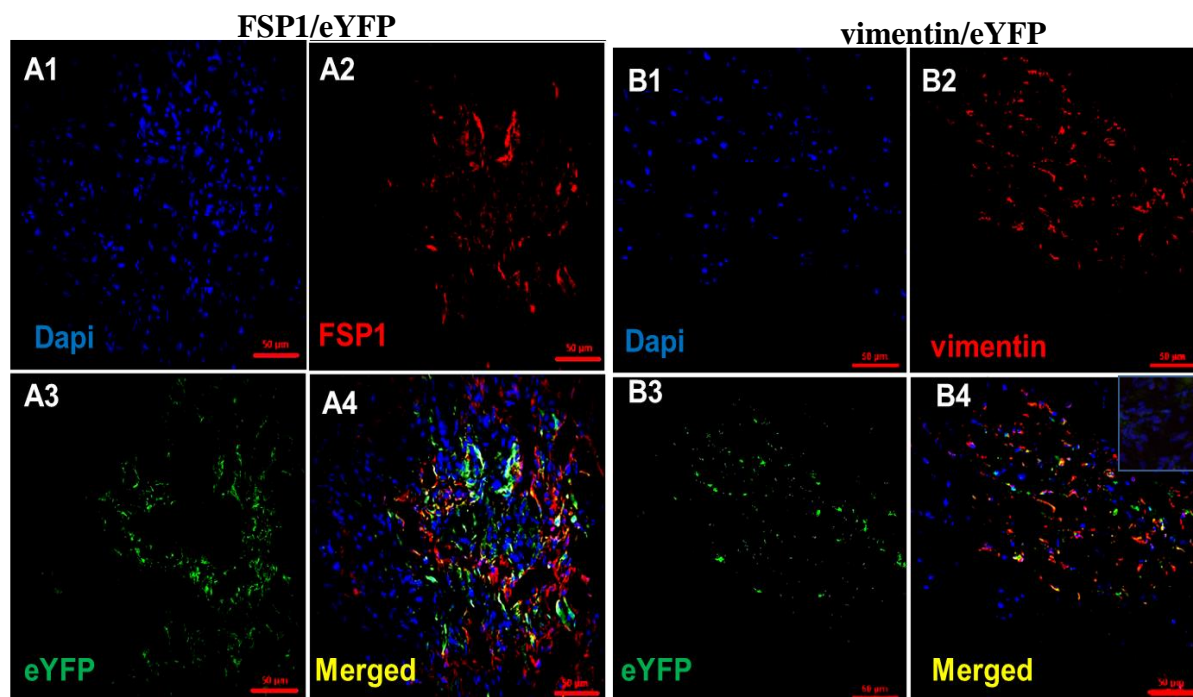


**Figure 5-8** Co localisation of FSP1 or vimentin with eYFP in the infarct region of *Colla2 CreERT; Rosa26-floxed STOP eYFP* mice, two weeks after MI. (A1-A4), a representative infarct region stained with anti-FSP1 antibody (red), anti-YFP (green) and nuclei stained with Dapi. (A1) Dapi, (A2) FSP1, (A3) eYFP and (A4) Merged. (B1-B4) a representative infarct region stained with anti-YFP (green), anti-vimentin (red). All mice and hearts were treated and processed as described in section 2.11. (B1) Dapi, (B2) vimentin, (B3) eYFP and (B4) merged. Autofluorescence in these images are removed by spectral unmixing, using confocal microscopy. The inset in image B4 is a no primary control from the infarct region. Co-localization analysis of eYFP/FSP1 or vimentin in the infarct region showed that the majority of cells do not co-express FSP1 and eYFP nor vimentin and eYFP. Scale bar = 50 µm.

A Fibroblast Marker	Cardiac Region	MIs						One way Anova p value
		1 week post MI (n=4)			2 weeks post MI (n=3)			
		Ventricle			Ventricle			
		RR	BZ	IR	RR	BZ	IR	
%YFP (Dapi cells)		16±2.5	24.1±2.3	25.5±1.6	17.4±5.7	22.3±2.3	24.7±2.7	0.000
%FSP1		25.7±4.4	30.2±2.1	43±5.7	30.7±3.1	31±2.4	41.1±6.4	0.000
%FSP1+/YFP+		7.9±3.2	10.1±3.1	8±2	10.3±5	9.7±2	8.1±2.2	0.4
%Total fibroblasts (YFP+FSP1)		32.01±5.2	42.5±3.8	52.3±4.3	33.9±4.2	41.2±3.9	52±6	0.000

B Fibroblast Marker	Cardiac Region	RR vs BZ p value		RR vs IR p value		BZ vs IR p value	
		1 W	2 W	1 W	2W	1W	2 W
% YFP (Dapi cells)		0.02	0.01	0.001	0.002	0.02	0.01
%FSP1		0.4	0.3	0.001	0.003	0.003	0.008
% Total fibroblasts (YFP+FSP1)		0.1	0.3	0.001	0.001	0.02	0.001

**Table 5-2 (A) The mean proportion of FSP1 and eYFP expression in *Col1a2 CreERT; Rosa26-floxed STOP eYFP* mice of infarcted hearts.** The table represents the summary of three independent quantifications of cells in each experimental group. Figures in the table are the percentage ± SEM of each cell type from 15-20 microscopic fields (10-12 sections) normalized to the total number of Dapi-positive nuclei. The summaries of one-way Anova tests showing the significance difference between the groups and the *p* values from the post-hoc (tukey) test on the experimental groups are shown in table B. The significant values are highlighted in red. The expression of fibroblast markers significantly increased in BZ and IR of MIs in comparison to RR. RR: remote region, BZ: border zone, IR: infarct region, 1W: 1 week post-MI, 2W: 2 weeks post-MI.

A Fibroblast Marker	Cardiac Region	MIs						One way <i>Anova</i> <i>p value</i>
		1 week post MI (n=4)			2 weeks post MI (n=3)			
		Ventricle			Ventricle			
		RR	BZ	IR	RR	BZ	IR	
%YFP (Dapi cells)		21±2.4	25±3.4	31±4.3	22.3±2.3	24.6±3.2	33±6.2	0.000
%vimentin		31.1±2	38±5.7	46.3±6.6	30±2.4	38.1±6.7	46.9±7	0.000
% vimentin <sup>+</sup> / YFP <sup>+</sup>		13.1±3	14.2±4.1	13.7±2.3	15±3.1	13.3±4.4	14±2.2	0.3
Total fibroblast(vimentin +%YFP)		46.2±7	44±3.3	54.7±7.7	44.5±9	44.5±3.7	55.5±5.5	0.000

B Fibroblast Marker	Cardiac Region	RR vs BZ <i>p value</i>		RR vs IR <i>p value</i>		BZ vs IR <i>p value</i>	
		1W	2W	1W	2W	1W	2W
%YFP (Dapi cells)		0.06	0.02	0.001	0.001	0.001	0.000
%vimentin		0.04	0.01	0.001	0.001	0.001	0.000
Total fibroblast(Vimentin +%YFP)		0.9	0.9	0.04	0.02	0.004	0.000

**Table 5-3 (A) The mean proportion of vimentin and eYFP expression in *Col1a2-CreERT*; *Rosa26-floxed-STOP-eYFP* mice of non-infarcts and MI models.** Figures in the table are the mean percentage ± SEM of each cell type from 15-20 microscopic fields (10-12 sections) normalized to the number of Dapi-positive nuclei per field of view. The summaries of one-way *Anova* tests showing the significance difference between the groups and the *p* values from the *post-hoc* (*tukey*) test on the experimental groups are shown in table B. The proportions of eYFP, vimentin and eYFP + vimentin-expressing cells increase significantly in BZ and IR of MIs in comparison to RR.

<b>A</b> Cardiac Region Fibroblast Marker	Non infarcted controls		MIs								One way Anova <i>p value</i>
	Atria (n=6)	Ventricle (n=6)	1 week post MI (n=4)				2 weeks post MI (n=3)				
			Atria	Ventricle			Atria	Ventricle			
				RR	BZ	IR		RR	BZ	IR	
%YFP <sup>+</sup> /FSP1 <sup>+</sup>	56.1±10.5	56.9±19.1	50.8±9.6	56.8±7.4	41.2±9	31.3±5.3	53.4±11.5	49.4±13	43±5.7	32.8±8.8	<b>0.001</b>
%FSP1 <sup>+</sup> /YFP <sup>+</sup>	30.5±7.6	30.4±10.4.5	31.7±11.8	34.7±8	34.8±10	19±4.8	35.4±11	31±10.5	31.2±6	20±6.5	<b>0.001</b>
% YFP <sup>+</sup> /vimentin <sup>+</sup>	60.3±13	58.8±10	59.2±12	58.3±7.6	62.7±9.4	46±5.8	55.5±12.3	56±11.2	66.6±10	48.3±7.8	<b>0.001</b>
%vimentin <sup>+</sup> / YFP <sup>+</sup>	42±10.6	39.2±9.7	41±9.7	32.7±7.4	46.1±8.7	30.3±7.5	39.5±6.7	40.3±8.8	48.1±11	31.7±6.5	<b>0.001</b>

<b>B</b> Cardiac Region Fibroblast Marker	RR vs BZ <i>p value</i>		RR vs IR <i>p value</i>		BZ vs IR <i>p value</i>	
	1W	2W	1W	2W	1W	2W
%YFP <sup>+</sup> /FSP1 <sup>+</sup>	<b>0.05</b>	0.5	<b>0.000</b>	<b>0.000</b>	<b>0.04</b>	<b>0.03</b>
%FSP1 <sup>+</sup> /YFP <sup>+</sup>	0.9	1.0	<b>0.001</b>	<b>0.001</b>	<b>0.003</b>	<b>0.03</b>
% YFP <sup>+</sup> /vimentin <sup>+</sup>	0.88	1.0	<b>0.001</b>	<b>0.001</b>	<b>0.001</b>	<b>0.001</b>
%vimentin <sup>+</sup> /YFP <sup>+</sup>	<b>0.01</b>	0.8	<b>0.02</b>	<b>0.04</b>	<b>0.03</b>	<b>0.01</b>

**Table 5-4 Evaluating the efficiency of *Colla2 CreERT; Rosa26-floxed STOP eYFP* transgenic mice in terms of eYFP co-localisation with FSP1 or vimentin *in vivo*.** (A) The table depicts the co-expression of two fibroblast markers; FSP1 or vimentin with YFP in healthy and MI mice from the atria and ventricles. Data show the mean percentage of eYFP cells which express FSP1 or vimentin and conversely. Each number is the mean number of cells  $\pm$  SEM, which is taken from 15-20 microscopic fields (10-12 sections). As shown in (A) approximately 30% of FSP1 fibroblasts from the normal atria and ventricles expressed eYFP, whilst approximately 40% of vimentin positive fibroblasts expressed eYFP, suggesting that the majority of FSP1 and vimentin-expressing cells did not express eYFP in healthy hearts. However, following MI, the co-expression of both markers with eYFP significantly reduces in IR in comparison to the RR. (B) The summary of one-way *Anova* showing the significance difference between the groups (table A) and the *post-hoc* test on the experimental groups shown in table B. (Abbreviations: RR: remote ventricular region, BZ: border zone, IR: infarct region, 1W: 1 week post-MI, 2W: 2 weeks post-MI).

### 5.2.7 Quantification of CFs in healthy and MI hearts and assessing eYFP co-staining with FSP1 or vimentin

To summarise, the efficiency of *Colla2 CreERT; Rosa26-floxed STOP eYFP* mice in CF lineage tracing and the calculation of the proportion of eYFP, FSP1, vimentin, eYFP/FSP1 and eYFP/vimentin were performed manually from 15-20 microscopic fields for each marker, taken from each mouse (x60 magnification from different regions of the atria and ventricles). As different regions in an infarcted heart (remote region, border zone and infarct region) contain different cell density therefore, I tried to take images from the regions which contained fairly similar cellular number in order to make sure that cell density has not a big impact on the final quantifications. Also the number of quantified cells for each marker were normalised to the total cell number (determined using Dapi positive nuclei per field of view). To assess the significant difference between the groups one-way *Anova* followed by *post-hoc* Tukey tests were performed. Three experimental groups from *Colla2 CreERT; Rosa26-floxed STOP eYFP* mice are given below:

1. Healthy mice (n=6)
2. 1 week post-MI (n=4)
3. 2 weeks post-MI (n=3)

In order to assess the efficiency of the STOP codon on *Rosa26-floxed-STOP-eYFP* mice 3 control groups were studied as follows.

1. Healthy mice (n=3)

2. 1 week post-MI (n=1)
3. 2 weeks post-MI (n=1)

In *Rosa26-floxed-STOP-eYFP* healthy and MI controls no eYFP expression was observed in the heart tissue (figure 5-4 and 5-6), which validated the STOP codon efficiency to inhibit unspecific labelling of cells. Further analysis of eYFP, FSP1 and vimentin expression showed that there is no significant difference between the following groups: healthy atria; infarct atria; healthy ventricle; and remote region (tables 5.1-3, Figures: 5-3 and 5-5). However, significant differences were observed between the infarct region versus the remote region and also between the infarct region versus the border zone (table 5-2 and table 5-3). Cells that showed co-expression of eYFP and FSP1 or eYFP/vimentin in the infarct region and the border zone decreased significantly in comparison with the remote region and the healthy hearts (table 5-4). To summarise the fibroblast content of murine healthy and MI hearts, quantification of YFP expressing cells showed that the healthy atria, healthy ventricle, MI atria and the remote region contain almost the same levels of eYFP cells but in the infarct zone YFP-expressing cells are significantly higher (table 5.2 A and 5.3 A). However, only 37.5% of collagen I expressing cells were activated to express eYFP using the *Colla2 CreERT; Rosa26-floxed STOP eYFP* transgenic mice. Therefore it is possible that the figures are an underestimate of collagen expressing fibroblasts that accumulate in the infarct zone. These results validated that CFs are heterogeneous and following myocardial infarction their proliferation rate increase significantly within the infarct and the border zone in comparison to the remote region.

Although *Colla2 CreERT; Rosa26-floxed STOP eYFP* was not efficient enough to detect all collagen 1 expressing cells *in vivo*, it could help us track cardiac fibroblasts and their derivatives at different stages of CDC culture.

### **5.2.8 eYFP expression at different stages of CDC culture**

*Colla2* has been shown to be an important type of collagen produced by CFs to form ECM, reviewed in [17], and it has already been shown that cardiac explants and Csphs express *Colla2* [78]. However there is some controversy over the extent of the CF contribution to CDCs. Therefore, having evaluated the efficiency of *Colla2-CreERT*;



*Rosa26-floxed-STOP-eYFP* transgenic mice as a tool to track CFs in lineage-tracing experiments I investigated the contribution of CF derived cells (by eYFP expression) to EDCs, Csphs and CDCs. To this end, nine *Colla2-CreERT; Rosa26-floxed-STOP-eYFP* mice (6-8 weeks old) were injected intraperitoneally with 2 mg tamoxifen per day, over 5 days. After 48 hours following the last injection, mice were euthanized by cervical dislocation and the hearts were dissected. Atrial explants were cultured on fibronectin-coated plates. To investigate the contribution of potential fibroblasts to EDCs, Csphs and CDCs I used confocal microscopy to analyse eYFP expression. However, I first had to resolve the problem of cell autofluorescence in cardiac explants and Csphs. Using the spectral unmixing option of the confocal microscope I digitally removed the autofluorescence from the cardiac tissue and phase bright cells. Figure 5-9 depicts a representative cardiac explant before and after the removal of autofluorescence. Detailed analysis of atrial explants from nine *Colla2-CreERT; Rosa26-floxed-STOP-eYFP* mice revealed that phase bright cells do not express eYFP, but stromal cells which grow underneath the phase bright cells do express eYFP. To quantify the proportion of cells expressing YFP, all EDCs (stromal cells and phase bright cells) were harvested with enzymatic digestion after 3 weeks of EDC culture and eYFP expression was assessed by FACS. These results showed that 9-11.5% of EDCs express eYFP. However, when considering the efficiency of the transgenic model the number of YFP-expressing cells in the EDC stage would be approximately 28-30%. The FACS data are derived from 4 independent experiments and presented as the mean percentage of eYFP-expressing cells  $\pm$  SEM.

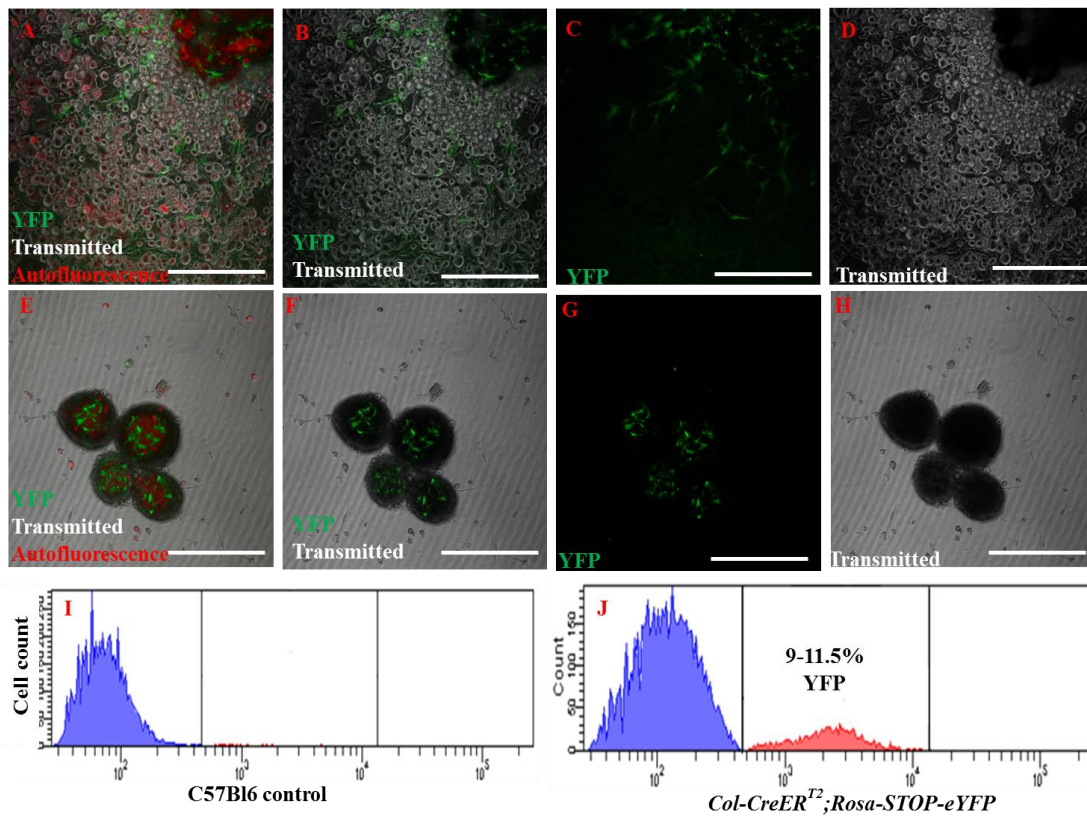


**Figure 5-9 eYFP expression in EDCs and Csphs cultured from the atria of *Col-CreERT*; *Rosa26-floxed-STOP-eYFP* mice.** eYFP expression was monitored by confocal microscopy with the additional white transmitted light option. High levels of autofluorescence were identified and removed using the spectral unmixing option of the confocal microscope. (A) A cardiac explant from *Col-CreERT*;*Rosa26-floxed-STOP-eYFP* mice with autofluorescence, indicated by the red colour. (B) The same explant after removing autofluorescence; and (C) eYFP is only expressed in stromal cells and not in phase bright cells. (D) Transmitted light image of phase bright cells (day 14). (E) Csphs showing autofluorescence (red) and eYFP (day 7). (F) eYFP expression in Csphs after removing the autofluorescence. (G) eYFP-expressing cells inside the Csphs. (H) Csphs imaged with transmitted light only. (I,J) After week 3, EDCs were enzymatically detached and eYFP expression was assessed by FACS. (I) eYFP expression is absent in EDCs prepared from C57BL/6 control mice. (J) eYFP expression in EDCs (at week 3 of culture) prepared from *Col-CreERT*; *Rosa26-floxed-STOP-eYFP* mice shows that 9-11.5% of EDCs express eYFP. This experiment was repeated four times independently and results presented as percentage eYFP expressing cells $\pm$  SEM. Scale bar = 500  $\mu$ m.

Having observed eYFP expression in Csphs after 7 days of culture (Figure 5-9), I next tried to evaluate how this occurred over time, and how early eYFP<sup>+</sup> cells were recruited to the Csphs. Following Cre-recombinase activation in adult *Col1a2 CreERT*; *Rosa26-floxed STOP eYFP* mice (age 8 weeks) with tamoxifen treatment, Csph culture was performed and eYFP expression was analysed with confocal microscopy over 2 weeks. Interestingly, the results showed that some cells inside the Csphs clearly express eYFP from the earliest stages of Csph formation and were seen at day 4. Figure 5-10 depicts eYFP expression in Csphs at day 4 (A,B,C) and day 14 (D,E,F) of culture.

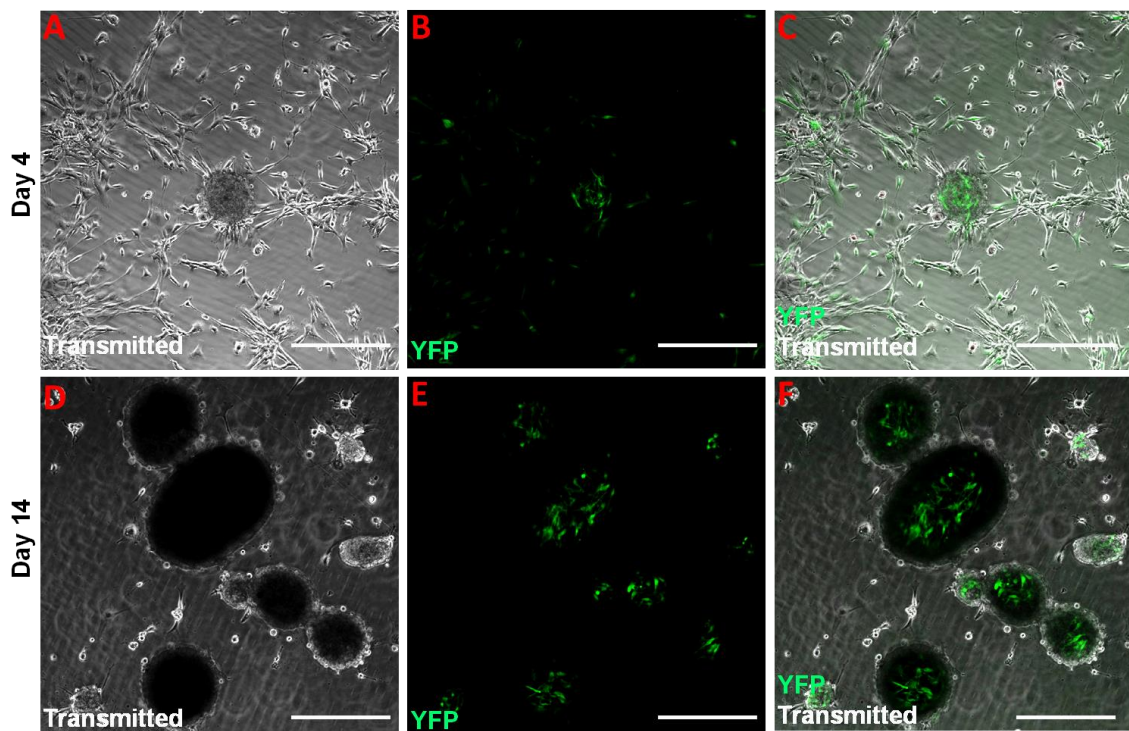


**Figure 5-10 eYFP expression in Csphs derived from *Col1a2 CreERT*; *Rosa26-floxed STOP eYFP* mice.** Csph culture from atrial explants from *Col1a2 CreERT*; *Rosa26-floxed STOP eYFP* mice after intraperitoneal injections (2 mg) of tamoxifen once per day over five days. After 48 hours from the last injection the hearts were removed and the atria were cultured as cardiac explants. After 3 weeks the EDCs were removed by enzymatic digestion and plated at  $10^5$  cells per well of a 24-well plate. eYFP expression was assessed from day 4 to day 14. The images in this figure show phase contrast and YFP fluorescence from Csphs at day 4 (A-C) and 14 (D-F) of culture. Images in B and E show eYFP expression in Csphs at day 4 (B) and day 14 (E); and in merged channels at day 4 (C) and day 14 (F). eYFP was expressed in all stages of Csph culture and indicates that Csphs contain fibroblasts or fibroblast-derived cells. This experiment was repeated 3 times independently. Scale bar = 500  $\mu$ m.

### 5.2.9 eYFP<sup>+</sup> EDCs from atria are able to form Csphs

Having shown that Csphs contain eYFP expressing cells, I next considered whether a pure population of eYFP expressing cells could form Csphs. Therefore, I compared Csph formation from YFP<sup>+</sup> versus YFP<sup>-</sup> EDCs. In order to do this, EDC culture was preformed from 6-8 week old *Coll1a2-CreERT; Rosa26-floxed-STOP-eYFP* mice following tamoxifen injection (please see section 2.11.1). After 3 weeks of culture, EDCs were disassociated and FACS sorted based on eYFP expression. Thereafter, eYFP<sup>+</sup> and eYFP<sup>-</sup> EDCs were placed at the same seeding density ( $10^5$  cells/well of a 24 well plate) in CGM in three separate wells and cultured for 2 weeks. Interestingly, the results showed that eYFP<sup>-</sup> EDCs formed significantly more Csphs than eYFP<sup>+</sup> EDCs, yet eYFP<sup>+</sup> EDCs also made Csphs but significantly lower numbers than eYFP<sup>-</sup> EDCs. As shown below (figure 5-11,C) eYFP<sup>-</sup> EDCs made 26-93 Csphs and eYFP<sup>+</sup> EDCs made 19-47 Csphs after 2 weeks of culture per well. However due to the heterogeneity of cardiac fibroblasts and incomplete activation of all collagen expressing cells using the eYFP reporter, it is likely that the eYFP<sup>-</sup> fraction of EDCs still contain significant number of cardiac fibroblasts.

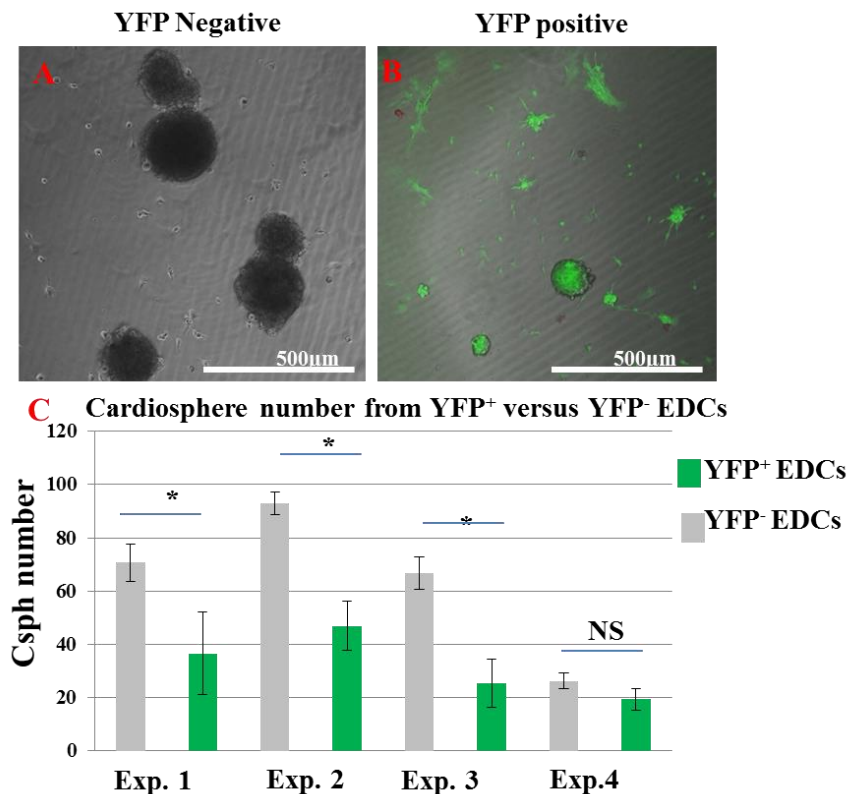


**Figure 5-11 Evaluating the potential of eYFP<sup>+</sup> versus eYFP<sup>-</sup> EDCs to generate Csphs.** A summary of four independent experiments showing Csph number from eYFP<sup>-</sup> EDCs (grey bars) and eYFP<sup>+</sup> EDCs (Green bars). 10<sup>5</sup> sorted EDCs were seeded in three different wells of a 24-well plate from each biological replicate and fully formed Csphs from both eYFP<sup>+</sup> and eYFP<sup>-</sup> cells were quantified at day 14. In three replicate experiments, eYFP<sup>-</sup> EDCs generated more Csphs than their eYFP<sup>+</sup> counterparts. However, in a fourth experiment no significant difference was observed between the two groups. (A) Csphs formed from eYFP<sup>-</sup> EDCs and (B) Csphs formed from eYFP<sup>+</sup> EDCs. Data analysed using student unpaired t test. (\* Denotes p<0.05). C) This experiment was repeated 4 times independently and results are presented as the mean number of Csphs ± SEM formed at day 14. Scale bar = 500 μm.

### 5.2.10 eYFP expression in passage 2 CDCs derived from *Colla2CreERT*; *Rosa26-floxed-STOP-eYFP* mice

So far my experiments showed that CF-derived cells are present in standard EDCs and Csph cultures. As passage 2 CDCs have been used frequently in this research and regenerative studies of the heart, it will be very useful to evaluate the fibroblast content of P2 CDCs. Previously, I observed that Sca-1 expression in CDCs increases by extending the passage number (please see section 4.2.11). This could be due to increasing passage numbers leading to increased fibroblast sub-populations of CDCs, as it has been shown that in wound healing, PECAM<sup>+</sup>/Sca1<sup>+</sup> vascular cells proliferate and transform into αSMA<sup>+</sup> myofibroblasts and αSMA expression was detected in 17% of

Sca-1<sup>+</sup> and 4.5% of PECAM1<sup>+</sup>/Sca1<sup>+</sup> cells[157]. Therefore, it is likely that some sub-populations of CDCs which express Sca-1 could also express fibroblast markers such as *Coll1α2*. In this respect, co-expression analysis of stem cell markers (Sca-1 or cKit) and eYFP in P2 CDCs could provide valuable information on the cell identities of CDCs. Using FACS immunophenotyping, P2 CDCs derived from the atria of 6-8 weeks old *Colla2 CreERT; Rosa26-floxed STOP eYFP* mice were assessed for co-expression of endogenous eYFP with cKit and Sca-1. FACS results showed that 8.3-12.9% of P2 CDCs express eYFP. Although I observed variability in eYFP-expressing CDCs in different culture preparations, it appears that eYFP CDCs are slightly distinct from Sca-1 and cKit-expressing cells as the majority of Sca-1<sup>+</sup> cells and cKit<sup>+</sup> cells were negative for eYFP. Figure 5-12 depicts a representative FACS analysis of P2 CDCs from *Colla2 CreERT; Rosa26-floxed STOP eYFP* mice and shows that 0.7-1.2% and 2.3-6.3% of CDCs are cKit<sup>+</sup>/YFP<sup>+</sup> and Sca-1<sup>+</sup>/YFP<sup>+</sup> respectively. Table 5-5 summarized the results of three independent analyses.

To elucidate what percentage of Sca-1<sup>+</sup> and cKit<sup>+</sup> CDCs express eYFP, I further analysed these CDC sub-populations and observed that ~19.6% and ~10.3% of Sca-1<sup>+</sup> and cKit<sup>+</sup> CDCs express eYFP, respectively. Figure 5-13 illustrates the percentage of Sca-1 and cKit CDCs at passage 2 which express eYFP. However, considering the efficiency of the *Colla2 CreERT; Rosa26-floxed STOP eYFP* transgenic mouse model the figures are likely to be higher.

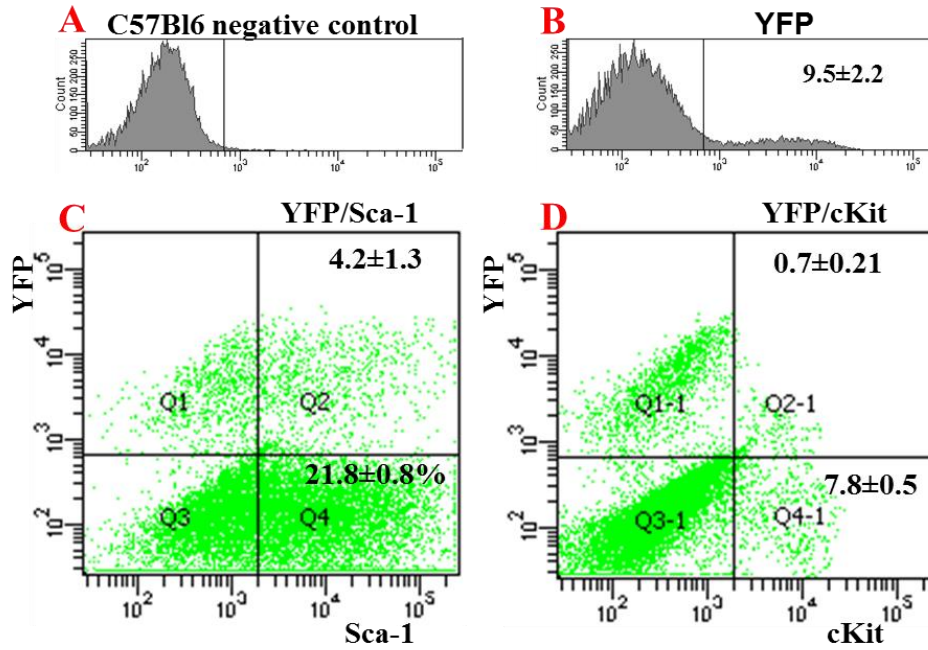


**Figure 5-12** eYFP<sup>+</sup>, eYFP<sup>+</sup>Sca-1<sup>+</sup> and eYFP<sup>+</sup>cKit<sup>+</sup> cells in P2 CDCs from *Colla2 CreERT*; *Rosa26-floxed STOP eYFP* mice. Mice received 2mg interaperitoneal injections of tamoxifen over 5 consecutive days. CDCs from the atria were expanded until passage 2 and then analysed for expression of eYFP, Sca-1 and cKit. Histogram (A) shows P2 CDCs from C57BL/6 mice used as a negative control for FACS analysis and confirm no YFP expression. Histogram (B) shows that 9.5±2.2% of P2 CDCs express eYFP. Dot plots (C) and (D) show the proportion of CDCs that co-express eYFP with Sca-1 (4.2±1.3%) and eYFP with cKit (0.7±0.21%) respectively.

Markers	Experiment 1	Experiment 2 *	Experiment 3
YFP	12.9±3.4	9.5±2.2	8.3±1.2
Sca-1	28.06±0.14	21.8±0.8	12.9±0.1
cKit	8.03±0.9	7.8±0.5	3.9±0.2
YFP/Sca-1	6.3±1.7	4.2±1.3	2.3±0.8
YFP/cKit	1.2±0.4	0.7±0.21	0.3±0.14

**Table 5-5** A summary of three independent FACS experiments for eYFP, Sca-1 and cKit expression in P2 CDCs from *Colla2 CreERT*; *Rosa26-floxed STOP eYFP* mice. Results are presented as the mean percentage of the total analysed CDCs per experiment ± SEM. \*Denote run is depicted in figure 5-12.

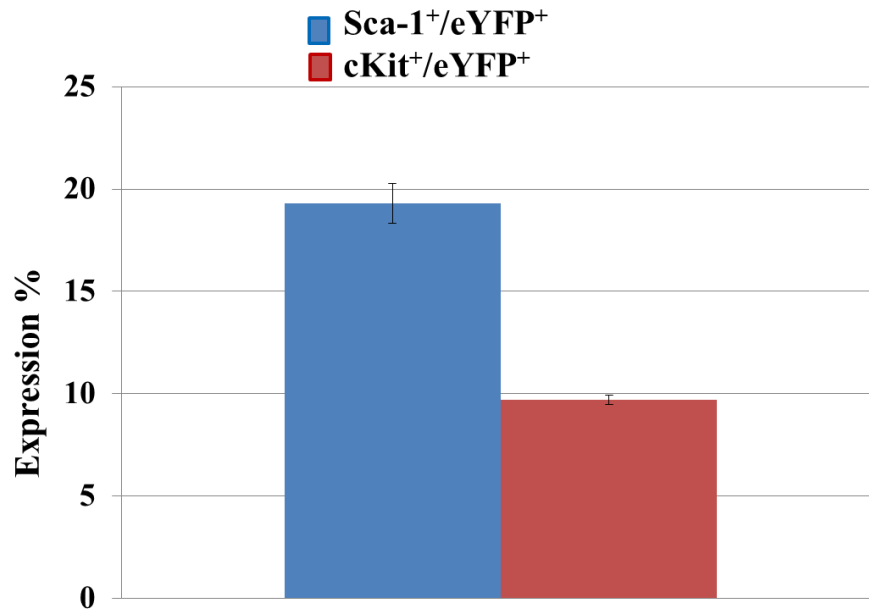


**Figure 5-13** The proportion of Sca-1<sup>+</sup> and cKit<sup>+</sup> CDCs which express eYFP in P2 CDCs cultured from *Colla2 CreERT; Rosa26-floxed STOP eYFP* mice. A summary of three independent FACS analyses, showing the proportion of Sca-1- and cKit-expressing CDCs that also express eYFP. Results showed that the majority of Sca-1- and cKit-expressing CDCs do not express eYFP.

### 5.2.11 eYFP expression (derived from *Colla2 CreERT; Rosa26-floxed STOP eYFP* mice) increases by extending CDC passage number

I observed that 8-13% of P2 CDCs derived from the atrium of 6-8 week-old *Colla2 CreERT; Rosa26-floxed STOP eYFP* mice express eYFP. However, it would be interesting to assess if passaging CDCs could change the proportion of eYFP-expressing cells in CDCs. To this end CDCs from *Colla2 CreERT; Rosa26-floxed STOP eYFP* mice were cultured for 4 passages and eYFP-expression was analysed with FACS at two time points. The results showed that eYFP-expression increased in P4 CDCs (12.9± 0.2%) in comparison with P2 (9.7±0.4%) (p<0.05 student t test was performed on 3 technical replicates). However, my experiment was performed only once and further biological replicates are necessary to validate this finding. Figure 5-14 depicts the effect of cell passaging on eYFP expression in P2 and P4 CDCs.



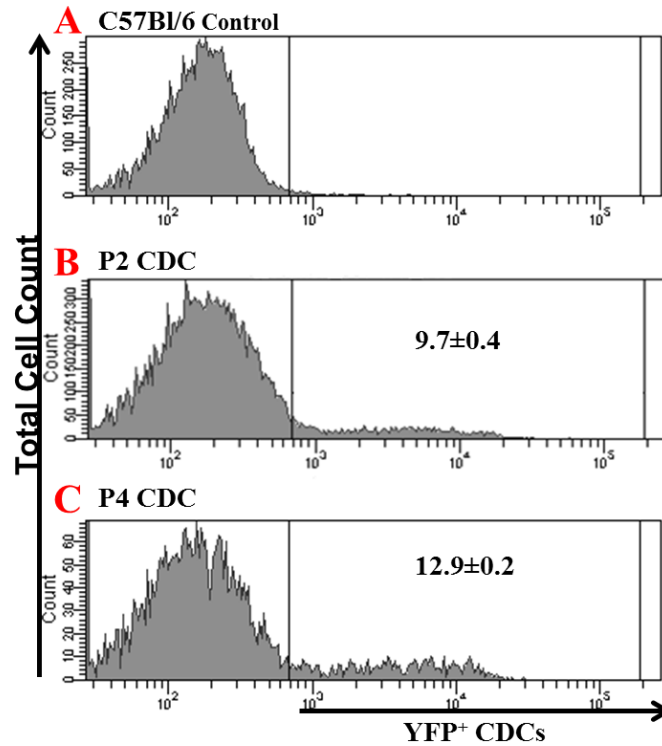


**Figure 5-14** The effect of cell passage on eYFP expression in P2 and P4 CDCs derived from *Col1a2 CreERT; Rosa26-floxed STOP eYFP* mice. CDCs cultured from *Col1a2 CreERT; Rosa26-floxed STOP eYFP* following Tamoxifen injection (section 2.11.1) and the expression of eYFP was measured with FACS. Histogram (A) depicts C57BL/6 P2 CDCs used as negative control for eYFP expression. (B) and (C) eYFP expression in P2 and P4 CDCs with 9.7±0.4% and 12.9±0.2 respectively. The results showed an increase in the proportion of eYFP-expressing cells in P4 CDCs in comparison with P2 CDCs. However, this experiment was done only once and more replicates are necessary to validate these findings.

### 5.3 Discussion

My studies in this chapter confirmed that murine hearts contain significant number of CFs, therefore it is likely that any cell culture of unselected cells from the heart tissue could potentially include considerable quantities of CFs. In this respect, CDC culture from cardiac explants is no exception, thus it is important to assess the quantity of CF in CDCs. As the rate of fibrosis in the infarct region of the myocardium dramatically increases, reviewed in [17], in any cell transplantation study for heart repair it is crucial to evaluate the CF content of the donor cells because, if the donor cells contain high levels of fibroblasts, this could potentially enhance the fibrosis process in the recipient heart. In the work described in this chapter, I tracked the potential CF content of CDC culture using transgenic *Colla2 CreERT; Rosa26-floxed STOP eYFP* mice, in which a eYFP reporter is expressed by the *Colla2* promoter, which corresponds partially ( $37.3 \pm 2.1\%$  efficiency) to collagen type 1 expressing cells in the heart (Figure 5.2). To identify CFs in the heart, I used FSP1 and vimentin immunostaining. FSP1 and vimentin have been reported to be useful markers for CF detection, reviewed in [15]. Immunohistochemical assessment of single staining for eYFP, FSP1 or vimentin showed that there was no significant difference between the atria and ventricles in the numbers of cells showing expression of these markers, which suggests that murine atria and ventricles share a similar fibroblast content (table 5-1). The manual quantification of total fibroblasts, which was obtained by adding eYFP with FSP1 or Vimentin normalised to the total number of cells per microscopic field showed that the atria and ventricles have fairly similar fibroblast content (34-36%) (table 5-1). However, co-localisation analysis of eYFP and FSP1 or vimentin showed that our transgenic mouse model is not able to detect all of the other cardiac fibroblast sub-populations *in vivo*. Detailed immunohistochemical analysis of the atria and ventricles from healthy murine hearts showed that ~ 30% of FSP1 and 39-42.3% of vimentin-expressing cells were labelled with eYFP and, conversely, almost 56% and 58-60% of eYFP cells were stained positive for either FSP1 or vimentin respectively (table 5-4).

There are several reasons which could possibly explain why this model failed to label the majority of cardiac fibroblasts:

The discrepancy between eYFP and FSP1 or eYFP and vimentin-expressing cells seen in this chapter could be due to the fact that CFs are heterogeneous cells originating from different sources and the fibroblast markers which are being used in CF studies are also

involved in other pathways. For instance, FSP1 is shown to be up regulated during neuronal differentiation [158], cell motility [159], angiogenesis [160,161], cardiomyogenesis [161] and heart repair [156]. It has also been shown that FSP1 is expressed in carcinoma cells [162] and macrophages [156]. On the other hand, vimentin, which was initially described as an endothelial cell marker [163], is also expressed in pericytes and myoepithelial cells [163,164], yet FSP1 and vimentin have been widely used to detect cardiac fibroblasts. Collagen 1 is shown to be expressed in fibroblasts, osteoblasts and odontoblasts, and its regulation is controlled by different genomic regions, reviewed in [165]. The collagen 1 promoter has numerous tissue-specific transcription activation sites located at different distances from the 5' transcription start site. Some enhancer sites are even located 19.5 Kb upstream to the transcription site. In *Colla2 CreERT; Rosa26-floxed STOP eYFP* mice a region, which was -19.5-kb to -13.5-kb upstream of the transcription start site, was used to make this transgenic line [110]. It is yet possible that part of the heart's tissue-specific enhancer of the Collagen 1 promoter was not included so leading to incomplete activation of the *Colla2* promoter in all CFs. According to the authors this enhancer drives *Coll1α2* in fibroblasts, as CFs in the hearts are believed to be heterogeneous; it is yet possible that this enhancer is only active in a subset of CFs.

Another potential reason for the lower than expected proportion of YFP+ CFs seen in the healthy hearts (from tamoxifen-activated *Colla2 CreERT; Rosa26-floxed STOP eYFP* mice) examined in this chapter is due to the incompletely ubiquitous expression of the *Rosa26* allele. Although the *Rosa26* promoter is generally considered to be ubiquitously expressed, it is possible that *Rosa26* has less activity in CFs. It is also possible that a proportion of cardiac fibroblasts have silenced their *Rosa* promoter by methylation mechanisms in *Colla2 CreERT; Rosa26-floxed STOP eYFP* mice which made it undetectable. Therefore, it would be interesting to assess the methylation status of CFs. Consequently, it would be useful to assess the expression of *Rosa* promoter and its epigenetic status *in vitro* in the CF cell culture. This will assist us in deciding which lineage-tracing mechanisms could be optimal to track cardiac fibroblasts. To activate Cre-recombinase I used the established protocol in my host laboratory with five consecutive IP injections of 2mg tamoxifen. It is possible that the amount of Cre-recombinase activation was below the threshold required to activate the eYFP reporter in all CFs. Therefore, further optimisation of tamoxifen injection in *Colla2 CreERT; Rosa26-floxed STOP eYFP* mice may be necessary. 4-hydroxytamoxifen is one early

functional metabolite of Tamoxifen with more activity [166]. It would be interesting to see whether the administration of 4-hydroxytamoxifen enhances Cre recombinase activation.

### **5.3.1 Myocardial infarction causes autofluorescence in the border zone and in the injured region**

Immunohistochemical analysis of infarcted heart sections from *Colla2 CreERT; Rosa26-floxed STOP eYFP* mice showed that the border zone and infarct region have high levels of tissue autofluorescence, which might be mistaken for an enhanced expression of any fluorescent reporter. To distinguish between the real eYFP, FSP1 and vimentin expression in the border zone and the infarct region, I used spectral unmixing with confocal microscopy. Although this approach reduced endogenous autofluorescence in the border zone and the injured regions, I observed that there remained some unidentified fluorescent spectra. As shown in the literature, tissue autofluorescence is either intrinsic (tissue type) or caused by tissue processing with different reagents [167]. In one study, researchers showed that the accumulation of lipofuscin granules and collagen fibres in skeletal muscles could cause autofluorescent artefacts. These cellular wastes are formed due to cell senescence and oxidative stress [168]. Therefore, autofluorescence is likely to be inevitable after MI, but it would be interesting to see if treatment with sudan black on the myocardial sections could reduce the autofluorescent level. It has been shown that treatment of the paraffin section of myocardial samples with sudan completely removed the autofluorescence from cardiomyocytes [167]. This could be accompanied with spectral unmixing with confocal to reduce further the level of autofluorescence.

### **5.3.2 Co-localisation of FSP1 and vimentin with eYFP in the border zone and the infarct region**

During my investigations of eYFP and FSP1, and vimentin expression from the healthy hearts, remote regions, the border zone and the infarct regions, I noticed that eYFP and FSP1 or eYFP and vimentin show incomplete co-localisation. To some extent my finding is partially in agreement with a previous study showing no co-localisation of

FSP1 and Collagen 1 in myofibroblasts in the fibrotic kidney; their study concluded that FSP1 was a poor marker to detect Collagen 1 expressing cells in the fibrotic kidney [169]. However, I noticed that following MI the expression of these fibroblast markers (eYFP, FSP1 and vimentin) significantly increases in the infarct region and border zone in comparison with the remote region and healthy hearts (see tables 5-1, 5-2 and 5-3). My finding is in agreement with work of other investigators. For instance, it has been shown that myocardial injury (MI or aortic banding) increases FSP1 protein expression 1.8-5.9 fold in comparison with sham operated groups [170,171]. My results also showed that following MI the number of total CFs (eYFP, FSP1 and vimentin-expressing cells) significantly increases in the border zone and the infarct region in comparison with the remote ventricular region (tables 5-2 and 5-3). However, there is a difference between my results and those of Camelliti *et al.* [172] who showed that, following MI induction in sheep, vimentin density increases in the remote region. In contrast, I did not see a significant change in the CF content of remote regions and healthy controls (Tables 5-2 and 5-3). This could be due to the different species used in these two studies. As shown in table 5-4 the co expression of YFP and FSP1 or vimentin significantly decreased in the infarct region versus the remote region which suggests the invasion of non-CFs into the infarct region. Indeed, it is known that MI activates immune responses and invasion of macrophages into the infarct region, which express FSP1 [156] and vimentin [173]. However, to investigate the fibroblast contribution to heart repair further, it would be useful to assess the expression of macrophage markers such as (CD11b) and collagen following MI.

There are some reasons that could potentially explain why not all eYFP cells stained with Collagen 1. (i) Un-specific activation of eYFP in some cells. Although I have always prepared biological controls from the *Rosa26-floxed STOP-eYFP* line in order to assess the specificity of eYFP expression to ensure that they are clear (no YFP expression), it is possible that in some cases eYFP has been activated un-expectedly and could have been detected as eYFP expression. (ii) Un-specific staining of Collagen 1 antibody, although technical negative controls for primary and secondary antibodies have always been included in all of fluorescent staining, it is possible that some un-specific collagen 1 staining has been detected and considered as a collagen 1 expressing cell. (iii) As I have quantified eYFP and Collagen 1 co-localisation in heart section with confocal microscopy, it is possible that I have missed a significant number of cells which co-express eYFP and Collagen1 in regions which have not been sectioned,

therefore assessing co-localisation of these two markers in single cells preps from freshly dissected healthy and infarcted *Coll1a2 CreERT; Rosa26-floxed STOP eYFP hearts* with FACS could potentially reveal more accurate results.

As shown in table 5-1 there is a considerable variation between the number of e-YFP and total fibroblast in two halves of the table. This variability is due to the fact that I used two different types of eYFP primary antibodies combined with either FSP1 or vimentin, in order to make compatible combinations of antibodies. However these results also suggest that neither of these anti-eYFP primary antibodies was fully efficient to detect all eYFP expressing cells. As discussed above several reasons could explain this incomplete co-staining between the antibodies such as; the heterogeneity of CFs (not all CFs express collagen-1) or the variable specificity of the antibodies used in this staining protocol.

### **5.3.3 Possible implications of MI experimental design on eYFP expression in CFs**

In this experiment the LAD ligation surgery was induced 7 days after the last tamoxifen injection and the hearts were dissected at 1 or 2 weeks post-MI. It is already known that in lineage tracing using the Cre-ER system, it takes just above 24 hours for Cre-ER to be detectable in the nucleus [174], although the authors reported variable time points for detecting labelled cells in different species following tamoxifen administration. Therefore, another approach is to administer tamoxifen after LAD ligation. It is likely that tamoxifen administration after surgery could increase eYFP localization within CFs with other fibroblast markers due to the fact that MI activates CF proliferation; so that recombination and eYFP accumulation may happen more efficiently in dividing CFs with active Cre-ER. Ideally, the *Coll1a2 CreERT; Rosa26-floxed STOP eYFP* transgenic model could be improved. It would be better to reconsider the 5' upstream region and assess if the sub-cloned region contains the heart tissue-specific transcription enhancer. As in the healthy myocardium and MI models, which had 2 and 7 days (respectively) of the window period between the last tamoxifen administration and heart dissection, the majority of CFs were not targeted with eYFP in both groups. This validates the consistency of the transgenic line in targeting Collagen 1 expressing cells. However, it would also be interesting to assess the expression of collagen receptors such as DDR2 co-localisation with eYFP, this could possibly be more helpful than FSP1 and vimentin

in further assessing the efficiency of *Colla2 CreERT; Rosa26-floxed STOP eYFP* in targeting CFs, as DDR2 is believed to be a collagen receptor, reviewed in [15].

#### **5.3.4 Cardiac fibroblasts are able to form Csphs**

To investigate whether eYFP<sup>+</sup> EDCs are able to form Csphs, I performed a Csph-forming assay from FACS sorted eYFP<sup>+</sup> and eYFP<sup>-</sup> EDC populations and found that both groups are able to form Csphs, suggesting the CFs or their derivatives could form Csph. These results are in agreement with a previous study [152] which showed that colon-derived fibroblasts can form spheroid aggregates. However, eYFP<sup>-</sup> EDCs did form more Csphs than eYFP<sup>+</sup> EDC, suggesting that either eYFP<sup>-</sup> EDCs have a shorter doubling time or release cytokines which encourage cell accumulation and Csph formation. However having eYFP<sup>-</sup> sorted cell fraction does not mean that they are fibroblast free cell population, as not all fibroblasts express Collagen 1 and not all collagen expressing cells were eYFP-positive in this study. Possibly sorting CDCs using alternative fibroblast markers (eg CD90) could tell us if fibroblast free CDCs are able to form Csphs. This would also emphasise the role of CFs in Csph formation and the consequences of CF depletion in terms of gene expression and cytokine production Csph biology. Although my findings indicate that Csph formation is not a very specific stem cell characteristic for CDC culture, it has previously been shown that Csphs contain more cKit<sup>+</sup> cells and express more stem cells related factors than monolayers [67]. It would be interesting to analyse and compare the growth factors released by eYFP<sup>-</sup> and eYFP<sup>+</sup> Csphs. Also it would be informative to perform a more complete immunophenotyping of CDCs derived from eYFP<sup>-</sup> and eYFP<sup>+</sup> EDCs, as this will provide more information in terms of stem cell sub-populations of CDCs derived from CFs. Measuring cell proliferation in eYFP<sup>+</sup> and eYFP<sup>-</sup> Csph cells could show whether the rate of cell doubling positively influences sphere formation in eYFP<sup>-</sup> Csph cells.

#### **5.3.5 Evaluation of eYFP expression at different stages of CDC culture**

The validity of potential cardiac regeneration by Csphs has been questioned by one laboratory which suggested that Csphs are not a suitable source for cardiac stem cell expansion [78]. The authors divided Csph-forming cells into CD45<sup>-</sup> and CD45<sup>+</sup>

phenotypes and showed that CD45<sup>-</sup> CDCs express the fibroblast marker, collagen 1. Although these results have been criticized, based on variations of the techniques used to prepare Csphs, the possibility that CDCs could contain some fibroblasts still remains open. However, another study showed by immunostaining and confocal microscopy that CDCs derived from congenital heart patients were negative for collagen 1 [79]. Nevertheless, having fibroblasts in Csphs does not mean that they are incapable of cardiac regeneration. Equally, lacking fibroblasts does not mean that Csphs and CDCs are all able to differentiate to the other cell lineages. Also Smith *et al.* (2007) showed that the existence of mesenchymal cells in CDC culture could be beneficial for cardiac sub-populations by providing physical and secretory support [68]. As CDC biology aims to provide a sufficient source of cardiac progenitor cells, it is necessary that CDCs are characterised in more detail. In this respect, lineage tracing of CFs during three stages of CDC culture (EDCs, Csph, CDCs) could provide valuable information and provide a better view of CDCs for future experimental designs. Confocal analysis of EDCs from tamoxifen treated *Colla2 CreERT; Rosa26-floxed STOP eYFP* mice showed that phase bright cells derived from explants are completely negative for eYFP expression, though approximately 10% of the stromal cells express eYFP (figure 5-9). As our lineage-tracing system could not target all the collagen 1 expressing cells (37.3±2.1% lineage-tracing efficiency) my interpretation is that there are more stromal cells that are derived from CFs and this may be as high as 27%. Previously, Andersen *et al.* (2009) showed by immunostaining that Csph-forming cells, and explant-derived cells overwhelmingly express collagen 1 [78]. To address this issue I further analysed eYFP expression in Csphs from *Colla2 CreERT; Rosa26-floxed STOP eYFP* mice with confocal microscopy. My results showed that Csphs are highly autofluorescent and it is possible that the autofluorescence could be mistaken for an enhanced expression of any fluorescent reporter (figure 5-9). Although I observed some eYFP-expressing cells within the Csphs, the majority were eYFP negative (figure 5-11). This is in agreement with Li *et al.* (2010)[67], who indicated that Csphs resemble a microenvironment niche with stem cells and an extracellular matrix. Although Smith *et al.* (2007) [68] concluded that phase bright cells are the possible source of Csphs, Csphs can be formed by both phase bright and stromal cells. This implies that a type of biological selection which recruits collagen 1 expressing cells into Csphs happens during Csph culture. For instance, a growth factor released by the Csph microenvironment could attract collagen-expressing cells. In this respect Li *et al.* (2010) showed by PCR array and



immunostaining that the expression of cell adhesion and ECM markers such as COL14A1, COL7A1 and ITGA2 was enhanced in Csphs in comparison with the monolayer culture [67]. However, we also need to consider the technical differences in Csph culture that could alter the fibroblast content. For instance, it is already shown that different approaches in Csph culture could cause significant differences in cardiosphere size, number and morphology [71]. As I used harsh enzymatic cell detachment at the EDC stage to harvest both stromal and phase bright cells, this could explain eYFP<sup>+</sup> stromal cell recruitment into Csphs. Although separating phase bright cells from stromal cells is technically very difficult, it would be interesting to assess eYFP expression in Csphs which form following a culture of either phase bright cells or stromal cells, independently.

To assess the importance of different stages of CDC culture based on the proportion of fibroblast and stem cell content, it would be interesting to quantify the ratio of eYFP-expressing cells and stem cell markers; this will allow us to focus on a specific stage of CDC culture in future functional experiments with a desired combination of fibroblast and stem cells in order to save time and increase cardiac progenitor cell efficiency.

I also analysed the level of eYFP expression in CDCs by FACS and noticed that 8-13% of CDCs express eYFP. Therefore, no significant change was observed between the expression of eYFP in CDC and EDC (8-13% versus 9-11.5%) (Sections: 5.2.9-5.2.10). I also analysed eYFP co-expression with stem cell markers, cKit and Sca-1, and noticed that the majority of stem cell sub-populations of CDCs are distinct from eYFP-expressing cells (figure 5-12). However, due to the limitations of our lineage-tracing method and possible influences of CDC culture on fibroblast-marker expression and phenotype, adding another CF marker such as DDR2 in FACS experiments could provide a better understanding of the CF contribution to different stages of CDC culture. Carr *et al.* [80] reported that 10±2% of rat-derived CDCs express DDR2, but the fibroblast content of mouse is likely to be different from rat as it is reported that approximately 27% of the cardiac cells were DDR2 positive whereas 56% of the cells were  $\alpha$ -MHC<sup>+</sup> (myocytes) [25]; conversely, the cellular populations of rat hearts were markedly different from the 70% non-muscle and 30% muscle cells [175]. Therefore, these data suggest that variations in cellular ratios which exist between species could generate different ratios of progenitor/fibroblast cells in CDC cultures.

I observed that preparing adult mouse CDCs takes a much longer culture time than neonatal CDCs (1 month neonatal and 2 months adult CDCs). Therefore, it is important to decide which passage number of CDCs is more suitable for cell delivery into the infarcted heart for regenerative purposes. Possibly quantifying the level of eYFP-expressing cells together with a stem cell marker profile in CDCs at different passage numbers could help to decide which passage number contains a more balanced number of fibroblast and stem cells. Here I compared the level of eYFP-expressing CDCs in passages 2 and 4 and noticed that serial passaging increased eYFP-expression from  $9.7 \pm 0.4\%$  at passage 2 to  $12.9 \pm 0.2\%$  at passage 4 ( $p < 0.05$ ). However, due to the efficiency of our lineage-tracing system ( $37.3 \pm 2.1\%$ ) these figures are expected to be higher. It would also be interesting to assess the functionality of CDCs which co-express eYFP and Sca-1 or cKit at higher passages. For example, this could be done by assessing the clonogenicity, multilineage differentiation and angiogenesis potential of eYFP-expressing CDCs at different passages, and extend this analysis to YFP/cKit and YFP/Sca-1 CDCs. Therefore, we could score different passages: (i) based on the quantity of fibroblasts and stem cells; and (ii) the proficiency of cells in *in-vitro* and *in-vivo* functional assays; and, finally, (iii) the ability to promote heart repair in MI models.

In this chapter, by the application of lineage tracing, I showed that CFs contribute to Csphs and form sub-populations of CDCs. It is likely that collagen 1 expressing cells within the Csphs are derived from stromal cells and not from phase bright cells as I did not observe any phase bright cells expressing eYFP; however, unfortunately, the lineage tracing was not able to label the majority of CFs *in vivo*. Using FACS, I showed that stem cell populations of CDCs are partially distinct from collagen-expressing cells. However, I believe the fibroblast content of CDCs is likely to be higher than shown in this chapter. Based on the manual quantification that I have done, almost 30-42% of CFs (FSP1- or vimentin-expressing cells) were labelled with eYFP reporter in healthy hearts (tables 5-4). This chapter showed the potential of using lineage tracing to interpret the fibroblast content of the different sub-populations of CDCs and brought more evidence of a CF presence in Csphs and CDCs.

In chapters 3 and 4, I showed that culturing CDCs in 3% O<sub>2</sub> increases stem cell and endothelial sub-populations of neonatal and adult CDCs, but whether 3% O<sub>2</sub> increases

the pro-angiogenic potential of CDCs *in vivo* is a question which I will address in the next chapter.

## **Chapter 6 Angiogenic potential of neonatal and adult CDCs in sub-dermal matrigel plugs**

## 6.1 Introduction

Stem cell transplantation studies following a heart attack aim to establish a way to supply adequate blood to the affected myocardium and minimise the infarct size or to replace lost myocardial cells. In the former case, transplantation of CDCs and Csphs have been shown to be effective either by being involved in direct vascular differentiation or by enhancing the host progenitor cells to form new vessels (please see section 1.5.7). However, a major dilemma in CDC and any other stem cell transplantation studies is the low survival after transplantation into the infarct and peri-infarct regions. Therefore, improving cell retention after transplantation is critical to enhance the efficiency of stem cell therapy. Hypoxia preconditioning has been shown to stimulate endogenous mechanisms resulting in multiple responses that protect against future lethal hypoxia such as reducing apoptosis and enhancing myocyte protection [138]. Studies have shown that hypoxia preconditioning of EDCs and CDCs markedly improves cell migration (*in vitro*) and cell recruitment into the ischemic myocardium (please see section 1.7.1). In chapters 3 and 4, I showed that the expression of stem cell (Sca-1, Abcg2), endothelial and angiogenic markers (Eng, Flk1, Vegf) increased significantly in CDCs preconditioned with 3% O<sub>2</sub> for 48 hours. I also observed that preconditioning adult CDCs for 48 hours in 3% O<sub>2</sub> elevates the level of secreted Vegf into the CDC media. It is possible that elevated levels of Sca-1, Abcg2, Eng, Flk1 and Vegf in CDCs treated with 3% O<sub>2</sub> are critical for their pro-angiogenic potential.

In order to test the ability of murine CDCs to promote neovascularisation *in vivo* I first established a mouse model of angiogenesis using subcutaneous injection of growth factor reduced matrigel combined with neonatal CDCs. CDCs were derived from *CAG-farnesyl-eGFP* transgenic mice to enable the tracking of GFP-labelled CDCs in the matrigel plugs.

The matrigel plug assay is an assay that does not require surgical procedures and allows for the screening of the potential pro-angiogenic state of different cells. Matrigel is an extract of the Engleberth-Holm-Swarm tumour and composed of basement membrane proteins that support neo-vessel formation. Microvasculature formation in the matrigel plug assay *in vivo* is a widely used angiogenesis assay. It mimics the formation of capillary networks *in vivo* and has advantages over other assays such as Suitable for large-scale screening and rapid quantitative analysis in chambers, reviewed in [176]. In this study adult CDCs treated with normoxia and 3% O<sub>2</sub> were directly injected

subcutaneously with growth factor reduced matrigel and after two weeks the effect of CDCs on neovascularisation was assessed by detailed quantification of the vessel density in the matrigel using immunofluorescence and histochemistry. The technical approach used in this study is based on two papers from the Bischoff laboratory [177,178] who showed that the combination of human endothelial and mesenchymal cells promotes their angiogenic function more efficiently than using each cell type alone.

## **6.2 Results**

### **6.2.1 Mouse model of angiogenesis using subcutaneous injection of CDCs**

I established a mouse model of angiogenesis using neonatal and adult CDCs to assess the vessel density inside the subcutaneous matrigel plug. Briefly, young adult (6 week old) C57BL/6 mice were selected as the recipients and CDCs from *CAG-farnesyl-eGFP* mice were passaged twice and mixed with matrigel before injecting the matrigel plug (300µl) subdermally in the flank regions. The use of *CAG-farnesyl-eGFP* mice allowed donor CDCs to be tracking using GFP expression as a marker. Two weeks later, the mice were humanely killed and the matrigel plugs were removed and processed to prepare cryosections to analyse angiogenesis (as described in section 2.12). One group of mice was given matrigel seeded with mouse lung endothelial cells (MLECS) as a positive control for *in-vivo* angiogenesis. As Melero-Martin *et al.* (2008) showed that the combination of mesenchymal cells with endothelial cells enhances their angiogenic and survival potential, in one of my experimental groups I combined CDCs (which have a high mesenchymal cell content) with MLECS (mouse lung endothelial cells) in the proportion of 40:60 to test if CDCs could provide a pro-angiogenic effect. Figure 6-1 schematically depicts the experimental design, different stages of CDC preparations and injection of subcutaneous matrigel plugs.

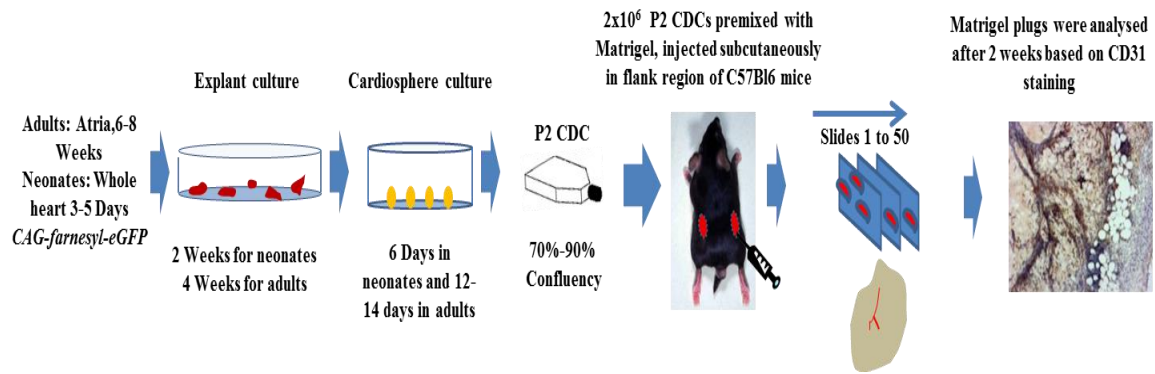


**Figure 6-1 Schematic depicting different stages of *in-vivo* angiogenesis with *CAG-farnesyl-eGFP* CDCs derived from neonatal and adult hearts and transplanted sub-dermally with matrigel in C57BL/6 recipient mice.** The figure depicts different stages of CDC culture and the duration of each stage for neonatal and adult CDCs, which were used in two separate experiments as summarised below.

**Experiment with neonatal CDCs:** Neonatal whole hearts from 3-6 days old neonates were used to prepare CDCs at passage 2, which were injected subcutaneously with matrigel. Each mouse received 2 matrigel plugs (200  $\mu$ l matrigel + 100 $\mu$ l PBS). Altogether four different groups were compared: 1) Matrigel; 2) Matrigel + CDCs ( $2 \times 10^6$ ); 3) Matrigel + MLECS ( $2 \times 10^6$ ) and 4) Matrigel + CDCs ( $8 \times 10^5$ ) + MLECS ( $1.2 \times 10^6$ ). Two weeks after the sub-dermal matrigel plugs were injected, the mice were humanely killed and plugs were dissected together with the surrounding skin and muscle. Tissue was frozen in OCT freezing medium on dry ice. From each plug 50 serial slides with 5-6 sections per slide were prepared, with each section of 10-25  $\mu$ m thickness. Every fifth slide was stained with anti-CD31 antibody as an angiogenic marker. For quantification, any positive staining for CD31 inside the matrigel section was quantified manually and normalized to the matrigel section area. The average values for 8-10 slides from each plug were used to derive the microvessel density (MVD= vessels/ $\text{mm}^2$ ).

**Experiment with adult atrial CDCs:** Angiogenesis was compared between the following groups: 1) Matrigel; 2) Matrigel + CDCs ( $2 \times 10^6$ ) pre-treated with normoxia for 48 hours; 3) Matrigel + CDCs ( $2 \times 10^6$ ) pre-treated with 3%  $\text{O}_2$  for 48 hours; 4) MLECS ( $2 \times 10^6$ ); and 5) Matrigel + CDCs ( $8 \times 10^5$ ) + MLECS ( $1.2 \times 10^6$ ). In each group, cells were re-suspended in matrigel on ice and then transferred into the syringes. All syringes were kept on ice till they were injected. Plugs were injected in three sites per mouse – 2 in the flanks and 1 in the scruff. All plugs were dissected after 2 weeks and were fixed in 0.2% PFA overnight at 4°C and transferred to 30% sucrose, overnight at 4°C, and finally all plugs were frozen on dry ice in OCT freezing medium. Serial sections were made and MVD assessed using image J software.

### 6.2.2 Investigating the role of neonatal CDCs on *in-vivo* angiogenesis in subcutaneous matrigel plugs

To test the ability of neonatal CDCs to contribute to angiogenesis,  $2 \times 10^6$  P2 CDCs were injected combined with growth factor reduced matrigel into the flank regions of recipient C57BL/6 mice. CDCs were re-suspended in 200  $\mu$ l of matrigel; however, due to the technical difficulties with pipetting the matrigel, I further added 100  $\mu$ l of PBS in order to dilute the matrigel. All syringes were kept on ice till the injection time and cells were in matrigel + PBS on ice for approximately 15-20 minutes prior to injection. Successful subcutaneous injections were obvious as no cell backwash was observed and the matrigel plugs were visible as slightly raised tissue in the flank following the injection, which indicated that the matrigel had solidified quickly following the injection.

To ensure that CDC viability was not affected following the injection with insulin syringes, I used the ViCell automated cell viability analyser. This system uses standard trypan blue assay to measure viability. CDCs were incubated for 20 minutes in matrigel + PBS mix and then passed once through the syringe, then the viability was assessed by ViCell. The analyser showed there was no significant difference between the viability of cells that passed through the syringe once and those that were not.

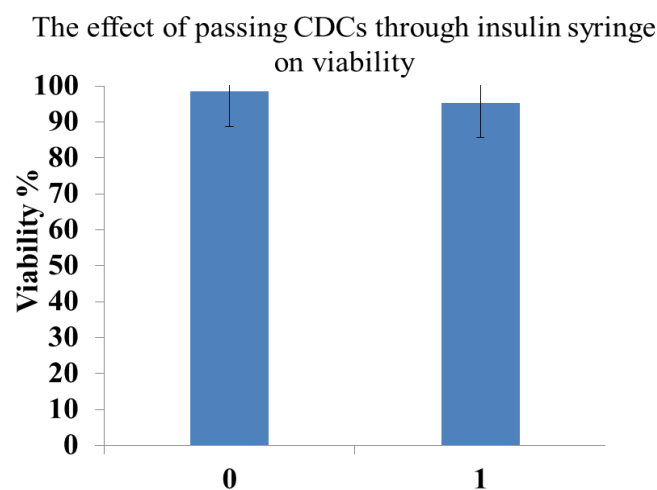


**Figure 6-2 Assessing the viability of neonatal CDCs after passing through an insulin syringe once.**  $2 \times 10^6$  P2 CDCs derived from neonates, re-suspended in 200 $\mu$ l of matrigel and 100 $\mu$ l of PBS. Then the matrigel + PBS + CDC mixture passed once through an insulin syringe and the viability was measured with the ViCell analyser. As shown in the figure no significant difference was observed in the viability of CDCs passed through an insulin syringe once in comparison to those which were not.



### 6.2.3 *In-vitro* expression analysis of GFP in P2 neonatal and adult-derived CDCs

In order to confirm the expression of GFP in the candidate P2 CDC cultures derived from *CAG-farnesyl-eGFP* mice, I stained samples from one representative cell culture of P2 neonatal and adult CDCs and observed that eGFP was expressed significantly in the majority of CDCs (Figure 6-3). The validity of GFP expression in neonatal CDCs has also been shown by an independent researcher, Dr. Redgrave, who used FACS to quantify GFP-expressing CDCs at passage 2 and showed that  $92.5 \pm 1.7\%$  of CDCs from *CAG-farnesyl-eGFP* mice express eGFP.

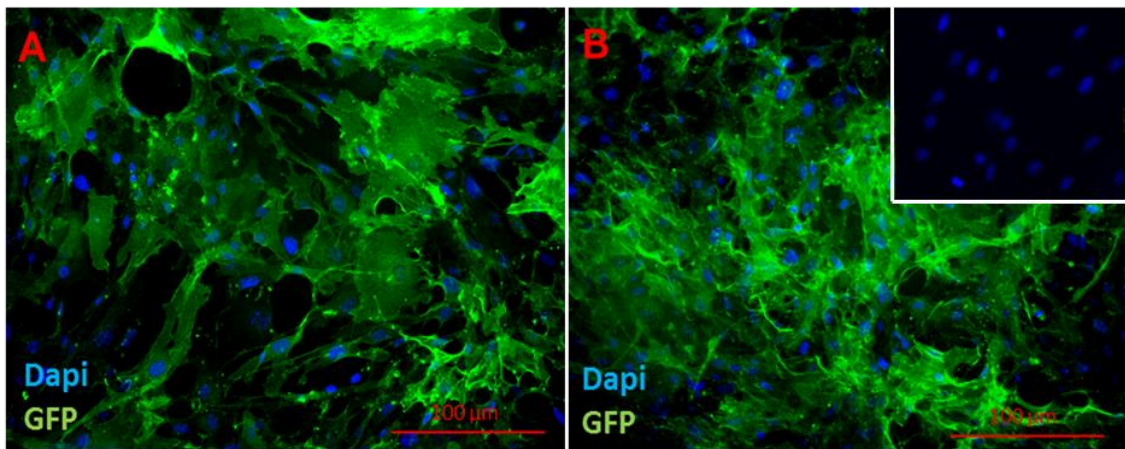


**Figure 6-3** *In-vitro* expression of eGFP in passage 2 CDCs derived from *CAG-farnesyl-eGFP* mice. Representative fluorescent microscopy image of passage 2 neonatal (A) and adult (B) CDCs showing eGFP expression from *CAG-farnesyl-eGFP* mice following immunostaining with a specific anti-GFP antibody conjugated to Alexa-488. This experiment was performed once for neonatal CDCs and once for adult CDCs. Scale bar = 100  $\mu\text{m}$ . The inset image B is no anti-GFP control.

### 6.2.4 Neonatal CDC transplantation with matrigel-increased microvessel density (MVD) in recipient C57BL/6 mice

10 slides (5-6 sections per slide) were prepared from matrigel plugs from 4 different groups (Matrigel, Matrigel + CDC, Matrigel + MLECS, Matrigel + CDC+ MLECS) and were stained with anti-CD31. The expression of CD31 was measured manually by quantifying CD31-expressing cells (any cell or cell-cluster showing CD31 expression within the matrigel was quantified as 1, without considering the size of the vessel) in all sections and normalized to the surface area of the matrigel to derive the mean of CD31 expression per matrigel area. The CD31-expression difference was analysed by one-way ANOVA ( $<0.001$ ) then the subsequent *post-hoc* Tukey test showed the significant

difference between the individual groups (table 6-1). Comparison of the vascularity between four groups showed that matrigel plugs with CDCs had significantly higher microvascular density compared to matrigel plugs alone (7.3-10 versus 1.6-2.7 vessels/mm<sup>2</sup>). Also the MLECs group showed a higher vascularity level in comparison with CDCs alone (18.5-28.3 versus 7.3-10 vessels/mm<sup>2</sup>). Interestingly, mixing CDCs with MLECs resulted in the highest level of vascularity (34.3-45.2 vessels/mm<sup>2</sup>). Figure 6-4 depicts a representative matrigel plug from each group showing CD31 immunostaining, while table 6-1 summarizes MVD quantification per matrigel plug in each group.

This experiment showed that sub-dermal injection of neonatal CDCs with matrigel results in an angiogenic response; however, the combination of CDCs with MLECs enhances the microvessel density, suggesting that CDCs may have a paracrine pro-angiogenic effect.

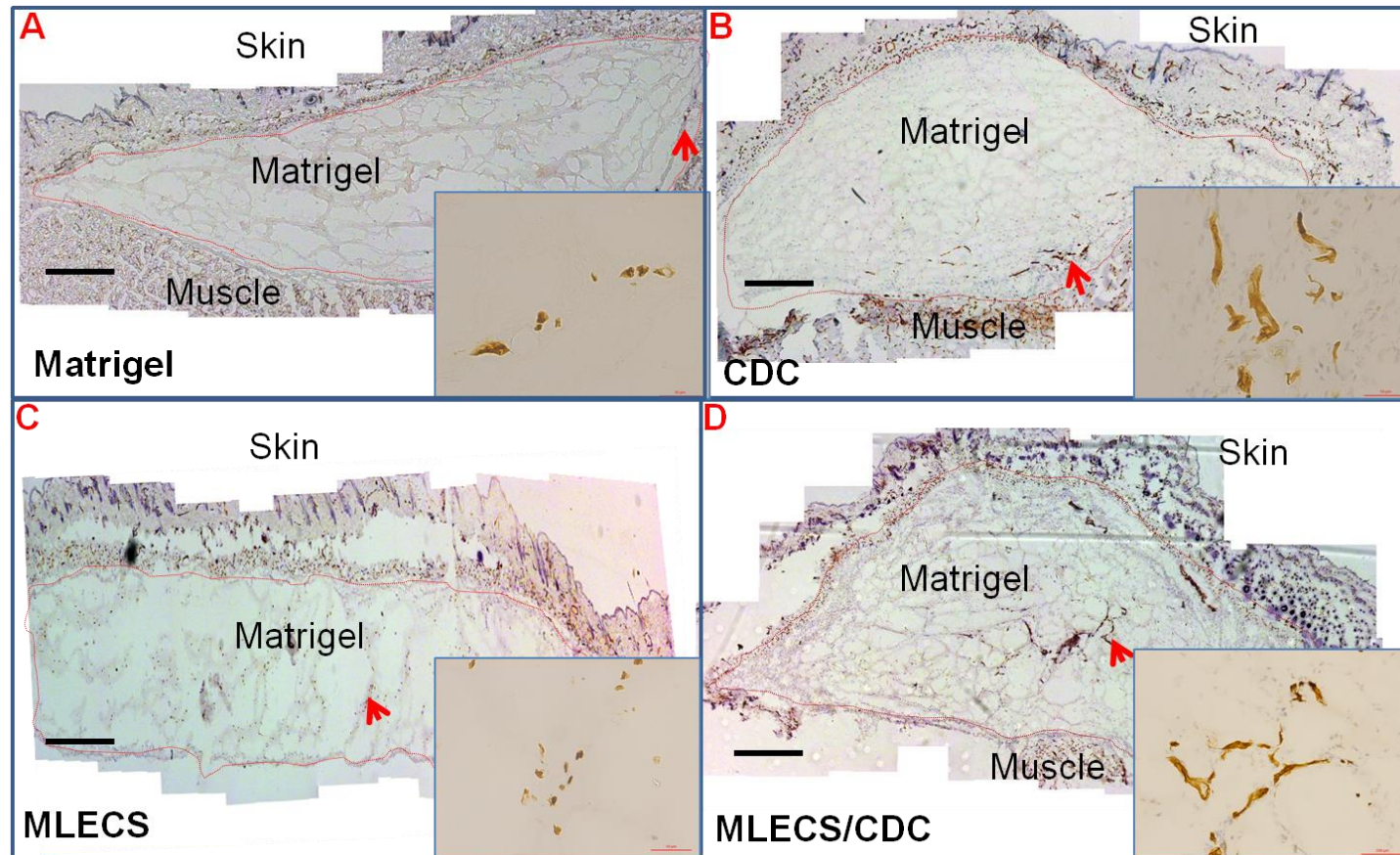


**Figure 6-4 Angiogenesis in subdermal matrigel plugs seeded with neonatal CDCs.** Representative images showing CD31 expression in matrigel alone (A), CDCs + matrigel (B), MLECS + matrigel (C) and CDCs + MLECS + matrigel (D). The matrigel boundaries are indicated by dashed lines. CD31 expression in matrigel plugs is highest in the CDC + MLECS + matrigel group. The inset images of the region are indicated by the red arrow. As shown in (A) and (C) positive expression for CD31 is mostly in single cells but in (B) and (D) the staining revealed a neo-vasculature like structure. To quantify the number of vessels formed in the matrigel any positive staining was quantified inside the matrigel manually. The quantification was done twice and blindly on several slides with the microscope; random slides were analysed by an independent researcher and similar results were obtained. 10-12 images (x5) were merged to generate each mosaic image. These data are representative of one experiment with 3 recipient mice per group. Scale bar = 1000 $\mu$ m.

A) Mean MVD in each group

	Matrigel only n=3	CDC n=3	MLECS n=3	CDC+MLECS n=3	Anova p value
Mean MVD	2.3±1.5	8.3±3.3	24.4±6.5	39.1±10.2	0.001

B) Tukey test results on MVD between the groups\*

Matrigel vs CDC <sup>N</sup> O <sub>2</sub>	Matrigel vs MLECS	Matrigel vs CDC+MLECS	CDC vs MLECS	CDC vs CDC + MLECS	MLECS vs CDC + MLECS
<0.001	<0.001	<0.001	<0.001	<0.001	<0.001

C) CD31 quantification from 10 slides of each matrigel plug

Blocks ID	Matrigel MVD			Matrigel/CDC MVD			Matrigel/MLECS MVD			Matrigel/MLECS/CDC MVD		
	MB1	MB2	MB3	MCB1	MCB2	MCB3	MMB1	MMB2	MMB3	MMCB1	MMCB2	MMCB3
Slide1	2.4	4.6	0.86	5.1	7.8	18.3	40.6	28.6	15.6	25	20	26.6
Slide 5	1.9	3.6	1.6	4.5	10.7	11.2	20.3	20.6	11.2	36.6	21	27.6
Slide10	1.3	3.0	1.2	8.7	6.5	6.0	30.0	29.6	13.4	34.4	31.0	37.1
Slide15	1.3	2.2	0.32	8.0	3.7	7.1	27.7	29.6	17.5	45.8	40.0	32.2
Slide20	1.8	2.1	0.38	12.2	7.4	5.1	25.0	25.2	22.9	53.7	38.5	36.7
Slide25	1.2	3.0	1.2	4.6	6.5	5.2	24.8	31.0	19.7	56.25	44.4	45
Slide30	2.6	1.6	2.6	6.4	6.0	9.0	25.8	26.1	21.25	58.5	43.2	35.2
Slide35	4.0	1.6	3.2	9.4	5.7	11.0	-	28.7	22.3	57.9	49.7	33.2
Slide40	7.8	1.5	3.5	13.0	8.8	10.2	35.5	27.2	-	41.02	48.3	37.8
Slide45	-	1.1	-	9.8	6.4	12.5	24.6	15.8	22.75	42.8	43.2	32.0
slide50	-	-	-	12.2	7.6	15.0	-	-	-	-	-	-
Mean MVD	2.7	2.4	1.6	8.5	7.3	10.07	28.3	26.2	18.5	45.2	37.9	34.3

**Table 6-1 Summary of MVD assessment in Matrigel, Matrigel/CDC, Matrigel/MLECS and Matrigel/MLECS/CDC in subcutaneous plugs 2 weeks after neonatal CDC injection.** Matrigel plugs were dissected following two weeks of injection and 50 slides made from each plug and every fifth slide was stained with CD31 antibody to identify endothelial cells. The figures in table (A) are mean MVD calculations which are a manual quantification of any positive expression for CD31 inside the matrigel and then normalised against the area of each matrigel. Table (B) is the *post-hoc* Tukey test for all 4 groups and table (C) shows the initial CD31 manual counts from several slides for each plug. MVD is the number of CD31 expressing cells/mm<sup>2</sup> of matrigel.

### **6.2.5 Tracking eGFP<sup>+</sup> neonatal CDCs in the neovasculature of the matrigel**

In order to allow donor cell tracking in matrigel plugs, CDCs were genetically labelled with eGFP using the *CAG-farnesyl-eGFP* line. In this line eGFP expression is controlled by the CAG promoter and the farnesyl group stabilises eGFP protein at the cell membrane. As the endogenous expression of eGFP was very difficult to detect, immunostaining using anti-GFP antibody was performed to test the expression of GFP in P2 CDCs in matrigel plug sections. Several cryosections from all four groups (Matrigel n=3, CDC+Matrigel n=3, MLECS+Matrigel n=3, CDC+MLECS+Matrigel n=3), approximately 8-10 sections per plug, were stained with anti-GFP antibody, directly conjugated with Alexa 488. No eGFP expression was observed in matrigel only (figure 6-6 C) or the MLECS+Matrigel group. In CDC+Matrigel and CDC+MLECS+Matrigel plugs, I observed very few GFP-expressing cells. To investigate whether any of these surviving CDCs had differentiated into vascular cells I performed double immunofluorescent staining for CD31 and GFP. Detailed analysis of different plugs (Matrigel+CDC, n=3 and Matrigel+CDC+MLECS, n=3) showed that very few GFP-expressing cells co-localised with CD31, suggesting a limited differentiation to endothelial cells. However, within one of the plugs (CDC+MLECS), I observed that some GFP-expressing cells were adjacent to a microvessel close to the border of the matrigel and occasionally some eGFP positive cells were co-stained with CD31 (figure 6-5). However, immunophenotyping experiments with neonatal CDCs showed that 4-16% of CDCs expressed CD31 and therefore it is possible these CDCs had been CD31 positive prior to the addition of these cells to the matrigel. I concluded that the vascular response achieved following neonatal CDC injection into sub-dermal matrigel plugs is likely due to paracrine mechanisms and that MLECs supports their angiogenic potential.

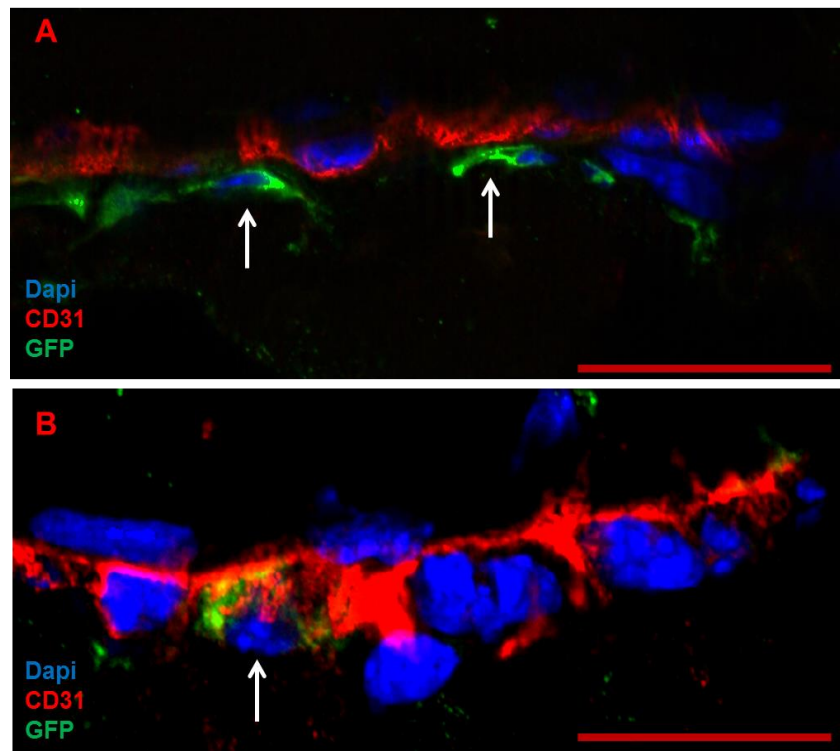


**Figure 6-5** Fluorescent staining of GFP and CD31 in matrigel plugs injected with neonatal CDCs+MLECs. P2 CDCs were prepared from *CAG-farnesyl-eGFP* neonates (3-6 days) and together with MLECs were used to seed matrigel in C57BL/6 recipient adult mice (6 weeks old). After 2 weeks the plugs were dissected and stained with anti-GFP and CD31 to test if any GFP expressing cells also expressed CD31. The majority of eGFP positive cells were not co-expressing CD31. (A) Rare eGFP expressing cells adjacent to endothelial cells in the matrigel plug and (B) depicting co-localisation of eGFP and CD31 in a microvessel (highlighted with white arrows). Scale bars =50µm.

### 6.2.6 Investigating the effect of adult-derived CDCs *CAG-farnesyl-eGFP* preconditioned with normoxia and 3% O<sub>2</sub> on *in-vivo* angiogenesis using matrigel plug assay

My pilot studies with neonatal CDCs showed that neonatal CDCs enhanced vasculogenesis in matrigel plugs (n=3) compared to the group that received matrigel alone (n=3). As severe (0.1%) and physiologic (5%) hypoxic preconditioning of mouse- and human-derived CDCs has been reported to show some improvements in angiogenic, cell survival and cardiogenic potential [73,103], I assessed the angiogenic potential of CDCs that had been preconditioned with 3% O<sub>2</sub> in the sub-dermal matrigel plug angiogenesis assay. Also because of the increased clinical relevance of adult (as opposed to neonatal) CDCs in heart repair, adult-derived CDCs were used for this part

of the study. As CDCs/MLECs combination enhanced the angiogenic response, I included the adult CDC+ MLECs group as before.

To do this experiment, three plugs were injected into three sites of each C57BL/6 recipient (two plugs were injected in the flanks and one in the scruff). Each study group was injected into one recipient mouse. Each plug contained  $2 \times 10^6$  cells (CDCs at P2 stage or MLECs or CDC+MLECs) that had been re-suspended in 300 $\mu$ l of growth factor reduced matrigel (table 6-2). As I observed from the neonatal CDC study above, using PBS to dilute the matrigel led to a poor structure of the matrigel plug, I did not dilute matrigel with PBS in this experiment. Furthermore, in my previous experiments I noticed that matrigel plugs needed light fixation with 0.2% PFA and processing through 30% sucrose to maintain good structure. Fixing the matrigel plugs with 0.2% PFA maintained the structure of the plug during the sectioning process and tissue destructions were avoided. This modification provided better slides and the empty areas within the matrigel which were evident in the neonatal CDC matrigel plug assay were resolved (freezing the plugs without fixation had resulted in a breakdown of the structure of the matrigel -compare matrigel structure in Figure 6-4 with 6-8). In addition, I assessed CDC survival by examining GFP expression in two protocols which have been used to prepare matrigel+cell suspension and tissue processing in adult and neonatal plugs (Figure 6-6).

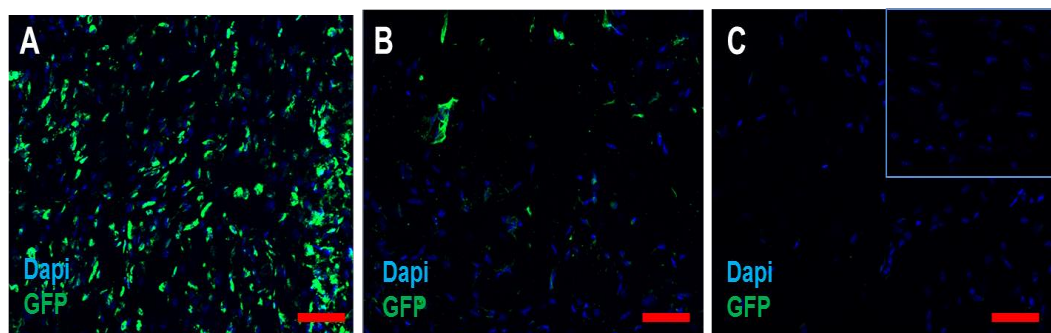


**Figure 6-6 eGFP expression in matrigel plugs harvested immediately after sub-dermal implantation of CDC-seeded matrigel plugs in recipient mice.** (A) adult CDC+ 300 $\mu$ l matrigel plugs (harvested 30 minutes after sub-dermal injection) fixed in 0.2% PFA, (B) neonatal CDC+ 200 $\mu$ l Matrigel + 100 $\mu$ l PBS (harvested 30 minutes after sub-dermal injection) fast frozen without fixation, (C) Matrigel only, (harvested 2 weeks after sub-dermal injection)(A) shows more efficient detection of CDCs in matrigel probably due to technical modifications applied to the sub-dermal matrigel plug implantation protocol in which the matrigel dilution step with PBS has been omitted and tissues were fixed with 0.2% PFA and 30% sucrose and slow-frozen with OCT on dry ice. (B) Low numbers of eGFP<sup>+</sup> cells were detected in neonatal CDC seeded plugs, possibly due to the fragile texture of the plugs which had been fast-frozen without fixation. The inset image (C) is no primary control. Scale bar= 50  $\mu$ m.

Sub dermal Plugs	Cell number
300 µl Matrigel only	-
CDC <sup>N</sup> O <sub>2</sub> +300 µl Matrigel	2x10 <sup>6</sup>
CDC <sup>3%</sup> O <sub>2</sub> +300 µl Matrigel	2x10 <sup>6</sup>
MLECS+300 µl Matrigel	2x10 <sup>6</sup>
CDC <sup>N</sup> O <sub>2</sub> /MLECS (40/60%)+300 µl Matrigel	8x10 <sup>5</sup> CDC+ 1.2x10 <sup>6</sup> MLECS

**Table 6-2 Number and type of cells injected with matrigel plugs in adult CDC angiogenesis study.**

**6.2.7 Adult CDCs led to increased microvessel density (MVD) in sub-dermal matrigel plugs in recipient C57BL/6 mice and preconditioning CDCs with 3% O<sub>2</sub> enhanced this process**

To compare the effect of normoxia and 3% O<sub>2</sub> on adult CDCs pro-angiogenic potential, CDCs (at P2) were cultured in normoxia and 3% O<sub>2</sub> for 48 hours. Initially, in chapter 4, I validated the hypoxic cell culture condition, by Hif-1 $\alpha$  protein stabilisation and the level of secreted Vegf, which was compared in normoxia and 3% O<sub>2</sub> preconditioned CDCs (shown in chapter 4: see Figure 4-2). However, in this chapter the level of Vegf in the supernatant of adult CDCs was also measured by Elisa assay. The results confirmed the data from chapter 4 and showed that 3% O<sub>2</sub> treatment led to an increase in the level of secreted Vegf in the supernatant of P2 CDCs compared with normoxic CDCs (367 $\pm$ 27 vs. 187 $\pm$ 30 pg/ml of supernatant, p<0.005).



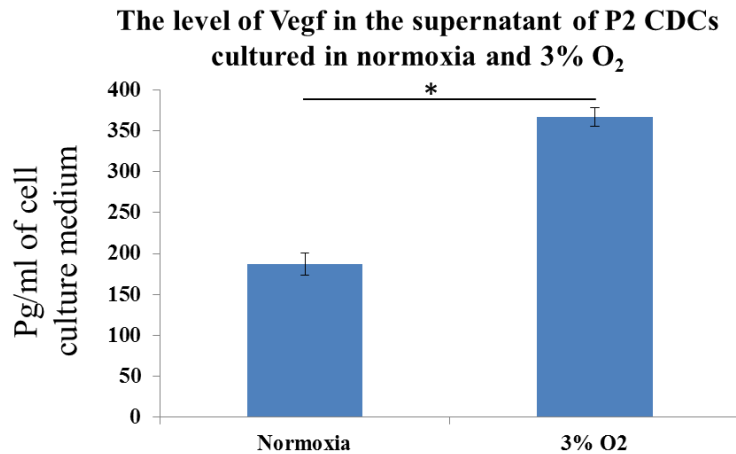


**Figure 6-7 The level of Vegf protein supernatant of adult P2 CDCs cultured in normoxia and 3% O<sub>2</sub>.** Adult P2 CDCs cultured in normoxia and 3% O<sub>2</sub> with the same cell seeding density and same total volume of cell culture media. At 48 hours of CDC culture time point the same aliquot (250 µl) was used to measure the Vegf level using a commercial Elisa assay. The data clearly show that Vegf secretion from P2 CDCs cultured in 3% O<sub>2</sub> is appreciably higher than CDCs cultured in normoxia. This experiment was repeated three times independently (\*P<0.005).

To assess the *in-vivo* angiogenic effect of 3% O<sub>2</sub> and normoxia on adult CDCs, 2 x 10<sup>6</sup> P2 CDCs were injected sub-dermally in matrigel plugs and after 2 weeks, the MVD was assessed, based on the expression of CD31 in the matrigel plugs. Plugs were cryosectioned and every fifth slide stained with CD31 antibody. Ten sagittal cryosections for each plug were used to make mosaic images (one mosaic image made from one section, created by merging 6-10, x5 images) and then the MVD was assessed, based on the percentage area of the matrigel that was positive for CD31 staining, using Image J software and normalised to the surface area of the matrigel to derive the mean percentage area of CD31 expression in each plug. CD31 expression was initially assessed using one-way ANOVA and found to be significantly different between the groups (p<0.001) and the subsequent *post-hoc* (Tukey) test was used to show the significant difference between any two groups.

Detailed analysis of CD31 expression in matrigel plugs showed that injection of adult-derived CDCs pre-treated with 3% O<sub>2</sub> resulted in enhanced CD31 expression compared to CDCs pre-treated with normoxia (5.1-6.5 versus 10.3-13.7, p<0.001). Furthermore, CDCs pre-treated with 3% O<sub>2</sub> showed higher levels of CD31 expression in the plugs than MLECs alone (10.3-13.7 versus 6.3-7.5, p<0.001). All groups showed higher levels of CD31 expression in comparison to the matrigel-only group (p<0.001), showing

this was a donor cell mediated effect. However the highest MVD was observed in MLECS+CDCs with 14.7-16.8 MVD.

These data suggest that although sub-dermal injection of adult-derived CDCs with matrigel enhanced the vascularity of the plugs, pre-treating adult CDCs with 3% O<sub>2</sub> resulted in significantly higher MVD. However, the combination of adult CDCs with MLECs showed the highest level of vascularity in the recipient plugs. The data show the potential angiogenesis of adult CDCs, but it is likely that pre-treating with 3% O<sub>2</sub> or a combination with another group of endothelial cells may increase their pro-angiogenic potential.

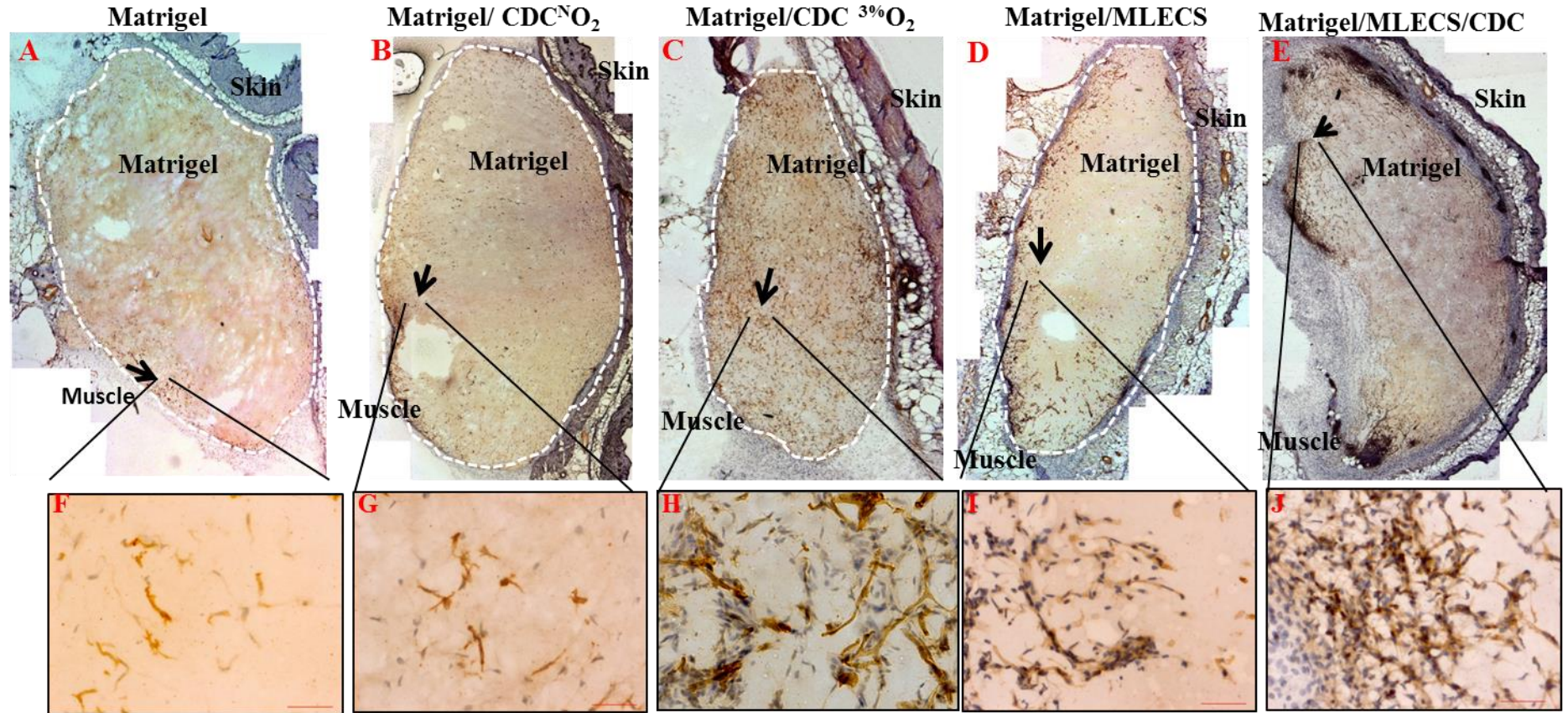


**Figure 6-8** Angiogenesis in matrigel plugs seeded with adult atrial CDCs, with and without pre-exposure to 3% O<sub>2</sub>. Representative immunohistochemical staining (brown) of three independent experiments (one animal was injected with three plugs) on matrigel plugs, showing the expression of CD31 in matrigel alone (A), CDC<sup>N</sup>O<sub>2</sub>/matrigel (B), CDC<sup>3%</sup>O<sub>2</sub>/matrigel (C), MLECS/matrigel (D) and CDC<sup>N</sup>O<sub>2</sub> /MLECS/matrigel (E). The matrigel boundaries are indicated by dashed white lines. CD31 expression was assessed using image J software and normalised to the surface area of each plug. The matrigel plugs containing CDCs that were pre-treated with exposure to 3% O<sub>2</sub> show higher levels of CD31 compared with normoxic CDC and matrigel controls. The strongest expression of CD31 was observed in the CDC<sup>N</sup>O<sub>2</sub> /MLECS/matrigel group. The areas highlighted by arrows are magnified in the corresponding images below.

**A) Mean MVD in each group**

	Matrigel only n=3	CDC <sup>N</sup> O <sub>2</sub> n=3	CDC <sup>3%</sup> O <sub>2</sub> n=3	MLECS n=3	CDC <sup>N</sup> O <sub>2</sub> + MLECS n=3	Anova p value
Mean MVD	1.1±0.58	5.7±2.02	11.7±3.08	6.7±1.9	15.6±3.02	<b>0.001</b>

**B) Tukey test (p values) results on MVD between the groups\***

Matrigel vs CDC <sup>N</sup> O <sub>2</sub>	Matrigel vs CDC <sup>3%</sup> O <sub>2</sub>	Matrigel vs MLECS	Matrigel vs CDC+MLECS	CDC <sup>N</sup> O <sub>2</sub> vs CDC <sup>3%</sup> O <sub>2</sub>	CDC <sup>N</sup> O <sub>2</sub> vs MLECS	CDC <sup>N</sup> O <sub>2</sub> vs CDC <sup>N</sup> O <sub>2</sub> + MLECS	CDC <sup>3%</sup> O <sub>2</sub> vs MLECS	CDC <sup>3%</sup> O <sub>2</sub> vs CDC <sup>N</sup> O <sub>2</sub> +MLECS	MLECS vs CDC <sup>N</sup> O <sub>2</sub> + MLECS
<b>&lt;0.001</b>	<b>&lt;0.001</b>	<b>&lt;0.001</b>	<b>&lt;0.001</b>	<b>&lt;0.001</b>	0.2	<b>&lt;0.001</b>	<b>&lt;0.001</b>	<b>0.007</b>	<b>&lt;0.001</b>

\* n=3 in all experimental groups

**C) CD31 quantification from 10 slides of each matrigel plug**

Blocks	Matrigel MVD			Matrigel/CDC <sup>N</sup> O <sub>2</sub> MVD			Matrigel/CDC <sup>3%</sup> O <sub>2</sub> MVD			Matrigel/MLECS MVD			Matrigel/CDC/MLECS MVD		
	MB1	MB2	MB3	MNB1	MNB2	MNB3	MHB1	MHB2	MHB3	MMB1	MMB2	MMB3	B1	B2	B3
Slide1	2.2	0.5	1.2	3.4	5.6	4	6.1	12.4	15.3	3.5	4.8	7.4	19.4	11.9	25.7
Slide5	1.4	0.7	0.8	3.5	8.9	8.9	12.4	14.7	7.2	4.3	10.9	4.1	12.9	17.5	19.4
Slide10	1.6	0.5	1.1	9.5	2.3	8.9	11.2	12.4	8.4	7.3	7.1	6.5	12.2	13	18.5
Slide15	1.9	0.7	0.9	5.7	9.7	5.5	8.2	6.9	9.2	8.2	5.2	7.3	13.1	17.6	17.4
Slide20	1.1	0.9	0.7	4	5.5	3.26	8.5	18.5	8.8	7.6	9.5	8.5	19.3	-	15.2
Slide25	0.4	0.7	-	3.5	4.7	5.4	10.4	11.4	12.5	7.5	9.7	9.8	12.8	13.7	14.8
Slide30	1.5	2	0.6	4.2	3.8	7.1	12	11.7	10.1	4.5	7.2	4.2	15.6	14.2	15.2
Slide35	1.3	0.7	1.4	5.2	6.2	5.7	13.2	15.2	9.1	5.2	8.6	4.1	16.2	17.8	14.12
Slide40	2.5	1.5	2.3	6.2	3.3	8.2	8.5	14.6	12.3	6.2	5.5	6.3	13.8	16.2	16.3
Slide45	1.4	0.4	0.5	6.3	5.12	8.3	-	15.6	14.1	7.2	8.12	7.89	12	15.2	17.2
Slide50	-	0.9	1.3	5.5	6.2	7.3	12.8	17.2	14	8.2	6.2	5.2	-	-	11.7
Mean MVD	1.53	0.86	1.08	5.18	5.5	6.5	10.33	13.7	11	6.3	7.5	6.4	14.73	15.2	16.8

**Table 6-3 Summary of MVD assessment in 1) Matrigel, 2) CDC<sup>N</sup>O<sub>2</sub>/matrigel, 3) CDC<sup>3%</sup>O<sub>2</sub>/matrigel, 4) Matrigel/MLECs and 5) Matrigel/CDC<sup>N</sup>O<sub>2</sub>/MLECs in subcutaneous plugs 2 weeks following sub-dermal implantation.** In each group, each mouse received three plugs. MLECS also used as the positive control for the *in-vivo* angiogenic model. One mouse received three plugs of a combination of CDC and MLECS with matrigel in the proportion of 40:60 respectively. Matrigel plugs were dissected following two weeks, 50 slides made from each plug and every fifth slide was stained with anti-CD31 antibody to identify endothelial cells. MVDs were analysed using Image J software and MVD calculated after CD31 staining was normalised against the matrigel area in each section. Results are presented as MVD from analysis of five sections from each slide one-way ANOVA (p=0.001) and the subsequent *post-hoc* (Tukey) test was used to show the significant difference between the pairs.

### **6.2.8 Tracking GFP positive adult CDCs two weeks following sub-dermal transplantation in matrigel plugs**

Transplanted adult CDCs were genetically tagged with GFP in order to allow tracking *in vivo*, in matrigel plugs. Several cryosections from all of the groups were stained with anti-GFP antibody. GFP-expressing cells were observed in all the plugs that were originally seeded with CDCs. No difference was observed in the pattern of GFP expression between these three groups. GFP-expressing cells within the plug were oval-shaped (figure 6.9 D) and not associated with CD31-expressing cells. However, I observed some GFP/CD31 co-expressing cells in MLECS/CDC and 3% O<sub>2</sub> pre-treated CDCs expressing cells very close to the vessels (figures 6-9 and 6-11).

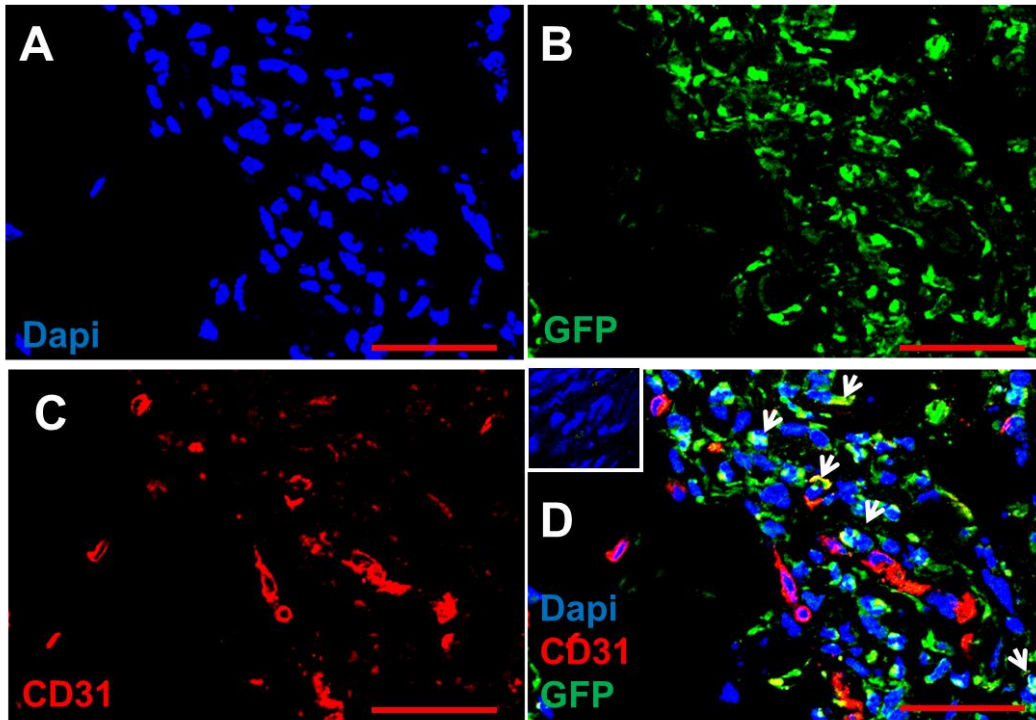


**Figure 6-9 Majority of eGFP positive adult CDCs do not express the vascular marker CD31.** Cryosections of matrigel plugs seeded with  $2 \times 10^6$  adult atria-derived CDCs and were stained with anti-GFP-Alexa488 antibody (green) and CD31 antibody detected by a secondary antibody conjugated to Alexa 594 (red). The image shows the survival of eGFP positive adult CDCs 2 weeks following the injection of matrigel plugs. It is also clear that the majority of CDCs do not co-express CD31. Here in this image, from 62 eGFP-expressing cells only 5 cells (8%) were co-expressing CD31. Inset image D is no GFP and no CD31 primary negative control.

To assess further whether transplanted adult CDCs co-express with endothelial and smooth muscle markers (CD31 and  $\alpha$ -SMA), I stained 3 slides (4-5 sections) from CDC<sup>N</sup>O<sub>2</sub>, CDC<sup>3%</sup>O<sub>2</sub> and CDC/MLECS plugs with anti-GFP antibody and CD31 (conjugated with Alexa 594) and  $\alpha$ -SMA (directly conjugated with Cy.3). Immunofluorescent analysis of the plugs showed that the majority of the GFP positive cells within the matrigel do not co-express CD31 or SMA (figures 6-10 & 6-11), although a limited number of GFP positive cells were also CD31 positive (figure 6.9 & 6.11). These data suggest that the pro-angiogenic effect generated in matrigel plugs is likely to be due to paracrine mechanisms. Within one CDC<sup>3%</sup>O<sub>2</sub> plug of three, I observed a number of eGFP positive cells that were accumulated around one big vessel (figure 6-11 A-D).

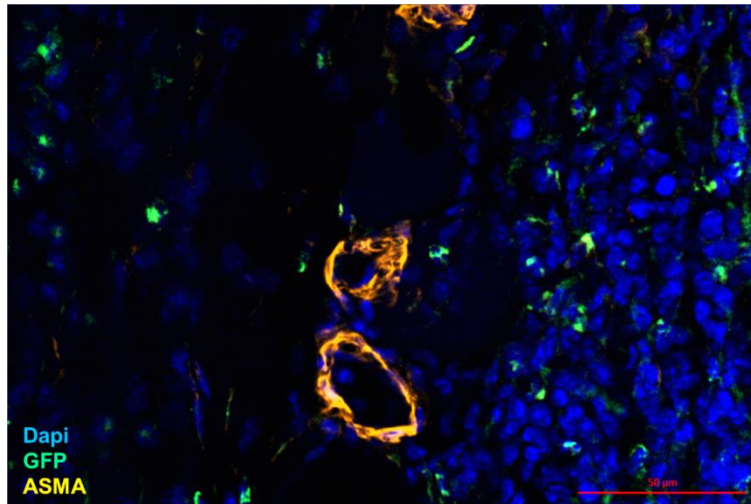


**Figure 6-10 GFP positive adult CDCs do not co-express  $\alpha$ -SMA within the vessels formed inside the matrigel.** The cryo-section of a matrigel plug received GFP-tagged adult CDCs with MLECS, stained with anti- $\alpha$ -SMA antibody (directly conjugated to Cy3) and anti-GFP antibody (directly conjugated to Alexa 488). As shown in the figure CDCs do not express  $\alpha$ -SMA and do not directly contribute to the neo-vessel formation.

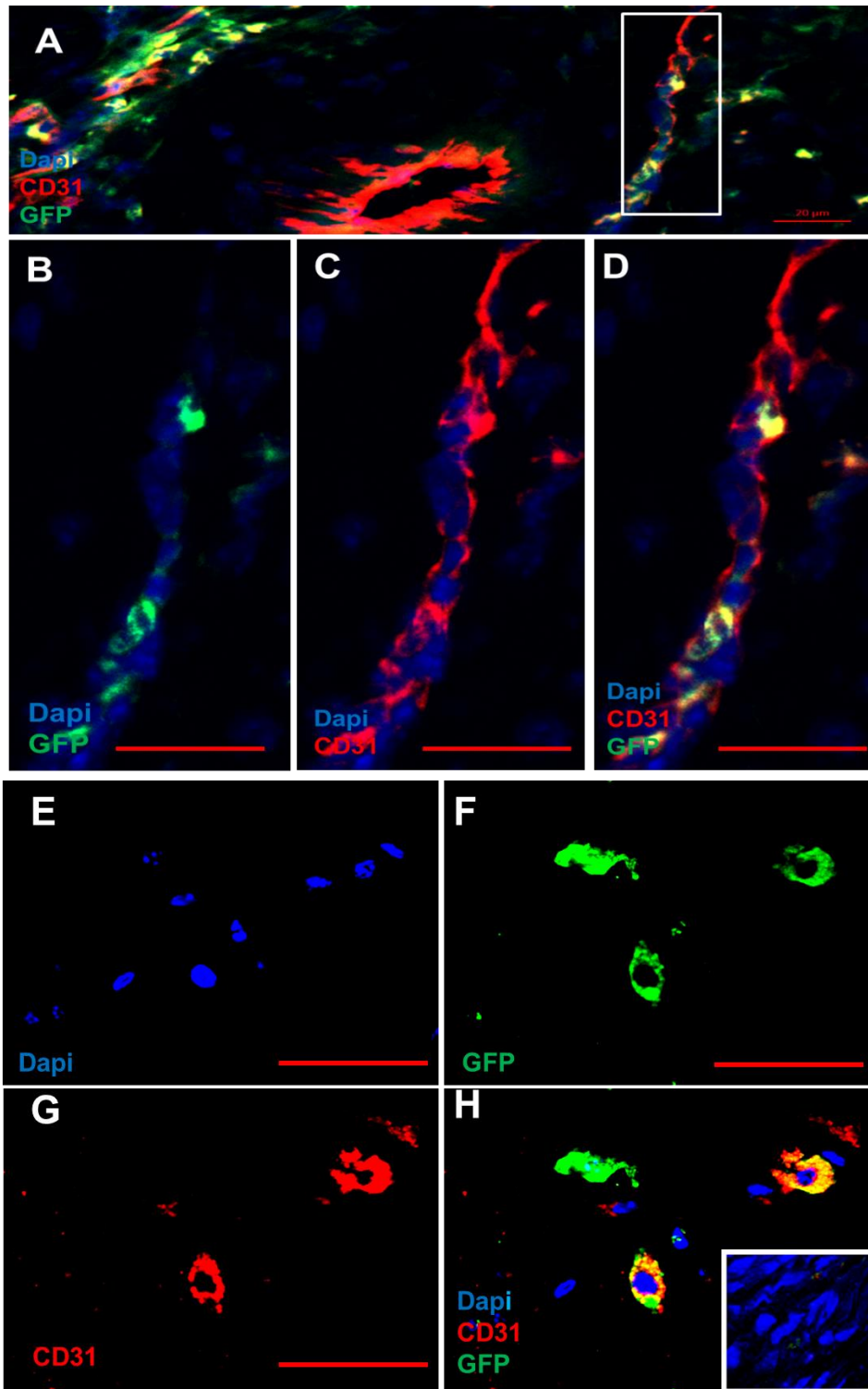


**Figure 6-11 eGFP and CD31 co-expression analysis in a CDC<sup>3%</sup>O<sub>2</sub> plug (A-D) and CDC<sup>N</sup>O<sub>2</sub> + MLECS plug (E-H) showing limited direct contribution of adult CDCs on neovascularisation in matrigel plugs 2 weeks after cell injection. Cryosections from CDC<sup>3%</sup>O<sub>2</sub> and CDC<sup>N</sup>O<sub>2</sub>+MLECS plugs stained with GFP antibody (green) and CD31 antibody (red). Images A-D show that GFP positive cells co-stained with CD31 and the highlighted region with a white box in A is magnified in B-D. Images in E-H show co-localization of GFP with CD31 in single cells from a plug seeded with CDC<sup>N</sup>O<sub>2</sub>+MLECS. The inset H is no primary CD31 and No GFP negative control, Scale bar = 20 μm.**



### 6.2.9 CDC<sup>3%</sup>O<sub>2</sub> matrigel implants showed more cytoplasmic protrusions than the other groups

Skovseth *et al.* (2002) showed that after 10 days of harvesting human umbilical vein endothelial cells (HUVECs) with sub-dermal matrigel plugs, some cells showed cytoplasmic protrusions resembling pseudopods and then made cellular arrays, which then formed tubular structures and contained erythrocytes [179]. I also observed such structures, especially in CDC<sup>3%</sup>O<sub>2</sub> plugs; interestingly, these cytoplasmic protrusions were not that obvious in CDC<sup>N</sup>O<sub>2</sub> and CDC<sup>N</sup>O<sub>2</sub>+MLECS. In this respect it is known that ICAM-1 modulates endothelial cell migration and modifies the organization of the actin cytoskeleton. Furthermore, they showed that by adding ICAM-1 to ICAM-1-deficient endothelium enhanced pseudopod formation [180]. It is also shown that hypoxia stimulates the expression of ICAM-1 in cultured human proximal tubular cells (HPTC) [181]. As shown in the figure 6-12 the elongated eGFP positive cells line up in cellular arrays and form cell-to-cell networks in which, occasionally, CD31 co-localised with eGFP. Figure 6-12 shows two representative images from CDC<sup>N</sup>O<sub>2</sub> and CDC<sup>3%</sup>O<sub>2</sub> plugs forming pseudopods.

To characterise and identify further the cellular component of the sub-dermal matrigel plugs and assess the immune response of the recipient mice to CDC transplantation (donor cells: *CAG-farnesyl-eGFP* and the recipients C57BL/6), I co-stained matrigel sections with GFP and CD11b (a marker which is expressed by monocytes, macrophages and natural killer cells). Results showed that CD11b shows two patterns of co-expression or ingestion of eGFP cells: (i) the majority of eGFP positive cells within the border of the matrigel express CD11b; but (ii) GFP positive cells within the middle of the matrigel were not positive for CD11b (figure 6-13). This possibly could be due to easier accessibility of eGFP cells for the immune system in the borders of matrigel than in the middle.

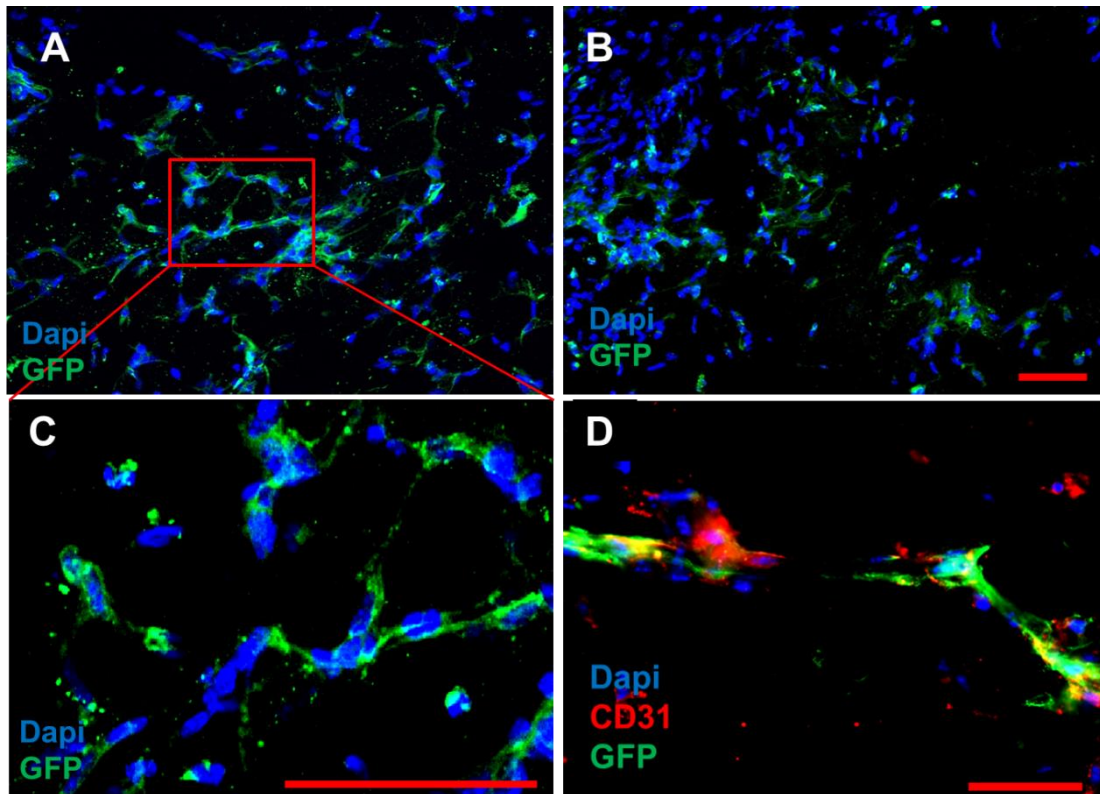


**Figure 6-12 Cytoplasmic protrusions formed more efficiently in matrigel plugs which received CDC<sup>3%</sup>O<sub>2</sub> than CDC<sup>N</sup>O<sub>2</sub>.** Several cryosections from three different experimental groups (CDC<sup>3%</sup>O<sub>2</sub>, CDC<sup>N</sup>O<sub>2</sub> and CDC<sup>N</sup>O<sub>2</sub>+MLECS) were analysed and stained with anti-GFP and CD31. As shown in (A) elongated cytoplasmic features known as cytoplasmic protrusions formed in CDC<sup>3%</sup>O<sub>2</sub> plugs are more obvious than in (B) CDC<sup>N</sup>O<sub>2</sub> counterpart. (C) High power image from the red box highlighted in image A. (D) In some regions of CDC<sup>3%</sup>O<sub>2</sub> plug close to the edges of matrigel, cytoplasmic protrusions co-express CD31 with eGFP. Scale bar = 50 μm.

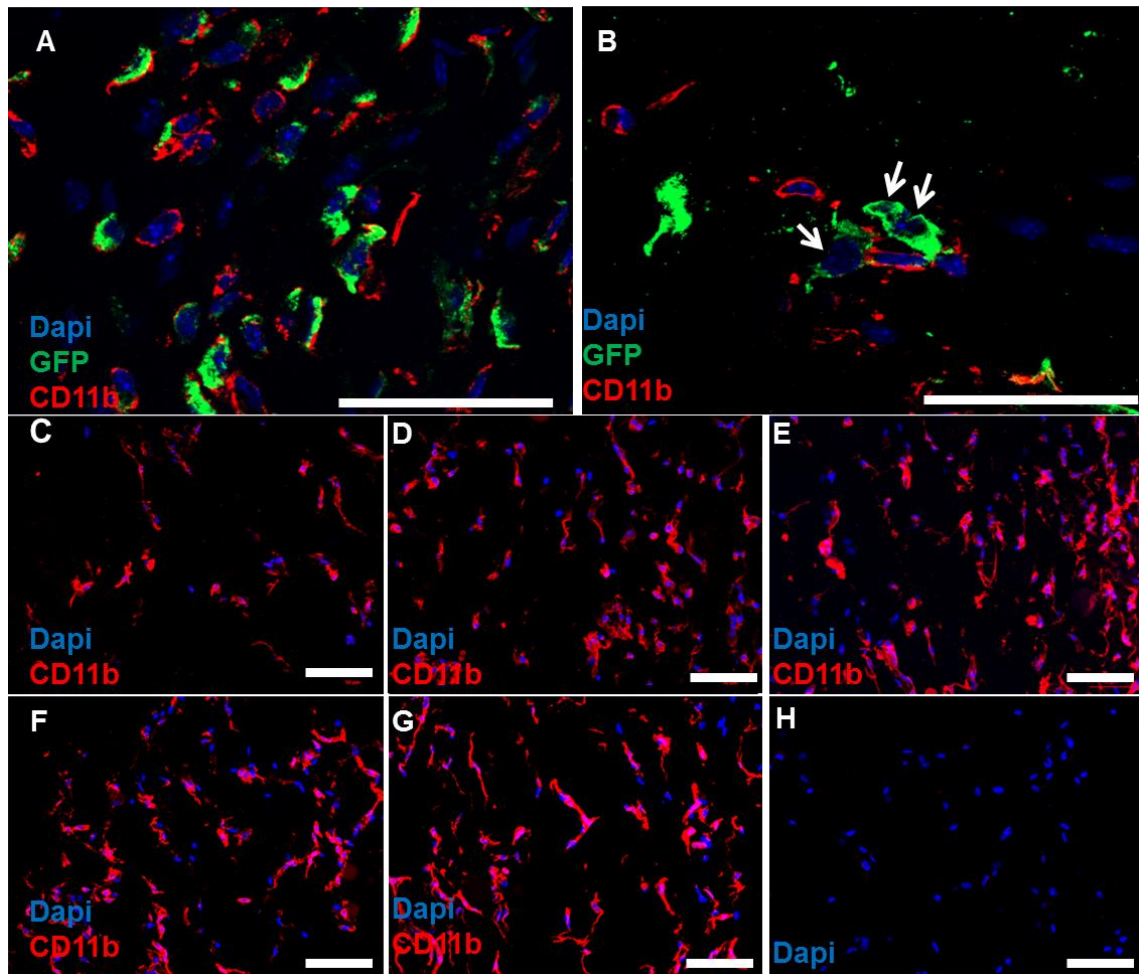


**Figure 6-13 The assessment of immune response within the matrigel plugs of the recipient mice using CD11b (macrophage marker) expression.** Serial matrigel sections from 5 experimental groups (CDC<sup>N</sup>O<sub>2</sub>, CDC<sup>3%</sup>O<sub>2</sub>, CDC<sup>N</sup>O<sub>2</sub>+MLECs, MLECs and matrigel only) were co-stained for GFP (green) and CD11b (red). The representative image (A) shows that the majority of eGFP-expressing cells within the border of matrigel plugs (in this case CDC<sup>N</sup>O<sub>2</sub> + MLECs) are positive for CD11b. (B) However, in B, three GFP positive cells are in the middle of the matrigel which do not express CD11b. The immune response of the matrigel plugs was assessed using multiple CD11b immunostained sections -examples are shown in (C-G) of plugs harvested 2 weeks post-injection. Images (5-8 images from 3-5 sections per plug) taken from different regions: middle and close to border of the matrigel were analysed using image J software (red colour stained area, normalised to the matrigel region) and CD11b expression is shown per microscopic field (x20). Although subcutaneous cell injection with matrigel led to an increase in CD11b cells in the plug, no significant differences were observed between the CDC<sup>N</sup>O<sub>2</sub>, (E) CDC<sup>3%</sup>O<sub>2</sub>, (F) CDC<sup>N</sup>O<sub>2</sub>+MLECs and (G) MLECs alone groups. However, all cell inoculated plugs showed a very significant increase in the CD11b expression level compared to the matrigel-only group. Data were analysed using one-way ANOVA (<0.001) and the *post-hoc* (Tukey) test was performed to identify significant differences between pairs of groups. Representative images of the plugs, (C) matrigel (n=3), (D) CDC<sup>N</sup>O<sub>2</sub> (n=3), (E) CDC<sup>3%</sup>O<sub>2</sub> (n=3) (F) CDC<sup>N</sup>O<sub>2</sub>+MLECS (n=3), (G) MLECS (n=3) and (H) no primary control. Scale bar = 50μm.

A)

Mean CD11b expression in each group

	Matrigel only n=3	CDC <sup>N</sup> O <sub>2</sub> n=3	CDC <sup>3%</sup> O <sub>2</sub> n=3	MLECS n=3	CDC <sup>N</sup> O <sub>2</sub> + MLECS n=3	Anova
Mean CD11b expression	1.3±0.38	8.9±1.8	9.5±1.4	7.0±1.6	8.1±1.8	0.001

B)

Tukey test results on CD11b expression between the groups\*

Matrigel vs CDC <sup>N</sup> O <sub>2</sub>	Matrigel vs CDC <sup>3%</sup> O <sub>2</sub>	Matrigel vs MLECS	Matrigel vs CDC+MLECS	CDC <sup>N</sup> O <sub>2</sub> vs CDC <sup>3%</sup> O <sub>2</sub>	CDC <sup>N</sup> O <sub>2</sub> vs MLECS	CDC <sup>N</sup> O <sub>2</sub> vs CDC <sup>N</sup> O <sub>2</sub> + MLECS	CDC <sup>3%</sup> O <sub>2</sub> vs MLECS	CDC <sup>3%</sup> O <sub>2</sub> vs CDC <sup>N</sup> O <sub>2</sub> +MLECS	MLECS vs CDC <sup>N</sup> O <sub>2</sub> + MLECS
<0.001	<0.001	<0.001	<0.001	0.9	0.4	<0.9	<0.1	<0.6	<0.3

\* n=3 in all experimental groups

**Table 6-4** The summary of immune response assessment with CD11b expression in CDC<sup>N</sup> O<sub>2</sub>, CDC<sup>3%</sup> O<sub>2</sub>, CDC<sup>N</sup> O<sub>2</sub>+MLECS, MLECS and matrigel only after 2 weeks of cell transplantation. (A) All parameters are expressed as mean ± SEM, the table shows the mean CD11b expression derived for each group. (B) Data were analysed using one-way ANOVA (<0.001) and *post-hoc* (Tukey) test was performed to identify significant differences between pairs of groups.(n=3). As shown in (B) the matrigel-only group had the lowest level of CD11b expression among the others and the entire cell-receiving groups did not show any significant difference in CD11b expression.

### **6.2.10 Perfusion analysis of microvasculature formed by adult CDCs cultured in normoxia and 3% O<sub>2</sub> within sub-dermal matrigel plugs**

To analyse whether the new vessels formed by CDC are functionally perfused and whether there is any difference between the potential perfusion of the vessels formed by normoxia or 3% O<sub>2</sub> pre-treated CDCs, a perfusion test with directly labelled isolectin (isolectin-Alexa 594) was performed. Three experimental groups were analysed for perfusion analysis: 1) matrigel alone; 2) CDC<sup>N</sup>O<sub>2</sub>; and 3) CDC<sup>3%</sup>O<sub>2</sub>. Each mouse received three plugs, two of the plugs injected into the left and right flanks and one in the scruff. On day 14 post-sub-dermal delivery of the matrigel plug, 50µg (prepared in 100 µl of PBS) of isolectin directly conjugated with Alexa 594 was injected via the tail vein and the mice were humanely culled after 15 minutes. To assess whether adult CDCs are participating in the structure of functionally perfused vessels, several cryosections (8-10 per plug) were stained with anti-GFP antibody directly conjugated with Alexa 488. After fluorescent microscopy I observed perfused microvessels only in one plug, which contained CDCs pre-treated with 3% O<sub>2</sub>. This suggests the microvessels in the plug are immature and not connected to the main vascular network of the mouse. As expected there was almost no co-expression of GFP with isolectin within the matrigel plugs, although GFP positive cells were easily distinguished in neighbouring regions of the perfused vessels.

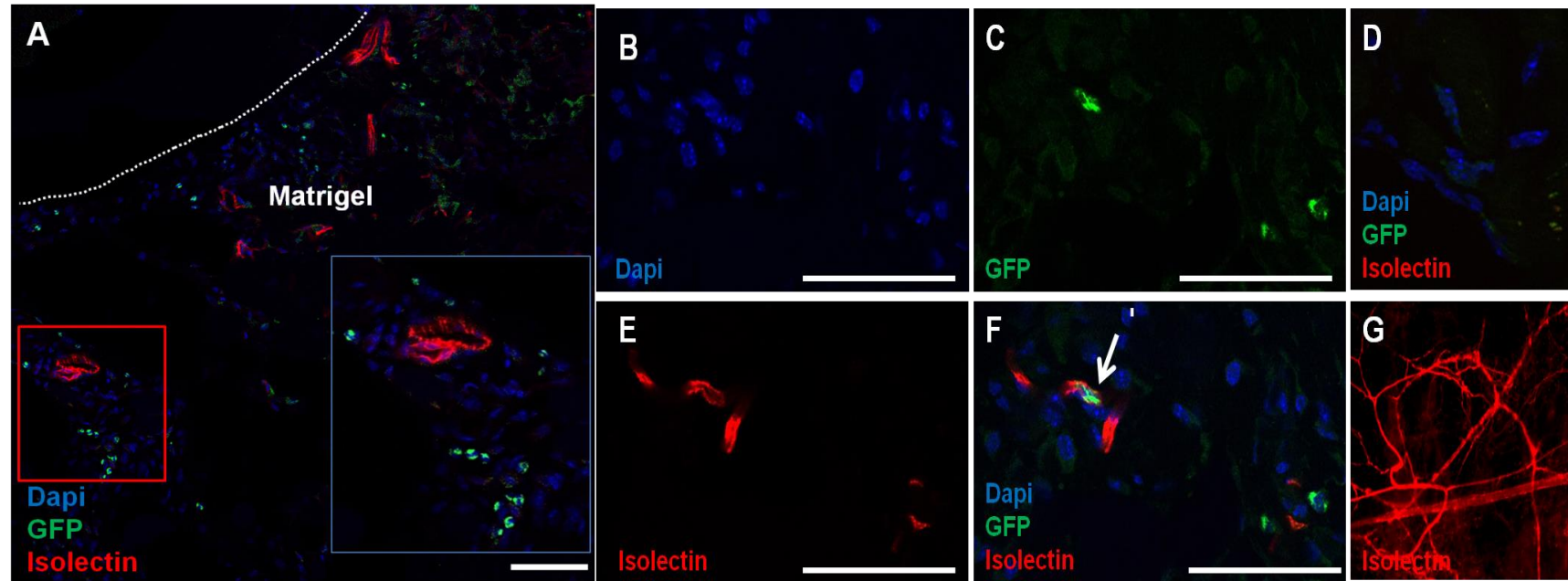


**Figure 6-14 Pre-treatment of adult CDCs with 3% O<sub>2</sub> has a limited effect on the *in-vivo* perfusion potential of adult CDCs.** Adult-derived CDCs at passage 2 pre-treated with 3% O<sub>2</sub> and normoxia for 48 hours.  $2 \times 10^6$  cells from both groups were combined with matrigel and injected sub-dermally (n=3). Plugs were harvested after 2 weeks, but immediately prior to this (at day 14) 50  $\mu$ g of isolectin - Alexa 594 was injected into the mice via the tail vein and the mice were culled humanly after 15 minutes. Serial cryosections were stained with anti-GFP antibody (green) and the co-expression of isolectin and eGFP was assessed. Among 3 matrigel plugs which received adult CDC<sup>3% O<sub>2</sub></sup>, I was able to observe in only one plug the positive perfused vessels within the matrigel. No positive perfusion response was observed from the CDC<sup>N O<sub>2</sub></sup> and matrigel alone. As shown in (A) the majority of eGFP-expressing cells do not co-localise with isolectin-expressing cells. The inset image is a digital zoom of the region of interest highlighted with a red box. However, in one specific region I noticed 2-3 eGFP-expressing cells (highlighted with a white arrow) which were co-localising with isolectin within the matrigel (F). (D) is the no primary control and (G) is a positive control showing perfused vessels in the same mouse left ear labelled with isolectin. Scale bars = 50 $\mu$ m.

## 6.3 Discussion

The aims of this chapter were to: (i) establish an *in-vivo* mouse model of angiogenesis using neonatally derived P2 CDCs; (ii) assess the angiogenic potential of adult-derived P2 CDCs; and (iii) determine whether pre-treating adult-derived CDCs with 3% O<sub>2</sub> could enhance their *in-vivo* pro-angiogenic potential.

### 6.3.1 MVD analysis of P2 neonatal CDCs in the matrigel plug angiogenesis assay

Using a sub-dermal matrigel plug assay I have successfully shown that seeding with neonatal P2 CDCs leads to significantly increased CD31 expression after 2 weeks, indicating an increased angiogenesis response. Using neonatal CDCs, I observed a 3.6 times increase in MVD compared with matrigel alone, indicating that matrigel itself is not the only agent responsible for vessel formation. However, the highest level of MVD was observed when neonatal CDCs were mixed with MLECS and MVD was 17.4 times higher than the matrigel-alone group (see table 6-1). This finding is similar to previous work showing that the combination of endothelial progenitor cells with mesenchymal progenitor cells increases their angiogenic potential compared with either cell type alone [177]. Although this is a small pilot study, this work showed the beneficial effect of neonatal CDCs on *in-vivo* angiogenesis and shows for the first time that the combination of neonatal CDCs with MLECs increases the efficiency of neo-vessel formation. The common finding among all of the groups with neonatal CDCs were that the highest level of angiogenesis was observed in the border of the matrigel compared with the centre which could be due to the host endothelial cell infiltration. It would be interesting to assess CDC-mediated angiogenesis in matrigel plugs after a longer time period. Indeed, it is possible that more incubating time could allow the endothelial cell fraction of CDCs, to make for more functional cell anastomosis with the recipient endothelial cells.

As standard matrigel preparations contains some growth factors such as epidermal growth factor, transforming growth factor (TGF-B) and bFGF, I used growth factor reduced matrigel in order to minimise the pro-angiogenic effect of matrigel alone. The results confirmed that very limited microvasculature formed within the matrigel after 2 weeks of plug injection (figures 6-4 and 6-8).

By using growth factor reduced matrigel, however, I observed variable MVD with neonatal CDCs between the plugs, which could be due to the following reasons: (i) matrigel implantation assay has been considered a technically challenging method of *in-vivo* angiogenesis study due to the difficulty of generating exactly the same three-dimensional plug even with the same matrigel volume, reviewed in [176]. (ii) I injected one plug per recipient mouse, which were all of the same age (6 weeks), it is possible that different animals exhibit different angiogenic responses. (iii) It is also possible the variability within the experimental groups is due to the heterogeneous nature of CDCs. In this respect in chapter 3 I showed variable levels of stem cell and endothelial cell marker expression from neonatal CDCs which was fluctuating in three independent experiments (please see table 3-5). Therefore, it is possible that CDCs within the matrigel are at different stages of differentiation and the microenvironment within the matrigel could all affect the angiogenic response.

I further analysed the eGFP-expressing cells within the matrigel and assessed their co-expression with CD31. Detailed analysis of cryosections from the CDC and CDC+MLECs groups revealed that majority of eGFP-expressing cells do not co-localise with CD31-expressing cells. In one plug of CDC+MLECs I observed a very small number of GFP cells co-stained with CD31 in the wall of new vasculature and some were located adjacent to CD31-expressing cells. This suggests that the neonatal CDCs' pro-angiogenic effect is most likely to be paracrine.

Doing *in-vivo* neonatal CDC angiogenesis helped me to improve the technical aspects of the assay. Initially, I diluted matrigel with PBS at 1:3 ratio in order to ease pipetting; although it helped, GFP cell survival was low and locating GFP positive cells within the plug was difficult. Therefore, in the subsequent angiogenesis study I used pure matrigel to mix with cells. I also found that matrigel plugs need a light fixation with 0.2% PFA and 30% sucrose in advance to cryosectioning; this improved tissue sectioning and staining significantly.

### **6.3.2 *In-vivo* angiogenesis with adult CDCs**

Due to the increased clinical relevance of using adult human CDCs rather than neonatal CDCs I investigated if adult CDCs are capable of promoting neo-vessel formation *in vivo* and whether pre-treating them with 3% O<sub>2</sub> could enhance their pro-angiogenic



potential. In chapter 4 my studies showed that preconditioning adult CDCs for 48 hours in 3% O<sub>2</sub> increased their stem cell (Sca-1, Abcg2) and endothelial (Vegf, Eng) at mRNA level. Sca-1 expression is already shown to be involved in neo-angiogenesis and its co-expression is shown with platelet/endothelial cell adhesion molecule-1 (PECAM-1) in the lung endothelium [182]. Vegf expression from endothelial precursors is an early response of angiogenesis and direct regulation of Vegf has been shown following hypoxia due to the stabilisation of the Hif-1 $\alpha$  protein, reviewed in [183]. As shown in figures 4-7 and 6-7, adult CDCs pre-treated with 3% O<sub>2</sub> showed higher levels of Vegf protein in comparison with their normoxia counterparts. On the other hand, Flk1 which is known to be one of three Vegf tyrosine kinase receptors (reviewed in [183]), was slightly increased in CDC<sup>3%</sup>O<sub>2</sub> compared with normoxia group (table 4-5). Therefore, the pro-angiogenic potential of CDC<sup>3%</sup>O<sub>2</sub> could have been primed prior to their delivery in the matrigel plug angiogenesis assay.

In this chapter I utilised a novel preconditioning strategy that related to the hypoxic environment of the infarct border zone to enhance CDC pro-angiogenic potential and I showed that sub-dermal delivery of adult CDC combined with matrigel leads to a significantly enhanced angiogenic response within the matrigel. I also showed that preconditioning adult CDCs for 48 hours with 3% O<sub>2</sub> increases their pro-angiogenic response almost two fold higher than the normoxia counterparts (5.1-6.5 vs. 10.3-13.7 MVD, p<0.001). However, combination of CDCs with MLECS increased their pro-angiogenic potential to 2.7 fold higher than CDCs treated with normoxia (5.1-6.5 vs. 14.7-16.8 MVD, p<0.001). Although I observed significant number of CD31 expressing cells within the matrigel plugs of all CDC recipient groups, further investigations with isolectin perfusion assay showed that only one of the three matrigel plugs showed inter-connection of the CD31-positive vessels with the main vasculature. However the limitation of the quantifications and angiogenesis assessment could have possibly affected the results. For instance as I only assessed 10/50 of slides for each matrigel plug, it is still possible that I have missed the true angiogenesis in those slides that I have not assessed. It is also possible that a proportion of the CD31<sup>+</sup> cells within the matrigel are circulating endothelial cells derived from bone marrow of the recipient mice which have infiltrated into the matrigel plugs. This could be more relevant in the plugs which received CDCs pre-treated with 3% O<sub>2</sub>. This is because co-relation of hypoxia pre-treatment and SDF1 expression has been shown in CDCs [73], therefore it is possible that 3% O<sub>2</sub> pre-treated CDCs has enhanced SDF1 production which has

attracted bone marrow CD31<sup>+</sup> cells into the plugs. However my findings are in agreement with previous reports showing the benefit of hypoxia preconditioning of adult CDCs and their increased angiogenic and cardioprotection potential [72,73,103]. However, there is an important difference between these studies and my own. In Yan [72] and Tang's [73] work CDCs were treated with severe hypoxic conditions (0.1%), equivalent to the injured region but in Li's study [103] CDCs were treated with 5% O<sub>2</sub> which is found in remote myocardium (away from the infarct) and healthy heart. I used 3% O<sub>2</sub> (the level approximately equivalent to the infarct border zone) [89]. This is an important distinction because the anatomical region of interest for cell delivery in preclinical and clinical studies is the border zone. If CDCs are pre-treated with severe hypoxic conditions and then delivered into the border zone, the new condition would be hyperoxic and if they are preconditioned with physiological O<sub>2</sub>, the pre-infarct border zone may be hypoxic for donor cells. In this way, either hyperoxic or hypoxic environments could produce unfavourable circumstances for donor cells and could alter their survival and cardioprotection potential. However, culturing CDCs with 3% O<sub>2</sub> could mimic similar conditions of their host region and could give better readouts of their *in-vitro* and *in-vivo* phenotypes.

### **6.3.3 eGFP and CD31 co-expression in matrigel plugs implanted with adult CDCs.**

The endothelial marker CD31 has a reliable epitope for immunostaining. Therefore, I used CD31 as the angiogenic marker in my study. I also analysed the proportion of eGFP cells which also co-localise with CD31. Although there was increased adult CDC survival in comparison to neonatal CDCs (likely due to the technical improvements of the matrigel angiogenesis model that I incorporated) the majority of CDCs did not co-localise with CD31 or with  $\alpha$ -SMA (figures 6-9 & 6-10). However, a small number of eGFP positive CDCs co-localized with CD31 in few regions of the neo-microvasculature and in single isolated cells (figure 6-11). However, there is a possibility that the limited number of eGFP<sup>+</sup>/CD31<sup>+</sup>-expressing cells which have been identified in the matrigel plugs were initially CD31 positive before sub-dermal injection, as my studies from FACS data showed that 1-2% of adult CDCs express CD31. This is also consistent with Davis *et al.* (2010) who showed that 3% of human cardiac progenitors express CD31 [70]. It is also possible that a fraction of the eGFP<sup>+</sup>/CD31<sup>+</sup> injected CDC sub-population has been removed by the recipient immune

system prior to our experiments. According to Li *et al.* (2009), less than 5% of transplanted CDCs are retained in the heart at three weeks following cell delivery [184]. Furthermore, it has been reported that 90% of delivered progenitor cells die due to apoptosis [87]. However, in one plug which received CDCs preconditioned in 3% O<sub>2</sub> some eGFP cells co-stained with CD31 and located within tubular structures that could be neo-vessels (figure 6-11). Angiogenesis is a complex process which involves four stages: 1) basement membrane degradation; 2) endothelial cell proliferation; 3) cell migration; and, finally, 4) tube or cellular array formation. After detailed analysis of several cryosections from five experimental groups I observed cytoplasmic protrusions and cellular array formations are common signatures of the plugs that contained CDC<sup>3%</sup>O<sub>2</sub>. In this respect Skovseth *et al.* (2002) showed the cytoplasmic protrusion formation and cellular accumulation (cell migration) to form cellular arrays are considered as positive angiogenic responses [179]. SDF1 is shown to induce endothelial cell migration and proliferation [185]; on the other hand the induction of SDF1 expression in murine adult CDCs with severe hypoxic preconditioning has been shown by two independent studies [72,73]. Therefore, it would be interesting to assess SDF1 expression in matrigel plugs which received CDC<sup>3%</sup>O<sub>2</sub> and compare it with CDC<sup>N</sup>O<sub>2</sub> counterparts. Ki-67, expressed in the nucleus, is also shown to be very specific in identifying proliferating cells [186]. Staining cryosections with Ki-67 and its co-expression analysis with eGFP and CD31 could give us valuable information about the proliferation rate of the endothelial sub-population of CDC<sup>3%</sup>O<sub>2</sub> and CDC<sup>N</sup>O<sub>2</sub>.

#### **6.3.4 Assessing eGFP and CD11b co-expression in matrigel plugs**

. I further quantified the level of CD11b expression in the matrigel plugs and noticed that in all of the plugs which received cells, either with CDC, MLECS or both, had the same level of CD11b expression, and all showed a significant increase of CD11b expression in comparison with the matrigel-only group, which suggests that the host's immune system has the same angiogenic impact on all four study groups which received cells. It is important to know the role of the endogenous immune response in CDC-mediated angiogenesis. One mechanism has been shown to be by secretion of the pro-angiogenic factors, such as Vegf and bFGF, by macrophages in ischemic wound healing repair [187]. Therefore, it is possible that CDCs stimulate the host's immune system to induce angiogenesis. Investigating the immune response at different time points with

matrigel plug assay will enable us to design experiments with the highest level of vascularity and the lowest level of CD11b response. Furthermore, to elucidate the angiogenesis pathway mediated by CDCs, the *in-vivo* angiogenesis would be tested on SCID mice. This would help us to understand better CDCs' role in angiogenesis, as SCID mice will not activate angiogenesis mediated by their immune response. Further analysis of cryosections showed that the location of CDCs in matrigel plugs affects the efficiency of CDC ingestion into the CD11b expressing cells. This is probably due to easier host animal macrophage infiltration into the border of matrigel plugs than into the middle of the plugs. As shown in figure 6-13 the majority of CDCs located in the border of the matrigel have been ingested by CD11b positive cells but the majority of CDCs in the middle of the gel have not. As it has been shown that the majority of CDCs are negative for inflammatory cell markers such as CD11b[71], therefore eGFP<sup>+</sup>/CD11b<sup>+</sup> cells within the matrigel plugs are probably the inflammatory cells which have engulfed GFP expressing CDCs as foreign bodies.

### **6.3.5 CDCs pre-treated with 3% O<sub>2</sub> may enhance connection of new vessels within the matrigel plugs to the host vasculature**

Perfusion analysis of the plugs made from CDC<sup>N</sup>O<sub>2</sub> and CDC<sup>3%</sup>O<sub>2</sub> showed that 1 out of 3 of the plugs with CDC<sup>3%</sup>O<sub>2</sub> showed positive isolectin-expressing cells within the middle and the borders of the matrigel, even though none of the plugs with CDC<sup>N</sup>O<sub>2</sub> and matrigel alone showed isolectin expression. This could be due to the fact that preconditioning CDCs with 3% O<sub>2</sub> has enhanced their pro-angiogenic potential. Due to the technical difficulties in adult CDC culture and preparation in this final experiment, I was only able to assess perfusion analysis in CDC<sup>N</sup>O<sub>2</sub> and CDC<sup>3%</sup>O<sub>2</sub>. Therefore, it would also be important to assess the perfusion of the vessels formed in CDC+MLECs plugs in a similar way to a previous study using mesenchymal cells and endothelial cells in a matrigel plug assay [177]. This work showed the combination of mesenchymal cells with endothelial cells enhances their angiogenesis potential. It would be also be useful to assess the perfusion analysis of the formed vessels following a longer period. My study was limited to matrigel angiogenesis assay of two weeks, but Skovseth *et al.* (2002) showed all of the vessels formed after 40 days within the matrigel plug contained erythrocytes [179]. In tumour angiogenesis studies, Das *et al.* (2005) showed the positive effect of hypoxia on the perfusion of the vessels formed in matrigel [188].

In my study it is possible that I have not noticed the perfused vessels with CDC<sup>N</sup>O<sub>2</sub> and CDC<sup>3%</sup>O<sub>2</sub> plugs due to the limitations of the technique. Another possibility is that the perfused plug with CDC<sup>3%</sup>O<sub>2</sub> was the plug which I injected in to the scruff region of the recipient, as different regions of the body may show different levels of angiogenic response. I divided each plug into three regions (beginning, middle and the end) and stained 3-5 slides containing 18-24 sections. Therefore, it is possible that perfused vessels were present in the regions that I have not assessed. It would be very accurate to assess the perfusion status of the matrigel plugs with imaging techniques such as contrast ultrasound imaging in future experiments. Using an ultrasound system Stieger *et al.* (2006) showed the efficacy of this system in detecting the angiogenesis in matrigel subdermal plugs of rats [189].

One of the longer-term aims of my study was to determine the optimal conditions for CDC-mediated angiogenesis by using a matrigel subdermal plug and to use the optimised conditions to deliver pro-angiogenic cells to promote angiogenesis in a surgical mouse model of cardiac infarction. From my data I would utilise adult CDCs pre-treated with 3% O<sub>2</sub>. An alternative would be to utilise human CDCs pre-treated with 3% O<sub>2</sub> and assess their angiogenic response in MI models of SCID mice, which, finally, helps us to design clinical trials to decide the desirable CDC pre-conditioning method in order to enhance angiogenesis and cardioprotection in humans.

My preliminary results also showed that the combination of CDC with endothelial cells (MLECs) enhanced their angiogenic potential. However this experiment has some limitations; (i) as I used different number of CDCs in CDC and CDC+MLECS plugs, this makes angiogenesis comparison between these groups difficult. It would be interesting to assess same number of CDCs with and without MLECS, this could also show the effect of CDC mediated angiogenesis when implanted alone or combined with MLECS sub-dermally. (ii) In this experiment I used un-labeled MLECS; therefore it is not possible to track MLECS contribution into the new vessels. Thus, to assess MLECS mediated angiogenesis, it would be useful to label them prior to implantation with a fluorescent reporter such as Ds-Red and combined with eGFP-CDCs, this experiment could tell us how these two cell populations contributing to in vivo angiogenesis in sub dermal matrigel plugs.

It is important to know if human-derived CDCs combined with autologous endothelial cells such as circulating endothelial cells enhance pro-angiogenic potential and survival after injection into the *in-vivo* matrigel model.

To summarise, the work described in this chapter confirms that CDC transfer can activate angiogenesis in sub-dermal matrigel plugs over 2 weeks post-cell-injection and 3% O<sub>2</sub> pre-treatment for 48 hours enhances this process. The mechanism underlying angiogenesis is likely to be paracrine with a limited autocrine contribution. However, the exact timing and pre-treatment of CDCs to get the optimum angiogenesis response remains uncertain and will require further study.

# **Chapter 7 Final discussion and future directions**

Cardiac stem cell therapy has recently brought new hope to coronary heart patients. As low cell survival and cell retention is the main barrier for myocardial cell transplantation strategies, hypoxia preconditioning of transplanted cells could improve their function in the recipient heart tissue. Hypoxic pre-treatment of CDCs has been shown to improve their pro-angiogenic and cardiogenic potential in human- [103] and mouse-derived [73] CDCs. The level of atmospheric O<sub>2</sub> used in conventional cell culture is 21% although the level of physiologic O<sub>2</sub> within the heart is 5-7% [89]. More importantly, the level of O<sub>2</sub> in the infarct border zone, the main target region for therapeutic cell delivery, is estimated to be 3% [89]. As described in this thesis I tested whether preconditioning of CDCs with 3% O<sub>2</sub> enhances their pro-angiogenic potential *in vitro* and *in vivo*. In addition, I characterised CDCs by using lineage tracing to estimate their fibroblast content, as this may affect their repair potential.

In chapter 3, I established culturing of neonatal CDCs in 3% O<sub>2</sub> and compared cell viability and proliferation with cells cultured in normoxia. While my data showed that expanding neonatal mice cardiac explants in 3%O<sub>2</sub> resulted in enhanced EDC outgrowth, Csph formation was delayed. This is in agreement with Koh *et al.* (2012), who showed that a prolonged hypoxic environment is shown to cause cell spreading rather than cell accumulations, so delaying sphere formation [121]. I also observed that culturing P2 neonatal CDCs at 3%O<sub>2</sub> for 72 hours did not change their viability, clonogenicity and cell proliferation. These findings are in agreement with Li *et al.* (2011) who showed that culturing human-derived CDCs in 5% O<sub>2</sub> did not change cell growth at early passages (from P1 to P3), but increased their proliferation at higher passages (P4 to P5) [103]. qRT-PCR and immunophenotyping results showed that pre-conditioning of neonatal CDCs with 3%O<sub>2</sub> for 72 hours significantly enhanced Sca-1 gene expression at the mRNA level, it also increased *Eng* and *Vegf* mRNA. These findings suggested that pre-conditioning CDCs could have clinical applications and may be used to prepare progenitor and endothelial sub-populations of CDCs. However, as the effect of hypoxia is context-specific, future studies should focus on the effect of 3% O<sub>2</sub> on human CDCs *in vitro* and assess the effect on stem cell and endothelial sub-populations. I also found that *Hprt* is not a trustworthy housekeeping gene for qRT-PCR studies with CDCs as it did not have a stable range of Ct values in CDCs cultured for different times in 3% O<sub>2</sub>. Therefore, in all subsequent qRT-PCR experiments only *Gapdh*, *B-actin* and *RPS-19* were used to normalise the data. This shows the importance of choosing valid housekeeping genes in quantitative gene experiments in CDCs.



Indeed, hypoxia has been shown to alter the level of housekeeping gene expression in CDCs [112]. Nevertheless, my findings do suggest that 3%O<sub>2</sub> pre-conditioning increases the progenitor and endothelial sub-populations of neonatal CDCs and may therefore prove to be of therapeutic value.

In chapter 4 I tested whether pre-conditioning adult-derived CDCs with 3% O<sub>2</sub> also increases the progenitor and endothelial sub-populations *in vitro*. The importance of using CDCs cultured from adult hearts is that it more closely models to the clinical situation, where autologous CDCs are used to treat coronary heart disease in adults. However, I first had to establish a culture of adult CDCs. Although I modified several steps of adult CDC culture, I observed lots of difficulties with CDC cultures from adult C57BL/6 mice, which produced a significantly lower cellular yield in all three stages of CDC culture and took a significantly longer time. For instance, CDC culture from neonatal mice takes 25-30 days, but from adults takes 55-60 days and their cellular yield is 1/2-1/3 in comparison to neonatal CDC culture. This is in agreement with a published study showing lower CPC yields in adults compared with neonates and young patients who had congenital cardiac surgery [79]. I further compared CDC culture efficiency between the atria and ventricles and noticed murine atrial explants generated higher yields of EDCs and Csphs in comparison to ventricles. This is in agreement with Chan *et al.* (2012) who showed that atrial samples generated a more sufficient number of EDCs than ventricles for Csph culture [140]. Mishra *et al.* (2011) suggested that the minimised stress wall in the atria favours cardiac progenitors and increases their proliferation potential [79]. However, it would be interesting to measure the level of growth factors and cytokines expressed in supernatant of atrial versus ventricular explant and Csph culture. It would be also interesting to assess the expression of the key regulators of cell mobility pathways such as Notch and SDF1/CXCR4, and compare them in atria and ventricles. Further immunophenotyping analysis of adult CDCs showed that Sca-1 positive CDCs are separate from cKit-expressing cells and, interestingly, Sca-1<sup>+</sup> and cKit<sup>+</sup> were predominantly CD45 negative which suggest that stem cell sub-populations of CDCs are not derived from BM. My findings agreed with Davis *et al.* (2009) who showed that CDCs are predominantly CD45 negative [83]. Although I showed the benefit of pre-conditioning adult CDCs with 3% O<sub>2</sub> in increasing the yield of progenitor and endothelial sub-populations, there were some limitations in

this study: (i) adult C57BL/6 is not an optimal model to study adult CDCs due to the poor yield; (ii) healthy mice are not a good model of coronary heart patients, therefore it would be interesting to generate CDCs from mice following MI or mice models of atherosclerosis. Among such models are the Apolipoprotein (ApoE) knockout mice. These mice show impaired clearing of plasma lipoproteins and develop atherosclerosis, reviewed in [190]. CDC culture from MI mice and ApoE-deficient mice and characterising them in normoxic and 3% O<sub>2</sub> environments could provide valuable information about CDC phenotypes in diseased models.

In chapter 5, I studied lineage tracing in a transgenic mouse *Colla2 CreERT; Rosa26-floxed STOP eYFP* to track CFs in CDC culture and *in vivo* in the healthy hearts of and following MI (1 and 2 weeks post-LAD ligation). This part of my thesis had two aims: (i) to assess the specificity of the *Colla2 CreERT; Rosa26-floxed STOP eYFP* mice in detecting CFs *in vivo*; and (ii) to investigate the CF contribution to CDC culture. The results showed that with this transgenic model, I was able to detect YFP expression in approximately 37% of Collagen 1 expressing cells. In addition, co-localisation experiments with YFP and additional fibroblast markers (FSP1 and vimentin) showed partial co-staining of eYFP with either FSP1 or vimentin. Lineage-tracing studies with fibroblasts has always been a difficult task as they lack a specific marker and all of the available markers have been shown to be expressed in other cell types, reviewed in [15]. Additional possible reasons for suboptimal labelling of CFs include incomplete Cre-activation. Potentially, this could be improved by further optimising the tamoxifen treatment, for example, by oral tamoxifen administration or by using 4-hydroxy tamoxifen, the active metabolite of tamoxifen. Nevertheless, the *in-vivo* experiments with healthy and MI models showed that, while the expression of eYFP, FSP1 and vimentin in the infarct regions significantly increased in comparison with healthy hearts and the remote myocardium of infarcted hearts, co-localisation of eYFP with FSP1 and vimentin decreased significantly. My results agreed with the findings of Schneider *et al.* (2007) who showed that fibroblasts are actively proliferating in the infarct region and border zone [156]. Further *in-vitro* experiments using confocal microscopy to analyse eYFP expression in CDCs derived from *Colla2 CreERT; Rosa26-floxed STOP eYFP* mice showed that phase bright cells are predominantly negative for eYFP expression. This suggests that there is a possibility of CDC enrichment against fibroblasts in the

CDC culture by selecting only phase bright cells. In fact, all EDCs were selected for culture using our standard culture protocol and FACS analysis showed that 9-11.5% of EDCs express YFP. Considering the 37% efficiency of our transgenic model in CF tracing, I estimate that the true proportion of CF derived cells in EDCs and CDCs is likely to be higher. I also showed that following Cre-activation in *Colla2 CreERT; Rosa26-floxed STOP eYFP* mice, Csph formed from both YFP<sup>+</sup> and YFP<sup>-</sup> EDCs. This suggests Csph formation occurs irrespective of fibroblast content, although eYFP<sup>+</sup> EDCs made spheroids more efficiently than eYFP<sup>-</sup> EDCs. It has been suggested that mesenchymal cells provide physical and secretory support to the progenitor sub-populations of CDCs [68]. To validate this hypothesis it would be informative to investigate the immunophenotype of the CDCs derived from YFP<sup>-</sup> or YFP<sup>+</sup> EDCs and measure the growth factors released to the cell culture medium. When CDCs were prepared in the standard way, 8.3-12.9% of CDCs express YFP. Moreover, FACS data showed that the majority of stem cell sub-populations of CDCs (Sca-1 or cKit-expressing cells) were YFP<sup>-</sup> suggesting that the stem cell populations were not derived from cardiac fibroblasts. This chapter showed the potential of using lineage tracing to interpret the fibroblast content of the different sub-populations of EDCs and CDCs.

In order to elucidate the effect of fibroblasts on the stem cell sub-populations of CDCs (Sca-1<sup>+</sup> and cKit<sup>+</sup>), it is possible to culture *Colla2 CreERT; Rosa26-floxed STOP eYFP*-derived CDCs and sort eYFP<sup>-</sup>/Sca-1<sup>+</sup> or eYFP<sup>-</sup>/cKit<sup>+</sup> cells and then assess their pro-angiogenic and cardiogenic capacity. The results could be compared with non-sorted CDCs and further valuable data would be achieved when the stem cell fraction of CDCs are used alone or with fibroblasts. The importance of this hypothesis is based on the fact that, after the infarction, cardiac fibrosis is activated, so CDCs without or having a lower CF sub-population is not likely to enhance this process. However, this hypothesis might bring an optimised strategy of delivering CDCs accompanied with nanoparticles carrying different paracrine factors.

In chapter 6 I assessed the pro-angiogenic potential of neonatal and adult CDCs derived from the *CAG-farnesyl-eGFP* transgenic line *in vivo* using a subdermal matrigel plug angiogenesis assay. The results showed that neonatal P2 CDCs lead to a significantly increased CD31 expression in the matrigel after 2 weeks, indicating an increased angiogenesis response. There was a significant increase in MVD compared with

matrigel alone, which suggests the pro-angiogenic potential of neonatal CDCs *in vivo* (please see table 6-1). Immunofluorescent staining showed that the majority of eGFP-expressing cells do not co-localise with CD31-expressing cells, which suggests that the pro-angiogenic effect of neonatal CDCs is most likely to be paracrine. I also investigated whether adult CDCs are capable of promoting neo-vessel formation *in vivo* and whether pre-treating them with 3% O<sub>2</sub> could enhance their pro-angiogenic potential. Here I showed that adult CDCs led to a significantly enhanced angiogenic response within the matrigel. I also showed that preconditioning adult CDCs for 48 hours with 3% O<sub>2</sub> increased the pro-angiogenic response significantly in comparison with their normoxia counterparts. In addition, the combination of CDCs with MLECS increased their pro-angiogenic potential significantly more than CDCs treated with normoxia or 3% O<sub>2</sub> (please see table 6-3). Further immunofluorescent staining with eGFP and CD31 or  $\alpha$ -SMA showed very limited co-localisation of eGFP CDCs with CD31 (consistent with my findings using neonatal CDCs) and confirming the low direct contribution of CDCs to new blood vessels. I observed that the majority of eGFP cells from 3% O<sub>2</sub> plugs show elongated cytoplasmic protrusions and form cellular arrays. Cytoplasmic protrusion formation and cellular accumulation (by cell migration) to form cellular arrays are considered as positive angiogenic responses and in this respect SDF1 has been shown to induce endothelial cell migration and proliferation [185]. As SDF1 is elevated in CDCs pre-treated with hypoxia [73], it would be interesting to assess SDF1 and CXCR4 expression in the matrigel plugs seeded with 3% O<sub>2</sub> treated CDCs.

CD11b analysis showed that matrigel plugs with CDC<sup>N</sup>O<sub>2</sub> and CDC<sup>3%</sup>O<sub>2</sub> had a similar type of immune response, and this was increased compared with the matrigel-only plugs. This suggests the enhanced angiogenic response in 3% O<sub>2</sub> in comparison with normoxia pre-treated CDCs is due to their enhanced pro-angiogenic potential and not due to an enhanced immune response. Perfusion analysis of the plugs made from CDC<sup>N</sup>O<sub>2</sub> and CDC<sup>3%</sup>O<sub>2</sub> showed that 1 out of 3 of the plugs with CDC<sup>3%</sup>O<sub>2</sub> showed positive isolectin-expressing cells in the matrigel. None of the plugs with CDC<sup>N</sup>O<sub>2</sub> or matrigel alone showed isolectin expression. This work would need to be repeated to determine whether CDC<sup>3%</sup>O<sub>2</sub> was able to promote increased numbers of perfused vessels. However, I showed that CDC transfer can activate angiogenesis in subdermal matrigel plugs over 2 weeks post-cell-injection and 3% O<sub>2</sub> pre-treatment for 48 hours enhances this process. Using eGFP to track the CDCs, it was clear that CDC-mediated angiogenesis was due to paracrine effects and there was limited autocrine contribution.

However, the exact timing and pre-treatment of CDCs to get the optimum angiogenesis response remains uncertain and requires further study. Nevertheless, this work had some limitations: (i) the optimal *in-vivo* model may be to utilise human CDCs pre-treated with 3% O<sub>2</sub> and assess their angiogenic response in MI models of SCID mice. This could also be combined with endothelial cells derived from BM to enhance angiogenesis and cardioprotection. It would also be interesting to investigate whether supplementing human CDCs with an endothelial cell source (for example human-circulating EPCs or human endothelial cells derived from induced pluripotent stem cells (iPSC)) would enhance CDC-mediated angiogenesis and improve cardiac function.

Future studies are needed to better understand the mechanisms underlying CDC-mediated repair as well as optimising neo-vessel formation potential following ischaemic heart injury.

So far, I have shown that preconditioning neonatal and adult CDCs with 3% O<sub>2</sub> *in vitro*, increases their progenitor, endothelial sub-populations and enhances their pro-angiogenic potential in subdermal matrigel plugs. However, to elucidate the exact mechanisms it will be important to investigate further the precise role of CDC-mediated pro-angiogenesis. Given that my findings suggest that subdermally transplanted CDCs act via paracrine mechanisms this suggests that it would be advantageous to assess which proteins are synthesised by CDCs treated with 3% O<sub>2</sub> compared with normoxia. This could be done using a custom qRT-PCR or protein array focusing on angiogenesis and cardiomyocyte differentiation pathways.

In addition, a time course would be helpful in determining the final pro-angiogenic effects of CDCs. In the matrigel plug assays only a 2-week time point was used for the analysis. It would be informative also to analyse matrigel plugs at 3-4 weeks when vascular networks and tubular structures would be more complete and vessel stability could be assessed. As the quantification method of the matrigel plugs is very time-consuming, it may also be easier to assess the vessel size and density with alternative methods such as ultrasound. One on-going project in our lab is studying the effect of Eng and TGFβ-signalling pathways on CDC-mediated heart repair. TGFβ signalling has been shown to be involved in infarct healing by enhancing angiogenesis and suppressing the immune response. For instance, the enrichment of Eng-expressing CDCs may lead to an enhanced pro-angiogenic response in the recipient MI models.

Recent clinical trials with CDC transplantation for MI patients have revealed some promising findings [77,107]. However, the exact characterisation of CDCs is still not complete. Here in this thesis, the results showed the importance of 3% O<sub>2</sub> preconditioning of CDCs on their pro-angiogenic potential. More preclinical studies (such as those mentioned above) will be required to validate and extend these findings and will help to design future clinical therapies.

## References

- 1 Iaizzo PA, SpringerLink ebooks - Medicine (2009): Handbook of cardiac anatomy, physiology, and devices: Current clinical oncology. New York, NY, Springer,, 2009.
- 2 Hutchins GM, Kessler-Hanna A, Moore GW: Development of the coronary arteries in the embryonic human heart. *Circulation* 1988;77:1250-1257.
- 3 Pérez-Pomares JM, Carmona R, González-Iriarte M, Atencia G, Wessels A, Muñoz-Chápuli R: Origin of coronary endothelial cells from epicardial mesothelium in avian embryos. *Int J Dev Biol* 2002;46:1005-1013.
- 4 Majesky MW: Development of coronary vessels. *Curr Top Dev Biol* 2004;62:225-259.
- 5 Cai CL, Martin JC, Sun Y, Cui L, Wang L, Ouyang K, Yang L, Bu L, Liang X, Zhang X, Stallcup WB, Denton CP, McCulloch A, Chen J, Evans SM: A myocardial lineage derives from tbx18 epicardial cells. *Nature* 2008;454:104-108.
- 6 Zhou B, Ma Q, Rajagopal S, Wu SM, Domian I, Rivera-Feliciano J, Jiang D, von Gise A, Ikeda S, Chien KR, Pu WT: Epicardial progenitors contribute to the cardiomyocyte lineage in the developing heart. *Nature* 2008;454:109-113.
- 7 Baudino TA, Carver W, Giles W, Borg TK: Cardiac fibroblasts: Friend or foe? *Am J Physiol Heart Circ Physiol* 2006;291:H1015-1026.
- 8 Frangogiannis NG: The immune system and cardiac repair. *Pharmacol Res* 2008;58:88-111.
- 9 Willems IE, Havenith MG, De Mey JG, Daemen MJ: The alpha-smooth muscle actin-positive cells in healing human myocardial scars. *Am J Pathol* 1994;145:868-875.
- 10 Desmoulière A, Geinoz A, Gabbiani F, Gabbiani G: Transforming growth factor-beta 1 induces alpha-smooth muscle actin expression in granulation tissue myofibroblasts and in quiescent and growing cultured fibroblasts. *J Cell Biol* 1993;122:103-111.
- 11 Siwik DA, Chang DL, Colucci WS: Interleukin-1beta and tumor necrosis factor-alpha decrease collagen synthesis and increase matrix metalloproteinase activity in cardiac fibroblasts in vitro. *Circ Res* 2000;86:1259-1265.
- 12 Dobaczewski M, Bujak M, Li N, Gonzalez-Quesada C, Mendoza LH, Wang XF, Frangogiannis NG: Smad3 signaling critically regulates fibroblast phenotype and function in healing myocardial infarction. *Circ Res* 2010;107:418-428.
- 13 Fukuda S, Kaga S, Sasaki H, Zhan L, Zhu L, Otani H, Kalfin R, Das DK, Maulik N: Angiogenic signal triggered by ischemic stress induces myocardial repair in rat during chronic infarction. *J Mol Cell Cardiol* 2004;36:547-559.
- 14 Kido M, Du L, Sullivan CC, Li X, Deutsch R, Jamieson SW, Thistlethwaite PA: Hypoxia-inducible factor 1-alpha reduces infarction and attenuates progression of cardiac dysfunction after myocardial infarction in the mouse. *J Am Coll Cardiol* 2005;46:2116-2124.
- 15 Zeisberg EM, Kalluri R: Origins of cardiac fibroblasts. *Circulation research* 2010;107:1304-1312.
- 16 Souders CA, Bowers SL, Baudino TA: Cardiac fibroblast: The renaissance cell. *Circ Res* 2009;105:1164-1176.

- 17 Krenning G, Zeisberg EM, Kalluri R: The origin of fibroblasts and mechanism of cardiac fibrosis. *J Cell Physiol* 2010;225:631-637.
- 18 Fan D, Takawale A, Lee J, Kassiri Z: Cardiac fibroblasts, fibrosis and extracellular matrix remodeling in heart disease. *Fibrogenesis Tissue Repair* 2012;5:15.
- 19 Chang HY, Chi JT, Dudoit S, Bondre C, van de Rijn M, Botstein D, Brown PO: Diversity, topographic differentiation, and positional memory in human fibroblasts. *Proc Natl Acad Sci U S A* 2002;99:12877-12882.
- 20 Norris RA, Borg TK, Butcher JT, Baudino TA, Banerjee I, Markwald RR: Neonatal and adult cardiovascular pathophysiological remodeling and repair: Developmental role of periostin. *Ann N Y Acad Sci* 2008;1123:30-40.
- 21 Zhou B, von Gise A, Ma Q, Hu YW, Pu WT: Genetic fate mapping demonstrates contribution of epicardium-derived cells to the annulus fibrosis of the mammalian heart. *Dev Biol* 2010;338:251-261.
- 22 de Lange FJ, Moorman AF, Anderson RH, Männer J, Soufan AT, de Gier-de Vries C, Schneider MD, Webb S, van den Hoff MJ, Christoffels VM: Lineage and morphogenetic analysis of the cardiac valves. *Circ Res* 2004;95:645-654.
- 23 Camelliti P, Borg TK, Kohl P: Structural and functional characterisation of cardiac fibroblasts. *Cardiovasc Res* 2005;65:40-51.
- 24 Snider P, Standley KN, Wang J, Azhar M, Doetschman T, Conway SJ: Origin of cardiac fibroblasts and the role of periostin. *Circ Res* 2009;105:934-947.
- 25 Banerjee I, Fuseler JW, Price RL, Borg TK, Baudino TA: Determination of cell types and numbers during cardiac development in the neonatal and adult rat and mouse. *Am J Physiol Heart Circ Physiol* 2007;293:H1883-1891.
- 26 Zeisberg EM, Tarnavski O, Zeisberg M, Dorfman AL, McMullen JR, Gustafsson E, Chandraker A, Yuan X, Pu WT, Roberts AB, Neilson EG, Sayegh MH, Izumo S, Kalluri R: Endothelial-to-mesenchymal transition contributes to cardiac fibrosis. *Nat Med* 2007;13:952-961.
- 27 van Meeteren LA, ten Dijke P: Regulation of endothelial cell plasticity by  $\text{tgf-}\beta$ . *Cell Tissue Res* 2012;347:177-186.
- 28 Widiantoro B, Emoto N, Nakayama K, Anggrahini DW, Adiarto S, Iwasa N, Yagi K, Miyagawa K, Rikitake Y, Suzuki T, Kisanuki YY, Yanagisawa M, Hirata K: Endothelial cell-derived endothelin-1 promotes cardiac fibrosis in diabetic hearts through stimulation of endothelial-to-mesenchymal transition. *Circulation* 2010;121:2407-2418.
- 29 Piera-Velazquez S, Li Z, Jimenez SA: Role of endothelial-mesenchymal transition (endomt) in the pathogenesis of fibrotic disorders. *Am J Pathol* 2011;179:1074-1080.
- 30 van Amerongen MJ, Bou-Gharios G, Popa E, van Ark J, Petersen AH, van Dam GM, van Luyn MJ, Harmsen MC: Bone marrow-derived myofibroblasts contribute functionally to scar formation after myocardial infarction. *J Pathol* 2008;214:377-386.
- 31 Höcht-Zeisberg E, Kahnert H, Guan K, Wulf G, Hemmerlein B, Schlott T, Tenderich G, Körfer R, Raute-Kreinsen U, Hasenfuss G: Cellular repopulation of myocardial infarction in patients with sex-mismatched heart transplantation. *Eur Heart J* 2004;25:749-758.



- 32 Haudek SB, Xia Y, Huebener P, Lee JM, Carlson S, Crawford JR, Pilling D, Gomer RH, Trial J, Frangogiannis NG, Entman ML: Bone marrow-derived fibroblast precursors mediate ischemic cardiomyopathy in mice. *Proc Natl Acad Sci U S A* 2006;103:18284-18289.
- 33 van Amerongen MJ, Harmsen MC, van Rooijen N, Petersen AH, van Luyn MJ: Macrophage depletion impairs wound healing and increases left ventricular remodeling after myocardial injury in mice. *Am J Pathol* 2007;170:818-829.
- 34 Carmeliet P: Angiogenesis in life, disease and medicine. *Nature* 2005;438:932-936.
- 35 ten Dijke P, Arthur H: Extracellular control of tgfbeta signalling in vascular development and disease. *Nat Rev Mol Cell Biol* 2007;8:857-869.
- 36 Scholz D, Ito W, Fleming I, Deindl E, Sauer A, Wiesnet M, Busse R, Schaper J, Schaper W: Ultrastructure and molecular histology of rabbit hind-limb collateral artery growth (arteriogenesis). *Virchows Arch* 2000;436:257-270.
- 37 Dor Y, Djonov V, Abramovitch R, Itin A, Fishman GI, Carmeliet P, Goelman G, Keshet E: Conditional switching of vegf provides new insights into adult neovascularization and pro-angiogenic therapy. *EMBO J* 2002;21:1939-1947.
- 38 Tendera M, Wojakowski W, Rużyło W, Chojnowska L, Kepka C, Tracz W, Musiałek P, Piwowarska W, Nessler J, Buszman P, Grajek S, Breborowicz P, Majka M, Ratajczak MZ, Investigators R: Intracoronary infusion of bone marrow-derived selected cd34+cxcr4+ cells and non-selected mononuclear cells in patients with acute stemi and reduced left ventricular ejection fraction: Results of randomized, multicentre myocardial regeneration by intracoronary infusion of selected population of stem cells in acute myocardial infarction (regent) trial. *Eur Heart J* 2009;30:1313-1321.
- 39 Tepper OM, Galiano RD, Capla JM, Kalka C, Gagne PJ, Jacobowitz GR, Levine JP, Gurtner GC: Human endothelial progenitor cells from type ii diabetics exhibit impaired proliferation, adhesion, and incorporation into vascular structures. *Circulation* 2002;106:2781-2786.
- 40 Heeschen C, Lehmann R, Honold J, Assmus B, Aicher A, Walter DH, Martin H, Zeiher AM, Dimmeler S: Profoundly reduced neovascularization capacity of bone marrow mononuclear cells derived from patients with chronic ischemic heart disease. *Circulation* 2004;109:1615-1622.
- 41 Bergmann O, Bhardwaj RD, Bernard S, Zdunek S, Barnabe-Heider F, Walsh S, Zupicich J, Alkass K, Buchholz BA, Druid H, Jovinge S, Frisen J: Evidence for cardiomyocyte renewal in humans. *Science* 2009;324:98-102.
- 42 Messina E, De Angelis L, Frati G, Morrone S, Chimenti S, Fiordaliso F, Salio M, Battaglia M, Latronico MV, Coletta M, Vivarelli E, Frati L, Cossu G, Giacomello A: Isolation and expansion of adult cardiac stem cells from human and murine heart. *Circ Res* 2004;95:911-921.
- 43 Lee ST, White AJ, Matsushita S, Malliaras K, Steenbergen C, Zhang Y, Li TS, Terrovitis J, Yee K, Simsir S, Makkar R, Marbán E: Intramyocardial injection of autologous cardiospheres or cardiosphere-derived cells preserves function and minimizes adverse ventricular remodeling in pigs with heart failure post-myocardial infarction. *J Am Coll Cardiol* 2011;57:455-465.

- 44 Martens A, Gruh I, Dimitroulis D, Rojas SV, Schmidt-Richter I, Rathert C, Khaladj N, Gawol A, Chikobava MG, Martin U, Haverich A, Kutschka I: Rhesus monkey cardiosphere-derived cells for myocardial restoration. *Cytotherapy* 2011;13:864-872.
- 45 Bearzi C, Rota M, Hosoda T, Tillmanns J, Nascimbene A, De Angelis A, Yasuzawa-Amano S, Trofimova I, Siggins RW, Lecapitaine N, Cascapera S, Beltrami AP, D'Alessandro DA, Zias E, Quaini F, Urbanek K, Michler RE, Bolli R, Kajstura J, Leri A, Anversa P: Human cardiac stem cells. *Proc Natl Acad Sci U S A* 2007;104:14068-14073.
- 46 Linke A, Müller P, Nurzynska D, Casarsa C, Torella D, Nascimbene A, Castaldo C, Cascapera S, Böhm M, Quaini F, Urbanek K, Leri A, Hintze TH, Kajstura J, Anversa P: Stem cells in the dog heart are self-renewing, clonogenic, and multipotent and regenerate infarcted myocardium, improving cardiac function. *Proc Natl Acad Sci U S A* 2005;102:8966-8971.
- 47 Urbanek K, Torella D, Sheikh F, De Angelis A, Nurzynska D, Silvestri F, Beltrami CA, Bussani R, Beltrami AP, Quaini F, Bolli R, Leri A, Kajstura J, Anversa P: Myocardial regeneration by activation of multipotent cardiac stem cells in ischemic heart failure. *Proc Natl Acad Sci U S A* 2005;102:8692-8697.
- 48 Massberg S, Schaerli P, Knezevic-Maramica I, Köllnberger M, Tubo N, Moseman EA, Huff IV, Junt T, Wagers AJ, Mazo IB, von Andrian UH: Immunosurveillance by hematopoietic progenitor cells trafficking through blood, lymph, and peripheral tissues. *Cell* 2007;131:994-1008.
- 49 Quaini F, Urbanek K, Beltrami AP, Finato N, Beltrami CA, Nadal-Ginard B, Kajstura J, Leri A, Anversa P: Chimerism of the transplanted heart. *N Engl J Med* 2002;346:5-15.
- 50 Uchida N, Weissman I: Searching for hematopoietic stem cells: Evidence that thy-1.1lo lin- sca-1+ cells are the only stem cells in c57bl/ka-thy-1.1 bone marrow. *J Exp Med* 1992;175:175-184.
- 51 Spangrude G, Brooks D: Mouse strain variability in the expression of the hematopoietic stem cell antigen ly-6a/e by bone marrow cells. *Blood* 1993;82:3327-3332.
- 52 Holmes C, Stanford W: Concise review: Stem cell antigen-1: Expression, function, and enigma. *Stem Cells* 2007;25:1339-1347.
- 53 Batts TD, Machado HL, Zhang Y, Creighton CJ, Li Y, Rosen JM: Stem cell antigen-1 (sca-1) regulates mammary tumor development and cell migration. *PLoS One* 2011;6:e27841.
- 54 Oh H, Bradfute SB, Gallardo TD, Nakamura T, Gaussin V, Mishina Y, Pocius J, Michael LH, Behringer RR, Garry DJ, Entman ML, Schneider MD: Cardiac progenitor cells from adult myocardium: Homing, differentiation, and fusion after infarction. *Proc Natl Acad Sci U S A* 2003;100:12313-12318.
- 55 Wang X, Hu Q, Nakamura Y, Lee J, Zhang G, From A, Zhang J: The role of the sca-1+/cd31- cardiac progenitor cell population in postinfarction left ventricular remodeling. *Stem Cells* 2006;24:1779-1788.
- 56 Ye J, Boyle A, Shih H, Sievers RE, Zhang Y, Prasad M, Su H, Zhou Y, Grossman W, Bernstein HS, Yeghiazarians Y: Sca-1+ cardiosphere-derived cells are enriched for isl1-expressing cardiac precursors and improve cardiac function after myocardial injury. *PLoS One* 2012;7:e30329.
- 57 Edling C, Hallberg B: C-kit--a hematopoietic cell essential receptor tyrosine kinase. *Int J Biochem Cell Biol* 2007;39:1995-1998.

- 58 Smith R, Barile L, Messina E, Marbán E: Stem cells in the heart: What's the buzz all about?--part 1: Preclinical considerations. *Heart Rhythm* 2008;5:749-757.
- 59 Hierlihy AM, Seale P, Lobe CG, Rudnicki MA, Megeney LA: The post-natal heart contains a myocardial stem cell population. *FEBS Lett* 2002;530:239-243.
- 60 Martin CM, Meeson AP, Robertson SM, Hawke TJ, Richardson JA, Bates S, Goetsch SC, Gallardo TD, Garry DJ: Persistent expression of the atp-binding cassette transporter, *abcg2*, identifies cardiac sp cells in the developing and adult heart. *Dev Biol* 2004;265:262-275.
- 61 Pfister O, Oikonomopoulos A, Sereti KI, Liao R: Isolation of resident cardiac progenitor cells by hoechst 33342 staining. *Methods Mol Biol* 2010;660:53-63.
- 62 Oyama T, Nagai T, Wada H, Naito AT, Matsuura K, Iwanaga K, Takahashi T, Goto M, Mikami Y, Yasuda N, Akazawa H, Uezumi A, Takeda S, Komuro I: Cardiac side population cells have a potential to migrate and differentiate into cardiomyocytes in vitro and in vivo. *J Cell Biol* 2007;176:329-341.
- 63 Meissner K, Heydrich B, Jedlitschky G, Meyer Zu Schwabedissen H, Mosyagin I, Dazert P, Eckel L, Vogelgesang S, Warzok RW, Böhm M, Lehmann C, Wendt M, Cascorbi I, Kroemer HK: The atp-binding cassette transporter *abcg2* (*bcrp*), a marker for side population stem cells, is expressed in human heart. *J Histochem Cytochem* 2006;54:215-221.
- 64 Khaitan D, Chandna S, Arya MB, Dwarakanath BS: Establishment and characterization of multicellular spheroids from a human glioma cell line; implications for tumor therapy. *J Transl Med* 2006;4:12.
- 65 Chimenti I, Smith RR, Li TS, Gerstenblith G, Messina E, Giacomello A, Marbán E: Relative roles of direct regeneration versus paracrine effects of human cardiosphere-derived cells transplanted into infarcted mice. *Circ Res* 2010;106:971-980.
- 66 Barile L, Gherghiceanu M, Popescu LM, Moccetti T, Vassalli G: Human cardiospheres as a source of multipotent stem and progenitor cells. *Stem Cells Int* 2013;2013:916837.
- 67 Li TS, Cheng K, Lee ST, Matsushita S, Davis D, Malliaras K, Zhang Y, Matsushita N, Smith RR, Marbán E: Cardiospheres recapitulate a niche-like microenvironment rich in stemness and cell-matrix interactions, rationalizing their enhanced functional potency for myocardial repair. *Stem Cells* 2010;28:2088-2098.
- 68 Smith R, Barile L, Cho H, Leppo M, Hare J, Messina E, Giacomello A, Abraham M, Marbán E: Regenerative potential of cardiosphere-derived cells expanded from percutaneous endomyocardial biopsy specimens. *Circulation* 2007;115:896-908.
- 69 Koninckx R, Daniëls A, Windmolders S, Carlotti F, Mees U, Steels P, Rummens JL, Hendrikx M, Hensen K: Mesenchymal stem cells or cardiac progenitors for cardiac repair? A comparative study. *Cell Mol Life Sci* 2011;68:2141-2156.
- 70 Davis DR, Kizana E, Terrovitis J, Barth AS, Zhang Y, Smith RR, Miake J, Marbán E: Isolation and expansion of functionally-competent cardiac progenitor cells directly from heart biopsies. *J Mol Cell Cardiol* 2010;49:312-321.
- 71 Davis DR, Zhang Y, Smith RR, Cheng K, Terrovitis J, Malliaras K, Li TS, White A, Makkar R, Marban E: Validation of the cardiosphere method to culture cardiac progenitor cells from myocardial tissue. *PLoS One* 2009;4:e7195.

- 72 Yan F, Yao Y, Chen L, Li Y, Sheng Z, Ma G: Hypoxic preconditioning improves survival of cardiac progenitor cells: Role of stromal cell derived factor-1 $\alpha$ -cxcr4 axis. *PLoS One* 2012;7:e37948.
- 73 Tang YL, Zhu W, Cheng M, Chen L, Zhang J, Sun T, Kishore R, Phillips MI, Losordo DW, Qin G: Hypoxic preconditioning enhances the benefit of cardiac progenitor cell therapy for treatment of myocardial infarction by inducing cxcr4 expression. *Circ Res* 2009;104:1209-1216.
- 74 Cheng K, Li T, Malliaras K, Davis D, Zhang Y, Marbán E: Magnetic targeting enhances engraftment and functional benefit of iron-labeled cardiosphere-derived cells in myocardial infarction. *Circ Res* 2010;106:1570-1581.
- 75 Bartosh TJ, Wang Z, Rosales AA, Dimitrijevič SD, Roque RS: 3d-model of adult cardiac stem cells promotes cardiac differentiation and resistance to oxidative stress. *J Cell Biochem* 2008;105:612-623.
- 76 Hodgkiss-Geere HM, Argyle DJ, Corcoran BM, Whitelaw B, Milne E, Bennett D, Argyle SA: Characterisation and cardiac directed differentiation of canine adult cardiac stem cells. *Vet J* 2012;191:176-182.
- 77 Malliaras K, Makkar RR, Smith RR, Cheng K, Wu E, Bonow RO, Marbán L, Mendizabal A, Cingolani E, Johnston PV, Gerstenblith G, Schuleri KH, Lardo AC, Marbán E: Intracoronary cardiosphere-derived cells after myocardial infarction: Evidence for therapeutic regeneration in the final 1-year results of the caduceus trial. *J Am Coll Cardiol* 2013.
- 78 Andersen DC, Andersen P, Schneider M, Jensen HB, Sheikh SP: Murine "Cardiospheres" Are not a source of stem cells with cardiomyogenic potential. *Stem Cells* 2009;27:1571-1581.
- 79 Mishra R, Vijayan K, Colletti EJ, Harrington DA, Matthiesen TS, Simpson D, Goh SK, Walker BL, Almeida-Porada G, Wang D, Backer CL, Dudley SC, Wold LE, Kaushal S: Characterization and functionality of cardiac progenitor cells in congenital heart patients. *Circulation* 2011;123:364-373.
- 80 Carr CA, Stuckey DJ, Tan JJ, Tan SC, Gomes RS, Camelliti P, Messina E, Giacomello A, Ellison GM, Clarke K: Cardiosphere-derived cells improve function in the infarcted rat heart for at least 16 weeks--an mri study. *PLoS One* 2011;6:e25669.
- 81 Thiele J, Varus E, Wickenhauser C, Kvasnicka HM, Lorenzen J, Gramley F, Metz KA, Rivero F, Beelen DW: Mixed chimerism of cardiomyocytes and vessels after allogeneic bone marrow and stem-cell transplantation in comparison with cardiac allografts. *Transplantation* 2004;77:1902-1905.
- 82 White AJ, Smith RR, Matsushita S, Chakravarty T, Czer LS, Burton K, Schwarz ER, Davis DR, Wang Q, Reinsmoen NL, Forrester JS, Marbán E, Makkar R: Intrinsic cardiac origin of human cardiosphere-derived cells. *Eur Heart J* 2013;34:68-75.
- 83 Davis DR, Zhang Y, Smith RR, Cheng K, Terrovitis J, Malliaras K, Li TS, White A, Makkar R, Marbán E: Validation of the cardiosphere method to culture cardiac progenitor cells from myocardial tissue. *PLoS One* 2009;4:e7195.
- 84 Barile L, Messina E, Giacomello A, Marbán E: Endogenous cardiac stem cells. *Prog Cardiovasc Dis* 2007;50:31-48.

- 85 Zakharova L, Mastroeni D, Mutlu N, Molina M, Goldman S, Diethrich E, Gaballa MA: Transplantation of cardiac progenitor cell sheet onto infarcted heart promotes cardiogenesis and improves function. *Cardiovasc Res* 2010;87:40-49.
- 86 Johnston PV, Sasano T, Mills K, Evers R, Lee ST, Smith RR, Lardo AC, Lai S, Steenbergen C, Gerstenblith G, Lange R, Marbán E: Engraftment, differentiation, and functional benefits of autologous cardiosphere-derived cells in porcine ischemic cardiomyopathy. *Circulation* 2009;120:1075-1083, 1077 p following 1083.
- 87 Robey TE, Saiget MK, Reinecke H, Murry CE: Systems approaches to preventing transplanted cell death in cardiac repair. *J Mol Cell Cardiol* 2008;45:567-581.
- 88 Teng CJ, Luo J, Chiu RC, Shum-Tim D: Massive mechanical loss of microspheres with direct intramyocardial injection in the beating heart: Implications for cellular cardiomyoplasty. *J Thorac Cardiovasc Surg* 2006;132:628-632.
- 89 Rumsey WL, Pawlowski M, Lejavardi N, Wilson DF: Oxygen pressure distribution in the heart in vivo and evaluation of the ischemic "Border zone". *Am J Physiol* 1994;266:H1676-1680.
- 90 Koh MY, Powis G: Passing the baton: The hif switch. *Trends Biochem Sci* 2012;37:364-372.
- 91 Déry M, Michaud M, Richard D: Hypoxia-inducible factor 1: Regulation by hypoxic and non-hypoxic activators. *Int J Biochem Cell Biol* 2005;37:535-540.
- 92 Brahim-Horn M, Pouyssegur J: Hif at a glance. *J Cell Sci* 2009;122:1055-1057.
- 93 Wenger R, Stiehl D, Camenisch G: Integration of oxygen signaling at the consensus hre. *Sci STKE* 2005;2005:re12.
- 94 Eliasson P, Jönsson JI: The hematopoietic stem cell niche: Low in oxygen but a nice place to be. *J Cell Physiol* 2010;222:17-22.
- 95 Wilson WR, Hay MP: Targeting hypoxia in cancer therapy. *Nat Rev Cancer* 2011;11:393-410.
- 96 Wang Y, Liu Y, Malek SN, Zheng P: Targeting hif1 $\alpha$  eliminates cancer stem cells in hematological malignancies. *Cell Stem Cell* 2011;8:399-411.
- 97 Grayson WL, Zhao F, Bunnell B, Ma T: Hypoxia enhances proliferation and tissue formation of human mesenchymal stem cells. *Biochem Biophys Res Commun* 2007;358:948-953.
- 98 Holzwarth C, Vaegler M, Gieseke F, Pfister SM, Handgretinger R, Kerst G, Müller I: Low physiologic oxygen tensions reduce proliferation and differentiation of human multipotent mesenchymal stromal cells. *BMC Cell Biol* 2010;11:11.
- 99 Ezashi T, Das P, Roberts RM: Low o<sub>2</sub> tensions and the prevention of differentiation of hescs. *Proc Natl Acad Sci U S A* 2005;102:4783-4788.
- 100 Kocabas F, Mahmoud AI, Sosic D, Porrello ER, Chen R, Garcia JA, DeBerardinis RJ, Sadek HA: The hypoxic epicardial and subepicardial microenvironment. *J Cardiovasc Transl Res* 2012;5:654-665.

- 101 van Oorschot AA, Smits AM, Pardali E, Doevendans PA, Goumans MJ: Low oxygen tension positively influences cardiomyocyte progenitor cell function. *J Cell Mol Med* 2011;15:2723-2734.
- 102 Ceradini DJ, Kulkarni AR, Callaghan MJ, Tepper OM, Bastidas N, Kleinman ME, Capla JM, Galiano RD, Levine JP, Gurtner GC: Progenitor cell trafficking is regulated by hypoxic gradients through hif-1 induction of sdf-1. *Nat Med* 2004;10:858-864.
- 103 Li TS, Cheng K, Malliaras K, Matsushita N, Sun B, Marbán L, Zhang Y, Marbán E: Expansion of human cardiac stem cells in physiological oxygen improves cell production efficiency and potency for myocardial repair. *Cardiovasc Res* 2011;89:157-165.
- 104 Bonios M, Chang CY, Terrovitis J, Pinheiro A, Barth A, Dong P, Santaularia M, Foster DB, Raman V, Abraham TP, Abraham MR: Constitutive hif-1 $\alpha$  expression blunts the beneficial effects of cardiosphere-derived cell therapy in the heart by altering paracrine factor balance. *J Cardiovasc Transl Res* 2011;4:363-372.
- 105 Li Z, Guo X, Guan J: An oxygen release system to augment cardiac progenitor cell survival and differentiation under hypoxic condition. *Biomaterials* 2012;33:5914-5923.
- 106 Eliasson P, Rehn M, Hammar P, Larsson P, Sirenko O, Flippin L, Cammenga J, Jönsson J: Hypoxia mediates low cell-cycle activity and increases the proportion of long-term-reconstituting hematopoietic stem cells during in vitro culture. *Exp Hematol* 2010;38:301-310.e302.
- 107 Makkar RR, Smith RR, Cheng K, Malliaras K, Thomson LE, Berman D, Czer LS, Marbán L, Mendizabal A, Johnston PV, Russell SD, Schuleri KH, Lardo AC, Gerstenblith G, Marbán E: Intracoronary cardiosphere-derived cells for heart regeneration after myocardial infarction (caduceus): A prospective, randomised phase 1 trial. *Lancet* 2012;379:895-904.
- 108 Bolli R, Chugh AR, D'Amario D, Loughran JH, Stoddard MF, Ikram S, Beache GM, Wagner SG, Leri A, Hosoda T, Sanada F, Elmore JB, Goichberg P, Cappelletta D, Solankhi NK, Fahsah I, Rokosh DG, Slaughter MS, Kajstura J, Anversa P: Cardiac stem cells in patients with ischaemic cardiomyopathy (scipio): Initial results of a randomised phase 1 trial. *Lancet* 2011;378:1847-1857.
- 109 Srinivas S, Watanabe T, Lin CS, William CM, Tanabe Y, Jessell TM, Costantini F: Cre reporter strains produced by targeted insertion of eyfp and ecfp into the rosa26 locus. *BMC Dev Biol* 2001;1:4.
- 110 Zheng B, Zhang Z, Black CM, de Crombrughe B, Denton CP: Ligand-dependent genetic recombination in fibroblasts : A potentially powerful technique for investigating gene function in fibrosis. *Am J Pathol* 2002;160:1609-1617.
- 111 Carmeliet P, Dor Y, Herbert J-M, Fukumura D, Brusselmans K, Dewerchin M, Neeman M, Bono F, Abramovitch R, Maxwell P, Koch CJ, Ratcliffe P, Moons L, Jain RK, Collen D, Keshet E: Role of hif-1[ $\alpha$ ] in hypoxia-mediated apoptosis, cell proliferation and tumour angiogenesis. *Nature* 1998;394:485-490.
- 112 Tan SC, Carr CA, Yeoh KK, Schofield CJ, Davies KE, Clarke K: Identification of valid housekeeping genes for quantitative rt-pcr analysis of cardiosphere-derived cells preconditioned under hypoxia or with prolyl-4-hydroxylase inhibitors. *Mol Biol Rep* 2012;39:4857-4867.
- 113 Pallen CJ, Tong PH: Elevation of membrane tyrosine phosphatase activity in density-dependent growth-arrested fibroblasts. *Proc Natl Acad Sci U S A* 1991;88:6996-7000.

- 114 Pieper RO, Lester KA, Fanton CP: Confluence-induced alterations in cpg island methylation in cultured normal human fibroblasts. *Nucleic Acids Res* 1999;27:3229-3235.
- 115 Drowley L, Okada M, Payne TR, Botta GP, Oshima H, Keller BB, Tobita K, Huard J: Sex of muscle stem cells does not influence potency for cardiac cell therapy. *Cell Transplant* 2009;18:1137-1146.
- 116 Crisostomo PR, Markel TA, Wang M, Lahm T, Lillemoe KD, Meldrum DR: In the adult mesenchymal stem cell population, source gender is a biologically relevant aspect of protective power. *Surgery* 2007;142:215-221.
- 117 Nayan M, Paul A, Chen G, Chiu RC, Prakash S, Shum-Tim D: Superior therapeutic potential of young bone marrow mesenchymal stem cells by direct intramyocardial delivery in aged recipients with acute myocardial infarction: In vitro and in vivo investigation. *J Tissue Eng* 2011;2011:741213.
- 118 Steinbrech DS, Mehrara BJ, Saadeh PB, Greenwald JA, Spector JA, Gittes GK, Longaker MT: Vegf expression in an osteoblast-like cell line is regulated by a hypoxia response mechanism. *Am J Physiol Cell Physiol* 2000;278:C853-860.
- 119 Nagelkerke A, Bussink J, Mujcic H, Wouters BG, Lehmann S, Sweep FC, Span PN: Hypoxia stimulates migration of breast cancer cells via the perk/atf4/lamp3-arm of the unfolded protein response. *Breast Cancer Res* 2013;15:R2.
- 120 Barry MA, Reynolds JE, Eastman A: Etoposide-induced apoptosis in human hl-60 cells is associated with intracellular acidification. *Cancer Res* 1993;53:2349-2357.
- 121 Koh MY, Lemos R, Liu X, Powis G: The hypoxia-associated factor switches cells from hif-1 $\alpha$ - to hif-2 $\alpha$ -dependent signaling promoting stem cell characteristics, aggressive tumor growth and invasion. *Cancer Res* 2011;71:4015-4027.
- 122 Berra E, Roux D, Richard DE, Pouyssegur J: Hypoxia-inducible factor-1 alpha (hif-1 alpha) escapes o(2)-driven proteasomal degradation irrespective of its subcellular localization: Nucleus or cytoplasm. *EMBO Rep* 2001;2:615-620.
- 123 Koshiji M, Kageyama Y, Pete EA, Horikawa I, Barrett JC, Huang LE: Hif-1alpha induces cell cycle arrest by functionally counteracting myc. *EMBO J* 2004;23:1949-1956.
- 124 Gordan JD, Bertout JA, Hu CJ, Diehl JA, Simon MC: Hif-2alpha promotes hypoxic cell proliferation by enhancing c-myc transcriptional activity. *Cancer Cell* 2007;11:335-347.
- 125 Keith B, Johnson RS, Simon MC: Hif1alpha and hif2alpha: Sibling rivalry in hypoxic tumour growth and progression. *Nat Rev Cancer* 2012;12:9-22.
- 126 Yao L, Chen X, Tian Y, Lu H, Zhang P, Shi Q, Zhang J, Liu Y: Selection of housekeeping genes for normalization of rt-pcr in hypoxic neural stem cells of rat in vitro. *Mol Biol Rep* 2012;39:569-576.
- 127 Holmes C, Stanford WL: Concise review: Stem cell antigen-1: Expression, function, and enigma. *Stem Cells* 2007;25:1339-1347.
- 128 Valorani MG, Germani A, Otto WR, Harper L, Biddle A, Khoo CP, Lin WR, Hawa MI, Tropel P, Patrizi MP, Pozzilli P, Alison MR: Hypoxia increases sca-1/cd44 co-expression in murine mesenchymal stem cells and enhances their adipogenic differentiation potential. *Cell Tissue Res* 2010;341:111-120.

- 129 Giaccia A, Siim BG, Johnson RS: Hif-1 as a target for drug development. *Nat Rev Drug Discov* 2003;2:803-811.
- 130 Tazuke SI, Mazure NM, Sugawara J, Carland G, Faessen GH, Suen LF, Irwin JC, Powell DR, Giaccia AJ, Giudice LC: Hypoxia stimulates insulin-like growth factor binding protein 1 (igfbp-1) gene expression in hepg2 cells: A possible model for igfbp-1 expression in fetal hypoxia. *Proc Natl Acad Sci U S A* 1998;95:10188-10193.
- 131 Rees BB, Bowman JA, Schulte PM: Structure and sequence conservation of a putative hypoxia response element in the lactate dehydrogenase-b gene of fundulus. *Biol Bull* 2001;200:247-251.
- 132 Jögi A, Øra I, Nilsson H, Lindeheim A, Makino Y, Poellinger L, Axelson H, Pählman S: Hypoxia alters gene expression in human neuroblastoma cells toward an immature and neural crest-like phenotype. *Proc Natl Acad Sci U S A* 2002;99:7021-7026.
- 133 Krishnamurthy P, Ross DD, Nakanishi T, Bailey-Dell K, Zhou S, Mercer KE, Sarkadi B, Sorrentino BP, Schuetz JD: The stem cell marker bcrp/abcg2 enhances hypoxic cell survival through interactions with heme. *J Biol Chem* 2004;279:24218-24225.
- 134 Valorani MG, Montelatici E, Germani A, Biddle A, D'Alessandro D, Strollo R, Patrizi MP, Lazzari L, Nye E, Otto WR, Pozzilli P, Alison MR: Pre-culturing human adipose tissue mesenchymal stem cells under hypoxia increases their adipogenic and osteogenic differentiation potentials. *Cell Prolif* 2012;45:225-238.
- 135 Adesida AB, Mulet-Sierra A, Jomha NM: Hypoxia mediated isolation and expansion enhances the chondrogenic capacity of bone marrow mesenchymal stromal cells. *Stem Cell Res Ther* 2012;3:9.
- 136 Sanchez-Elsner T, Botella LM, Velasco B, Langa C, Bernabeu C: Endoglin expression is regulated by transcriptional cooperation between the hypoxia and transforming growth factor-beta pathways. *J Biol Chem* 2002;277:43799-43808.
- 137 López-Novoa JM, Bernabeu C: The physiological role of endoglin in the cardiovascular system. *Am J Physiol Heart Circ Physiol* 2010;299:H959-974.
- 138 Hu X, Yu SP, Fraser JL, Lu Z, Ogle ME, Wang JA, Wei L: Transplantation of hypoxia-preconditioned mesenchymal stem cells improves infarcted heart function via enhanced survival of implanted cells and angiogenesis. *J Thorac Cardiovasc Surg* 2008;135:799-808.
- 139 Han Y, Kuang SZ, Gomer A, Ramirez-Bergeron DL: Hypoxia influences the vascular expansion and differentiation of embryonic stem cell cultures through the temporal expression of vascular endothelial growth factor receptors in an arnt-dependent manner. *Stem Cells* 2010;28:799-809.
- 140 Chan HH, Meher Homji Z, Gomes RS, Sweeney D, Thomas GN, Tan JJ, Zhang H, Perbellini F, Stuckey DJ, Watt SM, Taggart D, Clarke K, Martin-Rendon E, Carr CA: Human cardiosphere-derived cells from patients with chronic ischaemic heart disease can be routinely expanded from atrial but not epicardial ventricular biopsies. *J Cardiovasc Transl Res* 2012;5:678-687.
- 141 Leri A, Kajstura J, Anversa P: Cardiac stem cells and mechanisms of myocardial regeneration. *Physiol Rev* 2005;85:1373-1416.
- 142 Fujita D, Tanabe A, Sekijima T, Soen H, Narahara K, Yamashita Y, Terai Y, Kamegai H, Ohmichi M: Role of extracellular signal-regulated kinase and akt cascades in regulating



hypoxia-induced angiogenic factors produced by a trophoblast-derived cell line. *J Endocrinol* 2010;206:131-140.

143 Hu X, Yu SP, Fraser JL, Lu Z, Ogle ME, Wang JA, Wei L: Transplantation of hypoxia-preconditioned mesenchymal stem cells improves infarcted heart function via enhanced survival of implanted cells and angiogenesis. *J Thorac Cardiovasc Surg* 2008;135:799-808.

144 Yan F, Yao Y, Chen L, Li Y, Sheng Z, Ma G: Hypoxic preconditioning improves survival of cardiac progenitor cells: Role of stromal cell derived factor-1 $\alpha$ -cxcr4 axis. *PLoS One* 2012;7:e37948.

145 Burstein B, Libby E, Calderone A, Nattel S: Differential behaviors of atrial versus ventricular fibroblasts: A potential role for platelet-derived growth factor in atrial-ventricular remodeling differences. *Circulation* 2008;117:1630-1641.

146 Vagima Y, Lapid K, Kollet O, Goichberg P, Alon R, Lapidot T: Pathways implicated in stem cell migration: The sdf-1/cxcr4 axis. *Methods Mol Biol* 2011;750:277-289.

147 Tang Y, Wu X, Lei W, Pang L, Wan C, Shi Z, Zhao L, Nagy TR, Peng X, Hu J, Feng X, Van Hul W, Wan M, Cao X: Tgf-beta1-induced migration of bone mesenchymal stem cells couples bone resorption with formation. *Nat Med* 2009;15:757-765.

148 Bar EE, Lin A, Mahairaki V, Matsui W, Eberhart CG: Hypoxia increases the expression of stem-cell markers and promotes clonogenicity in glioblastoma neurospheres. *Am J Pathol* 2010;177:1491-1502.

149 Zuba-Surma EK, Abdel-Latif A, Case J, Tiwari S, Hunt G, Kucia M, Vincent RJ, Ranjan S, Ratajczak MZ, Srouf EF, Bolli R, Dawn B: Sca-1 expression is associated with decreased cardiomyogenic differentiation potential of skeletal muscle-derived adult primitive cells. *J Mol Cell Cardiol* 2006;41:650-660.

150 Hidestrand M, Richards-Malcolm S, Gurley CM, Nolen G, Grimes B, Waterstrat A, Zant GV, Peterson CA: Sca-1-expressing nonmyogenic cells contribute to fibrosis in aged skeletal muscle. *J Gerontol A Biol Sci Med Sci* 2008;63:566-579.

151 Janson D, Rietveld M, Willemze R, El Ghalbzouri A: Effects of serially passaged fibroblasts on dermal and epidermal morphogenesis in human skin equivalents. *Biogerontology* 2013.

152 Koninckx R, Daniels A, Windmolders S, Carlotti F, Mees U, Steels P, Rummens JL, Hendriks M, Hensen K: Mesenchymal stem cells or cardiac progenitors for cardiac repair? A comparative study. *Cellular and molecular life sciences : CMLS* 2011;68:2141-2156.

153 Cox BC, Liu Z, Lagarde MM, Zuo J: Conditional gene expression in the mouse inner ear using cre-loxp. *Journal of the Association for Research in Otolaryngology : JARO* 2012;13:295-322.

154 Jackson KA, Snyder DS, Goodell MA: Skeletal muscle fiber-specific green autofluorescence: Potential for stem cell engraftment artifacts. *Stem Cells* 2004;22:180-187.

155 Nussbaum J, Minami E, Laflamme MA, Virag JA, Ware CB, Masino A, Muskheli V, Pabon L, Reinecke H, Murry CE: Transplantation of undifferentiated murine embryonic stem cells in the heart: Teratoma formation and immune response. *FASEB J* 2007;21:1345-1357.

156 Schneider M, Kostin S, Strøm CC, Aplin M, Lyngbaek S, Theilade J, Grigorian M, Andersen CB, Lukanidin E, Lerche Hansen J, Sheikh SP: S100a4 is upregulated in injured

myocardium and promotes growth and survival of cardiac myocytes. *Cardiovasc Res* 2007;75:40-50.

157 Etich J, Bergmeier V, Frie C, Kreft S, Bengestrategie L, Eming S, Mauch C, Eckes B, Ulus H, Lund FE, Rappl G, Abken H, Paulsson M, Brachvogel B: Pecam1(+)/sca1(+)/cd38(+) vascular cells transform into myofibroblast-like cells in skin wound repair. *PLoS One* 2013;8:e53262.

158 Kiryushko D, Novitskaya V, Soroka V, Klingelhofer J, Lukanidin E, Berezin V, Bock E: Molecular mechanisms of ca(2+) signaling in neurons induced by the s100a4 protein. *Molecular and cellular biology* 2006;26:3625-3638.

159 Ambartsumian N, Klingelhofer J, Grigorian M, Christensen C, Kriajevska M, Tulchinsky E, Georgiev G, Berezin V, Bock E, Rygaard J, Cao R, Cao Y, Lukanidin E: The metastasis-associated mts1(s100a4) protein could act as an angiogenic factor. *Oncogene* 2001;20:4685-4695.

160 Semov A, Moreno MJ, Onichtchenko A, Abulrob A, Ball M, Ekiel I, Pietrzynski G, Stanimirovic D, Alakhov V: Metastasis-associated protein s100a4 induces angiogenesis through interaction with annexin ii and accelerated plasmin formation. *J Biol Chem* 2005;280:20833-20841.

161 Stary M, Schneider M, Sheikh SP, Weitzer G: Parietal endoderm secreted s100a4 promotes early cardiomyogenesis in embryoid bodies. *Biochem Biophys Res Commun* 2006;343:555-563.

162 Sugimoto H, Mundel TM, Kieran MW, Kalluri R: Identification of fibroblast heterogeneity in the tumor microenvironment. *Cancer biology & therapy* 2006;5:1640-1646.

163 Franke WW, Schmid E, Osborn M, Weber K: Intermediate-sized filaments of human endothelial cells. *J Cell Biol* 1979;81:570-580.

164 Mørk C, van Deurs B, Petersen OW: Regulation of vimentin expression in cultured human mammary epithelial cells. *Differentiation* 1990;43:146-156.

165 Manabe I, Shindo T, Nagai R: Gene expression in fibroblasts and fibrosis: Involvement in cardiac hypertrophy. *Circulation research* 2002;91:1103-1113.

166 Desta Z, Ward BA, Soukhova NV, Flockhart DA: Comprehensive evaluation of tamoxifen sequential biotransformation by the human cytochrome p450 system in vitro: Prominent roles for cyp3a and cyp2d6. *J Pharmacol Exp Ther* 2004;310:1062-1075.

167 Baschong W, Suetterlin R, Laeng RH: Control of autofluorescence of archival formaldehyde-fixed, paraffin-embedded tissue in confocal laser scanning microscopy (clsm). *J Histochem Cytochem* 2001;49:1565-1572.

168 Tohma H, Hepworth AR, Shavlakadze T, Grounds MD, Arthur PG: Quantification of ceroid and lipofuscin in skeletal muscle. *J Histochem Cytochem* 2011;59:769-779.

169 Lin SL, Kisseleva T, Brenner DA, Duffield JS: Pericytes and perivascular fibroblasts are the primary source of collagen-producing cells in obstructive fibrosis of the kidney. *Am J Pathol* 2008;173:1617-1627.

170 Iwasaki T, Mukasa K, Yoneda M, Ito S, Yamada Y, Mori Y, Fujisawa N, Fujisawa T, Wada K, Sekihara H, Nakajima A: Marked attenuation of production of collagen type i from cardiac fibroblasts by dehydroepiandrosterone. *American journal of physiology Endocrinology and metabolism* 2005;288:E1222-1228.

- 171 Schneider M, Kostin S, Strom CC, Aplin M, Lyngbaek S, Theilade J, Grigorian M, Andersen CB, Lukanidin E, Lerche Hansen J, Sheikh SP: S100a4 is upregulated in injured myocardium and promotes growth and survival of cardiac myocytes. *Cardiovasc Res* 2007;75:40-50.
- 172 Camelliti P, Devlin GP, Matthews KG, Kohl P, Green CR: Spatially and temporally distinct expression of fibroblast connexins after sheep ventricular infarction. *Cardiovasc Res* 2004;62:415-425.
- 173 Mor-Vaknin N, Punturieri A, Sitwala K, Markovitz DM: Vimentin is secreted by activated macrophages. *Nat Cell Biol* 2003;5:59-63.
- 174 Hayashi S, McMahon AP: Efficient recombination in diverse tissues by a tamoxifen-inducible form of cre: A tool for temporally regulated gene activation/inactivation in the mouse. *Developmental biology* 2002;244:305-318.
- 175 Nag AC: Study of non-muscle cells of the adult mammalian heart: A fine structural analysis and distribution. *Cytobios* 1980;28:41-61.
- 176 Norrby K: In vivo models of angiogenesis. *J Cell Mol Med* 2006;10:588-612.
- 177 Melero-Martin JM, De Obaldia ME, Kang SY, Khan ZA, Yuan L, Oettgen P, Bischoff J: Engineering robust and functional vascular networks in vivo with human adult and cord blood-derived progenitor cells. *Circulation research* 2008;103:194-202.
- 178 Allen P, Melero-Martin J, Bischoff J: Type I collagen, fibrin and permatrigel matrices provide permissive environments for human endothelial and mesenchymal progenitor cells to form neovascular networks. *J Tissue Eng Regen Med* 2011;5:e74-86.
- 179 Skovseth DK, Yamanaka T, Brandtzaeg P, Butcher EC, Haraldsen G: Vascular morphogenesis and differentiation after adoptive transfer of human endothelial cells to immunodeficient mice. *Am J Pathol* 2002;160:1629-1637.
- 180 Kevil CG, Orr AW, Langston W, Mickett K, Murphy-Ullrich J, Patel RP, Kucik DF, Bullard DC: Intercellular adhesion molecule-1 (ICAM-1) regulates endothelial cell motility through a nitric oxide-dependent pathway. *J Biol Chem* 2004;279:19230-19238.
- 181 Combe C, Burton CJ, Dufourco P, Weston S, Horsburgh T, Walls J, Harris KP: Hypoxia induces intercellular adhesion molecule-1 on cultured human tubular cells. *Kidney Int* 1997;51:1703-1709.
- 182 Kotton DN, Summer RS, Sun X, Ma BY, Fine A: Stem cell antigen-1 expression in the pulmonary vascular endothelium. *Am J Physiol Lung Cell Mol Physiol* 2003;284:L990-996.
- 183 Hoeben A, Landuyt B, Highley MS, Wildiers H, Van Oosterom AT, De Bruijn EA: Vascular endothelial growth factor and angiogenesis. *Pharmacol Rev* 2004;56:549-580.
- 184 Li Z, Lee A, Huang M, Chun H, Chung J, Chu P, Hoyt G, Yang P, Rosenberg J, Robbins RC, Wu JC: Imaging survival and function of transplanted cardiac resident stem cells. *J Am Coll Cardiol* 2009;53:1229-1240.
- 185 Kuhlmann CR, Schaefer CA, Reinhold L, Tillmanns H, Erdogan A: Signalling mechanisms of sdf-induced endothelial cell proliferation and migration. *Biochem Biophys Res Commun* 2005;335:1107-1114.

- 186 Scholzen T, Gerdes J: The ki-67 protein: From the known and the unknown. *J Cell Physiol* 2000;182:311-322.
- 187 Unemori EN, Lewis M, Constant J, Arnold G, Grove BH, Normand J, Deshpande U, Salles A, Pickford LB, Erikson ME, Hunt TK, Huang X: Relaxin induces vascular endothelial growth factor expression and angiogenesis selectively at wound sites. *Wound Repair Regen* 2000;8:361-370.
- 188 Das B, Yeger H, Tsuchida R, Torkin R, Gee MF, Thorner PS, Shibuya M, Malkin D, Baruchel S: A hypoxia-driven vascular endothelial growth factor/flt1 autocrine loop interacts with hypoxia-inducible factor-1alpha through mitogen-activated protein kinase/extracellular signal-regulated kinase 1/2 pathway in neuroblastoma. *Cancer Res* 2005;65:7267-7275.
- 189 Stieger SM, Bloch SH, Foreman O, Wisner ER, Ferrara KW, Dayton PA: Ultrasound assessment of angiogenesis in a matrigel model in rats. *Ultrasound Med Biol* 2006;32:673-681.
- 190 Meir KS, Leitersdorf E: Atherosclerosis in the apolipoprotein-e-deficient mouse: A decade of progress. *Arterioscler Thromb Vasc Biol* 2004;24:1006-1014.